

**UTILISATION OF VARIOUS BONDING MODES OF
NITROGEN-RICH HETEROCYCLES IN GOLD(I)
CHEMISTRY**

by

WILLIAM FULLARD GABRIELLI

DISSERTATION

submitted in fulfilment of the requirements
for the degree of

PHILOSOPHIAE DOCTOR



in the

FACULTY OF SCIENCE

at the

UNIVERSITY OF STELLENBOSCH

SUPERVISOR: PROF. H.G. RAUBENHEIMER

CO-SUPERVISOR: DR S CRONJE

APRIL 2006

Declaration

I, the undersigned, hereby declare that the work contained in this dissertation is my own original work and that I have not previously in its entirety or in part submitted it at any university for a degree.

Signature:

Date: 2006-03-08

SUMMARY

This study describes the exploitation of numerous donor ligand possibilities presented by selected nitrogen-rich heterocyclic ligands towards gold(I). The preparation and structural characterisation of novel gold(I) complexes, apart from conventional gold(I) bonding possibilities, also encompassed a study of bi- and polytopic bonding modes within a range of multifunctional ligands. Very few examples exist in the literature describing gold(I) compounds derived from tetrazoles. As main focus of our study, this fascinating class of ligands was employed in unique and unprecedented fashions towards the preparation of novel gold(I) complexes. The main objective of this work was to obtain a better understanding of the stability of the metal-ligand interactions involved and, eventually, to gain insight into the reactivity of the gold(I) centre, with an eye on future application.

A series of gold(I) complexes derived from (azolyl)phosphines that contain natural azoles such as imidazoles and thiazoles were prepared. As a representative example, chloro[(1-benzylimidazol-2-yl)diphenyl]phosphinegold(I) was prepared after the *in situ* formation of a tertiary (azolyl)phosphine, (1-benzylimidazol-2-yl)diphenylphosphine, followed by reaction with [AuCl(tht)] (tht = tetrahydrothiophene). In addition to this strongly-bonded gold(I) phosphine complex, another compound chloro[tris(1-methylimidazol-2-yl)phosphine]gold(I), was further employed as a secondary N-donor ligand towards the formation of aurophilically-coupled metallocyclic compounds. During this investigation, a fascinating self-assembly of molecules resulted in the formation of a tetranuclear bicyclic complex, dichloro[{*N*-pentafluorophenylgold(I)-1-methylimidazol-2-yl}(1-methylimidazol-2-yl)]phosphinitegold(II). This mixed Au(I)-Au(II) complex also represents the first example of two Au(II) centres stabilised by a P,N-bridging ligand, through phosphinite (P) and imine (N) donor atoms.

Interesting structural behaviour was also unearthed both in solution and in solid state for the new compounds. Single crystal X-ray crystallography revealed that chloro[tris(thiazol-2-yl)phosphine]gold(I), chloro[tris(4-methylthiazol-2-yl)phosphine]gold(I) and chloro[(1-benzylimidazol-2-yl)diphenyl]phosphinegold(I) independently self-associate through aurophilic interactions into discrete dimeric molecules. Chloro[tris(thiazol-2-yl)phosphine]gold(I) was further isolated in two true polymorphic crystalline forms. An unusual coupling of the phosphorus atom in this compound to the proton in the 4-position

on the thiazole ring *via* the sulphur atom, was confirmed by selective homonuclear proton decoupling as well as heteronuclear phosphorus decoupling.

A number of stable, neutral, N-coordinated pentafluorophenylgold(I) complexes were also prepared. The complexes 1-methylimidazole(pentafluorophenyl)gold(I), 1-benzylimidazole (pentafluorophenyl)gold(I), 1-methylbenzimidazole(pentafluorophenyl)gold(I), and [1,4-bis(imidazol-1-yl)butane]bis[(pentafluorophenyl)gold(I)] were obtained by the reaction of $[\text{Au}(\text{C}_6\text{F}_5)(\text{tht})]$ with 1-methylimidazole, 1-benzylimidazole, 1-methylbenzimidazole and 1,4-bis(imidazole-1-yl)butane. N-coordination of the imine complexes was confirmed by single crystal X-ray structure analysis and ^{15}N NMR measurements.

The methodology developed above was then applied in the successful preparation of the first tetrazolyl gold(I) imine complex. The molecular structure of 1-benzyltetrazole(pentafluorophenyl)gold(I), confirmed the inequivalency of the four ring nitrogen atoms and revealed that only the N^4 nitrogen coordinates to the gold(I) centre. Furthermore, a ^{15}N NMR-study and results based on the structure analyses of simple tetrazole ligands, 1-benzyltetrazole and 5-chloro-1-phenyltetrazole, allowed prediction of imine coordination potential of a given ligand to a neutral $(\text{C}_6\text{F}_5)\text{Au}$ moiety. Under very green conditions, a series of tetrazoles were prepared by a 2,3-cycloaddition reaction of inorganic azides and carbonitriles or amines. Microwave irradiation compared to conventional heating afforded a dramatic reduction in reaction times, increased production yields and high purity of these compounds.

Contributing to the rapidly expanding chemistry of N-heterocyclic carbene complexes of gold(I), we synthesised the first tetrazole-derived carbene complexes of gold(I), using two classical methodologies. First, by a lithiation-transmetallation-alkylation approach, to afford a bis(1-benzyl-4-methyltetrazol-5-ylidene)gold(I) triflate, and, second, by 1,2-cycloaddition of an isocyanide to $[\text{Au}(\text{N}_3)(\text{PPh}_3)]$ to furnish the precursors [1-(2,6-dimethylphenyl)tetrazol-5-yl](triphenylphosphine)gold(I). Alkylation of latter compound yielded the corresponding cationic carbene complex, [1-(2,6-dimethylphenyl)-4-methyltetrazol-5-ylidene](triphenylphosphine)gold(I) triflate in excellent yield. The first X-ray structure analysis performed on a tetrazolylidene gold(I) complex, bis(1-benzyl-4-methyltetrazol-5-ylidene)gold(I) triflate, further confirmed that alkylation to afford carbene complex formation occurs selectively on the nucleophilic N^4 heteroatom.

Other C-tetrazolyl complexes of gold(I) prepared include, [1-(*tert*-butyl)tetrazol-5-yl](triphenylphosphine)gold(I) and [1-(cyclohexyl)tetrazol-5-yl](triphenylphosphine)gold(I). Neutral and cationic tetrazolylidene gold(I) complexes derived from the lithiated tetrazoles, (pentafluorophenyl)(1-benzyltetrazol-5-ylidene)gold(I) and (1-benzyltetrazol-5-ylidene)(triphenylphosphine)gold(I) triflate, in accord with the related imidazolyaurate and imidazolylidene complexes, displayed a rapid homoleptic rearrangement of ligands when in solution. In the presence of an ammonium salt during the preparation of (pentafluorophenyl)(1-benzyltetrazol-5-ylidene)gold(I), this reaction was confirmed by the isolation and structural characterisation of [bis(pentafluorophenyl)gold(I)][TMEDAMe].

Finally, two novel and closely related coordination polymers, [Li(CF₃SO₃)₂][TMEDAMe] and [Li(CF₃SO₃)(diethyl ether)], in which the coordinated Li⁺-ions play an important ligand coupling role within the extended structures, were also isolated and characterised by molecular and crystal structure determination.

OPSOMMING

Hierdie studie behels 'n ondersoek na die reaktiwiteit van stikstofryk, heterosikliese verbindings teenoor goud(I). Die bereiding en struktuurkarakterisering van nuwe goud(I) komplekse sluit benewens konvensionele goud(I)verbindings bi- en politopiese bindingstipes van multifunksionele ligande in. Slegs enkele voorbeelde van tetrasool-bevattende goud(I)verbindings is voorheen in die literatuur beskryf. As 'n belangrike fokus van hierdie studie, word hierdie fassinerende tipe ligande op 'n nuwe en unieke wyse in goudkoördinasie aangewend. Die hoofdoelwitte van hierdie studie is om 'n beter begrip van die stabiliteit van die gekose metaal-ligand interaksies te bekom asook om 'n insig in die reaktiwiteit van goud(I)-eenhede met die oog op verdere toepassings te verkry.

'n Reeks asoeliëfosfien-gebaseerde goud(I)verbindings waarin natuurlike asole voorkom, onder andere imidasole en tiasole, is berei. As 'n verteenwoordigende voorbeeld, chloro[(1-bensielimidazol-2-iel)difeniel]fosfiengoud(I) is verkry deur die *in situ* vorming van die tersiêre asoeliëfosfien, (1-bensielimidazol-2-iel)difenielfosfien, gevolg deur reaksie met [AuCl(tht)] (tht = tetrahidrotiofeen). Addisioneel tot hierdie stabiele goud(I)kompleks, is chloro[tris(1-metielimidazol-2-iel)fosfien]goud(I) ook gebruik as sekondêre N-donorligand in die vorming van aurofiliese-gekoppelde metallosikliese verbindings. Tydens hierdie ondersoek, lei 'n spontane selfassosiasie-reaksie tot die bereiding van 'n tetrakernige, bisikliese kompleks, dichloro[{*N*-pentafluorofenielgoud(I)-1-metielimidazol-2-iel}(1-metielimidazol-2-iel)]fosfinietgoud(II). Hierdie gemengde Au(I)-Au(II)-kompleks verteenwoordig die eerste voorbeeld waarin twee Au(II)-atome gestabiliseer word deur 'n P,N-gebrugde ligand, deur middel van fosfiniet(P)- en imien(N) - donoratome.

Interessante struktuurgedrag in oplossing en in die vastetoestand is 'n kenmerk van hierdie nuwe verbindings. Deur middel van enkelkristal X-straalkristallografie is gevind dat chloro[tris(tiasol-2-iel)fosfien]goud(I), chloro[tris(4-metieliasol-2-iel)fosfien]goud(I) en chloro[(1-bensielimidazol-2-iel)difeniel]fosfiengoud(I) deur middel van aurofiliese interaksies in diskrete dimeriese molekules assosieer. Chloro[tris(tiasol-2-iel)fosfien]goud(I) is verder in twee ware polimorfiese kristalvorme geïsoleer. Met behulp van selektiewe homokernige protonontkoppeling en heterokernige fosforontkoppeling, kon 'n ongewone fosforatoom-koppeling met 'n proton in die 4-posisie van die tiasoolring, *via* die swaelatoom, bevestig word.

Verskeie stabiele en neutrale, N-gekoördineerde pentafluorofenielgoud(I)komplekse is berei. Die komplekse, 1-metielimidasool(pentafluorofeniel)goud(I), 1-bensielimidasool (pentafluorofeniel)goud(I), 1-(metiel)bensimidasool(pentafluorofeniel)goud(I), en 1,4-bis(imidasol-1-iel)butaan]bis[(pentafluorofeniel)goud(I) is bekom vanuit die reaksie van $[\text{Au}(\text{C}_6\text{F}_5)(\text{tht})]$ met 1-metielimidasool, 1-bensielimidasool, 1-metielbensimidasool en 1,4-bis(imidasool-1-iel)butaan onderskeidelik. N-koordinasie in hierdie imienkomplekse is bevestig deur enkelkristal X-straalkristallografie asook met behulp van ^{15}N -KMR-bepalings.

Laasgenoemde sintetiese metode is ook verder toegepas in die suksesvolle bereiding van die eerste tetrasoelgoud(I)-imienkompleks. Die molekulêre struktuur van 1-bensieltetrasool(pentafluorofeniel)goud(I), bevestig dat die vier stikstofatome in die tetrasool ring beslis verskil in hul koördinasievoorkeure en dui daarop dat slegs die N^4 -stikstofatoom aan die goud(I)kern bind. Uit ^{15}N -NMR-studies en struktuuranalitiese data van die tetrasoolligande 1-bensieltetrasool en 5-chloro-1-fenieltetrasool, kon die imienkoördinasiepotensiaal van hierdie ligande aan 'n $(\text{C}_6\text{F}_5)\text{Au}$ -groep voorspel word. Deur gebruik te maak van omgewingsvriendelike eksperimentele kondisies is 'n reeks tetrasoolverbindings berei deur 2,3-sikloaddisiereaksies van anorganiese asiede en karbonitriële of amiene. Mikrogolfbestraling in vergelyking met konvensionele verhittingsmetodes, bring 'n dramatiese afname in reaksietyd asook hoër opbrengste en beter suiwerheid van reaksieprodukte mee.

Die bereiding van die eerste tetrasool-gebaseerde karbeenkomplekse van goud(I), is 'n belangrike bydrae tot die vinnig-groeiende chemie van N-heterosikliese karbeenkomplekse van goud(I). Hierdie verbindings is deur middel van twee klassieke metodes daargestel: eerstens, deur gebruik te maak van agtereenvolgende litiëring, transmetilering en alkilering kon bis(1-bensiel-4-metieltetrasol-5-ilideen)goud(I)triflaat berei word; tweedens, deur middel van 'n 1,2-sikloaddissie van isosianied aan $[\text{Au}(\text{N}_3)(\text{PPh}_3)]$ is die karbeenvoorgangerverbinding, [1-(2,6-dimetielfeniel)tetrasol-5-iel](trifeniel-fosfien)goud(I), verkry. Alkilering van hierdie verbinding het die vorming van die ooreenstemmende kationiese karbeenkompleks, [1-(2,6-dimetielfeniel)-4-metieltetrasol-5-ilideen](trifeniel-fosfien)goud(I)triflaat tot gevolg. Die eerste enkelkristal X-straal kristallografiese analise van 'n tetrasool-afgeleide goud(I) karbeenkompleks, bis(1-bensiel-4-metieltetrasol-5-ilideen)goud(I)triflaat, bevestig dat alkilering wat lei tot karbeenvorming slegs op die nukleofiliese N^4 -heteroatoom plaasvind.

Ander goud(I) C-tetrasolielkomplekse wat berei is sluit in [1-(*tert*-butiel)tetrasol-5-iel](trifenielfosfien)goud(I) en [1-(sikloheksiel)tetrasol-5-iel](trifenielfosfien)goud(I). Neutrale en kationiese tetrasolilidien goud(I)komplekse, afgelei van gelitieceerde tetrasoolverbindings, nl. (pentafluorofeniel)(1-bensieltetrasol-5-ilideen)goud(I)- en (1-bensieltetrasol-5-ilideen)(trifenielfosfien)goud(I)triflaat, in ooreenstemming met soortgelyke imidasolielauraat- en imidasolilideenkomplekse, ondergaan homoleptiese herrangskikking in oplossing. Tydens die bereiding van (pentafluorofeniel)(1-bensieltetrasol-5-ilideen)goud(I) in die teenwoordigheid van ammoniumsoute, lei hierdie herrangskikking tot die isolering en struktuurkarakterisering van [bis(pentafluorofeniel)goud(I)][TMEDAMe].

Ten slotte, is twee nuwe en verwante koördinasiepolimere, [Li(CF₃SO₃)₂][TMEDAMe] en [Li(CF₃SO₃)(diëteleter)], waarin die gekoördineerde Li⁺-ione 'n belangrike rol in ligandkoppeling en die daarstelling van uitgebreide ('extended') strukture speel, geïsoleer en deur middel van molekulêre- en kristalstruktuurbeplating gekarakteriseer.

Joey

1945-04-04

2003-11-25

ACKNOWLEDGEMENTS

There are so many people and events that shapes one, and inspires you to attempt and complete goals, with this in mind there are a few people I would like to thank for making this a memorable decade.

This work is dedicated to both my parents; my late mother, whom has shown me that there is always a funnier and more colourful side to life, my dad for his enormous kind and warm heart that has inspired me in so many ways. Babbo, ti ringrazio per aivermi insegnato tutto quanto é necessario per il cammino della vita, la dedizione e l'amore. Questo lo dedico a te.

Elvi en Nello, vir julle liefde en ondersteuning.

Jakesy, dankie vir die mooiste twee jaar op Stellenbosch en dat jy my altyd herinner en laat uitsien na die mooi in die lewe.

Stephanie, for your important contribution to this study; all your advise, proof reading kindness and support. Prof Helgard Raubenheimer, for always demanding excellence. Dr Stefan Nogai, "My Don of crystal structure refinement" for your patient and meticulous care in X-ray data collections and refinements. I will not forget our *five month reign* of Sunday afternoon crystal structures, it made this work so much more pleasant to report. I will always cherish the conversations and friendship shared around good food and wine. Uli, you crazy Austrian!, for your kind proof reading through my scribble, your advise, friendship, a million smiles and many laughs. All the members of the Chemistry Department at Stellenbosch University for creating such a pleasant and enjoyable working environment. Elzet, vir jou vriendskap, die *peptalks*, en jou kliphard lag. Karolien, dit was lekker om saam met jou 'n kabouter te wees, dankie dat jy my geleer het om 'n grasiouse een te wees - *This one is for the little people !*. Gerrit, kollega dankie dat jy die standaard so hoog gestel het. Leon, meester en *vader van IUPAC*, ek sal ons koffiesessies en gesprekke altyd onthou en regtig mis, jou vriendskap die laaste agt jaar sal my altyd by bly.

Drs. Elma van der Lingen and Judy Caddy and colleagues in the AuTek Biomed. consortium, for a stimulating collaboration. Jean and Elsa for excellent NMR data collection, service and kindness. Mr Ward, thank you for the outstanding *service with a smile* the last three years, all the humorous conversations and for the time that we were champions on the golf course. Stefan Louw and Tommie van der Merwe for collection of

mass spectrometry data. Proff. Wim de Haen and Erick van der Eycken, at the Katolieke Universiteit Leuven, for the opportunity to complete part of this study in their laboratories.

For financial support, I would like to thank Harmony Gold (*via* Mintek) and Stellenbosch University.

Different aspects of the work in this study have been presented in the form of:

- A series of communications by the author within the Autek Biomed. Consortium, in the form of oral presentations and written reports at Mintek, Randburg, South Africa, 2003 to 2005.
- A lecture presented by the author at the Gold Workshop, April 2003, Arniston South Africa, titled “Gold usage in Medicine: Gold(I) complexes derived from biologically active azoles”.
- A lecture presented by Dr. Ulrike Horvath at the 37th National Convention of the South African Chemical Society (SACI), 4 to 9th July 2004, Pretoria, South Africa, titled “Mono- and binuclear gold(I) compounds of purine derivatives”.
- A series of lectures presented by Prof. Helgard Raubenheimer at various European Universities, July to December 2004.
- A lecture presented by the author at the South African Chemical Institute (SACI) - Young Chemists meeting (Western Cape section), 5th July 2005, Stellenbosch South Africa, titled “Unusual modifications to simple carbene complexes”.
- A lecture presented by Dr. Ulrike Horvath at “The Cape Organometallic Symposium, 22nd October 2005, Cape Town South Africa, titled “First steps towards new applications of gold in medicine”.
- A poster presentation by the author at the South African Chemical Society (SACI) conference on Inorganic Chemistry, June 2003, Pretoria, South Africa, entitled “Gold usage in medicine: Gold(I) coordinated to biologically active ligands”.
- A poster presentation by the author at the Cape Organometallic Symposium, October 2004, Cape Town, South Africa, entitled “Gold(I): A versatile coordination centre.”

“.....what is essential is invisible to the eye”
Antoine de Saint-Exupéry – *“Le Petit Prince”*

“Chi si ferma é perduto”
Nello Gabrielli – Benito Mussolini

CONTENTS

SUMMARY	iii
OPSOMMING	vi
ACKNOWLEDGMENTS	x
CONTENTS	viii
ABBREVIATIONS	xvi

CHAPTER 1

General Introduction

1.1	Nitrogen-containing compounds of gold(I)	1
1.1.1	Electronic considerations in bonding	1
1.1.2	Phosphine donor ligands in gold(I) complexes	2
1.1.3	Nitrogen donor ligands in gold(I) complexes	4
1.1.4	Carbon donor ligands in gold(I) complexes	5
1.1.5	Gold(I) complexes in cancer therapy	7
1.2	Research objectives and thesis outline	8

CHAPTER 2

Preparation and characterisation of gold(I) complexes derived from azolyphosphines, and their functionalisation to include other coordination modes

2.1	Introduction	11
2.2	Results and discussion	20
2.2.1	Tris-azoyl phosphines and their gold(I) complexes	21
2.2.2	Gold(I) complexes of diphenylphosphine C-,N-tetrazoyl- and imidazolyphosphines	38
2.2.3	Reactions involving azolyphosphine gold(I) complexes	49
2.2.3.1	Reactions with azolythium; reactions towards the preparation of monocarbene gold(I) complexes	50
2.2.3.2	Azolyphosphine complexes 3 and 5 as P,N-ligands-Reactions towards metallocyclic complexes	55
2.3	Conclusion	68
2.4	Experimental	70
2.4.1	General procedures and instruments	70

CHAPTER 3

Preparation and characterisation of neutral mono- and dinuclear gold(I) imine and amido complexes derived from simple nitrogen rich heterocycles

3.1	Introduction	81
3.2	Results and discussion	88
3.2.1	Mono- and dinuclear gold(I) imine complexes derived from imidazoles	89
3.2.2	Mono- and dinuclear gold(I) imine complexes derived from tetrazoles	98
3.2.3	Attempted synthesis of a dinuclear gold(I) imine complexes derived from bis(thiazole)	110
3.2.4	Neutral phosphine gold(I) amido complexes derived from tetrazoles	115
3.2.5	Attempted complexation reaction of gold(I) to pyridine and imidazole ligands containing C- and N-tetrazolyl substituents	118
3.3	Conclusion	124
3.4	Experimental	125
3.4.1	General procedures and instruments	125
3.4.2	Preparations and procedures	126

CHAPTER 4

Preparation and characterisation of novel gold(I) *N*-heterocyclic carbene (NHC) and acyclic carbene complexes, derived from lithiated and isocyanide precursors

4.1	Introduction	136
4.2	Results and discussion	147
4.2.1	Tetrazolylidene complexes of gold(I) derived from lithiated tetrazoles	147
4.2.2	Unexpected reactions observed in the attempted preparation of carbene complexes derived from lithiated tetrazoles	154

4.2.3	C-tetrazolyl and NHC-carbene complexes of gold(I) derived from isocyanide precursors	173
4.2.4	Acyclic nitrogen-rich carbene complexes of gold(I) derived from isocyanide precursors	185
4.3	Conclusion	195
4.4	Experimental	196
4.4.1	General procedures and instruments	196
4.4.2	Preparations and procedures	197

ADDENDUM 1

A1.1	Reactions of ligands IV, V, VIII, X and XI with gold(I) substrates	206
A1.1.1	Attempted synthesis of (pentafluorophenyl)gold(I) imine complexes	206
A1.1.2	Attempted synthesis of (phosphine)gold(I) amide complexes	207
A1.1.3	Attempted synthesis of cationic(phosphine)gold(I) imine complexes	208
A1.2	Experimental	209
A1.2.1	Preparations and procedures	209

ABBREVIATIONS

Å	Ångstrom (10^{-10} m)	
Bu	Butyl	
BzimPPh ₂	Benzylimidazolyl(diphenyl)phosphine	
Cy	Cyclohexyl	
DFT	Density functional theory	
diglyme	Diethylene glycol dimethyl ether	
DMF	<i>N,N'</i> -dimethylformamide	
DMSO	Dimethylsulfoxide	
dppe	(Diphenylphosphine)ethane	
Et	Ethyl	
Ebtz	1,2-di(tetrazol-2-yl)ethane	
FAB-MS	Fast atom bombardment mass spectrometry	
FT	Fourier Transform	
gHMQC	Gradient heteronuclear multiple quantum coherence	
Im	Imidazole	
ⁱ Pr	Isopropyl	
IR	Infrared	
M ⁺	Molecular ion	
M.p.	Melting point	
M _r	Molecular weight	
Mw	Microwave	
Me	Methyl	
<i>m/z</i>	Mass/charge	
NMR	Nuclear Magnetic Resonance	
NHC	N-heterocyclic carbene	
PPh ₃	Triphenylphosphine	
Ph	Phenyl	
ppm	Parts per million	
Py	Pyridyl	
pype	(Pyridylphosphine)ethane	
R	Alkyl, aryl or hydrogen group	
TMEDA	tetramethylenediamine	
^t Bu	Tertiary butyl	
thf	Tetrahydrofuran	
tht	Tetrahydrothiophene	
UV	Ultraviolet	
NMR	br	Broad
	d	Doublet
	dd	Doublet of doublets
	ddd	Doublet of doublet of doublet
	δ	Chemical shift (ppm)
	<i>J</i>	Coupling constant (Hz)
	m	Multiplet
	ppm	Parts per million
	q	Quartet
	s	Singlet
	t	Triplet

CHAPTER 1

General Introduction

1.1 Nitrogen-containing compounds of gold(I)

1.1.1 Electronic considerations in bonding

The vast array of compounds of gold(I) described in recent reviews^{1,2,3} serve as testimony to the versatility of the relatively soft metal centre to form stable complexes with a host of different organic ligands. This feature is elegantly displayed in the realm of numerous nitrogen-containing heterocyclic gold(I) complexes prepared and structurally characterised to date. These often multifunctional ligands, encompass a number of possible coordination modes which have on occasion translated into interesting inter- and intramolecular assemblies. In this regard structural analysis by single crystal X-ray diffraction has become a salient tool in understanding the stability of metal-ligand interactions, ligand preferences and ultimately an insight into the reactivity of the gold(I) centre.

Gold(I) has a closed shell $5d^{10}$ electron configuration and two-coordinated complexes can be obtained from predominantly soft donor ligands, although various examples exist where gold(I) complexes adapt three or four coordination. The most stable gold(I) complexes contain π -acceptor ligands, thus ligands capable of accepting back donation from the electron-rich metal centre. Both these attributes have been described as a consequence of relativistic effects which reaches a local maximum for gold.¹ Relativistic effects lead to a contraction of the $6s$ -orbitals, and an expansion of the $5d$ -orbitals affording a reduced energy separation between the valence shells of gold. Thus, the relative equivalency in s , p and d -orbital energies allows for the formation of stable two-coordinate complexes of gold(I) but furthermore, the $5d^{10}$ electrons are no longer chemically inert and readily participate in bonding, albeit in lesser bond contributions. Bonding between gold(I) centres of equal charges and with closed shell $5d^{10}$ electron configurations can now be better understood in the light of these considerations.⁴ It is well established that mononuclear gold complexes, which are not sterically hindered, participate in intermolecular aggregation *via* short gold-gold contacts, in the order of ca.

¹ M. C. Gimeno and A. Laguna, in *Comprehensive Coordination Chemistry II, Vol 6*, eds. J. A. McCleverty and T. J. Meyer, Elsevier Pergamon, Oxford, 2003, pp. 911, and references cited therein.

² P. Pyykkö, *Angew. Chem., Int. Ed., Engl.*, 2004, **43**, 4412.

³ H. Schmidbaur, *Chem. Soc. Rev.*, 1995, 391.

⁴ H. Schmidbaur, S. Cronje, B. Djordjevic and O. Schuster, *Chem. Phys.*, 2005, **311**, 151.

3.05 Å. These sub-van der Waals or aurophilic interactions are of comparable bond energy (5-10 kcal/mol) to hydrogen bonding and similarly play an important role in the stabilisation and organisation of crystalline gold compounds.² The extent of this stabilisation is best described in polyaurated molecules. Schmidbaur and co-workers⁵ illustrated that the normally low affinity that gold(I) has for nitrogen can be enhanced by the introduction of multiple gold(I) coordination to single nitrogen atom. Metallation of *tert*-butylamine proceeded less readily than subsequent auration of the nitrogen substrate. Within these cluster aggregates the synergistic Au(I)...Au(I) interactions lead to an overall stabilisation. Soft donor ligands as substituents L and X, in stereochemically not inhibited compound types, [LAuX], can contribute to the bond energies of these interactions.⁶ However, both steric effects in the solid state and solvation by solvent molecules in solution, prohibits the extrapolation of this observation to more complex molecules.⁷

A brief overview of the relevant donor ligand types described in gold(I) chemistry and encountered in our research are given here, with due emphasis on the unique reactivity displayed within nitrogen-rich heterocycles. Important concepts will be introduced to rationalise some of the unique behaviour in chemical reactions. In recent times, the application of gold(I) complexes in cancer therapy, has received increasing attention and due to the potential future relevance of our research in this regard, a brief discussion of the most important findings will be given here.

1.1.2 Phosphine donor ligands in gold(I) complexes

An overwhelming majority of gold(I) complexes described are those that contain phosphine donor ligands. This can partly be ascribed to the facile functionalisation of AuPPh₃-containing precursors to include other coordination modes. Although many complexes of the type [AuX(PR₃)] (where R = alkyl or aryl and X = halide, amide, thiolate, etc.) have been described, it was the predictable organisation in the crystal lattice of these complexes that captured the interest of many research groups.⁸ Many gold(I) phosphine complexes display inter- and intramolecular attractive interactions between gold(I) centres. The aurophilic interaction normally occurs perpendicular to the X-Au-PR₃ axis, and has been shown to organise molecular units in pairs, rings or chains. The constituents in dimeric units are often arranged parallel or approach one another in almost

⁵ A. Grohmann, J. Riede and H. Schmidbaur, *J. Chem. Soc., Dalton Trans.*, 1991, 783.

⁶ P. Pyykkö, J. Li and N. Runeberg, *Chem. Phys. Lett.*, 1994, **218**, 133.

⁷ F. Scherbaum, A. Grohmann, G. Müller and H. Schmidbaur, *Angew. Chem., Int. Ed. Engl.*, 1989, **28**, 463.

⁸ M. Jansen, *Angew. Chem., Int. Ed. Engl.*, 1987, **26**, 1098.

perpendicular fashion.^{9, 10} When utilising bi-, tri- or polydentate phosphine ligands, the various structural patterns that complexes can adopt as a result of Au...Au bonds become less predictable and more dependant on the coalescence of factors. For example, complex $[\mu\text{-}1,2\text{-bis}(\text{diphenylphosphine})\text{ethane}]_2[\text{chlorogold}(\text{I})]$, $\{[\text{AuPPh}_2\text{Cl}]_2\text{en}\}$, crystallise as dimeric units in the absence of dichloromethane, however in the presence of the solvent the complex aggregates in polymeric chains.^{11, 12}

The isolobal analogy that exists for $[\text{AuPR}_3]^+$ and H^+ due to similar frontal orbitals, has provided a means of understanding the structural similarities between different homo- and heteronuclear compounds with $[\text{AuPR}_3]^+$ fragments and those of the corresponding hydrogen derivatives.¹³ This analogy has especially found relevance in gold cluster chemistry and the hyperauration of various centres.¹⁴ Another peculiarity of many gold complexes that contain short Au...Au separations is the visible luminescence observed under UV excitation. This feature has either been ascribed to metal-centred p_z - d_{σ} phosphorescence *via* intermetallic interactions or to ligand-centred or ligand-metal charge transfer absorption modes.¹⁵

In order to initiate, to a certain degree, intramolecular aurophilic interactions within dinuclear complexes, certain bridging diphosphine ligands are specifically tailored to position gold centres in close proximity. Apart from many interesting homobridged diauracycles with similar bridging ligands, a few heterobridged species have also been prepared.^{16, 17} The facile preparation of dinuclear gold(I) complexes that contain apart from phosphines, dithiolates, bis(yldes), dithiocarbamates and other bridging ligands also triggered the preparation of the first isolable gold(II) complexes, as well as contributing greatly to the vast number of gold(II) complexes described to date.¹⁸ Dinuclear complexes with multifunctional ligands that contain apart from phosphorus also nitrogen donor ligands, are especially equipped to afford complexes with short intramolecular metal-

⁹ H. Schmidbaur, G. Weidenhiller, A. M. Aly, O. Steigelmann and G. Müller, *Chem. Ber.*, 1990, **123**, 285.

¹⁰ D. B. Dyson, R. V. Parish, C.A. McAuliffe, R. G. Prichard, R. Fields and B. Beagley, *J. Chem. Soc., Dalton Trans.*, 1989, 907.

¹¹ P. M. V. Calcar, M. M. Olmstead and A. L. Balch, *J. Chem. Soc., Chem. Commun.*, 1995, 1773.

¹² H. Schmidbaur, P. Bissinger, J. Lachmann and O. Steigelmann, *Z. Naturforsch., Teil B.*, 1992, **47**, 1711.

¹³ J. W. Lauher and K. Wald, *J. Am. Chem. Soc.*, 1981, **103**, 7648.

¹⁴ M. I. Bruce, P. E. Corbin, P. A. Humphrey, G. A. Koutsantonis, M. J. Lidell and E. R. T Tiekink, *J. Chem. Soc., Chem. Commun.*, 1990, 674.

¹⁵ Z. Assefa, B. G. McBurnett, R. J. Staples, J. P. Fackler, Jr, B. Assmann, K. Angermaier and H. Schmidbaur, *Inorg. Chem.*, 1995, **34**, 75.

¹⁶ M. Badají, A. Laguna and M. Laguna, *J. Chem. Soc., Dalton Trans.*, 1995, 1255.

¹⁷ M. A. Bennet, D. R. Hockless, A. D. Rae, L. L. Welling and A. C. Willis, *Organometallics*, 2001, **20**, 79.

¹⁸ A. Laguna, *Coord. Chem. Rev.*, 1999, **193**, 837.

metal interaction. It is thus surprising that only a few gold(I) complexes have been described with bridging phosphine-nitrogen donor ligands.¹⁹ Especially considering the fact that phosphine ligands with azolyl functionalities have found both application in catalysis and medicine (also see 1.1.5).^{20,21} However, gold(I) complexes derived from phosphines containing natural azoles, such as imidazoles and in particular thiazoles and tetrazoles, remain largely unexplored. Probing both these ligand functionalities, of different donor strengths simultaneously in a single ligand system, should provide an insight into the reactivity of the gold(I) centre.

1.1.3 Nitrogen donor ligands in gold(I) complexes

In contrast to the chemistry of gold(I) phosphines, gold(I) complexes with nitrogen donor ligands have received limited attention, due in part to the instability of these complexes. Sadler and co-workers²² were the first to structurally characterise a gold(I) complex coordinated to two nitrogen donor-ligands. The sodium salt of bis(1-methylimidazolidine-2,4-dionato)gold(I) tetrahydrate, was isolated in moderate yields and is stable for only a limited period in solution. During the same period the isolation and crystal structure of a mono-substituted gold(I) complex derived from a nitrogen donor ligand, piperidine was also reported.²³ The incompatibility of the soft gold(I) metal centre and predominantly hard nitrogen donor ligand was not only being questioned but interesting intermolecular interactions that are displayed in order to stabilise these unstable compounds were revealed. It is thus not surprising that a large number of amine complexes derived from aliphatic and aromatic amines, azoles and others, described in literature, are those stabilised by phosphine ligands. In the organisation of these complexes in the crystalline state, conventional geometries are often compromised in order to afford such stability. Secondary stabilisation may be provided by comparable intermolecular bonding, i.e. aurophilic interactions of gold centres or hydrogen bonding in the presence of N-H groups. This is elegantly illustrated for compounds of the type, [AuCIL], where L = dicyclohexylamine, piperidine and pyridine groups, which show the aggregation of the complexes as dimers, associated by Au...Au contacts and N-H...Cl hydrogen bonds.²⁴

¹⁹ A. Burini, B. R. Pietroni, R. Galassi, G. Valle and S. Calogero, *Inorg. Chim. Acta*, 1995, **229**, 299.

²⁰ F. Favre, H. Olivier-Bourbigou, D. Commereuc and L. Saussine, *Chem. Commun.*, 2001, 1360.

²¹ M. J. Mckeage, S. J. Berners-Price, P. Galettis, R. J. Bowen, W. Brouwer, L. Ding, L. Zhuang and B. C. Baguley, *Cancer Chemother. Pharmacol.*, 2000, **46**, 343.

²² N. A. Malik, P. J. Sadler, D. Neidle and G. L. Taylor, *J. Chem. Soc., Chem. Commun.*, 1978, 711.

²³ J. J. Guy, P. G. Jones, M. J. Mays and G. M. Sheldrick, *J. Chem. Soc., Dalton Trans.*, 1977, 8.

²⁴ E. M. Barranco, O. Crespo, M. C. Gimeno, P. G. Jones, A. Laguna and M. D. Villacampa, *J. Organomet. Chem.*, 1999, **592**, 258.

Often, these complexes rearrange in solution to yield ionic homoleptic gold(I) complexes of the type $[\text{AuCIL}_2]$.²⁵

The seminal contribution of Mingos and co-workers^{26,27} in the preparations of stable forms of $[\text{Au}(\text{NCPH})_2]_2^+$ and $\text{Au}(\text{NH}_3)_2^+$ compounds, have elevated this unexplored chemistry into the domain of other coordination possibilities. Ironically, it was the lability of these gold complexes that provided their application as synthons for the synthesis of a wide range of gold(I) amines and as starting material for the preparation of other organometallic gold(I) complexes. It is now possible by substitution of the labile ligand in the $[\text{Au}(\text{NCPH})_2]_2^+$ cation, by nitrogen donor ligands such as pyridine (py), to obtain the corresponding gold(I) amine complex, $[\text{Au}(\text{py})_2]\text{BF}_4$, in high yields. In a similar fashion, $[\text{Au}_2(\text{dien})_2][\text{BF}_4]_2$ (dien = diethylenetriamine) and $[\text{Au}_2(\text{cyclam})_2][\text{BF}_4]_2$ (cyclam = 1,4,8,11-tetraazacyclotetradecane) are obtained.²⁸ The latter complex is especially interesting due to the fact that only a few examples are described where a Au(I) centre is encapsulated by cavity of a macrocyclic nitrogen donor ligand.²⁹ Finally, the related gold amines, $[\text{Au}(\text{NH}_2\text{R})_2]^+$ (R = H and Bu^t) provide efficient precursor molecules for the preparation of new organometallic complexes, $[\text{Au}(\text{C}\equiv\text{CR})(\text{NH}_3)]$ (R = Ph or Bu^t).³⁰

1.1.4 Carbon donor ligands in gold(I) complexes

Carbon-bonded derivatives of gold(I) were first isolated from isocyanide ligands.³¹ These ligands have mainly σ -donor ligands characterised with only minor π -acceptor contributions. Of the contributing resonance structures possible in gold(I) isocyanide complexes, the one form with the highest C-N bond order (ii, Scheme 1.1) depicts the bond situation most accurately. The same holds true for the related gold-carbene bond, which can be described by two major contributing resonance structures (iv and v).³² However, in recent times a significant π -donor contribution from the metal centre to especially carbenes derived from N-heterocycles (NHC ligands), have been indicated by quantum chemical calculation.³³

²⁵ B. Ahrens, P. G. Jones and A. K. Fischer, *Eur. J. Inorg. Chem.*, 1999, 1103.

²⁶ D. M. P. Mingos, J. Yau, S. M. Menzer and D. J. Williams, *J. Chem. Soc., Dalton Trans.*, 1995, 319.

²⁷ D. M. P. Mingos and J. Yau, *J. Organomet. Chem.*, 1994, **479**, C16.

²⁸ J. Yau, D. M. P. Mingos, S. M. Menzer and D. J. Williams, *J. Chem. Soc., Dalton Trans.*, 1995, 2575.

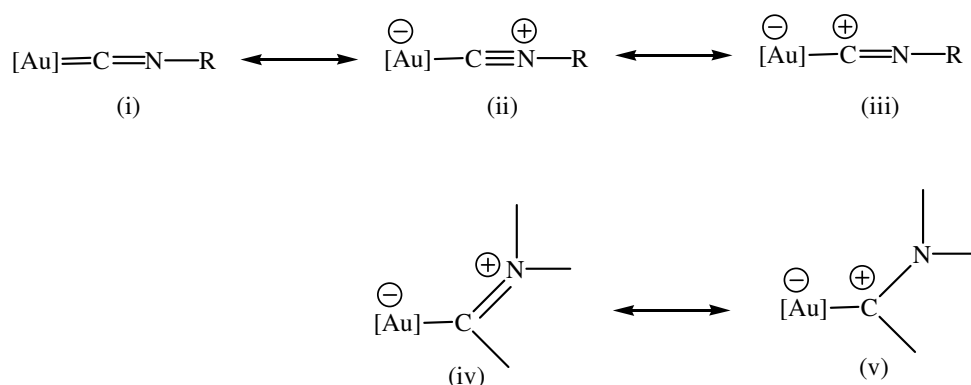
²⁹ J. Yau, D. M. P. Mingos and H. R. Powell, *Polyhedron*, 1996, **15**, 367.

³⁰ J. Yau and D. M. P. Mingos, *J. Chem. Soc., Dalton Trans.*, 1997, 1103.

³¹ A. Sacco and M. Freni, *Gazz. Chim. Ital.*, 1956, **86**, 195.

³² H. G. Raubenheimer and S. Cronje, in *Gold: Progress in Chemistry, Biochemistry and Technology*, ed. H. Schmidbaur, John Wiley & Sons Ltd., Chichester, 1999, pp. 558.

³³ G. Frenking, K. Wichmann, N. Fröhlich, C. Loschen, M. Lein, J. Frunzke and V. M. Rayon, *Coord. Chem. Rev.*, 2003, **238**, 55.



Scheme 1.1 The major contributing resonance structures possible in gold(I) isocyanide complexes.

Nonetheless, carbenes can be broadly defined as containing divalent carbon atoms, which are predominantly σ -bonded *via* an sp^2 orbital to only two other atoms. The two non-bonding electrons are intrinsically unstable and there are two main approaches to stabilise these electrons on the carbon atom. Firstly, as ligands to strong electron-withdrawing metal fragments – a method first introduced by Fischer and Maasbol³⁴ and secondly, within stable heterocyclic molecules. Öfele and Wanzlick^{35,36} independently reported on the remarkable stability of transition metals reacted with deprotonated imidazolium and pyrazolium salts. The stability in these compounds were first largely ascribed to the high electron densities on the heteroatoms flanking the carbene centre which repels nucleophiles that might otherwise react with the carbene carbon.³⁷ However, in the last decade both cyclic and acyclic carbenes, derived from both azoles and alternatives to azoles, have been described. Furthermore, the adjacent heteroatoms which at first appeared to be crucial for stabilisation in azoles can now be further removed from the metal-bonded carbon and even placed outside the coordination ring.^{38,39}

Gold(I) carbene complexes are accessible by a number of synthetic routes of which a few have been described in the last decade. The nucleophilic addition of alcohols and amines to isocyanide complexes of gold(I) was the first of these.⁴⁰ Many gold(I) carbene complexes derived from N-heterocyclic azoles are accessible by the reaction of lithiated azoles with gold(I) chloride precursor compounds, followed by alkylation or

³⁴ E. O. Fischer and M. A. Maasböl, *Angew. Chem. Int., Ed. Engl.*, 1964, **3**, 580.

³⁵ K. Öfele, *J. Organomet. Chem.*, 1968, **12**, 42.

³⁶ H. W. Wanzlick, H.J. Schönherr, *Angew. Chem.*, 1968, **80**, 154.

³⁷ D. Bourissou, O. Guerret, F. P. Gabbaï and G. Bertrand, *Chem. Rev.*, 2000, **100**, 39.

³⁸ M. Desmet, H. G. Raubenheimer and G. J. Kruger, *Organometallics*, 1997, **16**, 3324.

³⁹ W. H. Meyer, M. Deetlefs, M. Pohlmann, R. Scholtz, M. W. Esterhuysen, G. R. Julius, H. G. Raubenheimer, *Dalton*, 2004, 413.

⁴⁰ G. Minghetti, L. Baratto and F. Bonati, *J. Organomet. Chem.*, 1975, **102**, 397.

protonation.⁴¹ The use of silver(I) carbene complexes as transfer agents, has developed into a preferred method of obtaining numerous N-heterocyclic carbene (NHC) complexes of this metal.⁴²

1.1.5 Gold(I) complexes in cancer therapy

The most promising gold(I) complexes for application in medicine, and specifically as potential anti-tumour agents, have been of two classes of gold(I) phosphines: i) neutral, two-coordinate gold(I) complexes, e.g. (tetraacetylthioglucose)(trimethylphosphine) gold(I) (Auranofin) and ii) cationic tetrahedral bis-chelated gold(I) complexes related to $[\text{Au}(\text{dppe})_2]^+$ [dppe = (diphenylphosphine)ethane]. Both these groups of complexes display enormous potential to overcome the two overriding impediments in cancer chemotherapy, i.e. drug-resistant tumour cells and low-tumour selectivity of cancer drugs. The role that the mitochondria, and indeed mitochondrial membrane permeability, plays in the regulation of apoptosis (cell death) both in healthy cells in pathological states, has led to numerous attempts at targeting this cell constituent in the development of new cancer therapeutic agents.⁴³ Recent reports have shown that auranofin, at submicromolar concentrations, is able to induce mitochondrial membrane permeability depicted in membrane swelling and ultimate loss of membrane potential.⁴⁴ Berners-Price and co-workers⁴⁵ have shown by employing hydrophilic analogues of $[\text{Au}(\text{dppe})_2]^+$ that contain (pyridyl)phosphine ligands, that a greater differentiating cytotoxicity can be gained for tumour cells in relation to healthy cells. By the modification of lipophilicity of (pyridyl)phosphines in gold(I) complexes, cellular uptake, the binding to plasma proteins and degree of host toxicity can be tailored to effect an optimal anti-tumour activity.²¹ Recently, it was assessed whether the phosphine ligand in these anti-tumour agents is essential for cytotoxicity by evaluation of analogous cationic NHC complexes of gold(I) for similar activity. This approach exploits the established similarity that exists in the structural behaviour of these two types of ligand systems in gold(I) complexes. Mitochondrial dissipation assays conducted on isolated rat liver mitochondria, suggest a significant variation in the degree and rate by which these compounds enter the cell constituents and that direct relationship exist between the swelling of the mitochondria and gold uptake.⁴⁶

⁴¹ H. G. Raubenheimer and S. Cronje, *J. Organomet. Chem.*, 2001, **617**, 170

⁴² H. M. J. Wang and I. J. B. Lin, *Organometallics*, 1998, **17**, 972.

⁴³ K. M. Debatin, D. Poncet and G. Kroemer, *Oncogene*, 2002, **21**, 8786.

⁴⁴ M. P. Rigobello, G. Scutari, R. Boscolo and A. Bindoli, *Brit. J. Pharmacol.*, 2002, **136**, 1162.

⁴⁵ M. J. Mckeage, L. Maharaj and S. J. Berners-Price, *Coord. Chem. Rev.*, 2002, **232**, 127.

⁴⁶ P. J. Barnard, M. V. Baker, S. J. Berners-Price and D. A. Day, *J. Inorg. Biochem.*, 2004, **98**, 1642.

1.2 Research objectives and thesis outline

The aim of the research described in this dissertation is foremost the exploitation of numerous donor ligand possibilities to gold(I), present in various nitrogen rich heterocyclic ligands. The investigation was planned to be concerned with the preparation and structural characterisation of gold(I) complexes derived from predominantly strong bonded ligands, although in a broadened approach, the coordination to weaker bonding ligands could also be addressed.

As a point of departure, a comprehensive literature search of gold(I) complexes containing tetrazoles, revealed that very few examples have been described which contain a gold(I) centre directly linked to the ring. Available examples include C-bonded tetrazolyl gold(I) complexes of the type, $[\text{Au}(\text{RNC})(\text{RN}_4\text{C})]$ (R = methyl, cyclohexyl, phenyl) prepared by Fehlhammer and co-workers⁴⁷, and a few N¹-bonded tetrazolyl gold(I) complexes of the type, $[\text{Au}(\text{RN}_4\text{C})(\text{PPh}_3)]$ [R = CF₃, Ph, NH₂ and N(CH₃)₃ and H] reported by Kieft and co-workers.⁴⁸ The latter example, is also the only entry in the Cambridge Crystallographic database, of a structurally characterised tetrazolyl gold(I) complex. This is surprising if one considers the rich chemistry that exists for this ligand precursor-type in combinations with other metal centres. However, the susceptibility of the ring to undergo fragmentation reactions combined with the idea that tetrazoles are predominantly hard donor ligands, could in part be responsible for their unexplored application in gold(I) chemistry.

Our multi-pronged approach towards the novel coordination of tetrazole derivatives to gold is best illustrated as in Figure 1.1. Although tetrazole derivatives in various forms were intended as various ligands to gold(I), they remained a pivotal area in our investigations, many reactions involving other natural azoles such as imidazoles, thiazoles and triazoles could also be explored. Sites that present themselves for functionalisation included predominantly N¹, N⁴ and C⁵. Because tetrazoles are not readily available, the means to prepare these compounds in less hazardous ways than described in the literature had to be sought. One such investigation, described in **Chapter 3** explores the use of green-chemistry, in the form of microwave irradiation, to obtain such compounds.

⁴⁷ W. Beck, K. Burger and W. P. Fehlhammer, *Chem. Ber.* 1971, **104**, 1816.

⁴⁸ R. L. Kieft, W. M. Peterson, G. L. Blundell, S. Horton, R. A. Henry and H. B. Jonassen, *Inorg. Chem.*, 1976, **15**, 7.

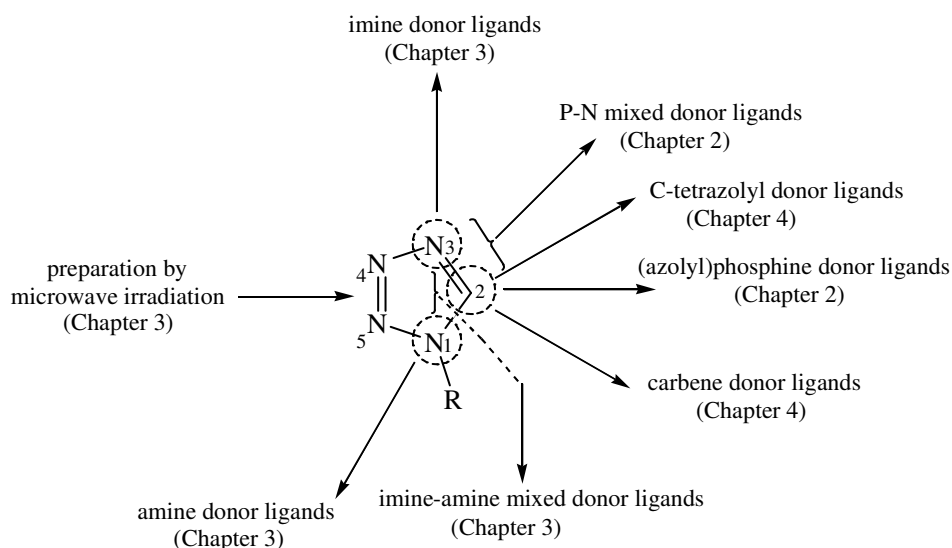


Figure 1.1 Gold(I) functionalisation of tetrazoles.

Thus, an exploration was undertaken which revisited a number of the conventional gold(I) coordination possibilities but with special emphasis towards the preparation of novel and stable gold(I) complexes derived from nitrogen-rich heterocycles. In **Chapter 2** attempts to contribute to the limited examples reported for gold(I) complexes containing (azolyl)phosphines are described. Apart from the predictable strong phosphine donor capabilities that should be present in these ligands, potential bi- and polytopic bonding possibilities could also be harnessed within these ligands. We addressed such possibilities by questioning whether gold(I) complexes that contain secondary donor ligands could in fact act as ligands towards other gold(I) centres. Understanding the stability of the metal-ligand interactions, ligand preference and ultimately gaining insight into the reactivity of the gold(I) centre are important goals of this work.

Neutral imines as donor ligands in gold(I), introduced in **Chapter 2** are then examined in **Chapter 3** but in a more simplistic manner by using simpler imidazole and thiazole substrates. Surprisingly, few examples of imine complexes exist. The developed methodology was then applied in the attempted preparation of the first tetrazolyl gold(I) imine complex. The outcome of imine donor-type reactions are related to the electron densities (derived from ^{15}N -NMR resonance and structural parameters) on the nitrogen atoms. The introduction of a multitude of different coordination modes in a single ligand is further explored in the attempted synthesis of binuclear gold(I) complexes containing gold-imine and gold-amide bonds. In **Chapter 4** the attempted synthesis of the first

tetrazolyl carbene complexes of gold(I) are described. The synthetic approaches followed in, utilise two classical methodologies.

Although each chapter is described individually, there are a few sub-themes that remain common to all three types of donor ligand systems, and these are emphasised throughout. Furthermore, by using X-ray diffraction methods, stabilising effects or geometric compromises that are often encountered in the crystal organisation of gold(I) complexes were carefully studied. This feature often translates in spontaneous self-assemblies, which have become quintessential to gold chemistry.

CHAPTER 2

Preparation and characterisation of gold(I) complexes derived from azolyphosphines, and their functionalisation to include other coordination modes.

Abstract

Tris(thiazol-2-yl)phosphine, **I**, tris(4-methylthiazol-2-yl)phosphine, **II**, tris(1-methylimidazole-2-yl) phosphine, **III**, reacted with [AuCl(tht)] (tht = tetrahydrothiophene) to afford chloro[tris(thiazol-2-yl)phosphine]gold(I), **1**, chloro[tris(4-methyl thiazol-2-yl)phosphine]gold(I), **2**, and chloro[tris(1-methylimidazol-2-yl)phosphine]gold(I), **3**. Single crystal X-ray crystallography reveals that **1**, **2** and **5** self-associate through aurophilic interactions into discrete dimeric molecules, with **1** appearing in two true polymorphic crystalline forms. An unusual coupling of the phosphorus atom in **1** to the proton in the 4-position on the thiazole ring *via* the sulphur atom, was confirmed by selective homonuclear proton decoupling as well as heteronuclear phosphorus decoupling. This distinctive C-P coupling pattern is not observed in the free tertiary phosphine **I**. The *in situ* formation of tertiary azole phosphines (1-benzyltetrazolyl-5-yl)diphenylphosphine, (1-benzylimidazole-2-yl)diphenylphosphine and (1-*H*-tetrazolyl)diphenylphosphine was followed by reaction with [AuCl(tht)] in producing chloro[(1-benzyltetrazolyl-5-yl)diphenyl]phosphinegold(I), **4**, chloro[(1-benzylimidazole-2-yl)diphenyl]phosphine gold(I), **5**, and chloro[(1-*H*-tetrazolyl)diphenyl]phosphinegold(I), **7**. Complex **4** spontaneously self-assembles in dichloromethane to form 1,2-digold(I)(1,1,2,2-tetraphenyl-diphosphine)chloride, **6**, representing the simplest dinuclear gold(I)bisphosphine bridged complex reported to date. These strongly bonded gold(I)phosphine complexes can be employed, in reactions with lithiated azoles followed by alkylation to afford for example (1-benzyl-4-methylimidazol-2-ylidene)tris(thiazolyl-2-yl)phosphinegold(I), **8**, or as secondary N-donor ligands towards the formation of metallocyclic complexes, **12-14**. A mixed Au(I)-Au(II) tetranuclear bicyclic complex, **14**, represents the first example of two gold(II) centres stabilised by a P,N-bridging ligand, through phosphinite and imine donor atoms.

2.1 Introduction

From the array of ligands used to stabilise transition metals in specific oxidation states and to achieve water-soluble coordination compounds, functionalised phosphines proved to be

the most effective and versatile class of ligands. Water-soluble phosphines, such as trisulfonated arylphosphines, $[P(m\text{-C}_6\text{H}_4\text{SO}_3\text{Na})_3]$, have found wide application in transition metal catalysis.¹ Alkylphosphines, containing hydrophilic moieties, e.g. tris(hydroxymethyl)phosphines, have facilitated the development of various organometallic compounds with potential use in homogeneous catalysis and biomedical application.² An overriding criterion in the development of new anti-tumour agents is the high degree of site-selectivity that is required for compounds to differentiate between healthy cells and fast proliferating cancer cells.

The most active research in medicinal gold chemistry involves the development of anti-tumour agents.³ One class of compounds that has attracted much attention is tetrahedral coordinated gold(I) complexes containing lipophilic phosphines.⁴ Gold(I) thiolates coupled to simple alkyl phosphines have found application in the treatment of rheumatoid arthritis.⁵ In recent times, the most promising new chrysotherapy agents have been anti-tumour compounds containing bidentate diphenylphosphines, such as $[\text{Au}(\text{dppe})_2]^+$ (Figure 2.1). The lipophilic-cationic character of these compounds allows for the distribution in mitochondria and showed preferential cytotoxicity to carcinoma cells with hyperpolarised membranes.⁶

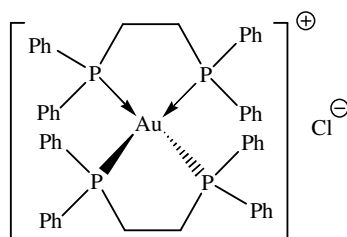


Figure 2.1 $[\text{Au}(\text{dppe})_2]\text{Cl}$

However due to the marked lipophilicity and subsequent non-selective targeting of mitochondria in all cells, including healthy hepatocytes, pre-clinical development of $[\text{Au}(\text{dppe})_2]^+$ was abandoned.⁷ Berners-Price and co-workers⁸ adopted an alternative

¹ W. A. Hermann and C. W. Kohlpainter, *Angew. Chem., Int. Ed., Engl.*, 1993, **32**, 1524.

² K. V. Katti, H. Gali, C. J. Smith and D. E. Berning, *Acc. Chem. Res.*, 1999, **32**, 9.

³ E. R. T. Tiekink, *Gold Bull.*, 2003, **36/4**, 117.

⁴ S. J. Berners-Price, G. R. Girard, D. T. Hill, B. M. Sutton, P. S. Jarrett, L. F. Faucette, R. K. Johnson, C. K. Mirabelli and P. J. Sadler, *J. Med. Chem.*, 1990, **33**, 1386.

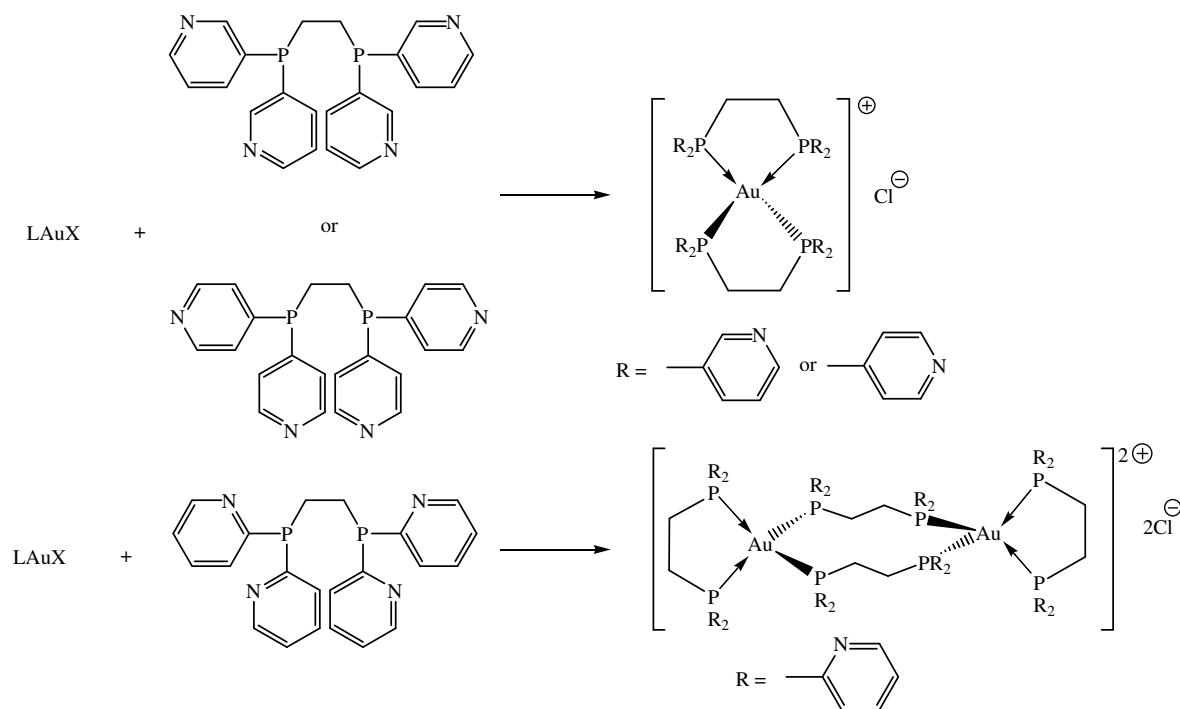
⁵ R. J. Puddephatt, in (eds. G. Wilkinson, F. G. A. Stone and E. W. Abel): *Comprehensive Organometallic Chemistry*, pp. 775 ff., Pergamon, Oxford, 1982.

⁶ S. J. Berners-Price, R. K. Johnson, A. J. Giovenella, L. F. Faucette, C. K. Mirabelli and P. J. Sadler, *J. Inorg. Biochem.*, 1988, **33**, 285.

⁷ M. J. Mckeage, L. Maharaj and S. J. Berners-Price, *Coord. Chem. Rev.*, 2002, **232**, 127.

⁸ S. J. Berners-Price, R. J. Bowen, P. Galettis, P. C. Healy and M. J. Mckeage, *Coord. Chem. Rev.*, 1999, **185-186**, 823.

approach of modifying the diphosphine ligand, in order to alter the hydrophilic character of the complexes and achieve greater selectivity for tumour cells versus normal cells. This was achieved by substitution of phenyl rings in the ligand (dppe), with hydrophilic pyridyl groups, which allowed for the retention of aromatic character without the loss of lipophilicity (Scheme 2.1).



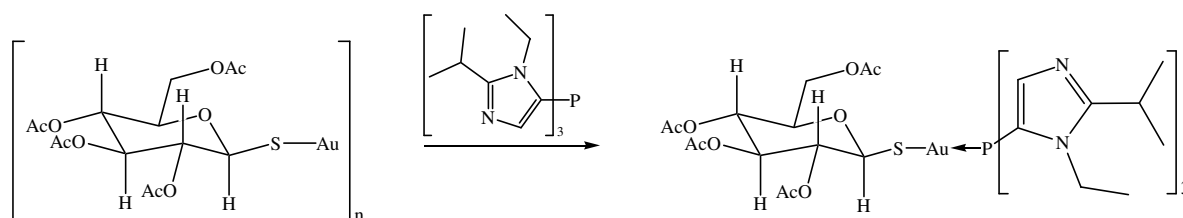
Scheme 2.1 The synthetic route to various bidentate pyridylphosphine gold(I) complexes.

Water solubility of gold(I) bidentate pyridylphosphine complexes exceed their phenyl analogues, and could be related to the position of the N atom on the pyridyl ring. Complexes of d3pype [where d3pype is 1,2-bis(di-3-pyridylphosphine)ethane] and d4pype as monomeric $[\text{Au}(\text{d3pype})_2]^+$ and $[\text{Au}(\text{d4pype})_2]^+$ species, revealed greater hydrophilicity compared to complexes of d2pype which exist in solution as equilibrium mixtures of monomeric, dimeric and tetrameric gold(I) clusters.⁸ It is notable that no evidence for the coordination of the pyridyl-N atoms to gold(I) centres in either the solid state or in solution was found. Alcock and co-workers⁹ have found that 2-pyridylphosphines coordinate as bidentate P,N-ligands, however only in instances where chloro/phosphorus coordination is not sufficient for coordinative stability.

⁹ N. W. Alcock, P. Moore, P. A. Lampe and K. F. Mok, *J. Chem. Soc., Dalton Trans.*, 1982, 207.

Schmidbaur and co-workers¹⁰ proposed that in bifunctional ligands, which contains two different donor atoms, gold(I) would coordinate to the donor site of greater donor strength, or the site which would effect the greater *trans*-influence on the substituent in the *trans*-position. For example, 2-pyridylphosphine will bind in a monodentate fashion through the phosphine atom to a gold(I) centre, due to the greater donor strength and *trans*-influence that the phosphine effects compared to the nitrogen atom.

Bell and co-workers¹¹ targeted the hydrophobic trialkylphosphine as the site of modification for the clinically applied chrysotherapeutic agent, triethylphosphinegold(I)*O*-acetylthioglucose or Auranofin. This group envisaged a substitution with a more hydrophilic tris(isopropylimidazole-5-yl)phosphine, which would lead to a more favourable distribution profile of the compound in biological systems (Equation 2.1).



Equation 2.1

Recent reports that lipophilic cations can find application as new classes of highly selective antitumour drugs, have stimulated the utilisation of gold(I)-halides, containing interesting phosphines, in transmetallation reactions with lithiated heterocycles (e.g. thiazole or imidazole).¹² This furnishes a unique class of cationic gold(I) complexes that contain both strongly bonded ligands, and which are derived from biologically active substrates.

Wu and Kurtz¹³ were the first to illustrate examples of tris(imidazolyl-2-yl)phosphines as tridentate capping ligands to hard metal centres such as Fe(III) and Mn(III). Apart from the N-donor capabilities of imidazoles to hard metal centres, coordination to softer metal centres such as gold(I) has received limited attention.¹⁴ Imidazolylphosphine ligands, in principle, should bind to both “soft” and “hard” metals simultaneously. Burini and co-

¹⁰ H. Schmidbaur and Y. Inoguchi, *Z. Naturforsch.*, 1980, **B35**, 1329.

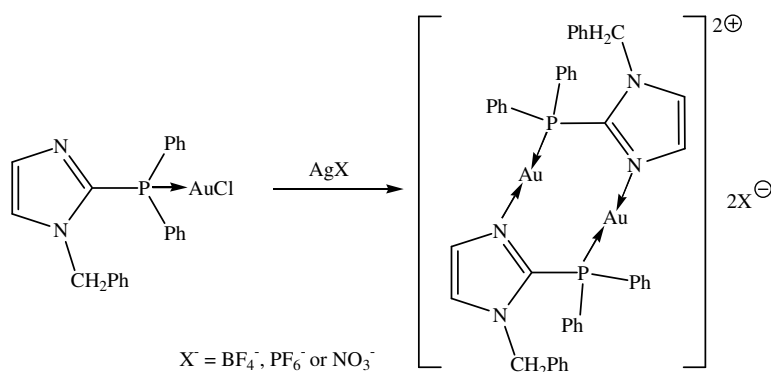
¹¹ R. A. Bell, C. J. L. Lock, C. Scholten and J. F. Valliant, *Inorg. Chim. Acta.*, 1998, **274**, 137.

¹² P. J. Barnard, M. V. Baker, S. J. Berners-Price and D. A. Day, *J. Inorg. Biochem.*, 2004, **98**, 1642.

¹³ F. Wu, D. M. Kurtz, Jr., K. S. Hagen, P. D. Nyman, P.G. Debrunner and V.A. Vankai, *Inorg. Chem.*, 1990, **29**, 5174.

¹⁴ S. Cronje, H. G. Raubenheimer, H. S. C. Spies, C. Esterhuysen, H. Schmidbaur, A. Schier and G. J. Kruger, *Dalton Trans.*, 2003, **14**, 2859.

workers¹⁵ illustrated this notion elegantly in the preparation of cationic gold(I) and silver(I) derivatives with bridging phosphines, containing imidazole rings such as 1-benzylimidazolyl(diphenyl)phosphine (BzimPPh₂) (Equation 2.2). In the study, dechlorination by various silver salts of chloro[(1-benzyl-2-imidazolyl)diphenylphosphine]gold(I), afforded P,N_{imine} coordinated products as dinuclear species. Other examples where phosphorus-imine mixed-donor ligands have been employed as bridging ligands, include pyridyl(diphenyl)phosphine (PyPPh₂) and pyridyl(dimethyl)phosphine (PyPMe₂).^{16,17,18}



Equation 2.2

The significance of employing short-bite P,N-ligands, is that gold(I) centres are brought in close proximity. In the crystalline state, gold(I) complexes show a pronounced partiality to self-associate *via* attractive aurophilic interactions. These metal interactions occur between closed shell, two coordinate gold(I) complexes when spatial separations are less than 3.6 Å.¹⁹ These weak bonding interactions are comparable to hydrogen bonding (*ca.* 29-46 kJ mol⁻¹ per Au...Au at a distance of 3.0 ± 0.2 Å) and often dictates the solid-state structures of gold complexes.^{20, 21}

Double-bridged complexes of gold(II) represent a rich chemistry, and are readily derived from dinuclear gold(I) precursor molecules, that by oxidative addition of halogens or pseudohalogens produce the corresponding dinuclear gold(II) halides (Scheme 2.2). The bridge moiety is important in holding the metal centres in close proximity, and hence the

¹⁵ A. Burini, B. R. Pietroni, R. Galassi, G. Valle and S. Calogero, *Inorg. Chim. Acta*, 1995, **229**, 299.

¹⁶ K. H. Leung, D. L. Phillips, M. Tse, C. Che and V. M. Miskowski, *J. Am. Chem. Soc.*, 1999, **121**, 4799.

¹⁷ L. M. Spencer, R. Altwer, P. Wei, L. Gelmini, J. Gauld and D. W. Stephan, *Organometallics*, 2003, **22**, 3841.

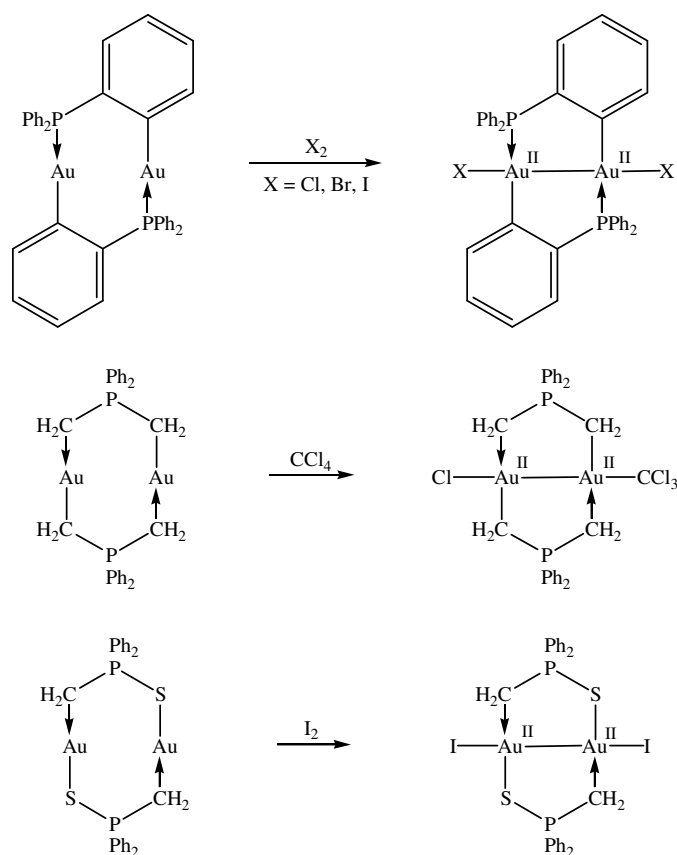
¹⁸ Y. Inoguchi, B. Milewski-Mahria and H. Schmidbaur, *Chem. Ber.*, 1982, **115**, 3085.

¹⁹ P. Pyykkö, *Angew. Chem., Int. Ed., Engl.*, 2004, **43**, 4412.

²⁰ H. Schmidbaur, W. Graf and G. Müller, *Angew. Chem., Int. Ed., Engl.*, 1988, **27**, 417.

²¹ C. Hollatz, A. Schier and H. Schmidbaur, *J. Am. Chem. Soc.*, 1997, **119**, 8115.

stabilisation in this oxidation state. Chelating ligands include organophosphines, ylides, organothiolates and others.²²



Scheme 2.2 Double-bridged complexes of gold(II) derived from chelating ligands. We assume that the deprotonated ylid reacts on one CH₂-unit as a carbanion and on the other by sharing one electron.

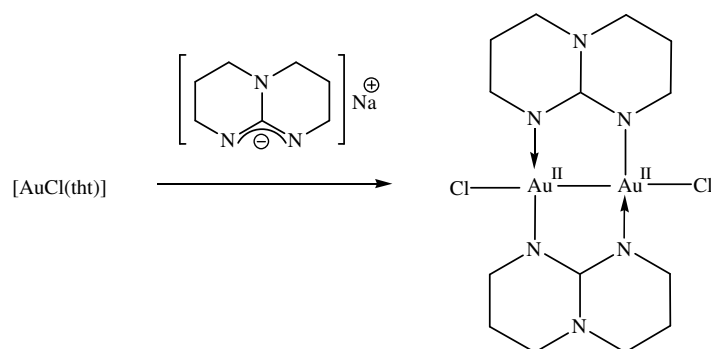
Not only are gold(II) complexes of nitrogen rare, but as a matter of future interest, dinuclear aurocycles containing phosphinite and imine bridging donor ligands have not been reported to date. Gold(I) complexes containing phosphinite [R₂PO]⁻ and diorgano phosphite [(RO)₂PO]⁻ anions appear exclusively as P-coordinated products, as are found in compound types, [R₂(O)P-Au-P(O)R₂]⁻, [R₃P-Au-P(O)R₂], [R₃P-Au-P(O)(OR)₂], [(R₂PO)Au]₃ and [R₂(O)P-Au-P(OH)R₂]₂.²³

Irwin and co-workers²⁴ have recently reported on the spontaneous formation of dinuclear gold(II) complexes, bridged by a guanidinate-type ligand, with a Au...Au separation of 2.47 Å, the shortest Au-Au bond to date (Equation 2.3). The dinuclear gold(I) amidinate complex that initially forms undergoes a self-redox reaction to form the gold(II) product from metallic gold.

²² A. Laguna and M. Laguna, *Coord. Chem. Rev.*, 1999, **193-195**, 837.

²³ C. Hollatz, A. Schier and H. Schmidbauer, *Inorg. Chem. Commun.*, 1998, **1**, 115 and reference cited therein.

²⁴ M. D. Irwin, H. E. Abdou, A. A. Mohamed and J. P. Fackler, Jr., *Chem. Commun.*, 2003, 2882.



Equation 2.3

When this reaction was repeated using dichloromethane as solvent, which can act as oxidant, higher yields of the gold(II) complex was obtained, supporting the belief that the type of ligand, could support the formation of metal-metal bonded Au(II)-Au(II) products.²⁵ It was further claimed that in dinuclear gold(I) complexes, reactive neighbouring metal centres and coordinated ligands can influence the oxidation of the metal centre. Electron-rich anionic complexes containing strongly donating ligands, would propagate this oxidative process. Fackler²⁶ proposed that the first step, an oxidative addition, proceeds by a nucleophilic attack of a gold(I) centre on the oxidant, simultaneous formation of a metal-metal bond, and then a nucleophilic attack by the remnant of the oxidant on the other gold centre.

Our two-pronged approach to the preparation of novel gold(I) complexes described in this chapter, involves bifunctional ligands containing biologically active heterocyclic rings, such as imidazoles, thiazoles and tetrazoles. These complexes could act as pro-drugs, thus designed to contain a labile ligand (which allows for ligand exchange reactions during *in vivo* transport) and a more strongly bonded ligand which allows for gold(I) as well as the biological functionality to enter cells. The employment of heterocyclic azole derivatives as substituents on tertiary phosphines further explores a possible synergism that could exist in one molecule containing two individually known biologically active functionalities. An important attribute of bifunctional nitrogen-rich ligands is that it lends itself to further application as ambidentate ligands.

The synthesis of tri-substituted heterocyclic tertiary phosphines, from lithiated azoles such as 2-lithiated-imidazole and -thiazoles is a well studied procedure.²⁷ However, limited attention has been given to gold(I) complexes that can be derived thereof, by simple ligand

²⁵ H. E. Abdou, A. A. Mohamed and J. P. Fackler, Jr., *Inorg. Chem.*, 2005, **44**, 166.

²⁶ J. P. Fackler, Jr., *Polyhedron*, 1997, **16**, 1.

²⁷ S. S. Moore and G. M. Whiteside, *J. Org. Chem.*, 1982, **47**, 1489.

substitution. With regards to the advent of supramolecular chemistry, and interesting self associations of gold complexes, the X-ray crystallographic characterisation of gold(I) complexes containing tri-substituted azoles, are an area of research that has been neglected.

A similar methodology can be employed to prepare other azole derived phosphines. Tetrazoles, have a rich history in biological applications, and act as bioequivalents to carboxylic acids.²⁸ Substituted tetrazoles, are versatile heterocycles that can be used in various coordination modes with metals. However tetrazole derivatives of gold(I) are limited to a few reports in literature. Nomiya and co-workers²⁹ have reported the synthesis and pharmaceutical activity of tetrazole-amido gold(I) complexes. The latter compound represents the only entry in the Cambridge Crystallographic Database of a gold(I) centre directly bonded to a tetrazole ring. Wehlan and co-workers³⁰ have isolated gold(III) carbene complexes of tetrazoles. Cationic and neutral mono and biscarbene gold(I) complexes of tetrazoles are discussed in Chapter 4 in this dissertation. Substituted tetrazoles can also act as soft-donor imine ligands to gold(I) complexes, illustrated herein for the first time (Chapter 3 in this dissertation).

Scheme 2.3, shows our approach to the preparation of various gold(I) complexes. The results described in this chapter firstly focus on the preparation, spectral characterisation and physical properties of mainly simple gold(I) chlorides (**i** and **ii**) that contain (predominantly water-soluble) phosphines derived from biologically active N-heterocyclic compounds (e.g. imidazole, thiazole and tetrazoles). Interesting, structural features were elucidated with analysis, in this investigation and will be discussed.

Secondly, the facile derivatisation of gold(I)phosphine halides should provide access to other coordination modes, such as strongly bonded N-heterocyclic carbene complexes (e.g. **iii** in Scheme 2.3). Bonati and co-workers³¹ reported that the treatment of lithiated 1-alkylimidazoles with [AuCl(PPh₃)] at room temperature resulted in the formation of a stable trimeric N-,C-imidazolato complex. In a related study from our laboratory an attempted preparation of various mono(carbene) complexes by the transmetallation

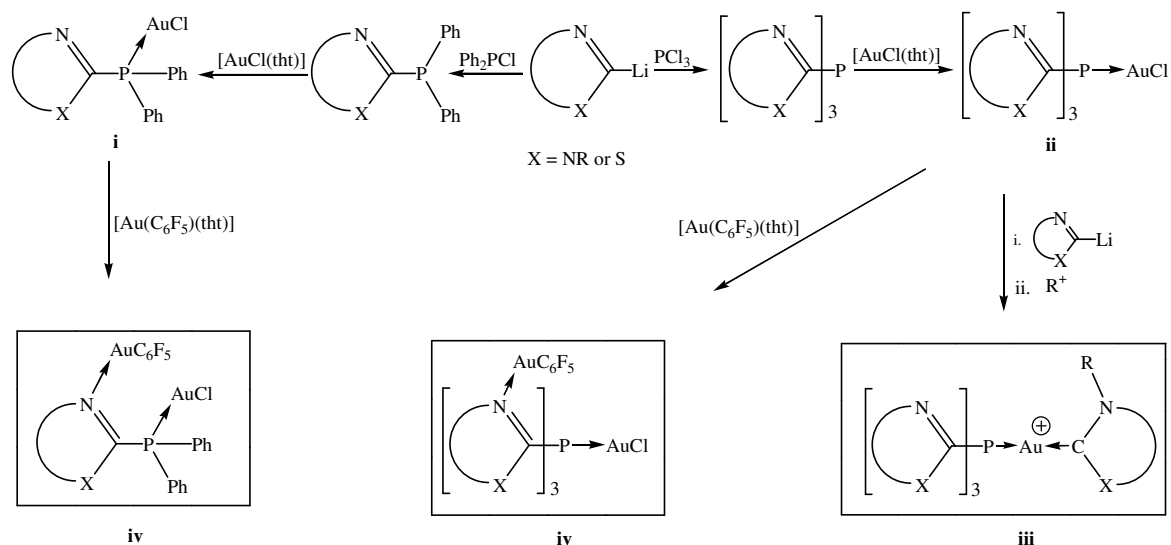
²⁸ S. Colarusso, B. Gerlach, U. Koch, E. Muraglia, I. Conte, I. Stansfield, V. G. Matassa and F. Narjes, *Bioorg. Med. Chem. Lett.*, 2002, **12**, 705.

²⁹ K. Nomiya, R. Noguchi and M. Oda, *Inorg. Chim. Acta.*, 2000, **298(1)**, 24.

³⁰ M. Wehlan, R. Thiel, J. Fuchs, W. Beck and W. P. Fehlhammer, *J. Organomet. Chem.*, 2000, 159.

³¹ F. Bonati, A. Burini and B. P. Pietroni, *J. Organomet. Chem.*, 1989, **375**, 147.

reaction of lithiated azoles with $[\text{AuCl}(\text{PPh}_3)]$, followed by protonation or alkylation of the aurate complexes has been reported.³²



Scheme 2.3 A general outline of the proposed preparation of gold(I) halides derived from biologically relevant azoles and subsequent further derivitisation.

Upon treatment of lithium 1-methylimidazol-2-yl with phosphine halides of gold(I) at -70 °C, the neutral azolyl complexes are formed. Alkylation and protonation of these compounds yield bis(carbene) complexes due to homoleptic rearrangements of cationic azolyl precursor gold(I) complexes. To further complement that study, we now investigated whether phosphine halides of gold(I), containing potentially stronger binding azolylphosphines, react similarly with lithiated azoles in forming gold(I) carbene complexes (**iii**).

Thirdly, tertiary phosphines that contain imidazole substituents, such as BzimPPh_2 , have proved to be very effective in bridging two gold centres, and arranging them in close separation. However, these examples only include cationic bi-aurocyclic complexes stabilized by symmetrical bidentate P,N ligands.¹⁵ The question arises whether similar mono-cyclic gold(I) complexes could be obtained by exploiting the same P,N-donor capability of the ligand (**iv** and **v**). This would require employing the imidazolyl phosphine gold(I) halide in the role of a ligand in secondary imine-coordination. The concept of using gold complexes as ligands for further gold coordination were best illustrated in the seminal report by Schmidbaur and co-workers on the hypercoordination

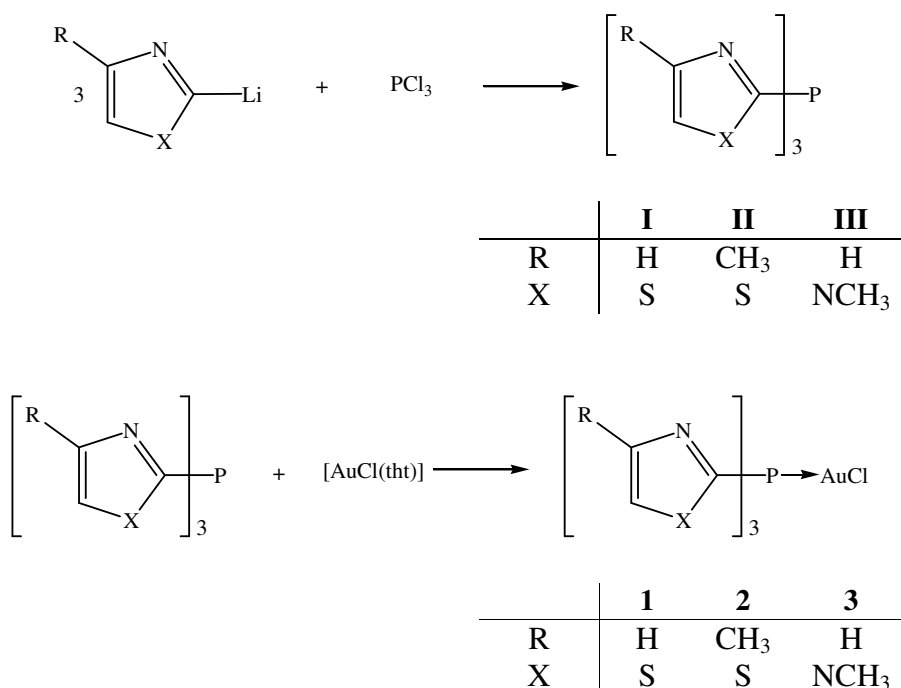
³² H.G. Raubenheimer, L. Lindeque and S. Cronje, *J. Organomet. Chem.*, 1996, **511**, 177.

of nitrogen, in which the reaction of $[\text{N}(\text{AuPPh}_3)_4]^+$ with AuPPh_3^+ afforded $[\text{N}(\text{AuPPh}_3)_5]^{2+}$.³³

Finally, the well documented affinity of gold to self-associate has often provided unexpected and novel results. We report here two examples that illustrates a self assembly that favours gold-gold interactions, firstly of a simple di(phosphinehalide)digold complex, and secondly the formation of a gold(II) compound stabilized by a novel bridging ligand.

2.2 Results and discussion

In Section 2.2.1 and 2.2.2 the general preparative route towards tertiary phosphines derived from natural azoles (e.g. thiazole, imidazoles and tetrazole) and their respective novel gold(I) complexes (Scheme 2.4) will be reported. Spectral characterisation, including NMR spectra and X-ray structure analysis, unearthed interesting phenomena and will be highlighted.



Scheme 2.4 Synthesis of tertiary azolyl phosphines, **I-III** and gold(I)-phosphine chlorides, **1-3**.

³³ A. Grohmann, J. Riede and H. Schmidbaur, *Nature*, 1990, **345**, 140.

2.2.1 Tris-azolyl phosphines and their gold(I) complexes

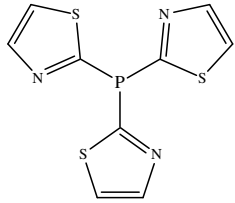
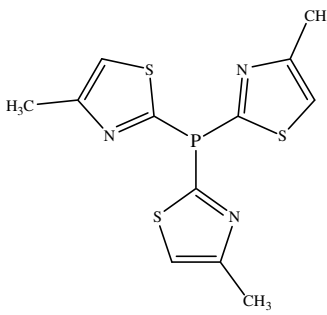
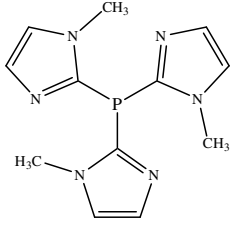
A. Preparation of tris(thiazol-2-yl)phosphine, **I**, tris(4-methylthiazol-2-yl)phosphine, **II**, tris(1-methylimidazol-2-yl)phosphine, **III**, chloro[tris(thiazol-2-yl)phosphine]gold(I), **1**, chloro[tris(4-methylthiazol-2-yl)phosphine]gold(I), **2**, chloro[tris(1-methylimidazol-2-yl)phosphine]gold(I), **3**.

The most general method towards the preparation of heterocyclic-substituted phosphines involves the nucleophilic displacement of halides on a phosphorus trihalide by an organometallic reagent.³⁴ The later is prepared either by metal-halogen exchange between for example 2-bromothiazole and *n*-butyllithium (in diethyl ether, -78 °C) or by the direct lithiation of the chosen thiazole by *n*-butyllithium at (-60 °C). The addition of freshly distilled PCl₃ in diethyl ether to the solution of the 2-lithiothiazole at -60 °C, followed by stirring for several hours, and quenching with aqueous NH₄Cl, afforded in our case tris(thiazol-2-yl)phosphine **I** and tris(4-methylthiazol-2-yl)phosphine **II** from the organic extract in acceptable yield (Scheme 2.2). This procedure could be further extended to the preparation of tris(1-methylimidazole-2-yl)phosphine **III**. However, it was found that during the two phase extraction with diethyl ether/water, the tris(1-methylimidazol-2-yl)phosphine was extracted into the aqueous rather than the organic phase. Sequential extraction of the separated water layer afforded the tertiary phosphine in modest yield (Scheme 2.2). Moore and Whiteside²⁷ reported an alternative strategy that was applied successfully to a range of heterocycles (benzothiazol-2-yl, 1-methylbenzimidazol-2-yl, thiazole-2-yl, 1-methylimidazol-2-yl), which involves the electrophilic cleavage of the C-Si bond of 2-(trimethylsilyl)-substituted heterocycles by various phosphorus halides (PCl₃, PhPCl₂, Ph₂PCl). We found with regards to the reaction of PCl₃ and silylated heterocycles, the procedure more laborious, but higher overall yields could be obtained using this method.

Recrystallisation of the free ligands **I** and **II** from methanol solution layered with *n*-hexane and **III** from toluene solution layered with *n*-hexane at -20 °C, was performed prior to the preparation of gold(I) complexes. All three phosphines are soluble in most organic solvents, with **III** particularly soluble in water. Analytical data for phosphines are summarised in Table 2.1.

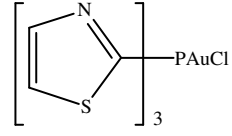
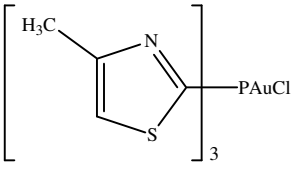
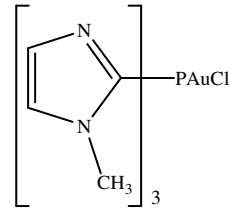
³⁴ W. E. Lynch, D. M. Kurtz, Jr., S. Wang and R. A. Scott, *J. Am. Chem. Soc.*, 1994, **116**, 11030.

Table 2.1 Analytical data for ligands **I-III**

Ligand			
	I	II	III
M.p.(°C)	95-96 (97-99) ²⁷	150-151	175-177
Colour	yellow	yellow	colourless
Yield(%)	35	28	70
<i>M_r</i>	282.95	324.99	274.11

A general method for obtaining gold(I) derivatives LAuCl, where L is a tertiary phosphine, consists of the use of [AuCl(tht)] as starting compound. By simple ligand substitution of the labile ligand by phosphines **I-III**, complexes **1-3** could readily be obtained. Final purification of complexes **1-3** was achieved by crystallisation from dichloromethane solution layered with diethyl ether at -20 °C. All the complexes are moisture and air stable. Analytical data for complexes **1-3** are summarised in Table 2.2.

Table 2.2 Analytical data for complexes **1-3**

Complex			
	1	2	3
M.p(°C)	131 (decomp.)	121 (decomp.)	155 (decomp.)
Colour	colourless	colourless	colourless
Yield(%)	90	93	89
<i>M_r</i>	514.88	556.93	506.04
Analysis (%) [*]	C ₉ H ₆ N ₃ S ₃ ClPAu	C ₁₂ H ₁₂ N ₃ S ₃ ClPAu	C ₁₂ H ₁₅ N ₆ ClPAu 0.2 CH ₂ Cl ₂
C	20.96 (21.18)	25.44 (25.84)	28.12 (27.98)
H	1.17 (1.21)	2.31 (2.17)	2.90 (2.96)
N	8.29 (8.15)	7.66 (7.53)	15.73 (16.05)

* Required calculated values given in parenthesis

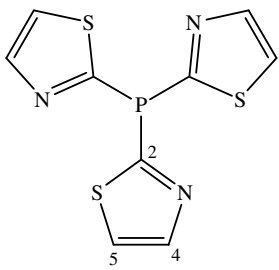
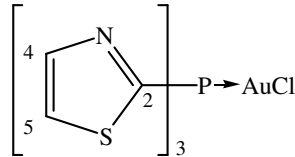
B. Spectroscopic characterisation of ligands I-III and complexes 1-3.

Nuclear magnetic resonance spectroscopy

The ^1H , $^{13}\text{C}\{^1\text{H}\}$, $^{31}\text{P}\{^1\text{H}\}$ and ^{15}N NMR spectroscopic data for compounds **I** and **1** are summarised in Table 2.3. The ^1H NMR data for the phosphine gold halide, **1**, shows that the proton chemical shifts are shifted downfield with respect to those in the free phosphine ligand **I**.

An unusual coupling of the phosphorus atom in **1** to the proton in the 4-position on the thiazole ring *via* the sulphur atom, was confirmed by selective homonuclear proton decoupling as well as heteronuclear phosphorus decoupling (Figure 2.2). This distinctive C-P coupling pattern is not observed in the free tertiary phosphine **I**.

Table 2.3 ^1H -, $^{13}\text{C}\{^1\text{H}\}$, $^{31}\text{P}\{^1\text{H}\}$ and ^{15}N NMR data for **I** and **1**

Compound		
	I	1
Solvent	CDCl_3	CD_2Cl_2
Temperature ($^\circ\text{C}$)	25	25
^1H NMR (300 MHz)	H^4 8.12 (d, 3H, $^3J = 3.23$ Hz) H^5 7.64 (d, 3H, $^3J = 3.21$ Hz)	8.28 (d, 3H, $^3J = 3.01$ Hz) 7.91 (dd, 3H, $^3J = 3.04$ Hz, $^4J = 2.43$ Hz)
$^{13}\text{C}\{^1\text{H}\}$ NMR (75 MHz)	C^2 165.4 (d, $^1J = 14.9$ Hz) C^4 145.6 (d, $^3J = 11.1$ Hz) C^5 124.9 (s)	156.8 (d, $^1J = 97.6$ Hz) 147.6 (d, $^3J = 22.8$ Hz) 128.33 (s)
$^{31}\text{P}\{^1\text{H}\}$ NMR (121 MHz)	P -31.33 (s)	0.87 (s)
^{15}N NMR (61 MHz)	N	-33.93 (d, $^2J_{\text{N-P}} = 27.81$ Hz)

The ^{13}C NMR data shows a downfield shift of the C^4 and C^5 resonances in complex **1** compared to ligand **I**, but the C^2 carbon (δ 156.8) of **1** resonates 8.6 ppm upfield from the

free ligand **1**. Upon complex formation the coupling constants of the phosphorus with C² (Δ^3J 82.7 Hz) and C⁴ (Δ^1J 11.7 Hz) increase significantly.³⁵

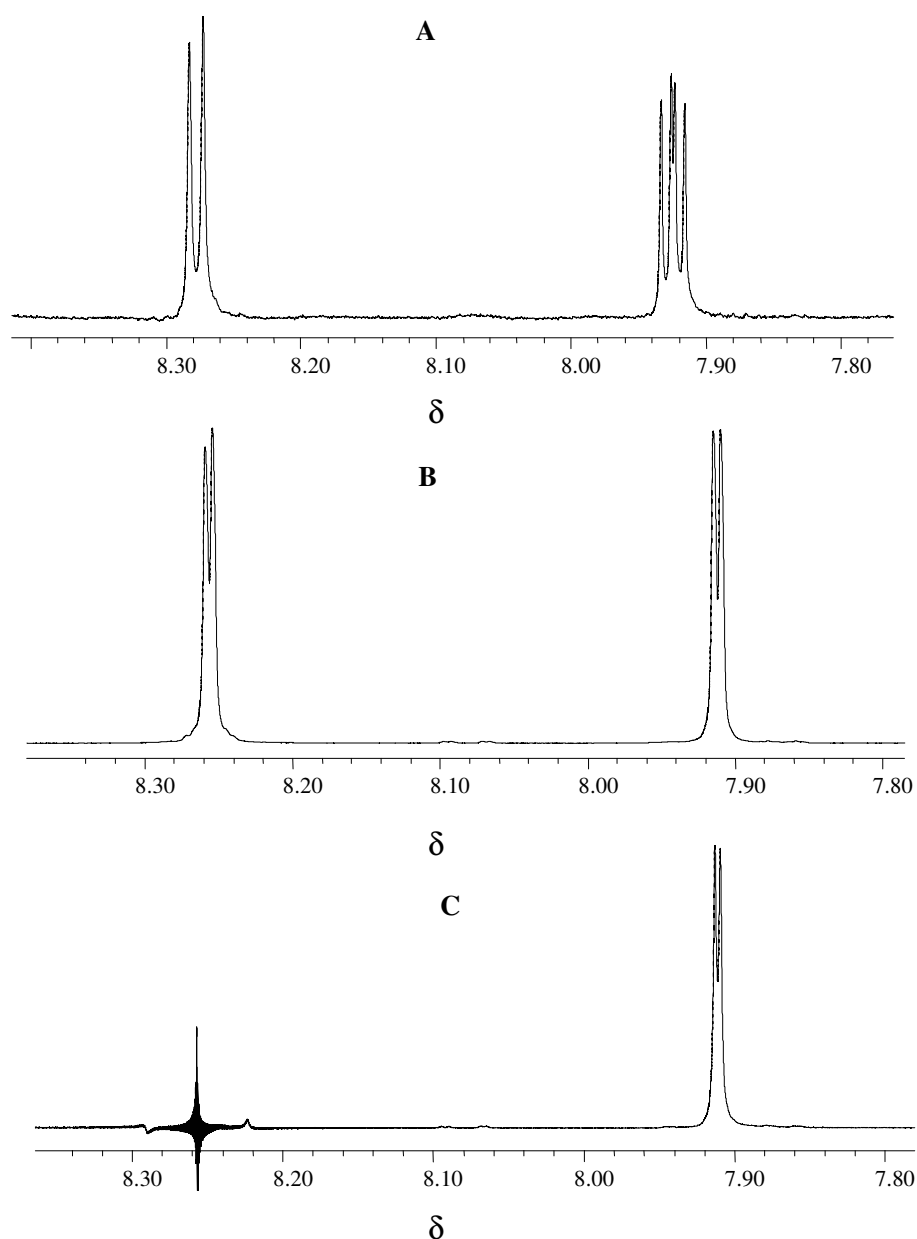


Figure 2.2 The signal of the protons in the 4 (δ 8.28) and 5 (δ 7.91) position on the thiazole ring in **1** (A); after selective heteronuclear phosphorus decoupling (B); and after selective homonuclear proton-proton decoupling (C).

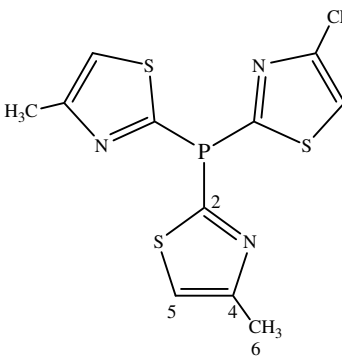
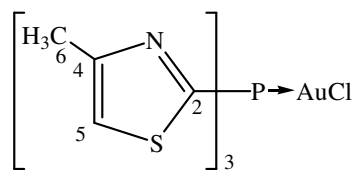
³¹P NMR data indicates a downfield shift ($\Delta\delta$ 30.46) of the phosphorus resonance in complex **1** relative to the free phosphine. The ¹⁵N NMR chemical shift of the nitrogen atom in **1** was determined in a direct detection ¹⁵N gHMQC (gradient heteronuclear multiple quantum coherence) experiment. The deshielded nitrogen resonance at δ -33.93

³⁵ R.F. Fenske, in B.L. Shapiro (Eds.): *Organometallic Compounds, Synthesis, Structure and Theory*, Texas A&M University Press, Texas, 1983, 305.

appears as a doublet and couples weakly to the phosphorus atom ($J = 27.8$ Hz). The ^{15}N NMR signals are, however, strongly dependant upon solvent, concentration and temperature.³⁶

The ^1H , $^{13}\text{C}\{^1\text{H}\}$, $^{31}\text{P}\{^1\text{H}\}$ NMR spectroscopic data for compounds **II** and **2** are summarised in Table 2.4. In the ^1H NMR spectra the proton in the 5-position on the thiazole ring in **II** and **2** resonates as a doublet of quartets due the long range coupling to the phosphorus atom *via* the sulphur atom. Furthermore, the CH_3 proton resonance appears as a doublet of doublets, testimony of a 5J -coupling to the phosphorus atom *via* the sulphur atom. This is well illustrated in the selective homonuclear CH and CH_3 decoupling of **2** (Figure 2.3).

Table 2.4 ^1H , $^{13}\text{C}\{^1\text{H}\}$, $^{31}\text{P}\{^1\text{H}\}$ and ^{15}N NMR data for **II** and **2**

Compound		
	II	2
Solvent	CDCl_3	CD_2Cl_2
Temperature ($^\circ\text{C}$)	25	25
^1H NMR (300 MHz)	H^5 7.20 (dq, 3H, $^4J = 0.92$ Hz, $^4J_{\text{H}5-\text{P}} = 0.49$ Hz) H^6 2.48 (d, 9H, $^4J = 0.93$ Hz)	H^5 7.43 (dq, 3H, $^4J_{\text{H}5-\text{P}} = 2.30$ Hz, $^4J = 0.90$ Hz) H^6 2.55 (dd, 9H, $^4J = 0.90$, $^5J_{\text{H}6-\text{P}} = 0.50$)
$^{13}\text{C}\{^1\text{H}\}$ NMR (75 MHz)	C^2 165.4 (d, $^1J = 11.8$ Hz) C^4 156.9 (d, $^3J = 13.2$ Hz) C^5 120.0 (s) C^6 16.9 (s)	C^2 155.6 (d, $^1J = 97.5$ Hz) C^4 158.5 (d, $^3J = 22.1$ Hz) C^5 123.0 (s) C^6 17.11 (s)
$^{31}\text{P}\{^1\text{H}\}$ NMR (121 MHz)	P -31.00 (s)	0.90 (s)
^{15}N NMR (61 MHz)	N -	- 29.49 (d, $^2J_{\text{N}-\text{P}} = 89.44$ Hz)

The ^{13}C NMR data indicates small downfield shifts of the C^4 , C^5 and C^6 carbon resonances, but an upfield shift for the C^2 carbon ($\Delta\delta$ 9.8) in complex **2** relative to **II**. In

³⁶ W. von Philipsborn and R. Müller, *Angew. Chem. Int. Ed., Engl.*, 1986, **25**, 383.

agreement with complex **1**, the phosphorus atom couples markedly stronger in the complex ($^1J_{C2-P}$ 97.5 Hz, $^3J_{C4-P}$ 22.1 Hz) than in the free ligand ($^1J_{C2-P}$ 11.8 Hz, $^3J_{C4-P}$ 13.2 Hz).

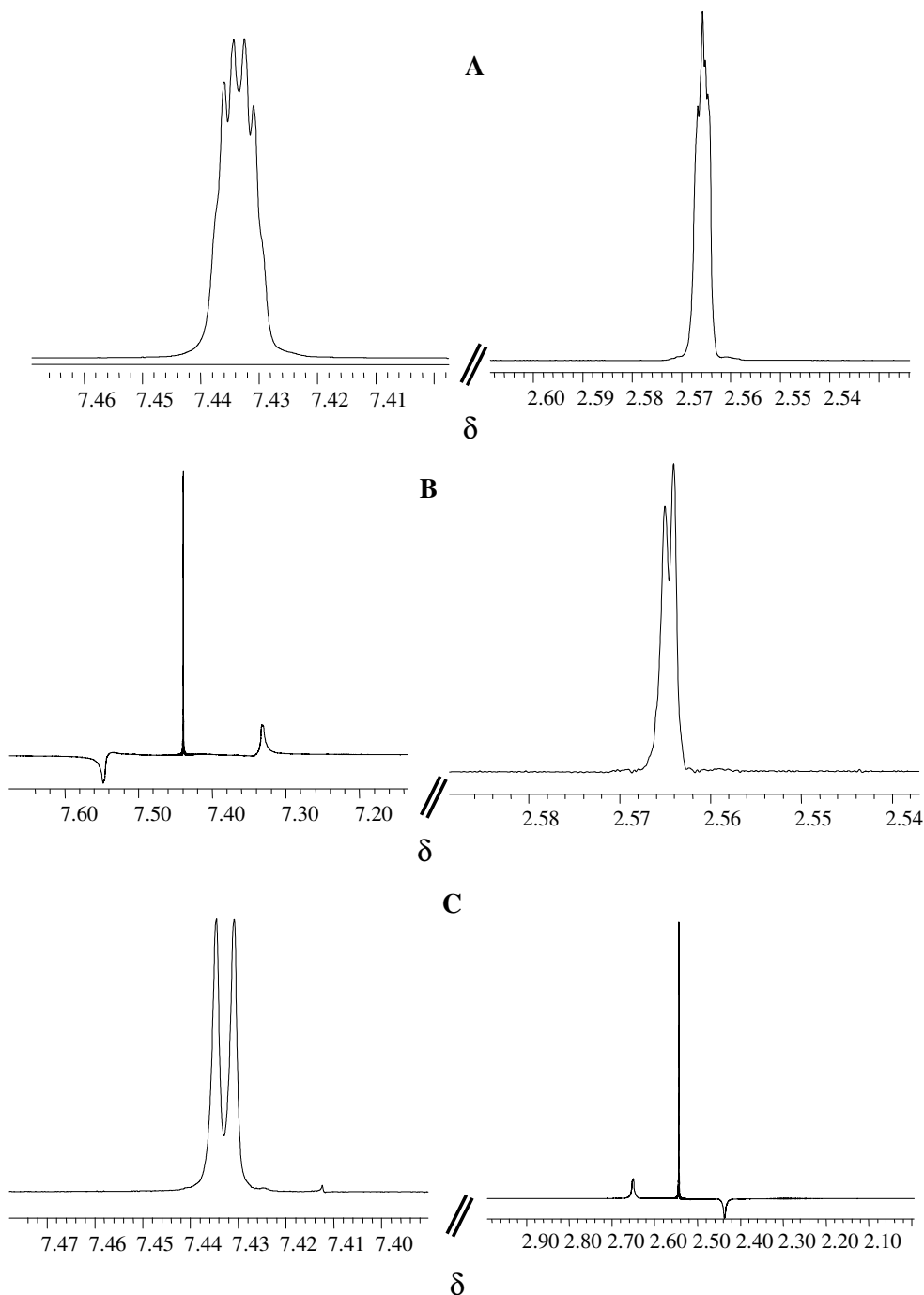
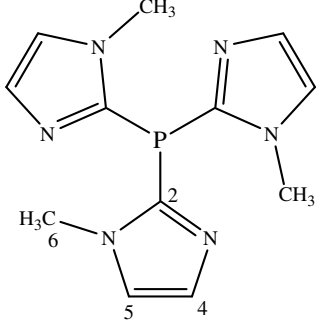
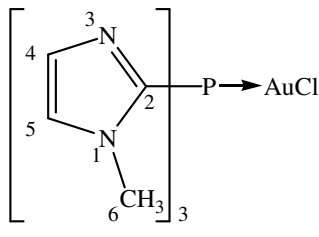


Figure 2.3 The signal of the CH protons (δ 7.43) in the 5 position and CH_3 protons (δ 2.55) on the thiazole ring in **2** (A); after selective homonuclear CH decoupling (B); and after selective homonuclear CH_3 coupling (C).

^{31}P NMR data indicates a downfield shift ($\Delta\delta$ 30.10) of the phosphorus resonance in the free phosphine relative to complex **2**. The ^{15}N NMR chemical shift of the nitrogen atom in **2** could be determined in a two dimensional ^1H , ^{15}N gHMQC experiment. The nitrogen

atom in **2** reveals a comparable chemical shift to the unsubstituted thiazole phosphine gold complex **1**, but exhibits a more than three times larger coupling constant to the phosphorus atom ($J = 89.44$ Hz) than in **1**. The ^1H , $^{13}\text{C}\{^1\text{H}\}$, $^{31}\text{P}\{^1\text{H}\}$ NMR spectroscopic data for compounds **III** and **3** are summarised in Table 2.5.

Table 2.5 ^1H , $^{13}\text{C}\{^1\text{H}\}$, $^{31}\text{P}\{^1\text{H}\}$ and ^{15}N NMR data for **III** and **3**

Compound	 <p style="text-align: center;">III</p>	 <p style="text-align: center;">3</p>
Solvent	CD_2Cl_2	$(\text{CD}_3)_2\text{SO}$
Temperature ($^\circ\text{C}$)	25	25
^1H NMR (300 MHz)	H^4 7.11 (m, 3H) H^5 7.11 (m, 3H) H^6 3.53 (s, 9H)	7.26 (m, 3H) 7.71 (m, 3H) 3.67 (s, 9H)
$^{13}\text{C}\{^1\text{H}\}$ NMR (75 MHz)	C^2 141.4 (d, $^1J_{\text{C}^2-\text{P}} = 12.0$ Hz) C^4 130.9 (d, $^3J = 8.8$ Hz) 130.9 (d, $^3J = 9.1$ Hz) 130.8 (d, $^3J = 8.9$ Hz)	132.4 (d, $^1J_{\text{C}-\text{P}} = 121.1$ Hz) 131.1 (d, $^3J = 17.6$ Hz) 131.1 (d, $^3J = 17.9$ Hz) 131.2 (d, $^3J = 17.8$ Hz)
$^{31}\text{P}\{^1\text{H}\}$ NMR (121 MHz)	C^6 34.3 (m) P -58.61 (s)	34.5 (m) -18.39 (s)
^{15}N NMR (61 MHz)	N^1 N^3	-206.31 (s) -90.64 (d, $^2J_{\text{N}-\text{P}} = 89.31$ Hz)

In the ^1H NMR spectrum of **III**, an unresolved multiplet is found at δ 7.10-7.12 for the allylic protons H^4 and H^5 . The protons of the N- CH_3 group appear as a singlet at δ 3.53. In the spectrum for **3** the signal for the allylic protons is resolved into two separate multiplets at δ 7.71 and 7.26 suggesting that apart from allylic coupling, coupling to the phosphorus also occurs across the heteroatoms in the complex. A sharp singlet peak assigned to the N- CH_3 , appears at slightly lower field (δ 3.67) relative to **III**.

In the ^{13}C NMR spectrum of **III** the C-atom in the 2-position resonates as a doublet ($J = 12.0$ Hz) at δ 141.4, in complex **3** an upfield shift ($\Delta\delta$ 9.0) occurs with a tenfold increase

in the C-P coupling constant (121.1 Hz). The assignment of signals to C⁴ and C⁵ were confirmed by gHSQC experiments. For both ligand **III** and complex **3** the carbons in the C⁴ position appear non equivalent and resonate as three doublets at δ 130.8 to 130.9 for **III** and δ 131.1 to 131.2 for **3**, with coupling constants approximately double for the latter compared to the free phosphine, **III**. Furthermore, the C⁵ carbon resonates as three separate singlets at δ 125.5, 125.6 and 125.6 in **III** thus showing no apparent long-range carbon-phosphorus coupling across the N-CH₃ group. The C⁵ carbon in **3** appears as an unresolved multiplet at δ 129.0.

The ¹⁵N NMR chemical shifts of the nitrogen atoms of **3** could be determined in a ¹H detected ¹H ¹⁵N gHMQC experiment. The most shielded nitrogen at δ -206.31 appears as a singlet and was assigned to N¹, the lesser shielded nitrogen resonates as a doublet ($J = 89.3$ Hz) at δ -90.64 showing strong N-P coupling. Both nitrogen atoms show a downfield shift relative to 1-methylimidazole (N¹, N³ at δ -220 and -122, respectively). The marked difference between the chemical shift of N¹ (sp³ hybridised) and N³ (sp² hybridised) nuclei is in agreement with literature reports.³⁶

Mass spectrometry

The mass-spectra of ligands **I**, **II** and complexes **1**, **2** are summarised in Table 2.6, and ligand **III** and complex **3** in Table 2.7. Both complexes **1** and **2** show weak molecular ion peaks at respectively m/z 517/515 (³⁷Cl/³⁵Cl) and 559/557 (³⁷Cl/³⁵Cl). The fragmentation patterns in the thiazole phosphine ligands comprise of the loss of a thiazole ring, which is preceded by the loss of AuCl in the complexes.

Table 2.6 Mass spectrometric data for **I**, **II**, **1** and **2**

Fragment	m/z (%)			
	I	II	1	2
{[M] ³⁷ Cl} ⁺	283 (13)	325 (24)	517 (3)	559 (1)
{[M]-AuCl} ⁺			283 (13)	325 (30)
{[M]-thiazole} ⁺	199 (100)	227 (100)	199 (100)	227 (100)
{[M]-thiazole(2)} ⁺	85 (27)	-	-	-

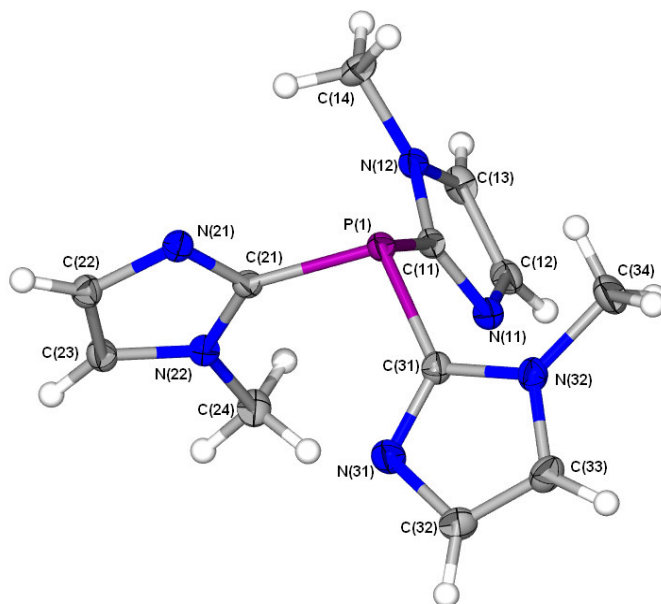
The mass-spectrum of tertiary imidazole phosphine, **III**, reveals the molecular ion peak as the base peak, which is verified by fragmentation peaks due to the loss of imidazole rings. Complex **3** shows weak molecular ion peaks at m/z 508/506 (³⁷Cl/³⁵Cl) followed by the loss of AuCl (m/z 274), which forms the base peak.

Table 2.7 Mass spectrometric data for **III** and **3**

Fragment	<i>m/z</i> (%)	
	III	3
{[M]- ³⁷ Cl} ⁺	274 (100)	508 (9)
{[M]-AuCl} ⁺		274 (100)
{[M]-methyl} ⁺	259 (6)	259 (7)
{[M]-imidazole} ⁺	193 (40)	193 (44)
{[M]-imidazole(2)} ⁺	112 (35)	112(30)

C. Structure determination of compounds **III**, **1** (as polymorphic forms **1a** and **1b**) and **2**.

The crystal and molecular structure of compounds **III**, **1** (**1a** and **1b**) and **2** was determined by single crystal X-ray diffraction. The molecular structure of tris(azolyl)phosphine, **III**, is depicted in Figure 2.4 and selected bond lengths and bond angles are summarised in Table 2.8. Compound **III** crystallises in the orthorhombic space group Pna2₁, and consist of discrete molecules. The geometry about the phosphorus atom is trigonal pyramidal, with the angles C(31)-P-C(11) [98.66(7)°], C(21)-P-C(31) [99.85(7)] and C(31)-P-C(11) [104.45(7)], largely in agreement with those of a related azolylphosphine, 2-PPh₂-6-CH₃C₅H₄N [100.90–102.29 °] and imPPh₂ [imidazolyl(diphenyl)phosphine] [100.3-104.1°].^{17, 37} The P-C distances [average 1.822(2)Å] are similar and correspond to separations in similar compounds, imPPh₂ [1.822(2)], BzimPPh [1.807(6)] and pyPPh₂ [1.837(3)].^{17, 38, 39}

**Figure 2.4** Molecular structure of **III** showing the numbering scheme.

³⁷ M. A. Jalil, T. Yamada, S. Fujinami, T. Honjo and H. Nishikawa, *Polyhedron*, 2001, **20**, 627.

³⁸ F. Bachechi, A. Burini, M. Fontani, R. Galassi, A. Macchioni, B. P. Pietroni, P. Zanello and C. Zuccaccia, *Inorg. Chim. Acta.*, 2001, **323**, 45.

³⁹ J. P. Charland, J. L. Roustan, N. Ansari, *Acta Crystallogr.*, **C 45**, 1989, 680.

In the crystal lattice (Figure 2.5), the unit cell consists of seventeen units and no important intermolecular interactions are noted.

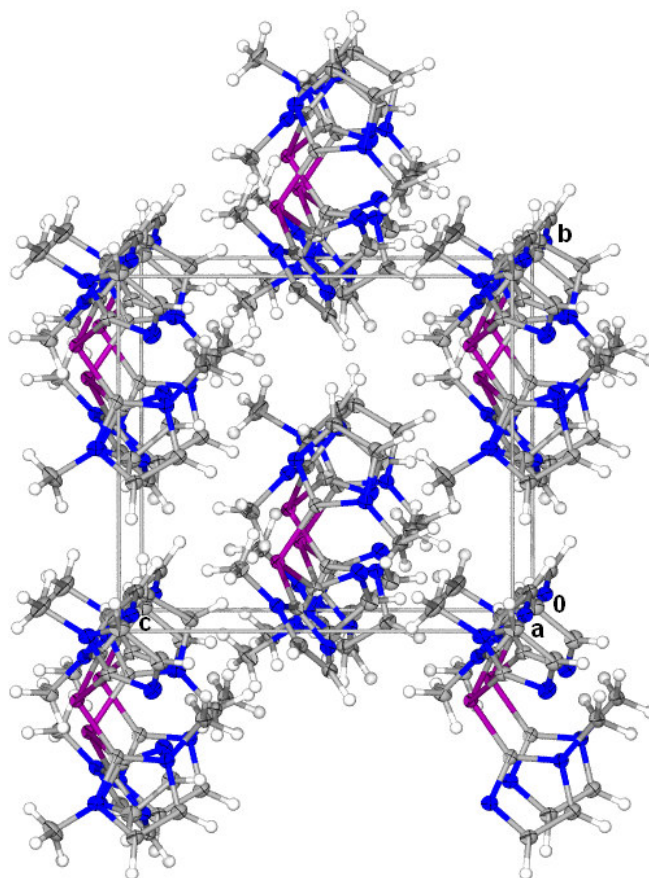


Figure 2.5 Unit cell and packing pattern in the crystal lattice of **III** viewed along the a-axis.

Table 2.8 Selected bond lengths (Å) and angles (°) for **III** with e.s.d.s in parenthesis

Bond lengths		Bond angles	
P(1)-C(11)	1.829(2)	C(21)-P(1)-C(11)	104.45(7)
N(11)-C(11)	1.323(2)	C(21)-P(1)-C(31)	99.85(7)
N(11)-C(12)	1.378(2)	C(31)-P(1)-C(11)	98.66(7)
C(12)-C(13)	1.359(2)	N(11)-C(11)-N(12)	111.4(1)
N(12)-C(13)	1.367(2)	N(11)-C(11)-P(1)	126.4(1)
N(12)-C(14)	1.466(2)	N(12)-C(11)-P(1)	122.3(1)
N(12)-C(11)	1.364(2)	N(21)-C(21)-P(1)	118.99(1)
		N(22)-C(21)-P(1)	129.7(1)
		C(11)-N(11)-C(12)	104.9(1)
		C(11)-N(12)-C(13)	107.3(1)
		C(11)-N(12)-C(14)	127.1(1)
		C(13)-N(12)-C(14)	125.6(1)
		C(13)-C(12)-N(11)	110.7(2)
		C(12)-C(13)-N(12)	105.8(1)

During the synthesis of azolygold(I) phosphines, we isolated two true crystalline polymorphs of chloro[tris(thiazol-2-yl)phosphine]gold(I) **1**. The polymorphs have exactly the same molecular connectivity and vary only in terms of crystal packing and minor

conformational effects. The molecular structures within the two forms of complex **1**, **1a** and **1b**, are represented in Figure 2.6. Selected bond lengths and angles are given in Table 2.9 and 2.10.

The space groups are monoclinic, $P2_1/c$ and triclinic, $P\bar{1}$, for forms **1a** and **1b** respectively. A search in the Cambridge Crystallographic database reveals that only a few examples of polymorphism, in other complexes of this type with gold(I) have been reported, chloro[tris(2-pyridyl)phosphine]gold(I),⁴⁰ chloro[tris(2-cyanoethyl)phosphine]gold(I)⁴¹ and $[\text{Au}(p\text{-}^t\text{BuNOC}_6\text{H}_4\text{PPh}_2)]\text{Cl}$.⁴²

The crystal structure of crystalline phase **1a** consists of two independent molecules in the asymmetric unit; they differ from each other by having slightly different conformational geometries of the thiazolyl rings. Whilst weak, intermolecular aurophilic interaction at 3.4563(2) Å aggregate the different conformers into dimers. The Au...Au contacts appear slightly shorter at 3.3459(3) Å in **1b**, and are generated by a centre of symmetry. Of note is that the few examples of tris(heterocyclic)phosphinegold(I) halides in the literature, e.g. chloro[tris(2-pyridyl)phosphine]gold(I),⁴⁰ chloro[tris(2-thienyl)phosphine]gold(I)^{43,44} and chloro[tris(2-furyl)phosphine]gold(I)^{45,46} are all devoid of any close (<4 Å) intermolecular aurophilic interactions, which is surprising in view of the fact that the phosphine substituent in such compounds is no more bulky than that found in **1a**, **1b** and **2**.

⁴⁰ C. J. L. Lock and M. A. Turner, *Acta Cryst.*, **C43**, 1987, 2096.

⁴¹ J. P. Fackler Jr., R. J. Staples, M. N. I. Khan and R. E. P. Winpenny, *Acta Cryst.*, **C50**, 1994, 1020.

⁴² D. B. Lesnoff, C. Rancurel, J.-P. Sutter, S. J. Rettig, M. Pink, C. Paulsen and O. Kahn, *J. Chem. Soc., Dalton Trans.*, 1999, 3593.

⁴³ S. Y. Ho and E. R. T. Tiekink, *Z. Kristallogr., New Chem. Struct.*, 2003, **218**, 73.

⁴⁴ U. Monkowius, S. Nogai and H. Schmidbauer, *Z. Naturforsch., B:Chem. Sci.*, 2003, **58**, 751.

⁴⁵ S. Y. Ho and E. R. T. Tiekink, *Z. Kristallogr., New Chem. Struct.*, 2002, **217**, 591.

⁴⁶ F. Bachechi, A. Burini, R. Galassi and B. R. Pietroni, *J. Chem. Cryst.*, 2004, **34**, 743.

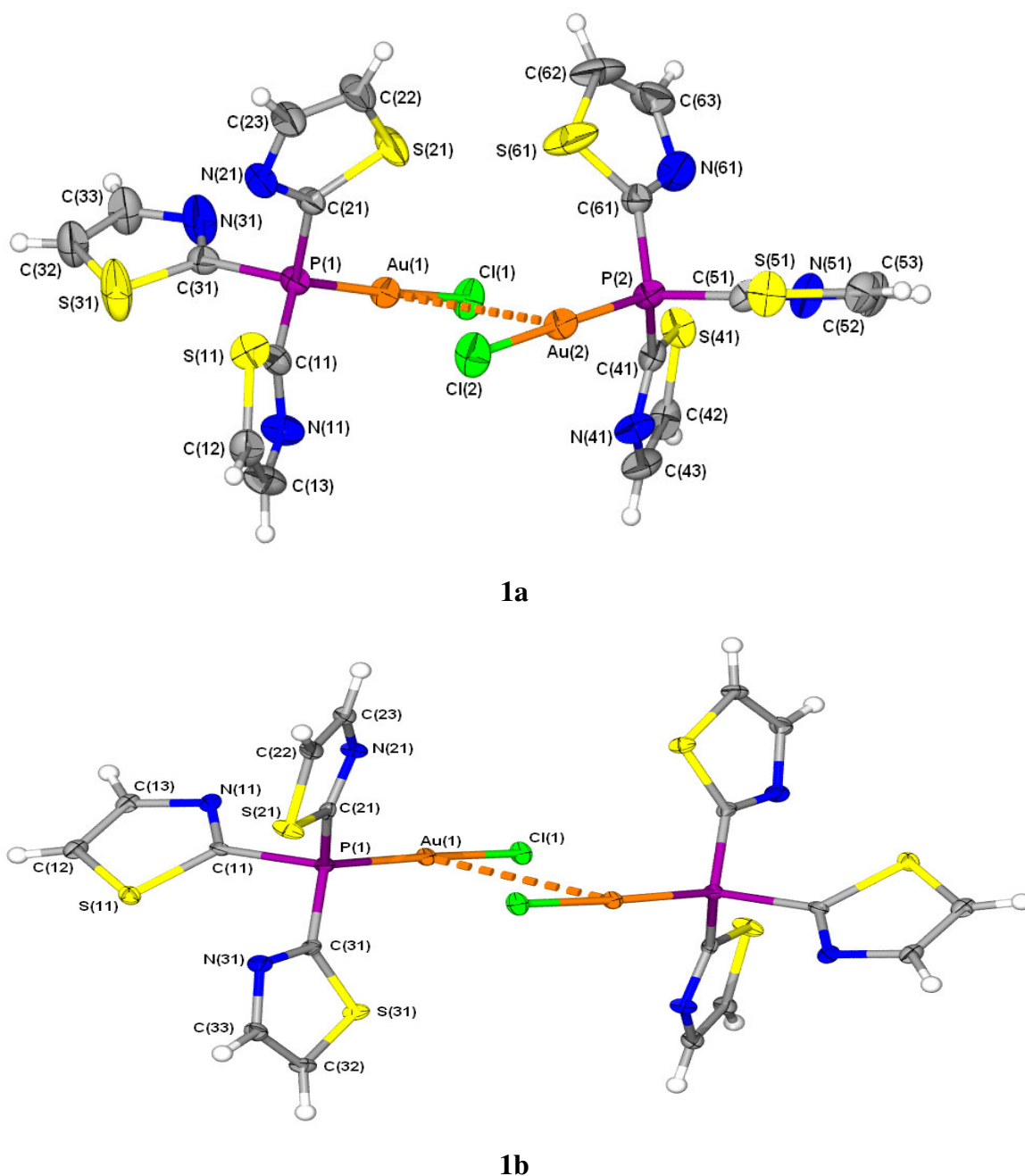


Figure 2.6 Molecular structures of polymorphs **1a** and **1b** showing their numbering schemes.

Furthermore, the presence of metal contacts is further manifested in the distortion from linearity of the P-Au-Cl angle, in **1a** [174.06(4) and 178.03(4)°] and **1b** [174.30(3)°]. The different spatial arrangement of the thiazole rings in **1a** bringing about an almost 4° deviation in the two polymorphs. The Au-P bond lengths of 2.2184(9) Å and 2.217(1) Å, in the two independent molecules of **1a**, and 2.2260(9) Å in **1b** are very similar and comparable with 2.227(1) Å in chloro[tris(2-thienyl)phosphine]gold(I),^{43, 44} and 2.214(4) Å in chloro[tris(2-pyridyl)phosphine]gold(I).⁴⁰ The Au-Cl separations [2.2774(9) and 2.276(1) in **1a**, 2.290(1) in **1b**] are similarly unremarkable. All relevant bond lengths and angles pertaining to the thiazole rings are normal.

Table 2.9 Selected bond lengths (Å) and angles (°) for polymorphic structure **1a** with e.s.d.s in parenthesis

Bond lengths		Bond angles	
Au(1)-P(1)	2.218(1)	P(1)-Au(1)-Cl(1)	174.06(4)
Au(1)-Cl(1)	2.277(1)	P(2)-Au(2)-Cl(2)	178.03(4)
Au(2)-P(2)	2.217(1)	P(1)-Au(1)-Au(2)	109.35(3)
Au(2)-Cl(2)	2.276(1)	P(2)-Au(2)-Au(1)	106.40(3)
C(11)-N(11)	1.300(5)	Cl(1)-Au(1)-Au(2)	76.33(3)
C(11)-S(11)	1.722(4)	Cl(2)-Au(2)-Au(1)	75.54(3)
C(11)-P(1)	1.804(4)	C(21)-P(1)-C(11)	103.9(2)
C(12)-C(13)	1.332(6)	C(21)-P(1)-C(31)	104.0(2)
C(12)-S(11)	1.694(4)	C(11)-P(1)-C(31)	104.4(2)
C(13)-N(11)	1.377(5)	C(21)-P(1)-Au(1)	113.6(1)
Au(1)-Au(2)	3.4563(2)	C(11)-P(1)-Au(1)	119.1(1)
Cl(1)-S(11)	3.373(1)	C(31)-P(1)-Au(1)	110.5(1)
		C(41)-P(2)-Au(2)	115.4(1)
		C(51)-P(2)-Au(2)	114.6(1)
		C(61)-P(2)-Au(2)	112.1(1)
		C(13)-C(12)-S(11)	110.9(3)
		C(12)-C(13)-N(11)	115.8(4)
		N(11)-C(11)-P(1)	120.4(3)
		S(11)-C(11)-P(1)	124.7(2)
		N(21)-C(21)-P(1)	122.7(3)
		S(21)-C(21)-P(1)	122.3(2)
		C(11)-N(11)-C(13)	109.5(4)
		C(12)-S(11)-C(11)	88.8(2)
		Au(1)-Cl(1)-S(11)	148.46(5)
		C(42)-S(41)-Cl(2)	82.2(2)
		C(41)-S(41)-Cl(2)	170.7(2)

Table 2.10 Selected bond lengths (Å) and angles (°) for polymorphic structure **1b** with e.s.d.s in parenthesis

Bond lengths		Bond angles	
Au(1)-P(1)	2.226(1)	P(1)-Au(1)-Cl(1)	174.30(3)
Au(1)-Cl(1)	2.290(1)	P(1)-Au(1)-Au(1)	108.50(2)
N(11)-C(11)	1.313(4)	Cl(1)-Au(1)-Au(1)	75.78(2)
S(11)-C(11)	1.728(3)	C(21)-P(1)-C(11)	103.5(2)
P(1)-C(11)	1.819(4)	C(31)-P(1)-C(21)	106.5(2)
C(12)-C(13)	1.346(5)	C(31)-P(1)-C(11)	101.6(2)
S(11)-C(12)	1.711(4)	C(31)-P(1)-Au(1)	113.3(1)
N(11)-C(13)	1.373(5)	C(21)-P(1)-Au(1)	119.3(1)
Au(1)-Au(1)	3.3459(3)	C(11)-P(1)-Au(1)	110.9(1)
		C(12)-S(11)-C(11)	89.1(2)
		N(11)-C(11)-S(11)	114.9(3)
		C(13)-C(12)-S(11)	110.0(3)
		C(12)-C(13)-N(11)	116.5(3)
		N(11)-C(11)-P(1)	120.3(2)
		N(31)-C(31)-P(1)	124.9(3)
		S(11)-C(11)-P(1)	124.7(2)
		S(31)-C(31)-P(1)	119.4(2)

A more apparent difference between the two structures is found, in the relative intermolecular arrangements in the crystal pattern as opposed to the molecular structure (Figure 2.7). Careful examination of the packing pattern in **1a** shows, apart from the weak aurophilic interactions, a system of non-bonding intermolecular Cl-S interactions [3.373(1) Å] along the a-axis of the unit cell (Figure 2.8). This interaction is made possible by the one thiazole group oriented with the sulphur atoms, S11 and S21, pointing towards the chlorine atom of the adjacent dimer. These interactions propagate the gold(I) dimers as polymeric chains in the a-axis.

No significant intermolecular forces other than the aurophilic interactions are present in the crystal lattice of polymorph **1b**. It shows a very efficient packing of rows of dimers along the a-axis, which are brought in close proximity to neighbouring aggregates due to the staggered conformation of the thiazole substituents on the phosphine ligands facing each other (Figure 2.9).

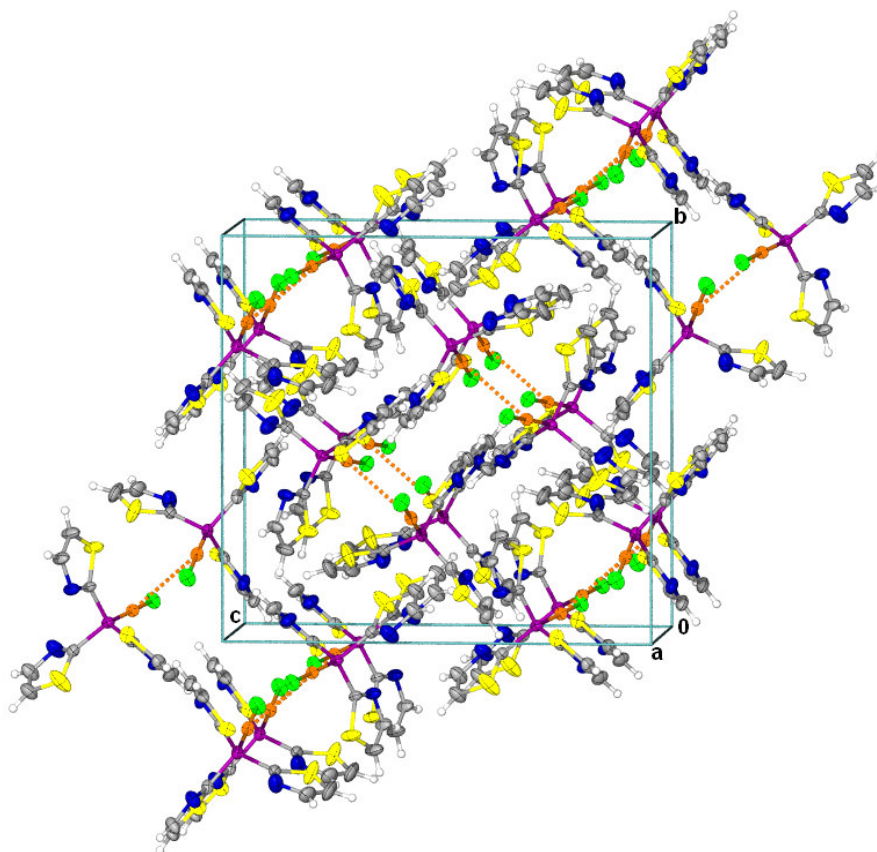


Figure 2.7 Unit cell and packing pattern in the crystal lattice of polymorphic form **1a** viewed along the a-axis.

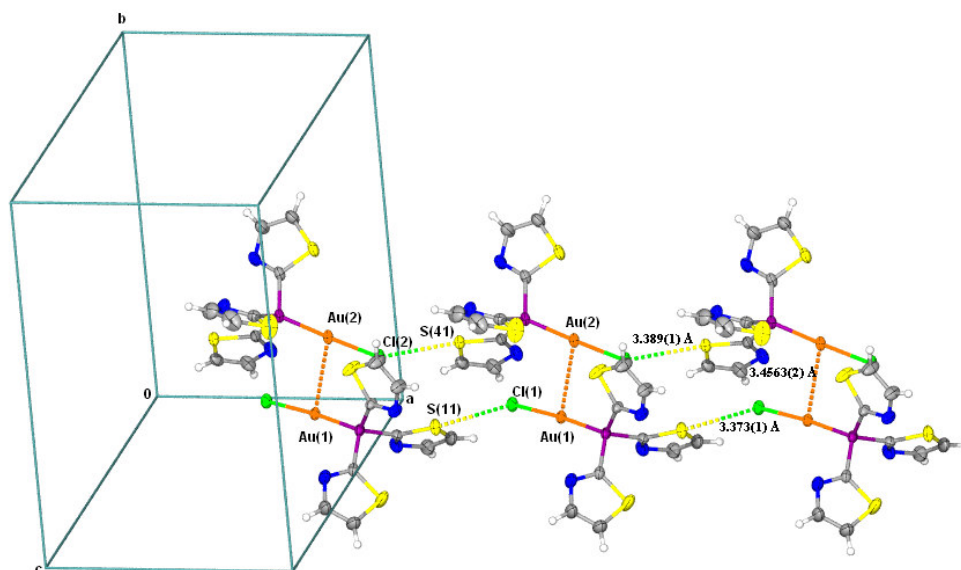


Figure 2.8 A system of non-bonding Cl-S interactions observed along the a-axis of the unit cell, present in polymorphic structure **1a**.

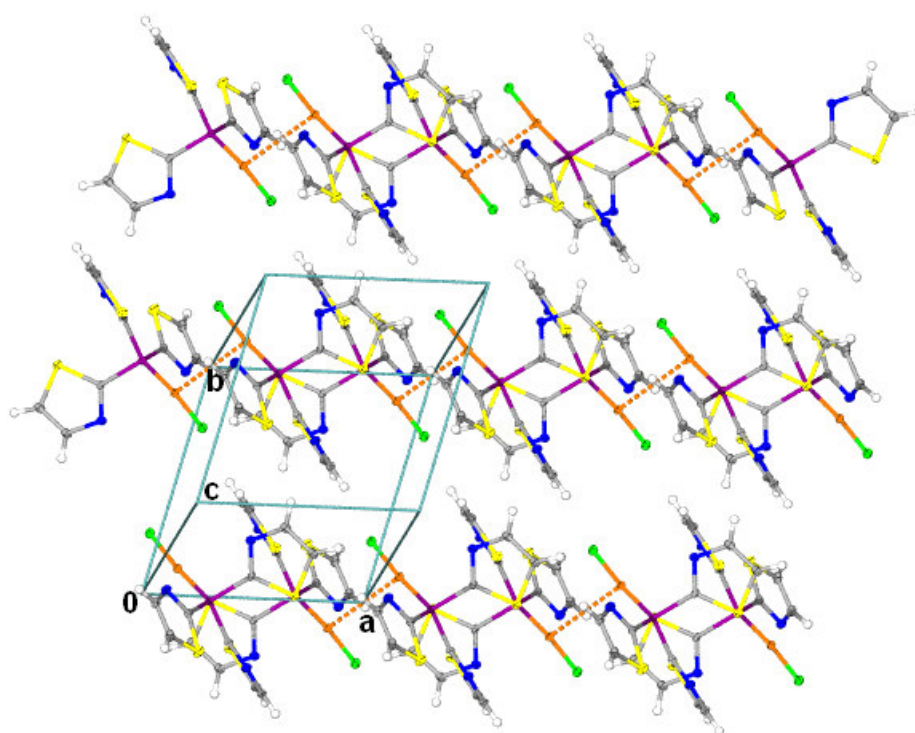


Figure 2.9 Unit cell and packing pattern in the crystal lattice of polymorphic form **1b** viewed along the c-axis, showing the staggered conformation of the thiazole rings.

A very distinguishing difference between the dimeric forms of **1a** and **1b**, is the torsion angle between the respective P-Au-Cl planes. In **1a** it is at approximately 18° (17.81° and 19.28°), in **1b** the inversion centre is located in the centre of the Au...Au vector and the planes are co-planar.

The molecular structure of **2** is discussed only with regard to noted differences to previously discussed **1a** and **1b**. The 4-methyl substituted analogue crystallises in the monoclinic, $C2/c$ space group. The molecular structure is shown in Fig 2.10 with selected bond lengths and angles in Table 2.11, numbered according to the figure.

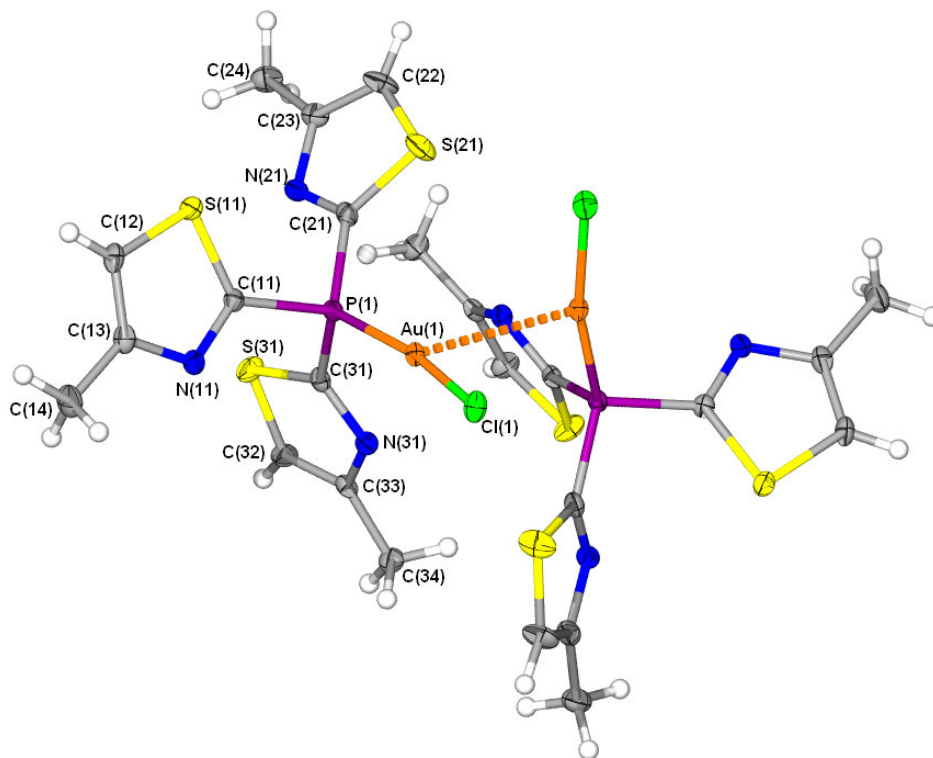


Figure 2.10 Molecular structure of **2** showing the numbering scheme.

The tris(4-methylthiazol-2-yl)phosphine ligand has a warped three fold symmetry, with the plane of two thiazolyl moieties containing the gold(I) centre. The third thiazole substituent forms a plane almost perpendicular to the aforementioned planes. Larger C-P-Au [108.42(10) to 121.44(11) $^\circ$] angles and smaller external angles about the phosphorus atom [101.54(14) to 105.25(14) $^\circ$] confer a pseudo-tetrahedral geometry on the complex.

Strong intermolecular gold contacts frequently disrupt the ideal linear coordination in gold(I) complexes.⁴⁷ As mentioned previously, an important precondition for linear complexes of the type PAuCl, that aggregate in the crystal lattice as dimers, is the absence of sterically bulky substituents on the phosphine ligands. This is no more apparent than in the crystal structure of **2**. The P-Au-Cl angle at 167.83(3) $^\circ$ shows a significant deviation from linearity, brought about to a large extent by the short Au...Au separation of 3.0393(4) Å. The empirical plane through the distorted coordination centre of the two

⁴⁷ H. Schmidbaur, P. Bissinger, J. Lachmann and O. Steigelmann, *Z. Naturforsch.*, 1992, **47b**, 1711.

parts of the dimer approach one another almost perpendicularly [torsion angle Au-Au(1)-P(1)-C(31) 83.90(11)°].

A view along the c-axis, shows how thirteen dimers of **2** are arranged in the unit cell, related by a twofold symmetry (Figure 2.11). Other than the short Au...Au interactions, notable intermolecular close contacts, include S-Cl non-bonding interactions [S(21)-Cl(1) 3.753 Å].

Table 2.11 Selected bond lengths (Å) and angles (°) for complex **2** with e.s.d.s in parenthesis

Bond lengths		Bond angles	
Au(1)-P(1)	2.2169(8)	P(1)-Au(1)-Cl(1)	167.83(3)
Au(1)-Cl(1)	2.2901(8)	P(1)-Au(1)-Au(1)	102.50(2)
N(11)-C(11)	1.304(4)	Cl(1)-Au(1)-Au(1)	89.66(2)
S(11)-C(11)	1.726(3)	C(21)-P(1)-C(11)	101.54(14)
P(1)-C(11)	1.810(3)	C(31)-P(1)-C(21)	105.25(14)
C(12)-C(13)	1.360(5)	C(31)-P(1)-C(11)	104.67(14)
C(13)-C(14)	1.502(4)	C(31)-P(1)-Au(1)	113.71(11)
S(11)-C(12)	1.707(3)	C(21)-P(1)-Au(1)	121.44(11)
N(11)-C(13)	1.380(4)	C(11)-P(1)-Au(1)	108.42(10)
Au(1)-Au(1)	3.0393(4)	C(12)-S(11)-C(11)	88.70(15)
		N(11)-C(11)-S(11)	115.2(2)
		C(13)-C(12)-S(11)	111.1(2)
		C(12)-C(13)-N(11)	114.5(3)
		C(12)-C(13)-C(14)	125.9(3)
		N(11)-C(13)-C(14)	119.6(3)
		N(11)-C(11)-P(1)	121.0(2)
		S(11)-C(11)-P(1)	123.28(17)

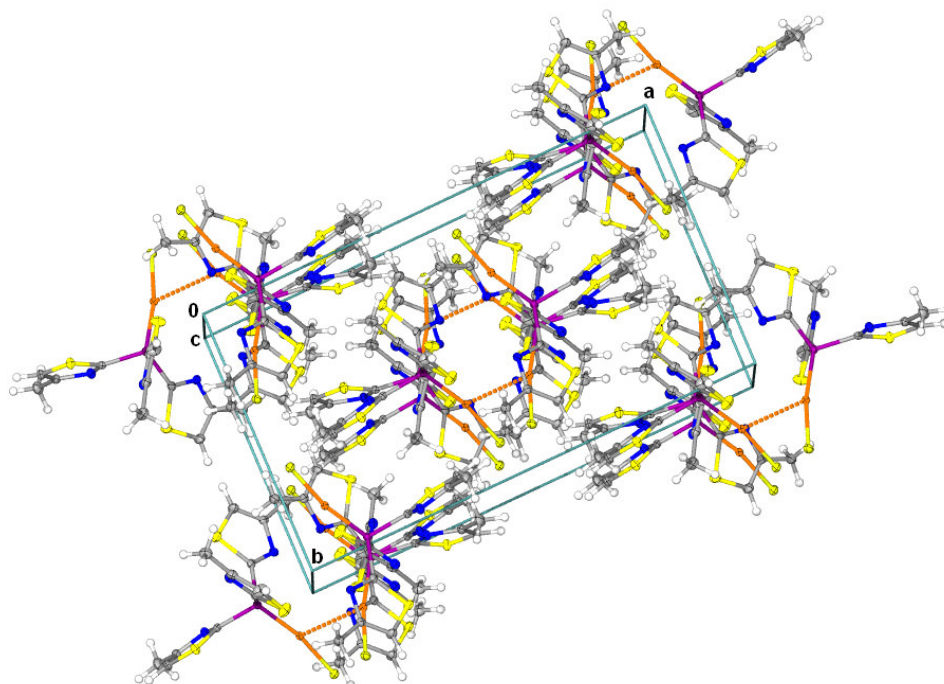
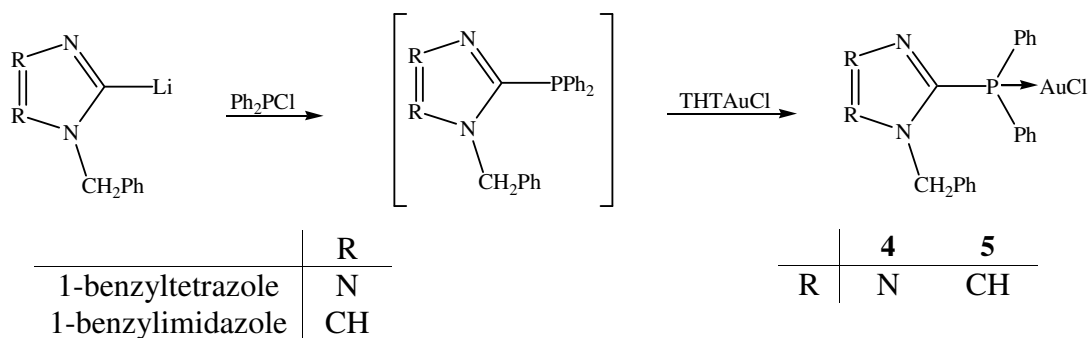


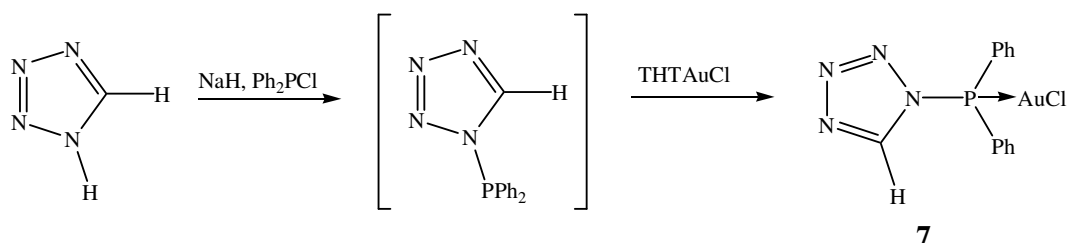
Figure 2.11 Unit cell and packing pattern in the crystal lattice of **2** viewed along the c-axis.

2.2.2 Gold(I) complexes of diphenylphosphine C-, N-tetrazolyl- and imidazolyl phosphines.

Using a similar approach which was successfully applied to the preparation of complexes **1-3**, the monosubstituted, azolyl(diphenyl)phosphinegold(I) complexes can be obtained from 1-benzylimidazole, 1-benzyltetrazole and 1*H*-tetrazole (Scheme 2.5 and 2.6).



Scheme 2.5 A one-pot synthetic approach to the preparation of azolyl(diphenylphosphine) gold(I)chloride **4** and **5**.



Scheme 2.6 A one-pot synthetic approach to the preparation of *N*-tetrazolyl(diphenyl phosphine)gold(I)chloride **7**.

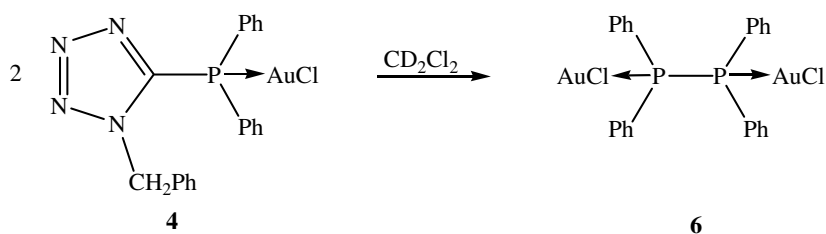
A Preparation of chloro[(1-benzyltetrazol-5-yl)diphenyl]phosphinegold(I), **4**, chloro[(1-benzylimidazol-2-yl)diphenyl]phosphine gold(I), **5**, chloro[(1-*H*-tetrazolyl)diphenyl]phosphinegold(I), **7** and the spontaneous formation of dichloro(1,1,2,2-tetraphenyl-diphosphine)digold(I), **6**.

In a first attempt to prepare the free phosphine, (1-benzyltetrazol-5-yl)diphenylphosphine, 5-lithiated-1-benzyltetrazole was treated with freshly distilled chlorodiphenylphosphine. However, a subsequent purification attempt by column chromatography, led to the formation of the phosphine oxide and thus reduced the yield significantly. Using a one-pot synthetic approach (Scheme 2.3), the isolation and purification of the phosphine was omitted, and the gold(I) precursor, [AuCl(tht)], added directly to the reaction mixture. Burini co-workers¹⁵ emphasised, in the preparation of the analogous (1-benzyl-2-imidazolyl)diphenylphosphine gold(I) complex, **5**, that by using [AuCl({CH₃})₂S] as starting material, an impure product is obtained due to the displacement of the thioether ligand also by the N donor atom of the dihapto ligand, (1-benzyl-2-

imidazolyl)diphenylphosphine. This was not observed when [AuCl(tht)] is employed as starting material, and phosphine complexes **4** and **5** were isolated in pure and good yield.

Final purification of complexes **4** and **5** were achieved by crystallisation from dichloromethane solution layered with *n*-hexane at -20 °C. The products are stable, even in the presence of moisture and air. Slow diffusion of the apolar solvent into a concentrated solution of **5** afforded suitable crystals for X-ray analysis. However, numerous attempts aimed at the recrystallisation of microcrystalline material of complex **4**, failed to provide suitable crystals for such structural analysis.

A complicating reaction that occurred during the NMR analysis of **4** in CD₂Cl₂, was the formation of a dinuclear diphosphinegold(I) chloride complex, dichloro(1,1,2,2-tetraphenyl-diphosphine)digold(I), **6**, (Scheme 2.7). Peculiar, highly insoluble colourless oval crystals formed overnight at 5 °C, and could be used for a structure determination. Complete characterisation of this novel but simple complex by NMR-studies was hampered by its low solubility in most organic solvents. Complex **6** represents the first dinuclear gold(I) chloride complex that contains a P-P bonded diphosphine and represents the missing link in the series of compounds ClAuP(Ph)₂[CH₂]_{*n*}P(Ph)₂AuCl, (*n* = 0,1,...5).



Scheme 2.7 The spontaneous formation of complex **6** from complex **4**, and the possible fragmentation to form cyanamide by-products.

The formation of complex **6** would require a formal cleavage of a P-C linkage in a σ -bond metathesis-type rearrangement reaction. Although fragmentations of 5-substituted tetrazole substrates have been reported in detail, such a reaction is unprecedented.⁴⁸ Analytical data for complexes **4**, **5** and **6** are summarised in Table 2.12.

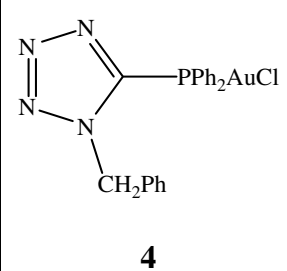
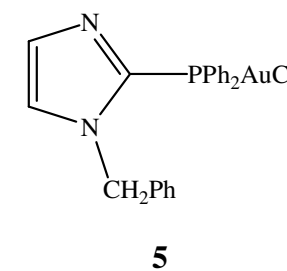
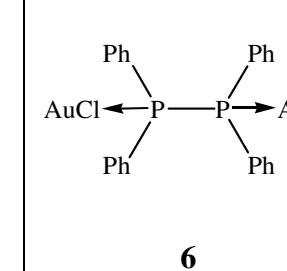
In recent times, phosphine ligands with P-N bonds have attracted much attention, due largely to the different electronic properties transferred by the nitrogen centre to the phosphorus nuclei.⁴⁹ Phosphinoamine ligands of tetrazoles, however, have not received

⁴⁸ R. Raap, *Can. J. Chem.*, 1971, **49**, 2139.

⁴⁹ Z. Fei, A. Scopelliti and P. J. Dyson, *Dalton Trans.*, 2003, 2772.

any attention. The most common nucleophilic type reactions occurring at tetrazole nitrogens arise from the acidity of the ring N-H, which in the case of 1*H*-tetrazole (pK_a 4.89) acts as the nitrogen analogue to formic acid (pK_a 4.75). The treatment of tetrazolic acids with bases (e.g. triethylamine, NaH, etc.) results in the formation of stable anions which are ambident in character and may afford the formation of 1- and to a lesser extent the 2-substituted tetrazoles (upon reaction with nucleophiles).⁵⁰

Table 2.12 Analytical data for complexes **4**, **5** and **6**

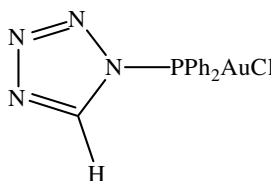
Complex			
	4	5	6
M.p./°C	87 (decomp.)	168-170(165-167 lit. ¹⁵)	146 (decomp.)
Colour	yellow	colourless	off-white/yellow
Yield(%)	78	85	42
M_r	576.05	574.06	833.47
Analysis(%)	$C_{20}H_{17}N_4ClPAu$ $\cdot 0.30 CH_2Cl_2$	$C_{22}H_{19}N_2ClPAu$	$C_{24}H_{20}Cl_2P_2Au_2$
C	40.61 (40.49)	45.83 (45.97)	34.52 (34.51)
H	3.02 (2.95)	3.29 (3.33)	2.41 (2.41)
N	9.14 (9.30)	4.80 (4.87)	

* Required calculated values given in parenthesis

Complex **7**, was prepared by the treatment of diphenylphosphine chloride with sodium tetrazolate, followed immediately by the addition of [AuCl(tht)] to afford the gold phosphine halide (Scheme 2.6). The isolation of the free phosphine, was not attempted. Unlike the stability of C-bonded imidazolyl- and tetrazolylphosphine complexes **4** and **5**, complex **7** decomposed readily in air and is most unstable in solution. Analytical data for complex **7** is summarised in Table 2.13.

⁵⁰ R. Bronisz, *Inorg. Chim. Acta*, 2002, **340**, 215.

Table 2.13 Analytical data for complex **7**

Complex	 7
M.p./°C	101-103 (decomp)
Colour	colourless
Yield(%)	59
M_r	486.01
Analysis(%)	$C_{13}H_{11}AuClN_4P$
C	32.41 (32.09)
H	2.31 (2.28)
N	11.75 (11.51)

* Required calculated values given in parenthesis

A. Spectroscopic characterisation of complexes 4-7.

Nuclear magnetic resonance spectroscopy

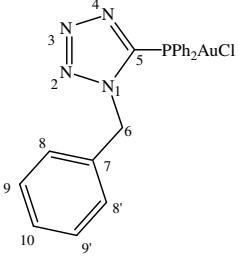
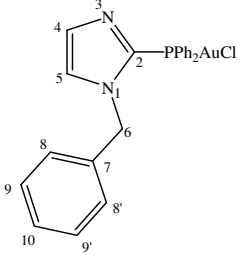
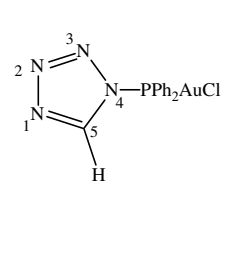
The 1H , $^{13}C\{^1H\}$, $^{31}P\{^1H\}$ and ^{15}N NMR spectroscopic data for complexes **4**, **5** and **7** are summarised in Table 2.14.

In the ^{13}C NMR spectrum of **4** the benzylic CH_2 resonance appears as a doublet ($^3J = 2.7$ Hz) at δ 57.7, indicative of a coupling across three bonds to the phosphorus atom. The azolyl carbon resonance features as a doublet ($^1J = 68.3$ Hz) at δ 151.2, and serves as a diagnostic signal for the presence of a carbon-bonded tetrazole-5-ylphosphine. Furthermore, the ^{15}N NMR spectrum of **4** exhibits two signals, a doublet ($J = 9.0$ Hz) at δ -136.8 for N1, and another at δ -33.0 ($J = 12.2$ Hz), indicating N-P coupling across two bonds. ^{31}P NMR analysis (d_6 -acetone) of the isolated reaction product has a single singlet (δ 7.3) pertaining to a coordinated phosphine.

In agreement with the characterisation of Burini co-workers¹⁵ of complex **5**, the 1H NMR spectrum, recorded in CD_2Cl_2 , shows the benzylic protons as a singlet signal at δ 5.62 (lit. δ 5.22 in DMSO). ^{31}P NMR records the phosphorus resonance as a singlet signal at δ 10.78 (lit. δ 10.67 in DMSO). The ^{13}C NMR spectrum, not previously reported, reveals

diagnostic C-P coupling patterns: both the benzylic carbon (C⁶) and the C²-*ipso* carbon appear as doublets, at δ 52.3 ($^3J = 4.6$ Hz) and δ 132.1 ($^1J = 68.7$ Hz), respectively.

Table 2.14 ^1H , $^{13}\text{C}\{^1\text{H}\}$, $^{31}\text{P}\{^1\text{H}\}$ and ^{15}N NMR data for **4**, **5** and **7**

Complex				
	4	5	7	
Solvent	(CD ₃) ₂ CO	CD ₂ Cl ₂	CD ₃ CN	
Temperature (K)	298	298	298	
^1H NMR (300 MHz)	H ⁴ H ⁵ H ⁶ H ⁸⁻¹⁰	7.37 (m, 1H) 7.71-7.78 (m, 1H) 5.62 (s, 2H) 6.97-7.16 (m, 5H)	9.05 (s, 1H)	
$^{13}\text{C}\{^1\text{H}\}$ NMR (75 MHz)	PPh PPh-C ^{ipso} PPh-C ^{ortho} PPh-C ^{meta} PPh-C ^{para} C ² C ⁴ C ⁵ C ⁶ C ⁷ C ⁸ , C ^{8'} C ⁹ , C ^{9'} C ¹⁰	7.53-7.93 (m, 10H) 7.37-7.63 (m, 10H)	7.47-7.87 (m, 10H)	
$^{31}\text{P}\{^1\text{H}\}$ NMR (121MHz)	P	137.9 (d, $^1J_{\text{C-P}} = 71.4$ Hz) 136.7 (d, $^2J_{\text{C-P}} = 16.1$ Hz) 131.7 (d, $^3J_{\text{C-P}} = 12.8$ Hz) 135.1 (d, $^4J_{\text{C-P}} = 2.5$ Hz) 151.2 (d, $^1J_{\text{C-P}} = 68.3$ Hz) 54.7 (d, $^3J_{\text{C-P}} = 2.7$ Hz) 130.8 (s) 130.9 (s) 130.8 (s) 130.4 (s) 7.3 (s)	128.2 (d, $^1J_{\text{C-P}} = 67.2$ Hz) 135.1 (d, $^2J_{\text{C-P}} = 14.7$ Hz) 129.7 (d, $^3J_{\text{C-P}} = 12.5$ Hz) 132.8 (s) 132.1 (d, $^1J_{\text{C-P}} = 68.7$ Hz) 129.4 (s) 128.0 (s) 52.3 (d, $^3J_{\text{C-P}} = 4.6$ Hz) 126.7 (s) 135.8 (s) 129.7 (s) 131.9 (s) 10.8 (s)	136.5 (d, $^1J_{\text{C-P}} = 72.7$ Hz) 130.1 (d, $^2J_{\text{C-P}} = 13.4$ Hz) 132.4 (d, $^3J_{\text{C-P}} = 10.2$ Hz) 133.9 (s) 144.9 (s) 117.4 (s)
^{15}N NMR (61MHz)	N ¹ N ^{2,3} N ⁴	-136.8 (d, $^2J_{\text{N-P}} = 9.0$ Hz) -2.2 (s), 11.7 (s) -33.0 (d, $^2J_{\text{N-P}} = 12.2$ Hz)		

NMR analysis of the mother liquor, after crystallisation, and separation of **6**, provided diagnostic signals that can be ascribed to the remnant moiety of starting complex **4**, either as the bis(1-benzyltetrazole) or the corresponding bis(benzylcyanamide) if dinitrogen elimination occurred. ^1H NMR spectra signals at δ 5.81 can tentatively be ascribed to the

benzyl protons. ^{13}C NMR singlet peaks at δ 52.9 and 145.7 are assigned to the benzyl- CH_2 and C_5 -*ipso* carbons, respectively.

The ^1H NMR data for the N-bonded tetrazolylphosphine gold halide **7**, shows the acidic CH resonance at δ 9.05, a small upfield shift with respect to 1*H*-tetrazole (δ 9.32). $^{13}\text{C}\{^1\text{H}\}$ NMR data indicates an insignificant downfield shift for the tetrazolyl carbon resonance (singlet at δ 144.9) relative to 1*H*-tetrazole (δ 143.3).

The ^{31}P NMR spectrum of **7** contains a single peak at δ 117.37, this significant downfield resonance can be attributed to the deshielding ability of the tetrazolate anion. The acquisition of high resolution ^{15}N NMR-spectra was not possible due to the instability of **7** in solution.

Mass spectrometry

Mass spectra data for complexes **4**, **5** and **6** are summarised in Table 2.15. The positive-ion FAB-MS spectrum of complex **4** contained apart from the matrix peaks (m/z 136, 154 and m/z 307), two strong molecular ion (M^+) peaks (m/z 578/576 $^{37}\text{Cl}/^{35}\text{Cl}$). Diagnostic fragmentation patterns include the loss of chlorine (m/z 541), and the dechlorinated cation with further loss of dinitrogen (m/z 513).

Table 2.15 Mass spectrometric data for **4-6**

Complex	m/z (%)		
	4	5	6
$\{[\text{M}]^{37}\text{Cl}\}^+$	578 (3)	576 (7)	-
$\{[\text{M}]-\text{Cl}\}^+$	541 (15)	539 (2)	-
$\{[\text{M}]-\text{ClN}_2\}^+$	513 (18)	-	-
$\{[\text{M}]-\text{AuCl}\}^+$	-	342 (65)	-
$\{[\text{M}]-\text{ClAuPPh}_2\}^+$	-	-	419 (2)
$\{\text{Ph}_2\text{PPPh}_2\}^+$	-	-	370 (16)

Electron ionisation mass spectra of complex **5** display a similar fragmentation to the analogous tetrazole compound. Distinctive molecular ion isotope peaks at (m/z 576/574 $^{37}\text{Cl}/^{35}\text{Cl}$) are present, which fragment with a loss of chlorine (m/z 539), and further loss of Au (m/z 342). The electron ionisation mass spectra of complex **6** has no molecular ion peak but showed distinct isotope peaks at (m/z 419/417 $^{37}\text{Cl}/^{35}\text{Cl}$) for ClAuPPh_2 which represents one half of the molecule. The free diphosphine ligand, Ph_2PPPh_2 appears at m/z 370. Due to rapid decomposition in air, identified by a violet discolouration as evidence of

fine metallic gold deposition, no significant mass spectrometric data could be obtained for complex **7**.

B. Structure determination of complexes of **5** and **6**.

The molecular structure of complex **5** is represented in Figure 2.12. Selected bond lengths and bond angles are given in Table 2.16, numbered according to Figure 2.7. The only entry of compound **5**, in the Cambridge Crystallographic database, was reported by Burini co-workers¹⁵ with crystal reflections in this instance collected at room temperature. Apart from a comparison to this given data, changes upon complexation observed from the structural characterisation of free ligand, BzimPPh₂, are discussed here.³⁸

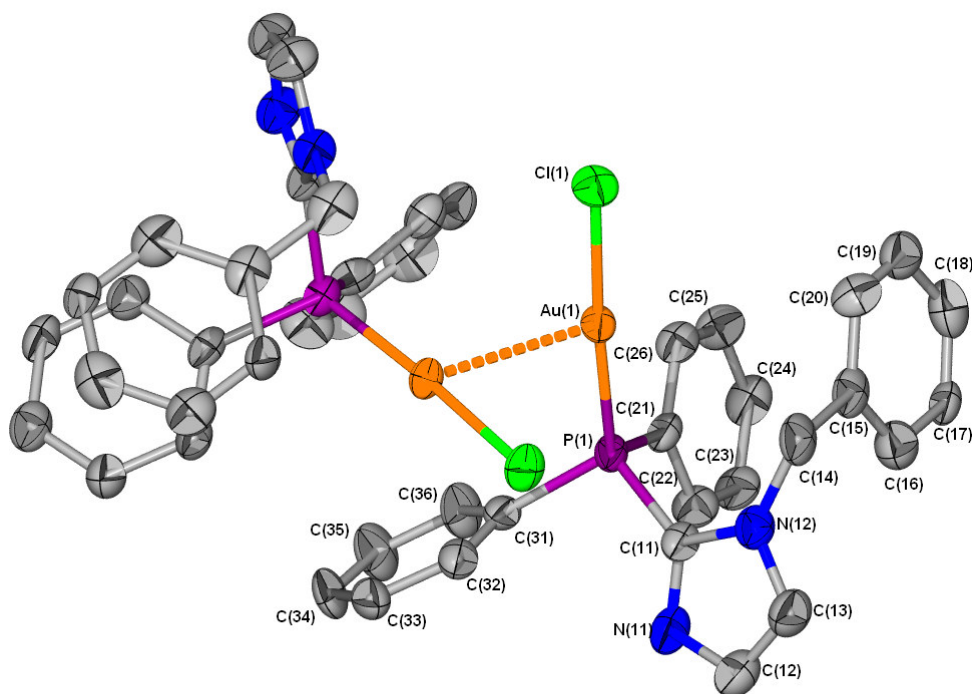


Figure 2.12 Molecular structure of **5** showing the numbering scheme; hydrogen atoms omitted for clarity.

Crystallisation of **5** from a concentrated dichloromethane solution layered with *n*-hexane at -20 °C, afforded colourless monoclinic crystals in the C2/c space group. The unit cell reported by Burini and co-workers for **5** [*a* = 18.068(2), *b* = 16.576(2), *c* = 15.391(2), $\alpha = \gamma = 90^\circ$, $\beta = 117.2(2)$, *V* = 4100(7)] is slightly larger than what we report here, [*a* = 17.978(3), *b* = 16.395(2), *c* = 15.163(2), $\alpha = \gamma = 90^\circ$, $\beta = 118.078(2)$, *V* = 3943.4(10), reflections collected at 100 K] which is to be expected from the crystal data acquisition at higher temperature.

The structure can be described as discrete linear two coordinate units, assembling in the unit cell as dimeric units. The Au-P [2.2325(16) Å] and Au-Cl [2.3055(15) Å] bond lengths are similar to those found in other gold(I) phosphine halides, e.g. [AuCl(PPh₃)], 2.235(3) Å and 2.279(3) Å for Au-P and Au-Cl bonds, respectively.⁵¹ This suggests that a mono-substitution of a phenyl for a heterocyclic ring does not alter the bond lengths substantially. However, this result is in contrast to, tri-substituted azole phosphine gold(I) chlorides **1a** [Au-P 2.2174(3) Å and Au-Cl 2.276(1) Å], **1b** [Au-P 2.226(9) Å and Au-Cl 2.290(9) Å] and **2** [Au-P 2.169(8) Å and Au-Cl 2.290(8) Å], which reveal a significant shortening of these bonds, indicative of a more tetrahedral coordination.

If bond distances (P-C_{Ph} and P-C_{im}) and bond angles (C_{Ph}-P-C_{Ph}, C_{Ph}-P-C_{im} and N1-P-N2) of the free ligand, BzimPPh₂, are compared to the same structural parameters in **5** after coordination, no significant variations are noted in the bond lengths. However, all the bond angles about the phosphorus atom, become larger and the most notable deviation, of 4-5° is for the C_{ph}-P-C_{ph} angle. The external angles about the phosphorus atom, Au(1)-P(1)-C(11), Au(1)-P(1)-C(21) and Au(1)-P(1)-C(31) are expanded from the ideal tetrahedral angles (109.5°) to 113.9(2)°, 112.7(2)° and 114.9(2)°, respectively. In addition,

Table 2.16 Selected bond lengths (Å) and angles (°) for complex **5** with e.s.d.s in parenthesis

Bond lengths		Bond angles	
Au(1)-P(1)	2.233(2)	P(1)-Au(1)-Cl(1)	175.58(6)
Au(1)-Cl(1)	2.306(2)	P(1)-Au(1)-Au(1)	97.84(4)
P(1)-C(11)	1.792(6)	Cl(1)-Au(1)-Au(1)	86.58(5)
P(1)-C(21)	1.809(7)	C(11)-P(1)-C(21)	105.2(3)
P(1)-C(31)	1.813(7)	C(11)-P(1)-C(31)	102.4(3)
N(11)-C(11)	1.308(8)	C(21)-P(1)-C(31)	106.8(3)
N(11)-C(12)	1.356(9)	C(11)-P(1)-Au(1)	113.9(2)
C(11)-N(12)	1.380(8)	C(21)-P(1)-Au(1)	112.7(2)
N(12)-C(13)	1.365(9)	C(31)-P(1)-Au(1)	114.9(2)
Au(1)-Au(1)	3.0296(7)	N(11)-C(11)-N(12)	110.0(5)
		N(11)-C(11)-P(1)	124.0(5)
		N(12)-C(11)-P(1)	125.9(5)
		C(26)-C(21)-P(1)	120.5(5)
		C(22)-C(21)-P(1)	121.0(6)

the external angles at the azolyl C11 in the phosphine ligand are altered upon coordination. The angle P-C11-N11 becomes smaller [128.6(5)° to 124.0(5)°] and the angle P-C11-N12 becomes larger [121.5(5) to 125.9(5)°]. The two-coordinate centre is distorted from the linearity of the P-Au-Cl angle, at 175.58(6)° [lit. 175.1(3)°]¹⁵ found in

⁵¹ N. C. Baenziger, W. E. Bennet and D. M. Soboroff, *Acta Crystallogr.*, **B32**, 1976, 962.

[AuCl(PPh₃)] [179.68(8)°].⁵¹ The angles about the gold centre are comparable to values reported above for **1a** [174.06(4)°] and **1b** [174.30(3)°]. Both the phenyl and the imidazolyl rings are planar.

Characteristic, short intermolecular aurophilic interactions at 3.0296(7) Å, which is less than the van der Waals radius for gold (3.4 Å), are observed. Compared to other gold(I)-halides, containing azolyphosphines, this distance is less than in the polymorphic structures **1a** [3.456(2) Å] and **1b** [3.3459(3) Å] and **2** [3.0393(3) Å]. This weak interaction, aggregates complex **5** as dimers, and governs the packing in the crystal lattice as shown in Figure 2.13. This is in contrast to the related compound, 2-(diphenylphosphine)-1-methylimidazolegold(I) chloride, which appears as a monomeric structure containing no intermolecular metal contacts, with the closest separation greater than 6.8 Å.⁵² Four pairs of dimers fill the monoclinic C2/c space group, and organise in regular rows along the a-axis, with the gold atoms pointing towards the centre. Each row is related to the next by a glide plane parallel to the c-axis. The torsion angle between the Au(1)-P-C(11) plane and the plane [Au(1)-Au(1)] parallel to the symmetry-generated gold centre approaches 90°, due to the steric bulk of the phosphorus substituents, allow for the most efficient packing in the crystal lattice.

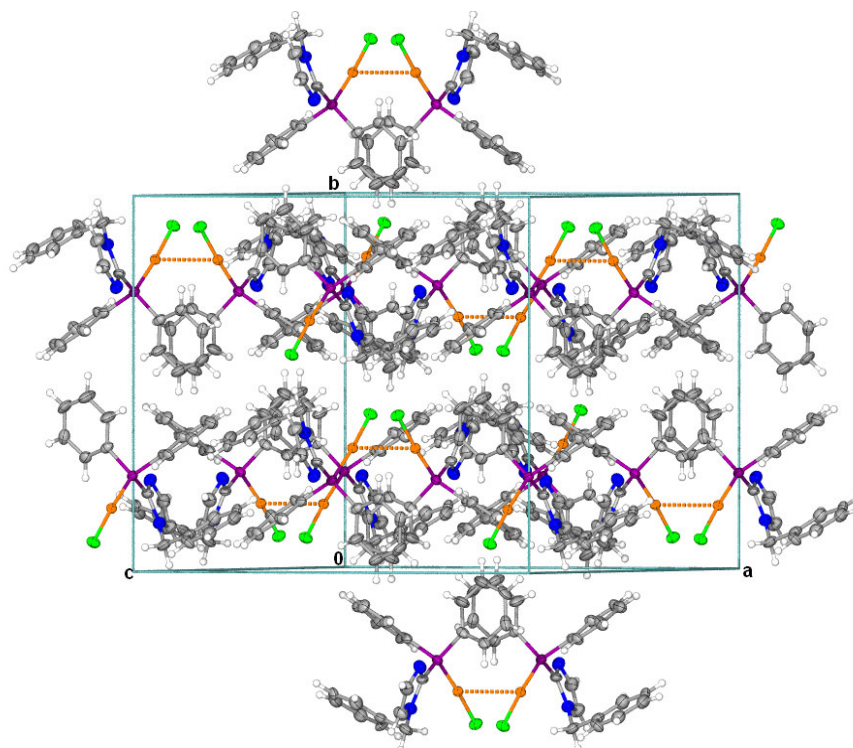


Figure 2.13 Unit cell and packing pattern in the crystal lattice of **5** viewed along the a-axis.

⁵² V. J. Catalano and S. J. Horner, *Inorg. Chem.*, 2003, **42**, 8430.

The molecular structure and numbering scheme of complex **6** is represented in Figure 2.14. Selected bond lengths and bond angles are given in Table 2.17, numbered according to Figure 2.14(a). Off-white, oval crystals of **6** crystallised from a concentrated dichloromethane solution at 5 °C, in an orthorhombic Pbcn space group. The asymmetric unit is shown in Figure 2.14(b).

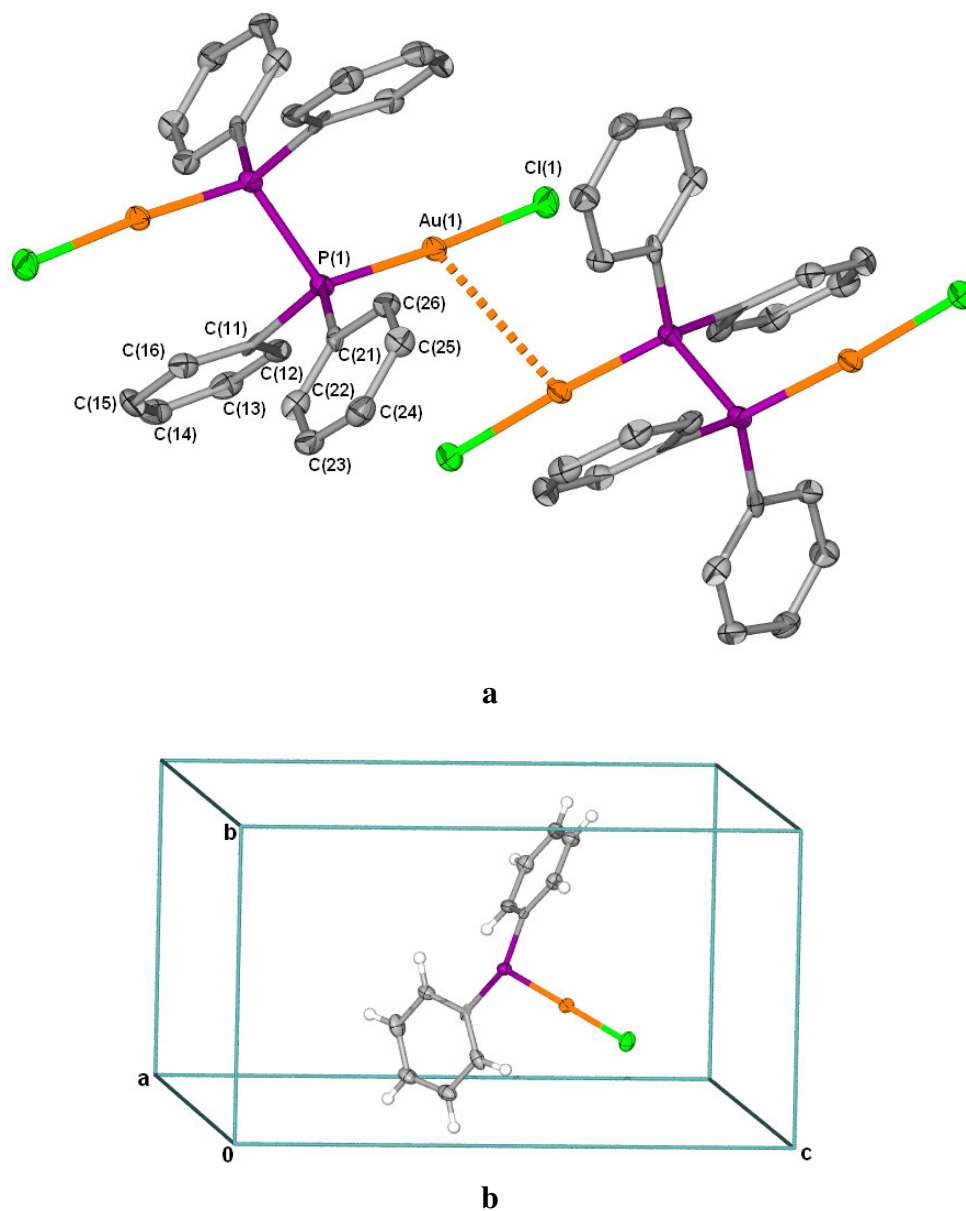


Figure 2.14 a) Two dinuclear molecules of **6**, related by a centre of symmetry and showing the intermolecular Au...Au contacts; hydrogen atoms omitted for clarity; b) unit cell containing the asymmetric unit viewed along the a-axis.

The structure can be described as a dinuclear molecule that is linear thus two-coordinate about the two metal centres, with the P-Au-Cl angle at 176.03(6)°. The Au-P [2.235(2) Å] and Au-Cl [2.281(2) Å] bond lengths are similar to those found in other gold(I)phosphine

halides, e.g. [AuCl(PPh₃)] [2.235(3) Å and 2.279(3) Å for Au-P and Au-Cl bonds, respectively].⁵¹ The typical shortening of the Au-P bond, compared to other group 11 elements, has been attributed to d_π-d_π back bonding.⁵³ The P-P bond of 2.233(3) Å is not greatly effected upon coordination, and is only slightly larger than the corresponding bond in the free diphosphine ligand (2.217 Å).⁵⁴ The most notable modifications after two coordination by the diphosphine ligand, are all the external bond angles about the phosphorus atom, with the angle C_{Ph}-P-C_{Ph} enlarged between 10-11°.

Table 2.14 Selected bond lengths (Å) and angles (°) for complex **6** with e.s.d.s in parenthesis

Bond lengths		Bond angles	
Au(1)-P(1)	2.235(2)	P(1)-Au(1)-Cl(1)	176.03(6)
Au(1)-Cl(1)	2.281(2)	P(1)-Au(1)-Au(1)	106.35(4)
P(1)-C(21)	1.863(6)	Cl(1)-Au(1)-Au(1)	77.26(4)
P(1)-C(11)	1.921(6)	C(21)-P(1)-C(11)	109.9(2)
P(1)-P(1)	2.233(3)	C(11)-P(1)-P(1)	103.3(2)
Au(1)-Au(1)	3.2933(7)	C(21)-P(1)-P(1)	103.5(2)
		C(11)-P(1)-Au(1)	114.9(2)
		P(1)-P(1)-Au(1)	110.70(9)
		C(22)-C(21)-C(26)	123.0(5)
		C(22)-C(21)-P(1)	121.8(4)
		C(22)-C(21)-P(1)	121.8(4)
		C(26)-C(21)-P(1)	115.2(4)

The dinuclear complex further assembles in the unit cell as dimeric units, by short intermolecular aurophilic interactions at 3.2933(7) Å. The Au...Au distance falls within the range typical of other gold(I) dimers reported in this work and in the literature (2.76-3.10 Å).^{55,56} Somewhat related 2:1 gold(I) chloride complexes of bis(diphenylphosphine), with the phosphorus atoms bridged by one to three carbon atoms, can assume different structural conformations.⁴⁷ Digold complexes of 1,2-bis(diphenylphosphine)methane, [(Ph₂P)₂CH₂](AuCl)₂, arrange as monomeric complexes with intramolecular Au...Au interactions, made possible by a staggered conformation of the Cl-Au-PPh₂ units about the P-CH₂ axis.⁵⁷ The complex of 1,2-bis(diphenylphosphine)ethane, [(Ph₂P(CH₂)₂PPh₂)(AuCl)₂, has been reported in two polymorphic forms, as dimeric units connected by intermolecular gold contacts related by a centre of symmetry and as polymeric chains, with metal contacts generated by translation.⁵⁸ The analogous propyl bridged complex, [(Ph₂P(CH₂)₃PPh₂)(AuCl)₂ aggregates in the crystal lattice as polymeric chains where

⁵³ P. Schwerdtfeger, H. L. Hermann and H. Schmidbaur, *Inorg. Chem.*, 2003, **42**, 1334.

⁵⁴ A. Dashti-Mommertz and B. Neumüller., *Z. Anorg. Allg. Chem.*, 1999, **625**, 954.

⁵⁵ H. C. Jaw, M. M. Savas, R. D. Rogers and W. R. Mason, *Inorg. Chem.*, 1989, **28**, 1028.

⁵⁶ M. N. I. Khan, J. P. Fackler, Jr., C. King, J. C. Wang and S. Wang, *Inorg. Chem.*, 1988, **27**, 1642.

⁵⁷ H. Schmidbaur, A. Wohlleben, F. Wagner, O. Orama and G. Huttner, *Chem. Ber.*, 1977, **110**, 1748.

⁵⁸ P. Bates and J. M. Waters, *Inorg. Chim. Acta.*, 1985, **98**, 125.

adjacent molecules are related by glide plane along the b-axis.⁵⁹ Similarly, complex **6**, forms polymeric chains by intermolecular aurophilic interactions, which can be reproduced by a glide plane along the c-axis. The individual gold coordination centres, Cl-Au-P, are arranged away from each other in the molecular unit, and are crossed to affect a dihedral angle, P-Au-Au-P and Cl-Au-Au-Cl, of approximately 45° to allow for efficient gold contact. Furthermore, as can be seen in Figure 2.15, the metal contacts arrange the sheets of molecules along the a-axis in a zigzag conformation.

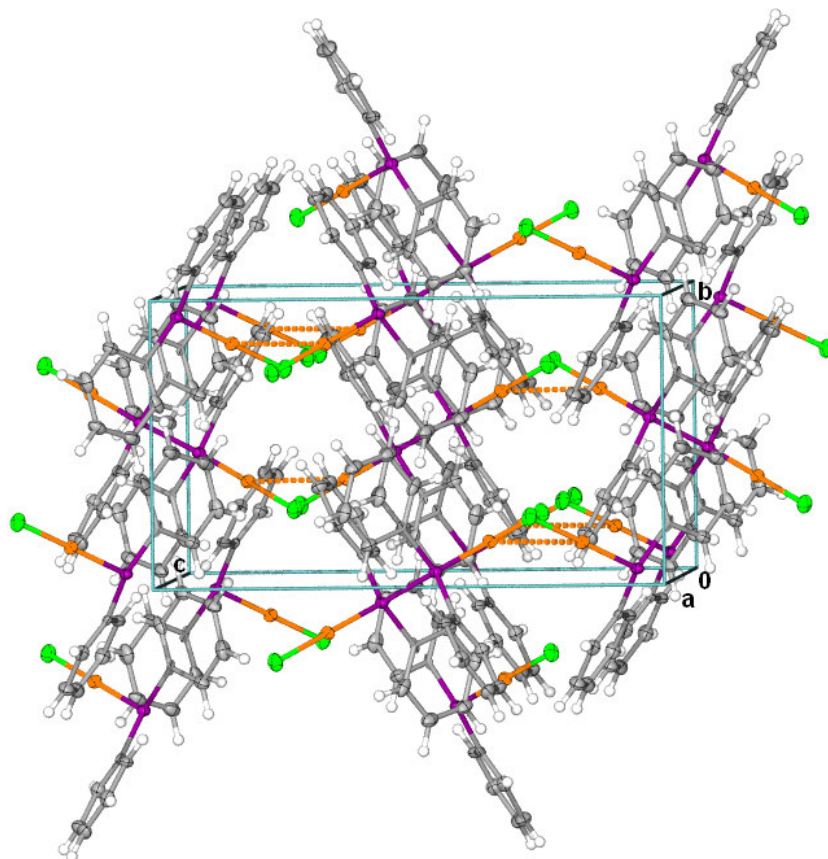


Figure 2.15 Unit cell and packing pattern showing the catenated lattice structure of **6** with Au(I)...Au(I) interactions, propagated in the c-axis, linking sheets in the a-axis in a zigzag pattern.

2.2.3 Reactions involving azolyphosphine gold(I) complexes

In section 2.2.3 the modification of simple gold(I) halides that contain functionalised phosphines as discussed in section 2.2.1 and 2.2.2, is described. A reported synthesis towards N-heterocyclic-carbene(NHC)(phosphine)gold(I) complexes, will be revisited. The idea of using gold(I) complexes containing bifunctional ligands as soft donor “ligands” to secondary gold centres, in the formation of unsymmetrical 5-membered

⁵⁹ M. K. Cooper, L. E. Mitchell, K. Henrick, M. Mcpartlin and A. Scott, *Inorg. Chim. Acta.*, 1984, **84**, L9.

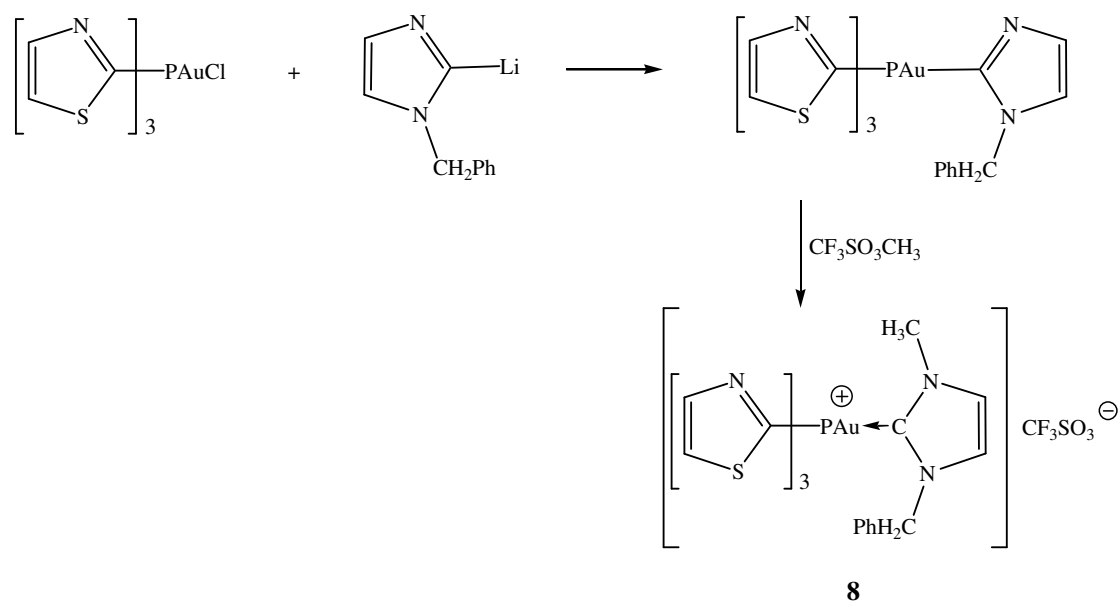
auracycles, will be explored. The unexpected spontaneous assembly of a novel mixed Au(I), Au(II) tetranuclear complex bridged by a unique ligand, will conclude the chapter.

2.2.3.1 Reactions with azolyllithium; reactions towards the preparation of monocarbene gold(I) complexes.

A. Preparation of (1-benzyl-4-methylimidazol-2-ylidene)tris(thiazolyl-2-yl)phosphinegold(I) **8**, from gold halide **1**.

The facile preparation of aurate complexes from thiazol- and imidazol-2-yl lithium reagents, has been developed into an eloquent route towards heterocyclic carbene complexes, which may then be obtained by alkylation or protonation of the carbene precursor aurate complexes.⁶⁰ Various neutral and cationic diamino and amino(thio) carbene complexes of gold(I) have since been prepared. A complicating reaction occurs during the preparation of gold(I) complexes with mixed ligands: monocarbene-phosphine complexes of gold(I), spontaneously rearranged to form preferred cationic homoleptic gold(I) compounds.⁶⁰

We attempted to apply this method to gold moieties that contain, stronger bonding tertiary phosphine ligands. Thus, the aim was to ascertain whether i) the phosphinegold(I) halide, **1**, could be transmetallated by lithium salts of 1-benzylimidazol-2-yl and 4,5-dimethylthiazol-2-yl; ii) similar spontaneous rearrangements would occur and iii) the new monocarbene gold(I) complexes could be isolated in pure form (Scheme 2.8).

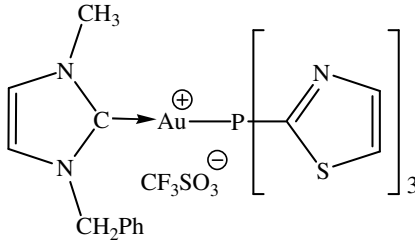


Scheme 2.8 Preparation of the cationic diamino carbene complex **8**.

⁶⁰ H. G. Raubenheimer and S. Cronje, *J. Organomet. Chem.*, 2001, **617-618**, 170-181.

Firstly, the reaction of 1-benzylimidazol-2-yllithium with chloro(azolyl)phosphinegold(I) **1**, followed by alkylation with CF₃SO₃Me (all at -78 °C) afforded **8** as colourless crystals in high yield after workup (Scheme 2.8). The analytical data for complex **8** is summarised in Table 2.14. Recrystallisation by slow diffusion of diethyl ether in a solution of dichloromethane at -20 °C, afforded off-white, cubic crystals. However, due to serious flaws within these crystals, no X-ray structure analysis could be performed.

Table 2.14 Analytical data for complexes **8**

Complex	 <p style="text-align: center;">8</p>
M.p./°C	138 (decomp)
Colour	off-white
Yield(%)	93
<i>M_r</i>	800.96
Analysis(%)*	C ₂₁ H ₁₈ N ₅ O ₃ S ₄ F ₃ PAu
C	31.33 (31.47)
H	2.29 (2.26)
N	8.90 (8.74)

* Required calculated values given in parenthesis

B. Spectroscopic characterisation of **8**

Nuclear magnetic resonance spectroscopy

The ¹H, ¹³C{¹H}, ³¹P{¹H} NMR spectroscopic data for complex **8** are summarised in Table 2.15.

In the ¹H NMR spectrum of **8**, signals for the N-CH₃ (δ 3.90) and thiazolylphosphine protons show distinct allylic coupling (δ 8.23, d, ³J_{H-H} = 3.0 Hz and 7.95, dd, ³J_{H-H} = 3.1 Hz, ⁴J_{H-P} = 2.1 Hz). All three sets of protons integrate for approximately three protons. The protons in the 4 and 5 position on the imidazole ring can not clearly be distinguished from the aromatic proton resonances. However, the broad multiplet (δ 7.36 - 7.43) integrates for the correct number of protons.

The ^{13}C NMR signals of the phosphine ligand are well resolved, showing phosphorus coupling to the *ipso*-carbon (δ 157.6, d, $^1J_{\text{C-P}} = 87.4$ Hz) and long range coupling to the carbon in the 4 position of the thiazole ring (δ 147.4 $^3J = 22.0$ Hz). The carbene carbon resonance appears as a weak singlet signal at δ 184.9, consistent with literature values of similar compounds (see also monocarbene gold(I) complexes of tetrazoles in Chapter 4).³²

Table 2.15 ^1H , $^{13}\text{C}\{^1\text{H}\}$, $^{31}\text{P}\{^1\text{H}\}$ NMR data for **8**

Complex	<p style="text-align: center;">8</p>
Solvent	CD_2Cl_2
Temperature (K)	298
^1H NMR (300 MHz)	$\text{H}^{4'}$ 8.23 (d, 3H, $^3J = 3.0$ Hz) $\text{H}^{5'}$ 7.95 (dd, 3H, $^3J = 3.1$ Hz, $^4J_{\text{H-P}} = 2.1$ Hz) H^6 5.37 (s, 2H) H^{8-10} 7.36-7.43 (m, 5H) H^{11} 3.90 (s, 3H) $\text{H}^{4,5}$ 7.37-7.38 (m, 2H)
$^{13}\text{C}\{^1\text{H}\}$ NMR (75 MHz)	C^2 184.9 (s) $\text{C}^{4,5}$ 122.6(s), 124.2(s) C^6 53.6 (s) C^7 136.9 (s) $\text{C}^8, \text{C}^{8'}$ 129.8 (s) $\text{C}^9, \text{C}^{9'}$ 129.2 (s) C^{10} 129.8 (s) C^{11} 36.5 (s) $\text{C}^{2'}$ 157.6 (d, $^1J_{\text{C-P}} = 87.4$ Hz) $\text{C}^{4'}$ 147.4 (d, $^3J = 22.0$ Hz) $\text{C}^{5'}$ 128.5 (s)
$^{31}\text{P}\{^1\text{H}\}$ NMR (121MHz)	CF_3SO_3 121.2 (q, $^1J_{\text{C-F}} = 322.1$ Hz) P -2.00 (s)

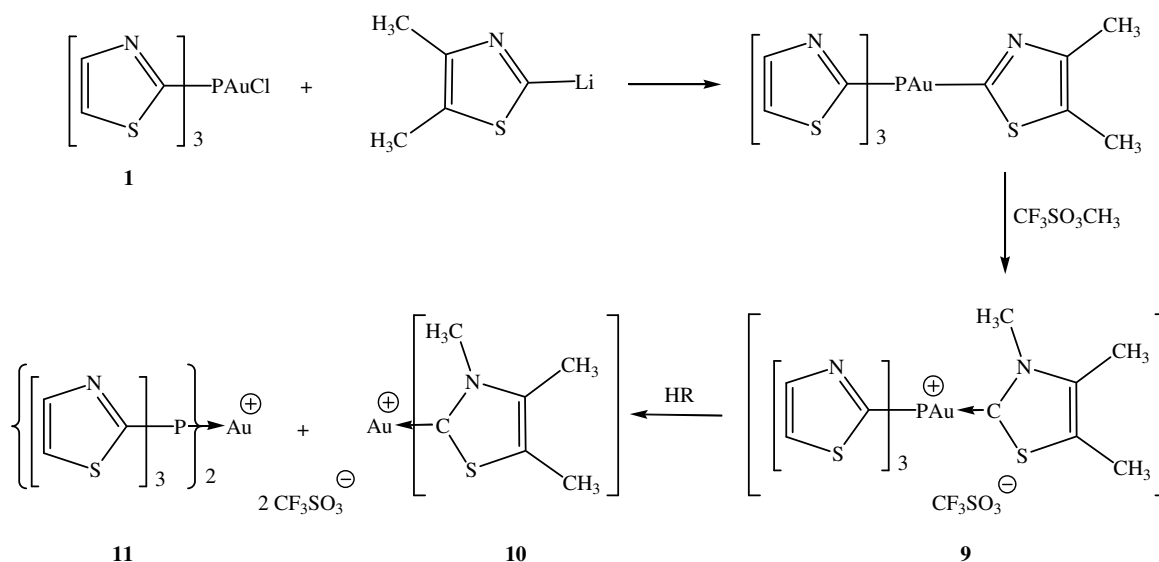
The ^{31}P NMR spectrum of complex **8** contains a single, signal at δ -2.0, which represents a insignificant upfield shift ($\Delta\delta$ 3.0) relative to the parent complex **1**.

Mass spectrometry

The molecular ion peak was not observed in the mass spectra, only m/z values pertaining to the free thiazolylphosphines [m/z 283 (13) and 199 (100)], and fragments thereof, as previously reported for complex **1**, were visible.

A. The homoleptic rearrangement of monocarbene complex **9**.

Various thiazolylidene complexes, containing strongly bonded neutral and anionic ligands (eg. PPh_3 , C_6F_5 and CN) as well as azolyls or carbenes - the latter obtained by the alkylation or protonation of gold aurates, have been described.⁶¹ Complementary to that study we now report the reaction of 2-lithio-4,5-dimethylthiazol-2-yl with chloro[tris(thiazol-2-yl)phosphine]gold(I) **1** (Scheme 2.9). The complex product spectrum that was obtained corresponded to cationic gold(I) products, **10** and **11**, that contain like ligands as propagated by spontaneous homoleptic rearrangement (HR).



Scheme 2.9 The reaction of 2-lithio-4,5-dimethylthiazol-2-yl with chloro[tris(thiazol-2-yl)phosphine]gold(I) **1**.

We now found the reaction of the lithium salt of 4,5-dimethylthiazol-2-yl and gold(I)-halide **1** at low temperature (-78°C), followed by alkylation with $\text{CF}_3\text{SO}_3\text{Me}$, produced a complex reaction mixture. Through careful interpretation of ^1H , ^{13}C and ^{31}P NMR spectra, assignments of resonances in the spectra were made by correlation with known literature compounds. It became clear that the products **10** and **11** each contain two similar ligands and that a homoleptic rearrangement had occurred.

⁶¹ H. G. Raubenheimer, F. Scott, G. J. Kruger, J. G. Toerien, R. Otte, W van Zyl, I. Taljaard, P. Olivier and L. Linford, *J. Chem. Soc., Dalton. Trans.*, 1994, 2091.

The ^{31}P NMR spectrum of the crude reaction mixture, shows broad singlet signals, which can be ascribed to the rearrangement and formation of phosphorus-containing like-ligand gold(I) cations (Figure 2.16). This is in contrast to the aforementioned complex **8**, which revealed a sharp singlet peak at δ -2.0 and indicated the absence of other products.

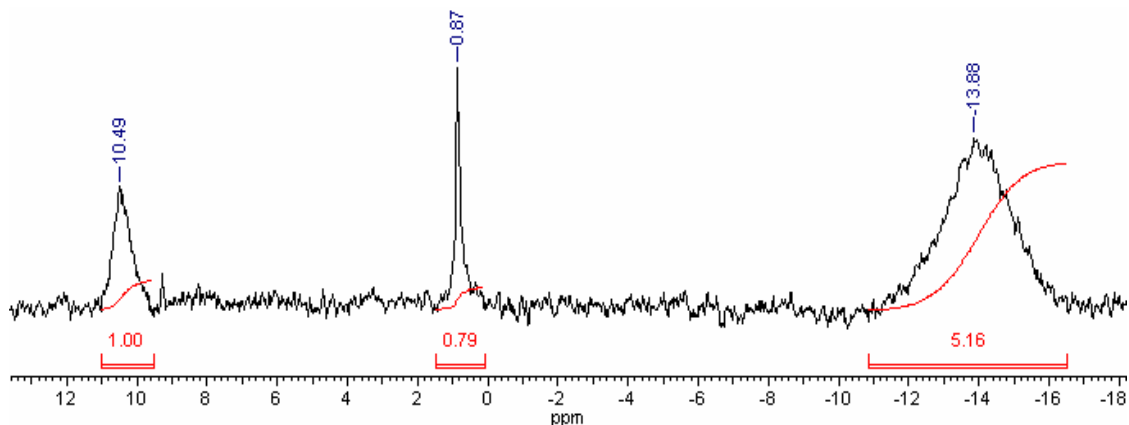


Figure 2.16 The broad signals (δ 10.49 and δ -13.88 ppm) in the ^{31}P NMR pertaining possibly to monocarbene complex **9** and the formation of rearranged phosphine complex **11**. The sharp singlet peak (δ 0.87) is assigned to the reactant complex **1**.

^1H NMR data reveals a duplication of proton resonance signals, which supports the presence of **10** (^{31}P at δ 10.49) and **9** (^{31}P at δ -13.88), assigned previously to the allylic protons on the thiazolyphosphine. These two sets integrate in a similar 1:5 ratio that is seen in the ^{31}P NMR spectra. This result is in contrast to the trend in related bis(phosphine)gold(I) cations, e.g. $[\text{AuCl}(\text{PPh}_3)]$ (δ ca. 34), $[\text{Au}(\text{PPh}_3)_2]$ (δ ca. 38), and $[\text{Au}(\text{PMe}_3)\text{Cl}]$ (δ ca. -9.0) and $[\text{Au}(\text{PMe}_3)_2]$ (δ ca. 8.4). A duplication of NCH_3 signals at δ 4.10 - 4.30 can be assigned to the biscarbene complex **11** which compares well with the analogous 4-methylthiazolylidene complex reported mentioned above (NCH_3 δ 4.33, Scheme 2.9). ^{13}C NMR reveals a carbene carbon as a doublet resonance at 202.79 ($J = 129$ Hz), with a phosphorus-carbon coupling comparable to that experienced by the monocarbene carbon reported previously (δ 209.8, $J = 129$ Hz).

Mass spectrometry

The low resolution positive-ion FAB-MS of the crude reaction mixture of **9** supports the formation of the rearranged gold(I) product. The molecular ion peak of **9b** (m/z 451) and fragmentation peaks thereof $\{m/z$ 421, $([\text{M}]-2\text{Me})^+\}$ can be identified. Attempts to resolve the complex product spectrum were hampered by the instability of the products. Attempted separation, using solvent extraction followed by selective crystallisation in

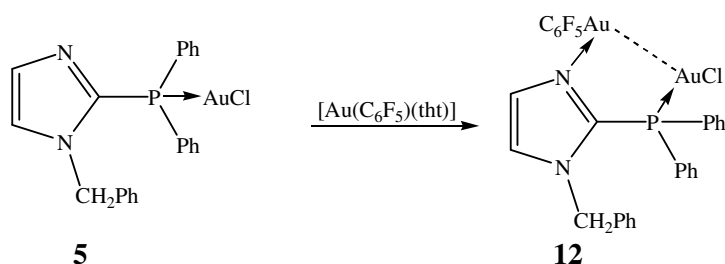
different solvent systems, failed to produce suitable crystals for single crystal structure determination.

2.2.3.2 Azolyphosphine complexes **3** and **5** as *P,N*-ligands-Reactions towards metallocyclic complexes.

An important feature of gold complexes derived from phosphine ligands containing imidazole moieties, is that they can act as secondary ligands to other metals. In our study we attempted to exploit the soft-donor potential of the nitrogen atom on the imidazole ring by coordinating gold atoms to these sites. This should furnish neutral dinuclear complexes with phosphine bridging ligands across two unlinked metal centres, from complex **5** and **3** respectively.

A. Preparation of chloro[1-benzyl-*N*-pentafluorophenylgold(I)imidazol-2-yl](diphenyl)phosphinegold(I), **12**, from complex **5**.

The treatment of equimolar amounts of substrate **5** with freshly prepared pentafluorophenyl(tetrahydrothiophene)gold(I), [Au(C₆F₅)(tht)], readily affects the substitution of the thioether ligand, to yield, after simple workup, neutral imine complex **12**, an air stable, colourless crystalline product (Scheme 2.10). This binuclear complex is readily soluble in polar solvents such as dichloromethane, thf and acetone. Recrystallisation from concentrated dichloromethane solution, carefully layered with *n*-hexane, at -20 °C, provided suitable crystals for X-ray analysis. The analytical data for complex **12** is summarised in Table 2.16.



Scheme 2.10 Preparation of dinuclear auracyclic complex **12**.

When this procedure was repeated in order to prepare the analogous product, chloro[1-benzyl-*N*-pentafluorophenylgold(I)tetrazol-2-yl(diphenyl)]phosphinegold(I), using **4** as ligand, low yields and an impure product containing colloidal gold were obtained. This result could not be attributed to the insufficient N-donor capabilities of 1-benzyltetrazole, considering that this compound readily forms the 3-*N*-imine pentafluorogold(I) complex

(Chapter 3 in this dissertation). The noted instability of **4** in solution (section 2.2.2), can partly be responsible for the failure to produce the P,N-coordinated derivative.

Table 2.16 Analytical data for complex **12**

Complex	<p style="text-align: center;">12</p>
M.p./°C	117 °C (decomp.)
Colour	colourless
Yield(%)	73
M_r	938.02
Analysis(%)*	$C_{28}H_{19}N_2F_5ClPAu_2$
C	36.10 (35.82)
H	2.22 (2.04)
N	3.14 (2.98)

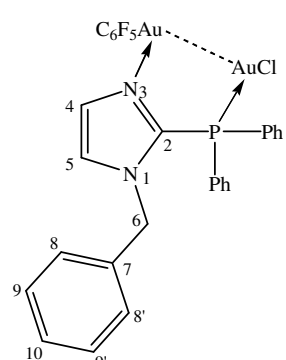
* Required calculated values given in parenthesis

B. Spectroscopic characterisation of **12**.

Nuclear magnetic resonance spectroscopy

The 1H , $^{13}C\{^1H\}$, $^{31}P\{^1H\}$ NMR spectroscopic data for compound **12** are summarised in Table 2.17. The relative chemical shifts of the dinuclear complex **12**, can be compared to that of the parent complex, **5**, as both NMR spectra were recorded in deuterated dichloromethane. The 1H NMR spectrum shows a slight upfield shift and broadening of the signal assigned to the benzylic protons ($\Delta\delta$ 0.32, δ 5.30). The broadened incompletely resolved signal can be ascribed to H-P coupling across N^1 , in contrast to the sharp singlet found for the same proton in **5**. The two distinct sets of doublets of doublets - both integrating for single protons and representing two chemically non-equivalent nuclei, are assigned to allylic protons H^4 and H^5 .

Table 2.17 ^1H , $^{13}\text{C}\{^1\text{H}\}$ and $^{31}\text{P}\{^1\text{H}\}$ NMR data for **12**

Complex	 <p style="text-align: center;">12</p>	
Solvent Temperature (K) ^1H NMR (300 MHz) $^{13}\text{C}\{^1\text{H}\}$ NMR (75 MHz) $^{31}\text{P}\{^1\text{H}\}$ NMR (121MHz) ^{19}F NMR (376 MHz)	CD_2Cl_2 298 H^4 6.83 (dd, 1H, $^3J = 7.2$ Hz, $^4J_{\text{H-P}} = 1.6$ Hz) H^5 7.23 (dd, 1H, $^3J = 7.8$ Hz, $^4J_{\text{H-P}} = 1.9$ Hz) H^6 5.30 (bs, 2H) H^{8-10} 7.18-7.44 (m, 5H) PPh 7.42-7.72 (m, 10H) PPh-C ^{ipso} 124.8 (d, $^1J_{\text{C-P}} = 65.3$ Hz) PPh-C ^{ortho} 134.8 (d, $^2J_{\text{C-P}} = 14.8$ Hz) PPh-C ^{meta} 130.5 (d, $^3J_{\text{C-P}} = 12.7$ Hz) PPh-C ^{para} 133.0 (s) C^2 133.4 (d, $^1J_{\text{C-P}} = 63.1$ Hz) C^4 129.8 (s) C^5 127.7 (s) C^6 53.3 (s) C^7 128.1 (s) $\text{C}^8, \text{C}^{8'}$ 141.2 (s) $\text{C}^9, \text{C}^{9'}$ 129.4 (s) C^{10} 133.4 (s) $\text{C}_6\text{F}_5\text{-C}^{\text{ipso}}$ 117.7 (m) $\text{C}_6\text{F}_5\text{-C}^{\text{ortho}}$ 149.6 (ddm, $J_{\text{C-F}} = 231.0$, $J_{\text{C-F}} = 28.0$ Hz) $\text{C}_6\text{F}_5\text{-C}^{\text{meta}}$ 127.0-135.0 (overlap, m) $\text{C}_6\text{F}_5\text{-C}^{\text{para}}$ 127.0-135.0 (overlap, m) P 17.24 (s) F^{ortho} -114.7 (m) F^{meta} -162.7 (m) F^{para} -161.4 (t, $J = 21.3$ Hz)	

Apart from an allylic $^3J_{\text{H-H}}$ coupling of 7.17 and 7.78 Hz, long range $^4J_{\text{H-P}}$ coupling of 1.60 and 1.95 Hz across the nitrogen atom was noted, for H^4 and H^5 respectively. Similar coupling patterns cannot be observed in complex **5** due to overlap with the aromatic signals. No assumption could thus be made on whether complexation at N^3 , favours longer range coupling of the allylic protons to the phosphorus atom or not.

The ^{13}C NMR spectrum of **12** shows distinctive C-P coupling patterns for the chemically non-equivalent phenyl carbons and diagnostic C^2 carbon. The azole carbon in the 2-position appears as a doublet, with an insignificant upfield shift ($\Delta\delta$ 1.3) compared to the corresponding “ligand” **5**. The characteristic and complicated C-F coupling patterns were partly (due to overlap with aromatic signals) assigned to the pentafluorophenyl moiety. The most apparent difference is noted in the ^{31}P NMR singlet resonance in **12** which showed a downfield shift ($\Delta\delta$ 6.54) to δ 17.24 relative to complex **5**.

Mass spectrometry

The electron impact mass spectrum of **12** is summarised in Table 2.18. Although the molecular ion (M^+) peak is absent, diagnostic fragmentation signals at m/z 706 (loss of AuCl) and m/z 574 (loss of AuC_6F_5) are noted. Interestingly, however, by employing a softer ionisation technique, in FAB-MS, the molecular ion peak m/z 938 (^{35}Cl), is represented by a relatively strong peak. The peak at m/z 342 as was found for complex **4**, was assigned to the free phosphine, BzimPPh₂ ligand, representing a loss of both gold substituents.

Table 2.18 Mass spectroscopic data for **12**

Fragment	m/z (%)
	12
{[M] ^{35}Cl } ⁺	938
{[M]-Au} ⁺	741(1)
{[M]-AuCl} ⁺	706(16)
{[M]-AuC ₆ F ₅ } ⁺	574(12)
{BzimPPh ₂ } ⁺	342(70)

C. Structure determination of complex **12**.

The molecular structure of complex **12** is given in Figure 2.17, and selected bond lengths and bond angles are given in Table 2.19, numbered according to the figure. The colourless complex crystallises together with one equivalent of dichloromethane in the triclinic space group $\text{P}\bar{1}$. Important structural parameters of **12** can be compared with its constituent molecular structures, **5** (Table 2.16) and **16** (Chapter 3, Table 3.5), which represent the two halves of the molecule (Figure 2.18). A further structural comparison can also be made to the related cationic bimetallic complex, $[\text{Au}_2(\text{imPPh}_2)_2]^{2+}$ reported by Catalano and Horner⁵² (Scheme 2.11).

The neutral binuclear structure shows the two metal centres bridged by a BzimPPh₂ ligand, with Au(1) coordinated to the phosphorus atom and Au(2) to the imine-N (N11) on

the imidazole ring. The C(41)-Au(2)-N(11) angle is almost linear $179.0(2)^\circ$ as is the situation in complex **14** [$178.97(2)^\circ$]. However, the P(1)-Au(1)-Cl(1) angle is distorted from linearity at $174.15(6)^\circ$, and shows a more than 1° deviation compared to the corresponding angle in complex **5** [$175.58(6)^\circ$]. This could be due to steric repulsion of the chlorine atom by the pentafluorophenyl substituent.

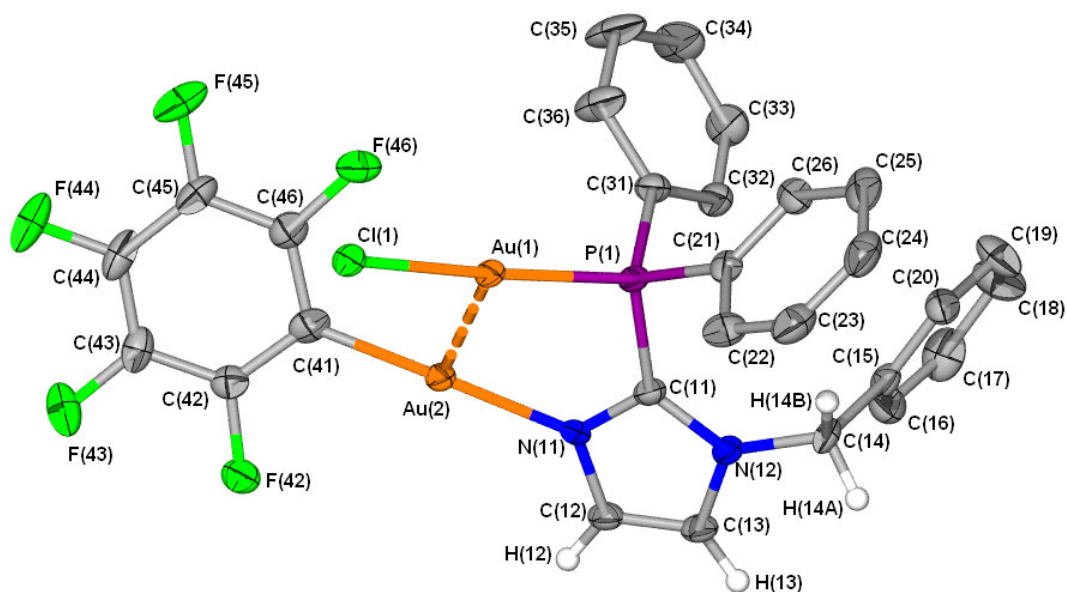


Figure 2.17 Molecular structure of **12** showing the numbering scheme; phenyl hydrogens and unlinked solvent (dichloromethane) omitted for clarity.

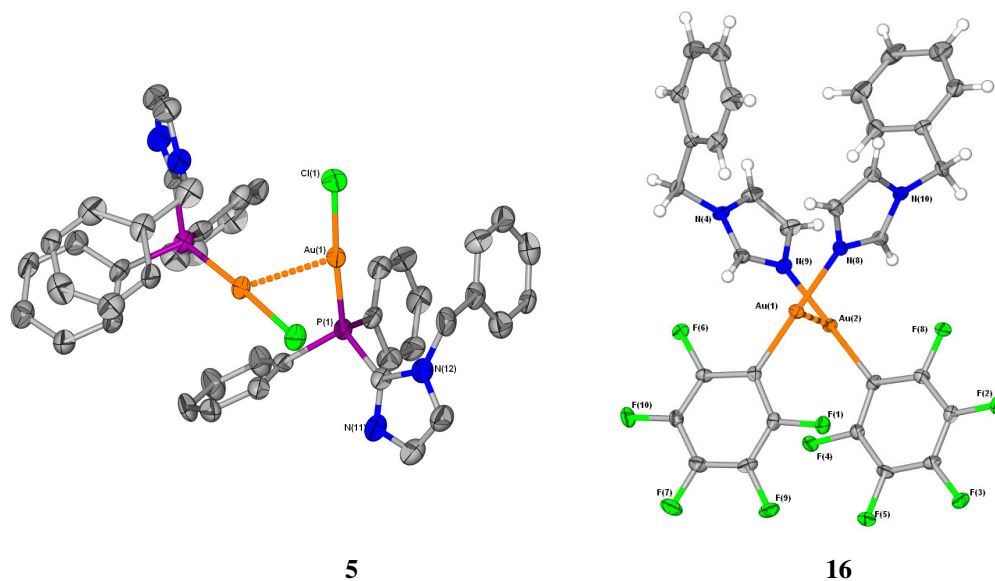
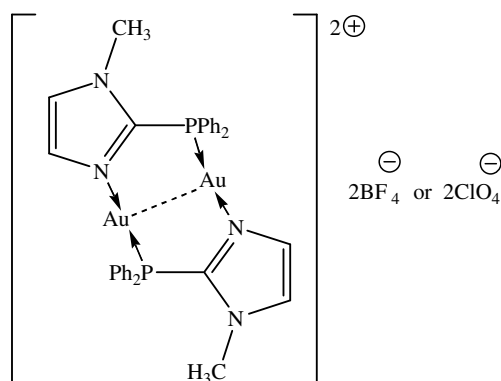


Figure 2.18 Molecular structure of **5** and **16** representing the two motifs of the molecular structure of **12** in dimeric forms.



Scheme 2.11 Binuclear complex, $[\text{Au}_2(\text{imPPh}_2)_2]^{2+}$ reported by Catalano and Horner.⁵²

The Au(1)-P [2.228 (2) Å] and slightly shortened Au(1)-Cl [2.290(2) Å] separations are comparable to **5** [2.233(2) Å and 2.306(2) Å, respectively], the Au-P bond in $[\text{Au}_2(\text{imPPh}_2)_2]^{2+}$ [2.238(3) Å] and relevant separations reported previously for azolyl(phosphines)gold(I) complexes **1a**, **1b** and **2**. The Au(2)-C(41) [1.986(7) Å] and Au(2)-N(11) [2.060(5) Å] bond distances in **12** correspond to the values in the complex **14**, and similar bonds in $[\text{Au}(\text{C}_6\text{F}_5)\{\text{NC}(\text{H})\text{SC}(\text{H})\text{C}(\text{CH}_3)\}]$ [2.00(1) Å and 2.081(8) Å respectively]¹⁴ and $[\text{Au}_2(\text{imPPh}_2)_2]^{2+}$ [2.090(11) Å].

Table 2.19 Selected bond lengths (Å) and angles (°) for complex **12** with e.s.d.s in parenthesis

Bond lengths		Bond angles	
Au(1)-P(1)	2.228(2)	P(1)-Au(1)-Cl(1)	174.15(6)
Au(1)-Cl(1)	2.290(1)	P(1)-Au(1)-Au(2)	80.68(4)
P(1)-C(11)	1.812(7)	Cl(1)-Au(1)-Au(2)	105.16(4)
P(1)-C(21)	1.807(7)	C(11)-P(1)-C(21)	108.0(3)
P(1)-C(31)	1.813(7)	C(11)-P(1)-C(31)	106.3(3)
N(11)-C(11)	1.338(8)	C(21)-P(1)-C(31)	107.6(3)
N(11)-C(12)	1.364(8)	C(11)-P(1)-Au(1)	109.8(2)
C(11)-N(12)	1.379(8)	C(21)-P(1)-Au(1)	111.0(2)
N(12)-C(13)	1.366(9)	C(31)-P(1)-Au(1)	113.9(2)
Au(2)-C(41)	1.986(7)	N(11)-C(11)-N(12)	108.5(6)
Au(2)-N(11)	2.060(5)	N(11)-C(11)-P(1)	119.2(5)
Au(1)-Au(1)	3.0079(5)	N(12)-C(11)-P(1)	132.3(5)
		C(26)-C(21)-P(1)	122.7(6)
		C(22)-C(21)-P(1)	117.5(5)
		C(41)-Au(2)-N(11)	179.0(2)
		C(41)-Au(2)-Au(1)	95.2(2)
		N(11)-Au(2)-Au(1)	84.7(2)
		C(11)-N(11)-C(12)	107.7(5)
		C(11)-N(11)-Au(2)	126.3(4)
		C(12)-N(11)-Au(2)	126.1(5)

The empirical bite distance for P,N-ligand **5** is about 2.75 Å (in **12** at 2.73 Å), which falls between values reported for other bidentate ligands, imPh₂P [2.84 Å]¹⁷ and Ph₂PPy [2.65 Å]³⁹ and proves to be effective at holding the two gold atoms in close proximity. The short

intramolecular aurophilic separation of 3.0079(5) Å falls within the range of intramolecular metal contacts of related monobridged dinuclear complexes, [(AuCl)₂{(Ph₂P)₂CH₂}] [3.351(2) Å],⁵⁷ dibridged compounds, [Au₂(imPPh₂)₂]²⁺ [2.8261(11) Å], and [(AuCl)₂{(Ph₂P)₂CH₂}₂] [2.962(1) Å]⁶² and the tetranuclear complex, [Au{SCNC(CH₃)C(H)S}]₄ [3.02(4) Å].¹⁴

The angles created by the bidentate P,N-coordination to Au(1) and Au(2) are modified in comparison to related angles in **5** and **14**. The Au(2)-N(11)-C(11) angle expands [123.11(1) to 126.3(4)°] and the Au(1)-P(1)-C(11) angle becomes smaller [113.9(2) to 109.8(2)°]. This ensues as the two centres of coordination, Cl-Au-P and C-Au-N are crossed, with the resultant plane of the five membered metallocyclic ring twisted by about 30° from planarity, [torsion angles Au(1)-P(1)-C(11)-N(11) and Au(1)-Au(2)-N(11)-C(11) at 35.7(6)° and -26.6(5)° respectively]. Literature examples of similar distorted metal-

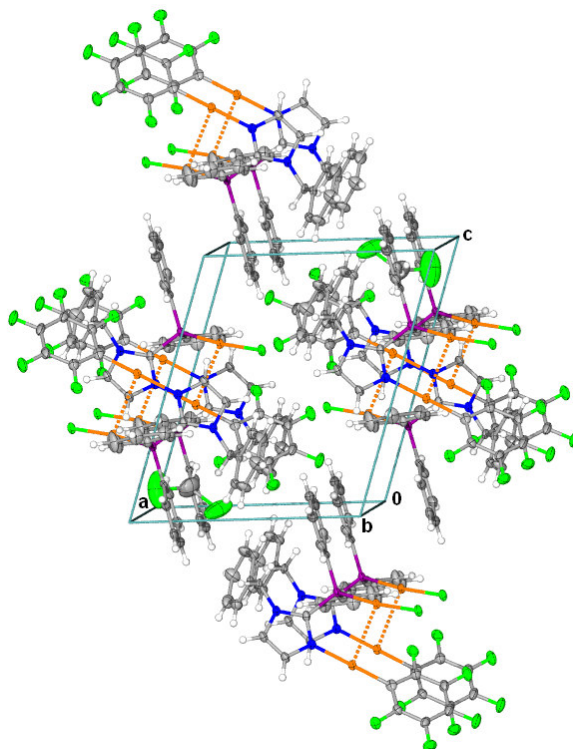


Figure 2.19 Unit cell and packing pattern showing the structure of **12** with Au(I)...Au(I) interactions shown as dashed lines, viewed along the b-axis. Dichloromethane molecules are evenly dispersed in the crystalline lattice.

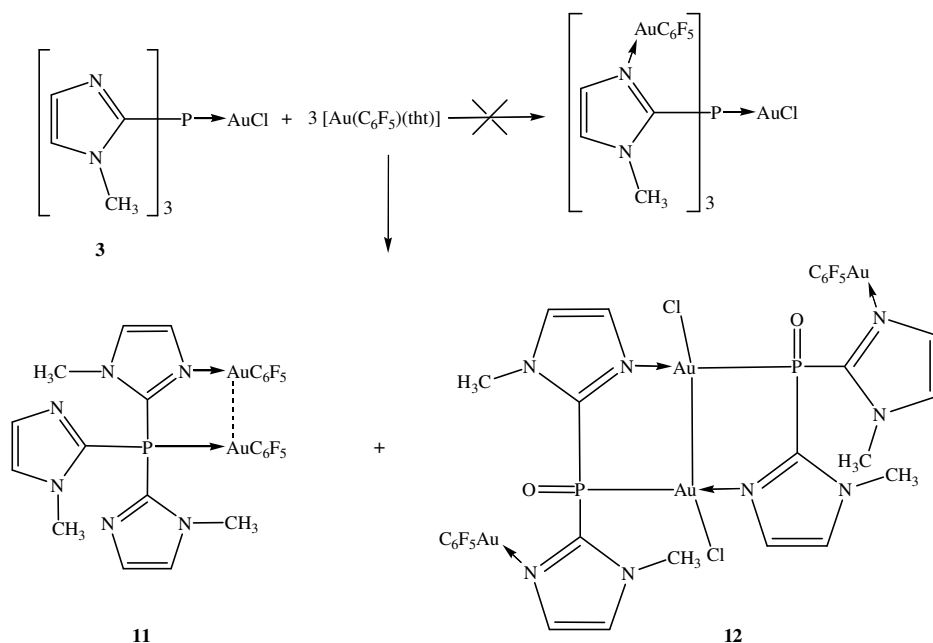
containing heterocyclic rings include [Au{SCNC(CH₃)C(H)S}]₄ [torsion angles approximately 17.2 - 19.6°].¹⁴ In contrast to analogous cationic complex [Au₂(imPPh₂)₂]²⁺ which shows almost perfect planarity.⁵²

⁶² H. Schmidbaur, A. Wohlleben, F. E. Wagner, D. F. Van de Vondel and G. P. Van der Kelen, *Chem. Ber.*, 1977, **110**, 2758.

In the unit cell molecules of **12** pack in regular rows along the a-axis, and are brought in close proximity to neighbouring rows by intercalated non-bonding planar phenyl-interactions (Figure 2.19). Along each of the packed rows of molecules, dichloromethane solvent molecules are dispersed. No other significant intermolecular interactions are noted.

A. Preparation of pentafluorophenyl[*N*-pentafluorophenylgold(I)](1-methylimidazol-2-yl)di(1-methylimidazol-2-yl)phosphinegold(I), **13, and the spontaneous self-association of dichloro[*N*-pentafluorophenylgold(I)-1-methylimidazol-2-yl](1-methylimidazol-2-yl)phosphinitegold(II), **14**.**

Using a similar synthetic approach to the preparation of **12**, complex **3** was employed as a potential multidentate “ligand”. What followed were the simultaneous formation of dinuclear metalocyclic complex **13**, due to Au...Au interactions in solid state, and a dinuclear gold(II) complex, bridged by a gold(I) substituted iminephosphinite ligand **14**. The formation of complex **13** can be rationalised by the excess amount of [Au(C₆F₅)(tht)] that effected a ligand substitution, to yield a bis[pentafluorophenylgold(I)] group bridged by ligand **III**. It is clear that the AuC₆F₅ neutral unit not only readily coordinates at the imine nitrogen but also replaces AuCl at the phosphine.

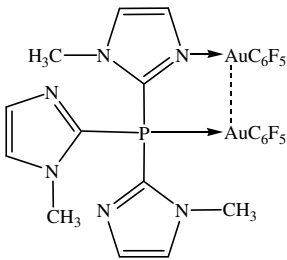
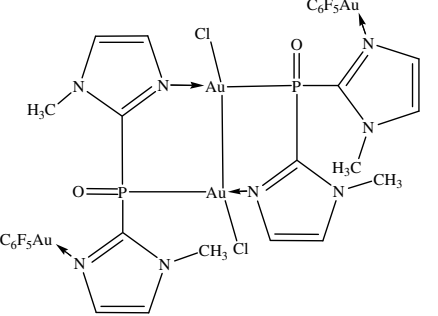


Scheme 2.8 The formation of dinuclear complex **13** and a tetranuclear Au(I)/Au(II) complex, that contains an imidazole-substituted iminephosphinite ligand.

The treatment of substrate **3** with three molar equivalents of freshly prepared [Au(C₆F₅)(tht)] afforded an unexpected substitution product. The insolubility of **3** in non-polar solvents prompted the use of a mixture of methanol:ether (10:1) as reaction solvent.

After simple work up of the resultant light yellow solution, a yellow luminescent product was isolated. Dissolution of the luminous product in dichloromethane results in a clear colourless solution, whereas in acetone it appears light yellow. Similar variations in luminescence have been credited to the formation of aggregates of cations which self-associate through aurophilic interactions.⁶³ A solution of the luminescent product mixture (40 mg) in deuterated acetone, contained in an NMR tube, was allowed to crystallise by vapour diffusion of *n*-hexane at -20 °C. This resulted in a simultaneous crystallisation of colourless cubic crystals **13** (together with 1 equivalent. acetone), and yellow needles of **14**. Both these crystals types were stable at room temperature. However, upon prolonged standing in a hydrocarbon oil the colourless crystals of **13**, lost morphology. This is most likely due to the loss of the acetone from the crystal lattice. The yellow needles of **14** in this regard, appeared stable. The analytical data for **13** and **14** are summarised in Table 2.20.

Table 2.20 Analytical data for complexes **13** and **14**

Complex	 <p style="text-align: center;">13</p>	 <p style="text-align: center;">14</p>
M.p./°C	174	136
Colour	colourless	yellow
M_r	1002.03	1609.91
Analysis(%)*	not pure	not pure

In a first attempt to prepare tetranuclear complexes from azolyl(phosphine)gold(I) halides, substrates **1** and **2** were employed as potential imine donor substrates. However, no significant substitution products could be isolated in either situation. Prolonged reaction times, with heating, only led to the decomposition of [Au(C₆F₅)(tht)] to metallic gold and the recovery of unsubstituted **1** and **2**. It is noteworthy that the ¹⁵N NMR chemical shift of **1** (δ -33.93) of **2** (δ -29.49) differ significantly from **3** (δ -90.64). The high field N³ resonance in **3** represents a more shielded nucleus than is found for the thiazole derivatives **1** and **2** and thus higher electron density. This in part can be responsible for the

⁶³ R. L. White-Morris, M. M. Olmstead and A. L. Balch, *J. Am. Chem. Soc.*, 2003, **125**, 1033.

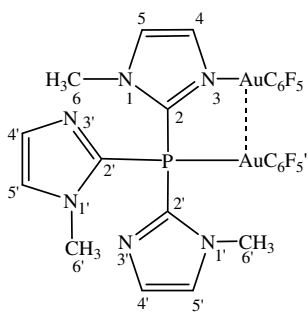
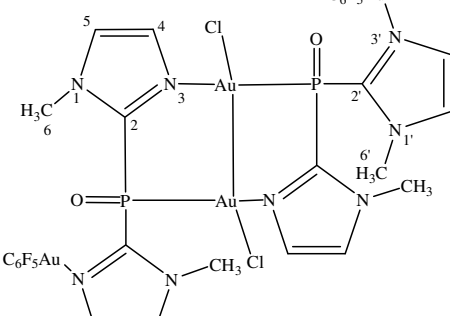
low imine coordination ability of the latter two electron density. As a working hypothesis, we propose that partial hydrolysis of the phosphine ligand, initiated by trace amounts of moisture afforded a di(imidasolyl)phosphinite ligand covalently bonded to a gold(I) chloride unit and coordinately attached to AuC_6F_5 . Such an anionic complex, with two metallic centres in close proximity, is subsequently further stabilised by self-assembly followed by a self-redox reaction (oxidation product unknown) to afford the gold(II) complex, not dissimilar to the formation of gold(II) complex reported by Irwin and co-workers.²⁴ This result represents a novel addition to the plethora of gold(II) complexes synthesised with hybrid dihapto ligands of the type P-O, P-N, P-P and P-S.

B. Spectroscopic characterisation of **13** and **14**.

Nuclear magnetic resonance spectroscopy

The ^1H and $^{31}\text{P}\{^1\text{H}\}$ NMR spectroscopic data for complexes **13** and **14** are summarised in Table 2.20. Assignments of ^1H -resonances are tentatively made, due to the great degree of overlap occurring for both complexes.

Table 2.20 ^1H and $^{31}\text{P}\{^1\text{H}\}$ NMR data for **13** and **14**

Complex	 <p style="text-align: center;">13</p>	 <p style="text-align: center;">14</p>
Solvent	$(\text{CD}_3)_2\text{CO}$	$(\text{CD}_3)_2\text{CO}$
Temperature (K)	298	298
^1H NMR (300 MHz)	H^4 7.62-7.80 (m, 1H) H^5 7.86-8.09 (m, 1H) H^6 2.83 (bs, 3H) $\text{H}^{4'}$ 7.62-7.80 (m, 2H) $\text{H}^{5'}$ 7.86-8.09 (m, 2H) $\text{H}^{6'}$ 3.07 (bs, 6H)	7.28 (bs, 2H) 7.80 (bs, 2H) 2.86 (bs, 2H) - - -
$^{31}\text{P}\{^1\text{H}\}$ NMR (121 MHz)	P -23.20 (s)	126.44 (s)

A well-resolved spectrum, could only be obtained of the colourless crystals of complex **13**, and was used to distinguish signals in the spectra of a mixture of both complexes. The signals in the ^1H NMR spectrum show a slight upfield shift and broadening of the signals

that have been assigned to the chemically non-equivalent N-CH₃ protons of 6' (δ 3.07) and 6 (δ 2.83) in **13**. The related protons in **14** showed a significant upfield shift and resonate as broad singlets at δ 7.28. These broadened singlets can be ascribed to H-P coupling of H⁶ and H^{6'} coupling across N1. The two sets of multiplet signals at δ 7.62-7.80 and 7.86-8.09 are assigned to the allylic protons H⁴, H^{4'} and H⁵, H^{5'} respectively in **13**. The related protons in **14** are assigned with difficulty, owing to overlap with other signals.

In the ³¹P NMR spectrum, a singlet resonance at δ -23.20 is assigned to the phosphorus nucleus in **13**, this shows an insignificant upfield shift from the parent complex **3**. A distinguishing singlet signal at δ 126.44 is assigned to the deshielded phosphinite phosphorus nucleus in **14** and is comparable to a value reported in the literature.⁶⁴ The signals at δ -23.20 and 126.44, integrates in a ratio of ca. 5:1 indicating that complex **14** is present in a ratio of 1:10 compared to complex **13**.

Mass spectrometry

The FAB mass spectrum of the yellow product residue gives an intense signal for the molecular ion of **13** at m/z 1003, as well as equally intense peaks corresponding to the fragmentation thereof, at m/z 835 (loss of C₆F₅), m/z 639 (loss of AuC₆F₅) and m/z 639 (loss of AuC₆F₅ and imidazole). No diagnostic peaks could be assigned to the molecular ion of **14**. A signal at m/z 1365 corresponds to ligand **III** with three AuC₆F₅ groups. The strong base peak, at m/z 1199 can be ascribed to a fragmentation (loss of C₆F₅) of the trisubstituted product.

C. Structure determination of complex 13 and 14.

The molecular structure of complex **13** is represented in Figure 2.20, and selected bond lengths and bond angles are given in Table 2.22, numbered according to Figure 2.20. The colourless complex co-crystallises with one equivalent of acetone in the triclinic space group P $\bar{1}$. Structure **13** will be discussed only with regard to noted differences to a similar complex **12** and related complexes from literature, [Au₂(imPPh₂)₂]²⁺⁵² and [Au₂(pyPMe₂)₂]²⁺.¹⁸

⁶⁴ J. Vicente, M. T. Chicote and P. G. Jones, *Inorg. Chem.*, 1993, **32**, 4960.

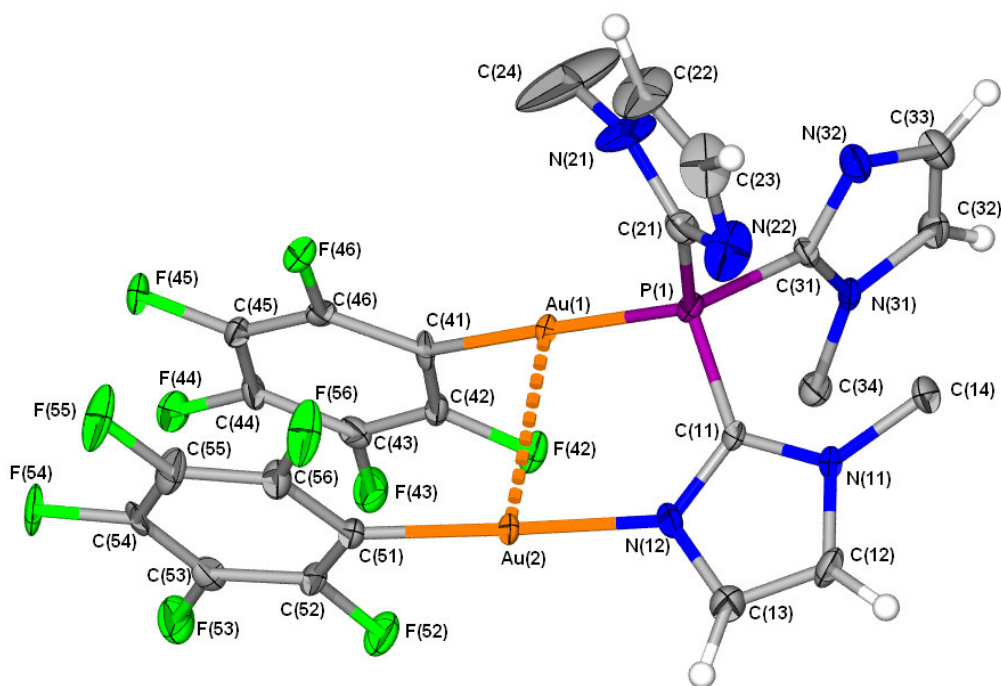


Figure 2.20 Molecular structure of **13** showing the numbering scheme. One equivalent of acetone co-crystallised with the complex and is omitted for clarity.

The neutral dinuclear structure shows two AuC₆F₅-substituents bridged by a tris(1-methylimidazol-2-yl) ligand, with Au(1) coordinated to the phosphorus atom and Au(2) imine coordinated to one of three possible nitrogens on the imidazole rings, N(12). The angles C(51)-Au(2)-N(12) [178.4(3)°] and P(1)-Au(1)-Cl(1) [175.9(2)°] are approaching linearity, in agreement with corresponding angles in complex **12**. The pentafluorophenyl rings are co-planar and are arranged off-centre to one another.

It is tempting to compare the bidentate coordination ability of ligands, BzimPPh₂ and **III** with respect to the structural parameters found in the binuclear complexes **12** and **13**. A more accurate assessment would be of a complex, with a chloro substituent in place of the pentafluorophenyl ring (C41-C46) as in **13**. However, the respective 5-membered rings formed by this bidentate coordination, shows a less distorted coordination in order to place gold atoms in close proximity. These contacts are comparable and slightly shorter in the case of **13** [2.9620(5) Å] than in **12** [3.0079(5) Å]. The empirical bite distance for the P,N-ligand **III** is approximately 2.72 Å [2.76 Å in **13**] which is similar to the spatial separation in ligand, BzimPPh₂. The resultant plane of the five membered metallocyclic ring is less distorted from planarity at approximately 20° [torsion angles Au(1)-P(1)-C(11)-N(12) and Au(1)-Au(2)-N(12)-C(11) at -20.8(8)° and 19.2(8)° respectively] than in **12**. The observed angle at which the two planes created by the gold coordination cross, is approximately 24°. It can be accepted that monodentate substituents attached to the respective metal

centres affect not only the separation between the gold atoms but also the geometry of the five-membered metallocyclic rings. Bonds around the two coordination centres [Au-P, Au-C(41), Au(2)-C(51) and Au(2)-N(21)] are normal.

Table 2.22 Selected bond lengths (Å) and angles (°) for complex **13** with e.s.d.s in parenthesis

Bond lengths		Bond angles	
Au(1)-P(1)	2.263(2)	P(1)-Au(1)-C(41)	175.9(2)
Au(1)-C(41)	2.028(8)	(N12)-Au(2)-C(51)	178.4(3)
P(1)-C(11)	1.810(8)	C(41)-Au(1)-Au(2)	96.2(2)
P(1)-C(21)	1.78(1)	C(11)-P(1)-C(21)	102.4(4)
P(1)-C(31)	1.812(8)	C(11)-P(1)-C(31)	105.4(4)
N(11)-C(11)	1.35(1)	C(21)-P(1)-C(31)	102.4(4)
N(11)-C(12)	1.36(1)	C(11)-P(1)-Au(1)	110.3(3)
C(11)-N(12)	1.32(1)	C(21)-P(1)-Au(1)	120.9(3)
N(12)-C(13)	1.375(1)	C(31)-P(1)-Au(1)	113.9(3)
Au(2)-C(51)	2.019(8)	N(11)-C(11)-N(12)	109.2(7)
Au(2)-N(12)	2.075(7)	N(11)-C(11)-P(1)	128.3(6)
Au(1)-Au(2)	2.9620(5)	N(12)-C(11)-P(1)	122.5(6)
		N(21)-C(21)-P(1)	124.3(8)
		N(22)-C(21)-P(1)	124.2(8)
		C(51)-Au(2)-Au(1)	93.0(2)
		N(12)-Au(2)-Au(1)	86.15(2)
		C(11)-N(11)-C(12)	109.1(7)
		C(11)-N(11)-C(14)	128.5(7)
		C(11)-N(12)-Au(2)	128.0(6)
		C(13)-N(12)-Au(2)	124.4(6)

An interesting assessment can be made as to whether ligand **III** has structurally changed to accommodate a bidentate coordination. Another look at the crystal structure shows (Figure 2.4) that the trigonal pyramidal geometry, places only one unsubstituted N-centre in close spatial proximity to the phosphorus atom, with the other two imine nitrogen atoms pointing away and to the base of the pyramidal structure. It is, however, not surprising to note that although all the external angles about the phosphorus atom are greater than in **III**, angles C(11)-P(1)-C(21) [102.4(4)°], C(11)-P(1)-C(31) [105.4(4)°] and C(21)-P(1)-C(31) [102.4(4)°] are largely similar.

In the unit cell, molecules of **13** pack in regular rows along the *ab*-plane, and show no significant intermolecular interactions. Apart from the intramolecular Au...Au interactions, the co-planarity of the pentafluorophenyl substituents govern the arrangement of molecules in the crystal lattice.

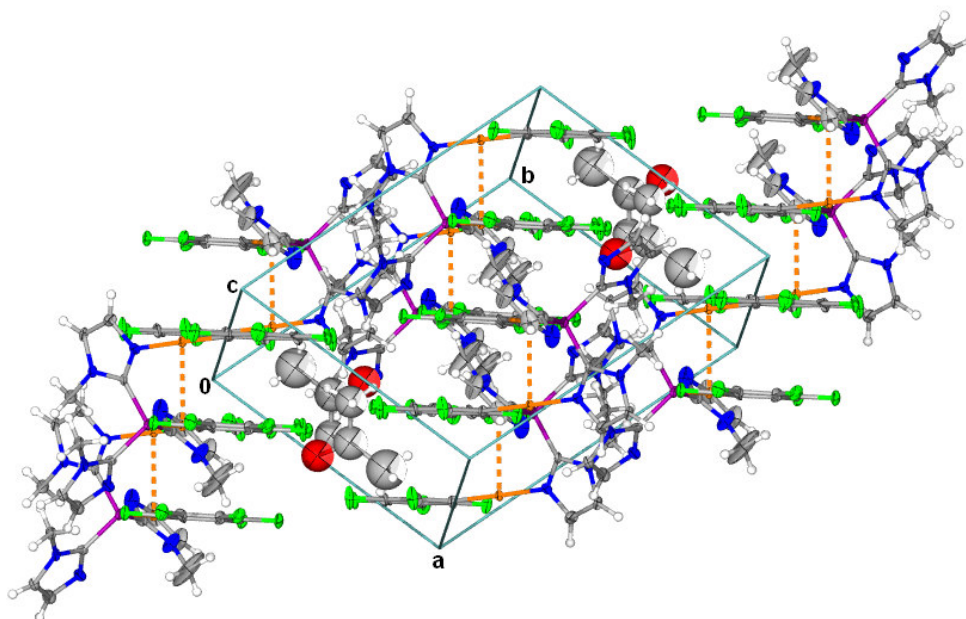


Figure 2.21 Unit cell and packing pattern of **13** viewed along the b-axis.

The molecular structure of **14** is represented in Figure 2.22. An acceptable structure refinement was hampered by a twinning of crystals. As a result of the disorder, the bond and angle parameters are severely affected and will not be discussed.

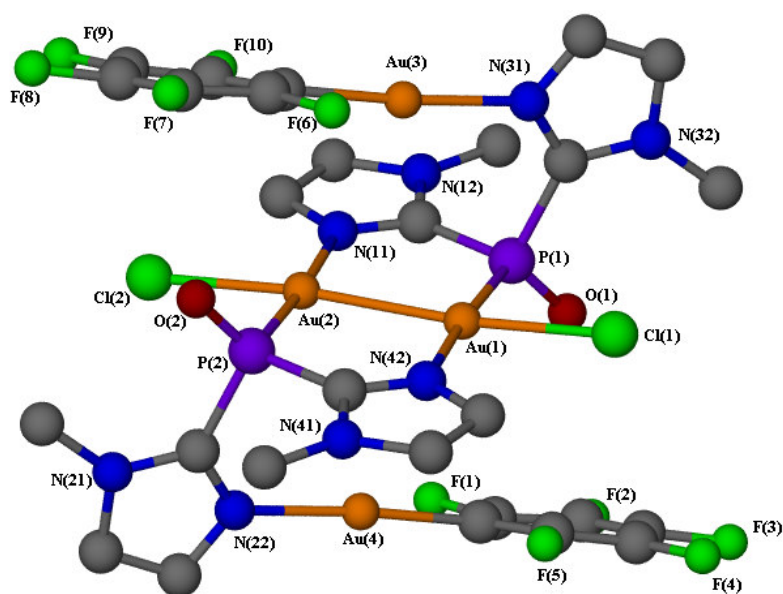


Figure 2.22 Molecular structure of **14**, hydrogen atoms omitted for clarity.

2.3 Conclusion

A series of novel gold(I) complexes derived from natural azoles have been synthesised and characterised. X-ray crystallographic investigation has revealed that chloro[tris(thiazol-2-yl)phosphine]gold(I), **1**, (in two polymorphic conformations **1a** and

1b), chloro[tris(thiazol-2-yl)phosphine]gold(I), **2**, and chloro[(1-benzylimidazol-2-yl)diphenyl]phosphinegold(I), **5**, aggregate in the solid state as gold(I) dimers, and that weak aurophilic interactions govern the arrangement of molecules within the crystal lattice. ^1H and ^{13}C NMR spectra revealed interesting phosphorus coupling patterns for gold(I) complexes derived from azolyphosphines, which were confirmed by selective nucleus decoupling experiments.

In a short investigation towards the synthesis of mono-carbene complexes of Au(I) that contain tertiary azolyphosphine ligands, it was found that chloro[tris(thiazol-2-yl)phosphine]gold(I), **1**, reacts in a similar manner with lithiated azoles than $[\text{AuCl}(\text{PPh}_3)]$. A novel, stable cationic di(amino)carbene complex was prepared and isolated. In the preparation of an amino(thio)carbene complex of gold(I), derived from the starting complex, chloro[tris(thiazol-2-yl)phosphine]gold(I), **1**, complicating side-reactions occurred which afforded various cationic gold(I) complexes.

The idea of using gold(I) complexes, with functionalised phosphine ligands, as “ligands” for coordination of a second metal was successfully implemented. Using chloro[tris(1-methylimidazol-2-yl)phosphine]gold(I), **3**, and chloro[(1-benzylimidazol-2-yl)diphenyl]phosphinegold(I), **5**, in this role, and exploiting the soft donor potential of the nitrogen atoms on the imidazole ring, two novel 5-membered auracyclic dinuclear complexes were obtained (complexes **12** and **13**). The bidentate $M-\eta^2 \text{P,N}$ -coordination, bridging two non-equivalent unbonded gold(I) centres has not previously been reported in the literature. The gold(I) complexes derived from azolyphosphine ligands (complexes **1-5**) differed in their ability to act as ligands to secondary metal coordination, and no second coordination products were identified with gold(I) complexes that contained thiazole phosphines (complexes **1** and **2**) and tetrazolyl phosphine (complex **4**).

During the investigation, unusual self-assembly of molecules resulted in the formation of a novel dinuclear gold(I) product that is bridged by a P-P unit, and aggregates in the solid state as polymeric chains. The tetranuclear bicyclic complex (**14**) represents the first example of a complex with two gold(II) centres stabilised by a phosphinite-imine bridge.

2.4 Experimental

2.4.1 General procedures and instruments

Reactions were carried out under argon using standard Schlenk- and vacuum-line techniques. Tetrahydrofuran (thf), *n*-hexane, pentane and diethyl ether were distilled under N₂ from sodium benzophenone ketyl, dichloromethane from CaH₂ and ethanol and methanol from magnesium. Thiazole, 4-methylthiazole, 4,5-dimethylthiazole, 1-methylimidazole, 1-benzylimidazole and CF₃SO₃Me were purchased from Aldrich, and butyllithium from Merck. Commercially available phosphorus trichloride and diphenylphosphine chloride were freshly distilled under argon prior to use. Literature methods were used to prepare 1-*H*-tetrazole,⁶⁵ 1-benzyltetrazole,⁶⁶ [AuCl(tht)]⁶⁷ and [Au(C₆F₅)(tht)].⁶⁸

Melting points were determined on a Stuart SMP3 apparatus and are uncorrected. Mass spectra were recorded on an AMD 604 (EI, 70 eV), VG Quattro (ESI, 70 eV methanol, acetonitrile) or a VG 70 SEQ (FAB, 70 eV, recorded in a *m*-nitrobenzylalcohol matrix) instrument. NMR spectra were recorded on a Varian 300 FT or INOVA 600 MHz spectrometer (¹H NMR at 300/600 MHz, ¹³C{¹H} NMR at 75/150 MHz, ³¹P{¹H} NMR at 121/243 MHz, ¹⁵N NMR at 60.8 MHz, ¹⁹F NMR at 376 MHz; δ reported relative to solvent resonance or external reference of 85 % H₃PO₄ (³¹P), NH₃NO₂ (¹⁵N) and CFCl₃ (¹⁹F). Elemental analysis were carried out at the School of Chemistry, University of the Witwatersrand. Certain characterisation data (elemental analysis, melting point and also yields) are given in the main text. For elemental analysis, products were evacuated under high vacuum for 10 h.

2.4.2 Preparations and procedures

2.4.2.1 Preparations of tris(thiazol-2-yl)phosphine, I.

A solution of thiazole (2.80 ml, 39.9 mmol) in diethyl ether (10 ml) was added drop wise *via* a syringe to a solution of *n*-BuLi in *n*-hexane (25.9 ml, 38.4 mmol) in diethyl ether (10 ml), which was cooled to -68 °C. After the addition the yellow solution was stirred at -68 °C for an additional hour. A solution of PCl₃ (1.52 g, 11.0 mmol) in diethyl ether (10 ml)

⁶⁵ R. Bronisz, *Inorg. Chim. Acta.*, 2002, **340**(1), 215.

⁶⁶ Y. Satoh, N. Marcopulos, *Tetrahedron Lett.*, 1995, **36**(1), 1759.

⁶⁷ R. Usòn and A. Laguna, in *Organometallic Synthesis*, eds. R. B. Lang and J. J. Eisch, Elsevier, Amsterdam, 1986, vol. 3, p. 325.

⁶⁸ R. Usòn and A. Laguna, in *Organometallic Synthesis*, eds. R. B. Lang and J. J. Eisch, Elsevier, Amsterdam, 1986, vol. 3, p. 326.

was added and the reaction mixture was stirred at $-68\text{ }^{\circ}\text{C}$ for 3 h. The mixture was then transferred with a cannula into degassed, saturated aqueous NH_4Cl (100 ml). The brown suspension was filtered through silica gel and MgSO_4 . The resultant clear solution was concentrated *in vacuo* to yield a solid yellow residue, which was dissolved in the minimum methanol and layered with *n*-hexane. Colourless crystals of tris(thiazol-2-yl)phosphine (1.10 g, 35 %) formed at $-20\text{ }^{\circ}\text{C}$.

2.4.2.2 Preparation of tris(4-methylthiazol-2-yl)phosphine, II.

A solution of 4-methylthiazole (3.0 ml, 30 mmol) in diethyl ether (7.5 ml) was added drop wise *via* a syringe to a solution of *n*-BuLi in *n*-hexane (19.5 ml, 28.8 mmol) in diethyl ether, which was cooled to $-68\text{ }^{\circ}\text{C}$. After the addition the yellow solution was stirred at $-68\text{ }^{\circ}\text{C}$ for an additional hour. A solution of PCl_3 (1.14 g, 8.25 mmol) in diethyl ether (7.5 ml) was subsequently added. The reaction mixture was stirred at $-68\text{ }^{\circ}\text{C}$ for 3 h and then transferred with a cannula into degassed, saturated aqueous NH_4Cl (100 ml). The orange biphasic mixture formed after stirring. The orange ether layer was extracted. The aqueous phase was washed with a further three portions of diethyl ether (40 ml). The combined organic extracts were subsequently dried over anhydrous Na_2SO_4 , filtered, treated with activated charcoal, filtered through celite and the filtrate concentrated *in vacuo*. The residue was dissolved in the minimum of methanol and layered with *n*-hexane. Colourless crystals of, tris(4-methylthiazol-2-yl)phosphine (0.75 g, 28 %) formed at $-20\text{ }^{\circ}\text{C}$.

2.4.2.3 Preparation of tris(1-methylimidazol-2-yl)phosphine, III.

A solution of 1-methylimidazole (0.82 g, 10 mmol) in diethyl ether (60 ml) was cooled to $-78\text{ }^{\circ}\text{C}$, and treated with a solution *n*-BuLi in *n*-hexane (6.6 ml, 10 mmol). After the addition the yellow solution was stirred at this temperature for an additional hour. Freshly distilled PCl_3 (0.30 ml, 3.3 mmol) was added to the reaction mixture at $-78\text{ }^{\circ}\text{C}$ and stirred for 3 h upon which the white slurry was allowed to reach room temperature. The mixture was treated with a concentrated NH_3 solution (20 ml) and stirred for 15 min. The aqueous layer was separated from the clear biphasic mixture and extracted with an equal volume of dichloromethane (20 ml). The organic extract was dried over anhydrous NaSO_4 , filtered, and the filtrate concentrated *in vacuo*, to yield a white solid. Recrystallisation from a solution of dichloromethane layered with diethyl ether afforded colourless crystals, tris(1-methylimidazol-2-yl)phosphine (0.64 g, 70 %), at $-20\text{ }^{\circ}\text{C}$.

2.4.2.4 Preparation of chloro[tris(thiazol-2-yl)phosphine]gold(I), 1.

A solution of [AuCl(tht)] (0.12 g, 0.39 mmol) in dichloromethane (5 ml) at room temperature was treated with tris(thiazol-2-yl)phosphine (0.12 g, 0.43 mmol) in dichloromethane (5 ml). The mixture was stirred at room temperature for 1 h, upon which MgSO₄ (5 g) was added. The suspension was filtered through celite and the filtrate concentrated *in vacuo* to yield a white solid. Recrystallisation from a solution of dichloromethane layered with diethyl ether afforded colourless crystals (**1b**), chloro[tris(thiazol-2-yl)phosphine]gold(I) (0.18 g, 90 %) at -20 °C.

X-ray quality single crystals for the polymorphic form **1b** was obtained accidentally from a mixture of the complex **1** and 2-lithio-4,5-dimethylthiazole in dichloromethane, which failed to react completely. Crystallisation of the mixture in dichloromethane layered with diethyl ether, ensued at -20 °C.

2.4.2.5 Preparation of chloro[tris(thiazol-2-yl)phosphine]gold(I), 2.

A solution of [AuCl(tht)] (0.11 g, 0.35 mmol) in dichloromethane (7.5 ml) at room temperature was treated with tris(4-methyl thiazol-2-yl)phosphine (0.13 g, 0.40 mmol) in dichloromethane (10 ml). The mixture was stirred at room temperature for 1 h, upon which MgSO₄ (5 g) was added. The suspension was filtered through celite and the filtrate concentrated *in vacuo* to yield a white solid. Recrystallisation from a solution of dichloromethane layered with diethyl ether afforded colourless crystals of, chloro[tris(thiazol-2-yl)phosphine]gold(I) (0.18 g, 93 %), at -20°C.

2.4.2.6 Preparation of chloro[tris(1-methylimidazol-2-yl)phosphine]gold(I), 3.

A solution of [AuCl(tht)] (0.20 g, 0.63 mmol) in dichloromethane (15 ml) at room temperature was treated with tris(1-methylimidazol-2-yl)phosphine (0.17 g, 0.63 mmol) in dichloromethane (10 ml). The mixture was stirred at room temperature overnight, upon which the solution turned a light yellow/green. The dried white residue was extracted with dichloromethane (70 ml), filtered through MgSO₄ and concentrated *in vacuo* to yield a white solid. Recrystallisation from a mixture of methanol/thf (10:2) layered with diethyl ether afforded colourless microcrystals of chloro[tris(1-methylimidazole)phosphine]gold(I) (0.28 g, 89 %) at -20 °C.

2.4.2.7 Preparation of chloro[(1-benzyltetrazol-5-yl)diphenyl]phosphinegold(I), 4.

A solution of 1-benzyltetrazole (0.16 g, 1.0 mmol) in thf (10 ml) was treated with *n*-butyllithium in *n*-hexane (0.70 ml, 1.0 mmol) at -98 °C. The light yellow solution turned orange almost immediately. After 2 h of stirring the solution was treated with diphenylphosphine chloride (0.20 ml, 1.0 mmol) and the reaction mixture was stirred for a further 2 h at -78 °C. The light yellow solution was warmed to 0 °C and treated with [AuCl(tht)] (0.32 g, 1.0 mmol) in thf (10 ml). The solution turned colourless and was stirred for 2 h, whereafter the mixture was allowed to reach room temperature. The solvent was removed *in vacuo* to yield a white solid residue. The residue was sequentially washed with *n*-hexane (30 ml), extracted with dichloromethane (30 ml) and filtered individually through anhydrous MgSO₄. The dichloromethane extract contained a gold complex and was concentrated *in vacuo* to yield colourless microcrystalline material, (0.45 g, 78 %) at -20 °C.

2.4.2.8 Preparation of chloro[(1-benzylimidazol-2-yl)diphenyl]phosphinegold(I), 5.

A solution of 1-benzylimidazole (0.31 g, 1.9 mmol) in thf (10 ml) was treated with *n*-butyllithium in *n*-hexane (1.30 ml, 1.97 mmol) at -78 °C. The colourless solution turned light yellow over a period of 2 h, and was treated with diphenylphosphine chloride (0.40 ml, 1.9 mmol) and the reaction mixture was stirred for a further 1 h at -78 °C. The resultant deep orange solution was treated with [AuCl(tht)] (0.57 g, 1.8 mmol) in thf (10 ml). The solution turned colourless and was stirred for 2 h, whereafter the mixture was allowed to reach room temperature. The solvent was removed *in vacuo* to yield a white solid residue. The residue was sequentially washed with ether/*n*-hexane (1:1, 30 ml), extracted with dichloromethane (30 ml) and filtered individually through anhydrous MgSO₄. The dichloromethane extract contained the desired gold complex and was concentrated *in vacuo* to yield a off-white solid. Recrystallisation by layering a dichloromethane solution with *n*-hexane afforded colourless crystalline material, (0.96 g, 85 %) at -20 °C.

2.4.2.9 The formation of 1,3-digold(I)(1,1,2,2-tetraphenyl-diphosphine)chloride, 6.

A sample of **4** (0.04 g, 0.07 mmol) was dissolved in dichloromethane (5 ml) and left at 5 °C for 48 hrs. An insoluble light yellow crystalline solid **6** (0.02 mg, 42 %) precipitated which contained off-white oval crystals.

2.4.2.10 Preparation of chloro[(1-tetrazolyl)diphenyl]phosphinegold(I), 7.

A solution of 1*H*-tetrazole (0.07 g, 2 mmol) in thf (20 ml) was treated with NaH (0.05 g, 2.0 mmol) at room temperature. After 30 min. of stirring, the clear solution was treated with diphenylphosphine chloride (0.40 ml, 2.0 mmol) and stirred for a further 2 h, whereafter the solution was filtered through anhydrous MgSO₄. The filtrate was subsequently treated with [AuCl(tht)] (0.64 g, 2.0 mmol) in thf (10 ml) and stirred at room temperature for 2 h. The solvent was removed *in vacuo* to yield a white solid residue, which was sequentially washed with *n*-hexane (30 ml), extracted with diethyl ether (30 ml) and filtered individually through anhydrous MgSO₄. The ether extract contained a gold complex and was concentrated *in vacuo* to yield colourless microcrystalline material, (0.6 g, 59 %).

2.4.2.11 Preparation (1-benzyl-4-methylimidazol-2-ylidene)tris(thiazolyl-2-yl)phosphinegold(I), 8

A solution of 1-benzylimidazole (0.067 g, 0.43 mmol) in dichloromethane (10 ml) was treated with *n*-butyllithium in *n*-hexane (0.30 ml, 0.43 mmol) at -78 °C. After 30 min. of stirring the light yellow solution was treated with, **1** (0.22 g, 0.43 mmol) and the reaction mixture was stirred for a further 2 h at -78 °C. The product was treated with CF₃SO₃CH₃ (0.10 ml, 0.43 mmol) at -78 °C and stirred for 30 min. whereafter the mixture was allowed to reach room temperature. The solvent was removed *in vacuo* to yield a dark yellow residue. The residue was extracted sequentially with diethyl ether/pentane mixture (1:1) (30 ml) and dichloromethane (10 ml) and the extracts were filtered individually through anhydrous MgSO₄. The dichloromethane extract was concentrated *in vacuo* to yield off-white microcrystalline product, (0.32 g, 93 %).

2.4.2.12 The reaction of 2-lithio-4,5 dimethylthiazole with 1, followed by methylation.

A solution of 4,5-dimethylthiazole (0.06 g, 0.5 mmol) in dichloromethane (10 ml) was treated with *n*-butyllithium in *n*-hexane (0.3 ml, 0.5 mmol) at -78 °C. After 30 min. of stirring the light yellow solution was treated with, **1** (0.3 g, 0.5 mmol) and the reaction mixture was stirred for a further 2 h at -78 °C. The product was treated with CF₃SO₃CH₃ (0.1 ml, 0.5 mmol) at -78 °C and stirred for 30 min. whereafter the mixture was allowed to reach room temperature. The solvent was removed *in vacuo* to yield a dark yellow residue. The residue was extracted sequentially with a diethyl ether/pentane mixture (1:1) (30 ml)

and dichloromethane (30 ml) and the extracts were filtered individually through anhydrous MgSO₄. The dichloromethane extract contained a mixture of gold containing products, and was concentrated *in vacuo* to yield yellow microcrystalline material, (0.3 g).

2.4.2.13 Preparation of chloro[1-benzyl-N-pentafluorophenylgold(I)imidazol-2-yl](diphenyl)phosphinegold(I), 12.

A solution of **5** (0.13 g, 0.22 mmol) in diethyl ether/thf (10:1, 20 ml) was treated with a solution of freshly prepared [Au(C₆F₅)(tbt)] (0.10 g, 0.22 mmol) in diethyl ether (20 ml). The clear solution was stirred for 48 hrs. at room temperature. The resultant cloudy solution was reduced to dryness under vacuum. The off-white oily residue was repeatedly washed with *n*-hexane to afford a white solid. Recrystallisation by layering a dichloromethane solution with *n*-hexane afforded colourless, crystalline material, (0.15 g, 73 %), at -20°.

2.4.2.14 Preparation of pentafluorophenyl[{N-pentafluorophenylgold(I)}(1-methylimidazol-2-yl)di(1-methylimidazol-2-yl)]phosphinegold(I), 13 and the spontaneous formation of, dichloro[{N-pentafluorophenylgold(I)-1-methylimidazol-2-yl}(1-methylimidazol-2-yl)]phosphinitegold(II), 14.

A solution of **3** (0.06 g, 0.1 mmol) in methanol (10 ml) was treated with a solution of freshly prepared [Au(C₆F₅)(tbt)] (0.16 g, 0.34 mmol) in diethyl ether (10 ml). The clear solution was stirred for 4 hrs. at room temperature. The resultant light yellow solution was filtered through celite, and the filtrate reduced to dryness under vacuum, to afford a yellow luminescent product (0.13 g). Recrystallisation by layering an acetone solution with *n*-hexane afforded a mixture of colourless cubic crystals of **13**, and yellow needles of **14**, at -20°.

2.4.2.15 X-Ray crystal structure determinations

Crystal data collection and refinement details for ligand **III** and complexes **1a**, **1b**, **2**, **5**, **6**, **12**, **13**, **14** are summarised in Tables 2.20-2.27. Data sets for compounds were collected on a Bruker SMART Apex CCD diffractometer⁶⁹ with graphite monochromated Mo-K α radiation ($\lambda = 0.71073 \text{ \AA}$). Data reduction was carried out with standard methods from software package Bruker SAINT.⁷⁰ Empirical corrections were performed using SCALEPACK⁷¹ and data were treated with SADABS.^{72,73}

⁶⁹ SMART Data Collection Software, Version 5.629, Bruker AXS Inc., Madison, WI, 2003.

⁷⁰ SAINT, Data Reduction Software, Version 6.45, Bruker AXS Inc., Madison, WI, 2003.

⁷¹ L.J. Ferrugia, *J. Appl. Crystallogr.*, 1999, **32**, 837.

⁷² R.H. Blessing, *Acta Crystallogr.*, 1995, **A51**, 33.

All the structures were solved in collaboration with Dr S. Nogai, using direct methods or interpretation of a Patterson synthesis which yielded the position of the metal atoms, and conventional difference Fourier methods. All non-hydrogen atoms were refined anisotropically by full-matrix least squares calculations on F^2 using SHELX-97⁷⁴ within the X-seed⁷⁵ environment. The hydrogen atoms were fixed in calculated positions. Figures were generated with X-seed⁷⁵ and POV Ray for Windows, with the displacement ellipsoids at 50% probability level. Further information is available from Prof. H.G. Raubenheimer at the Department of Chemistry and Polymer Science, Stellenbosch University.

Crystallisation procedures for complexes, are described in the preparation and procedure part of section 2.4.2.

⁷³ SADABS, Version 2.05, Bruker AXS Inc., Madison, WI, 2002.

⁷⁴ G.M. Shelrick, SHELX-97. Program for Crystal Structure Analysis, University of Göttingen, Germany, 1997.

⁷⁵ L.J. Barbour, *J. Supramol. Chem.* 2001, **1**, 189.

Table 2.23 Crystallographic data for polymorphs **1a** and **1b**

	1a	1b
Empirical formula	C ₉ H ₆ AuCIN ₃ PS ₃	C ₉ H ₆ AuCIN ₃ PS ₃
M_r	515.73	515.73
Temp. (K)	203 (2)	100 (2)
Wavelength (Å)	0.71073	0.71073
Crystal system	Monoclinic	Triclinic
Space group	P2 ₁ /c	P $\bar{1}$
a (Å)	10.3829(1)	8.0705(4)
b (Å)	16.2935(1)	8.6077(4)
c (Å)	17.2073(2)	10.5184(5)
α (°)	90	72.425(1)
β (°)	92.32	84.882(1)
γ (°)	90	75.120(1)
Volume (Å ³)	2908.63(5)	673.20(6)
Z	8	2
d_{calcd} (g/cm ³)	2.355	2.544
Absorption coefficient (μ , mm ⁻¹)	10.823	11.690
Absorption correction	none	Semi-empirical from equivalents (SADABS)
F(000)	1920	480
Crystal size (mm)	0.15 x 0.07 x 0.05	0.20 x 0.15 x 0.10
θ -range for data collection (°)	3.02 to 26.00	2.56 to 26.73
Index range	-12 ≤ h ≤ 12 -20 ≤ k ≤ 20 -21 ≤ l ≤ 21	-10 ≤ h ≤ 10 -10 ≤ k ≤ 10 -13 ≤ l ≤ 13
No. of reflections collected	21538	7454
No. independent reflections	5711 ($R_{\text{int}} = 0.0250$)	2842 ($R_{\text{int}} = 0.0251$)
Max. and min. transmission	0.6137 and 0.2936	0.3102 and 0.1668
Refinement method	Full-matrix least-squares on F ²	Full-matrix least-squares on F ²
Data/restraints/parameters	5711 / 0 / 325	2842 / 0 / 163
Goof on F ²	1.033	1.028
Final R-indices [$I > 2\sigma > (I)$]	$R_1 = 0.0207$ $wR_2 = 0.0422$	$R_1 = 0.0192$ $wR_2 = 0.0449$
R indices (all data)	$R_1 = 0.0272$ $wR_2 = 0.0439$	$R_1 = 0.0202$ $wR_2 = 0.0453$
Largest diff. peak and hole (e.Å ⁻³)	0.817 and -0.802	1.384 and -0.786
Weighing scheme		a = 0.0223 / b = 0.2556

Table 2.24 Crystallographic data for **III** and **2**

	III	2
Empirical formula	C ₁₂ H ₁₅ N ₆ P	C ₁₂ H ₁₂ AuClN ₃ PS ₃
<i>M_r</i>	274.27	557.81
Temp. (K)	100(2)	100(2)
Wavelength (Å)	0.71073	0.71073
Crystal system	Orthorhombic	Monoclinic
Space group	Pna2 ₁	C2/c
a (Å)	13.9779(15)	23.574(2)
b (Å)	9.2492(10)	10.7660(9)
c (Å)	10.2439(11)	17.201(2)
α (°)	90	90
β (°)	90	128.280(1)
γ (°)	90	90
Volume (Å ³)	1324.4(2)	3426.9(5)
Z	4	8
<i>d</i> _{calcd} (g/cm ³)	1.376	2.162
Absorption coefficient (μ, mm ⁻¹)	0.204	9.195
Absorption correction	none	Semi-empirical from equivalents (SADABS)
F(000)	576	2112
Crystal size (mm)	0.30 x 0.20 x 0.20	0.20 x 0.20 x 0.15
θ-range for data collection (°)	2.64 to 26.73	2.19 to 26.73
Index range	-13 ≤ h ≤ 17 -8 ≤ k ≤ 11 -12 ≤ l ≤ 12	-29 ≤ h ≤ 29 -7 ≤ k ≤ 13 -21 ≤ l ≤ 21
No. of reflections collected	7514	9974
No. independent reflections	2762 (R _{int} = 0.0190)	3639 (R _{int} = 0.0222)
Refinement method	Full-matrix least-squares on F ²	Full-matrix least-squares on F ²
Data/restraints/parameters	2762 / 1 / 175	3639 / 0 / 193
Goof on F ²	1.070	1.058
Final R-indices [I > 2σ > (I)]	R ₁ = 0.0275 wR ₂ = 0.0719	R ₁ = 0.0204 wR ₂ = 0.0473
R indices (all data)	R ₁ = 0.0281 wR ₂ = 0.0724	R ₁ = 0.0225 wR ₂ = 0.0482
Largest diff. peak and hole (e.Å ⁻³)	0.283 and -0.165	1.039 and -0.530
Weighing scheme	a = 0.0435 / b = 0.2775	a = 0.0245 / b = 1.1125

Table 2.25 Crystallographic data for **5** and **6**

	5	6
Empirical formula	C ₂₂ H ₁₉ AuClN ₂ P	C ₂₄ H ₂₀ Au ₂ Cl ₂ P ₂
M_r	574.78	835.17
Temp. (K)	100(2)	150(2)
Wavelength (Å)	0.71073	0.71073
Crystal system	Monoclinic	Orthorhombic
Space group	C2/c	Pbcn
a (Å)	17.978(3)	17.616(3)
b (Å)	16.395(2)	8.561 (2)
c (Å)	15.163(2)	15.186(3)
α (°)	90	90
β (°)	118.078(2)	90
γ (°)	90	90
Volume (Å ³)	3943.4(10)	2290.3(7)
Z	8	4
d_{calcd} (g/cm ³)	1.936	2.422
Absorption coefficient (μmm^{-1})	7.687	13.180
Absorption correction	Semi-empirical from equivalents (SADABS)	Semi-empirical from equivalents (SADABS)
F(000)	2208	1544
Crystal size (mm)	0.20 x 0.10 x 0.10	0.1 × 0.15 × 0.25
θ -range for data collection (°)	1.79 to 26.73	2.31 to 26.73
Index range	-15 ≤ h ≤ 22 -19 ≤ k ≤ 20 -19 ≤ l ≤ 18	-22 ≤ h ≤ 21 -10 ≤ k ≤ 10 -19 ≤ l ≤ 16
No. of reflections collected	11306	12650
No. independent reflections	4179 ($R_{\text{int}} = 0.0356$)	2426 ($R_{\text{int}} = 0.0406$)
Max. and min. transmission	0.4622	0.2678 and 0.1955
Refinement method	Full-matrix least-squares on F^2	Full-matrix least-squares on F^2
Data/restraints/parameters	4179 / 0 / 244	2426 / 18* / 137
Goof on F^2	1.041	1.056
Final R-indices [$I > 2\sigma > (I)$]	$R_1 = 0.0381$ $wR_2 = 0.0941$	$R_1 = 0.0317$ $wR_2 = 0.0773$
R indices (all data)	$R_1 = 0.0535$ $wR_2 = 0.1022$	$R_1 = 0.0390$ $wR_2 = 0.0805$
Largest diff. peak and hole ($e \cdot \text{Å}^{-3}$)	2.961 and -0.794	1.779 and -0.604
Weighing scheme	a = 0.0621	a = 0.0413 / b = 7.8660
*Restraints		ISOR to C11

Table 2.26 Crystallographic data for **12** and **13**

	12	13
Empirical formula	C ₂₉ H ₂₁ Au ₂ C ₁₃ F ₅ N ₂ P	C ₂₄ H ₁₅ Au ₂ F ₁₀ N ₆ P
M_r	1023.73	1002.03
Temp. (K)	100(2)	100(2)
Wavelength (Å)	0.71073	0.71073
Crystal system	triclinic	triclinic
Space group	P $\bar{1}$	P $\bar{1}$
a (Å)	10.505(2)	10.2802(15)
b (Å)	12.697(2)	12.7070(18)
c (Å)	13.241(2)	13.1407(19)
α (°)	113.914(3)	81.504(2)
β (°)	103.872(2)	81.244(3)
γ (°)	90.991(3)	72.231(2)
Volume (Å ³)	1554.2(4)	1606.3(4)
Z	2	2
d_{calcd} (g/cm ³)	2.187	2.192
Absorption coefficient (μmm^{-1})	9.791	9.264
Absorption correction	Semi-empirical from equivalents (SADABS)	Semi-empirical from equivalents (SADABS)
F(000)	956	992
Crystal size (mm)	0.20 x 0.10 x 0.10	0.05 x 0.15 x 0.15
θ -range for data collection (°)	1.75 to 26.73	2.19 to 28.17
Index range	-7 ≤ h ≤ 13 -13 ≤ k ≤ 16 -16 ≤ l ≤ 16	-12 ≤ h ≤ 13 -15 ≤ k ≤ 16 -16 ≤ l ≤ 10
No. of reflections collected	9244	9403
No. independent reflections	6419 ($R_{\text{int}} = 0.0146$)	6595 [$R_{\text{int}} = 0.0262$]
Max. and min. transmission	0.3749 and 0.2408	0.3310 and 0.6545
Refinement method	Full-matrix least-squares on F^2	Full-matrix least-squares on F^2
Data/restraints/parameters	6419 / 0 / 379	6595 / 2 / 408
Goof on F^2	1.104	1.001
Final R-indices [$I > 2\sigma > (I)$]	$R_1 = 0.0350$ $wR_2 = 0.0837$	$R_1 = 0.0449$ $wR_2 = 0.1056$
R indices (all data)	$R_1 = 0.0400$ $wR_2 = 0.0860$	$R_1 = 0.0638$ $wR_2 = 0.1145$
Largest diff. peak and hole (e.Å ⁻³)	2.140 and -1.464	2.955 and -1.784
Weighing scheme	a = 0.0360 / b = 11.0208	a = 0.0685
*Restraints		SADI to acetone

CHAPTER 3

Preparation and characterisation of neutral mono- and dinuclear gold(I) imine and amido complexes derived from simple nitrogen rich heterocycles.

Abstract

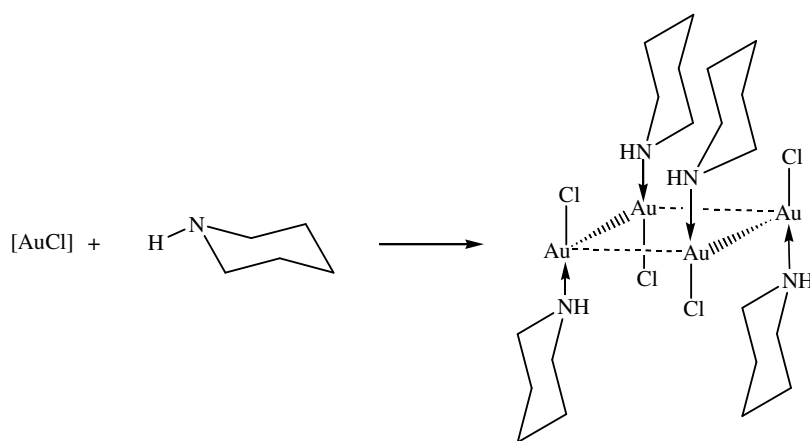
Stable neutral N-coordinated pentafluorophenylgold(I) complexes, 1-methylimidazole(pentafluorophenyl)gold(I), **15**, 1-benzylimidazole(pentafluorophenyl)gold(I), **16**, 1-methylbenzimidazole(pentafluorophenyl)gold(I), **17**, and [1,4-bis(imidazol-1-yl)butane]bis[(pentafluorophenyl)gold(I)], **18**, can be obtained by the reaction of $[\text{Au}(\text{C}_6\text{F}_5)(\text{tht})]$ with 1-methylimidazole, 1-benzylimidazole, 1-methylbenzimidazole and 1,4-bis(imidazole-1-yl)butane. N-coordination of the imine complexes was confirmed by single crystal X-ray structure analysis (**15**, **16** and **17**) and ^{15}N NMR measurements (**18**). Treatment of $[\text{Au}(\text{C}_6\text{F}_5)(\text{tht})]$ with 1-benzyltetrazole affords the first reported imine coordinated gold(I) tetrazole complex, **19**. X-ray crystallography of **19** reveals that only the N^4 nitrogen coordinates to the gold(I) centre. Lithiation of **19** followed by quenching with dimethyldisulphide affords the thiolate complex, **22**. The attempted synthesis of a binuclear tetrazole gold(I)imine complex resulted in the formation of a polymeric chelated lithium salt of the $\text{Au}(\text{C}_6\text{F}_5)_2$ aurate salt, **21**. Reaction of 2,2'-bis(4,5-dimethylthiazole) with various mole quantities of $[\text{Au}(\text{C}_6\text{F}_5)(\text{tht})]$ results in the formation of 2,2'-bis(4,5-dimethylthiazol-2-yl)(pentafluorophenyl)gold(I), **23**. Amido complexes, (triphenylphosphine)(tetrazol-1-yl)gold(I), **22**, and (trimethylphosphine)(tetrazol-1-yl)gold(I), **25**, can be prepared by reaction of sodium tetrazolate with $[\text{AuCl}(\text{PMe}_3)]$ or $[\text{AuCl}(\text{PPh}_3)]$. The synthesis of various bicyclic and tricyclic tetrazole ligands by microwave-irradiation methods dramatically improves yields, purity and reaction times.

3.1 Introduction

The ability of gold(I), as an innately soft metal centre, to coordinate to both soft and hard ligands, is well established and evident in the diversity of gold(I) derivatives reported in literature.¹ In relation to its affinity for sulphur-donor and phosphine ligands, gold(I) has a moderate tendency to form complexes with nitrogen ligands. Although many gold(I) complexes that contain gold-nitrogen bonds have been prepared, the structural analysis of stable neutral imine complexes derived from azoles such as imidazoles, thiazoles, and

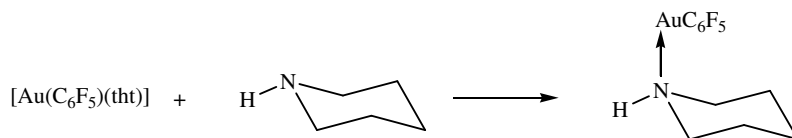
¹ J. Strähle, in *Gold: Progress in Chemistry, Biochemistry and Technology*, ed. H. Schmidbaur, John Wiley & Sons Ltd., Chichester, 1999, pp. 311-313.

tetrazoles remain limited. The propensity of gold(I) atoms to aggregate *via* inter and intramolecular aurophilic interactions often provides additional stabilisation to such complexes, affording interesting and unpredictable extended coordination structures in the solids (also see binuclear complexes **12-14**, Section 2.2.3.2).^{2,3,4} Gold(I) complexes derived from neutral nitrogen-donor ligands are predominantly of the type AuXL_n where X constitutes a halide or pseudo-halide anion, and L a neutral Lewis base nitrogen compound. Molecular or ionic forms of the type AuXL exist in solid state with the structure L-Au-X or [AuL₂]⁺ and [AuX₂]⁻, respectively. However, certain complications sometimes arise. Chloro(piperidine)gold(I) exists in the solid state as a neutral tetrameric complex, stabilised by extensive Au(I)...Au(I) contacts with the gold atoms arranged in square clusters (Equation 3.1).⁵



Equation 3.1

By the reaction of [Au(C₆F₅)(tht)] with piperidine, the related organometallic complex pentafluorophenyl(piperidine)gold(I) is obtained as a neutral monomeric derivative (Equation 3.2).⁶ This compound appears more stable in solution and in solid state than the chloro equivalent.



Equation 3.2

² S. D. Bunge, O. Just and W. S. Rees, Jr., *Angew. Chem., Int. Ed., Engl.*, 2000, **39**, 3082.

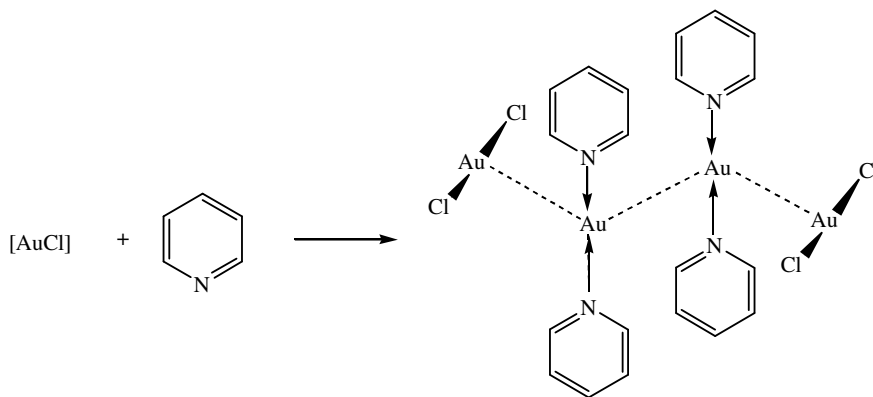
³ K. Nomiya, R. Noguchi, K. Ohsawa and K. Tsuda, *J. Chem. Soc., Dalton Trans.*, 1998, 4101.

⁴ A. Hayashi, M. M. Olmstead, S. Attar and A.L. Balch, *J. Am. Chem. Soc.*, 2002, **124**, 5791.

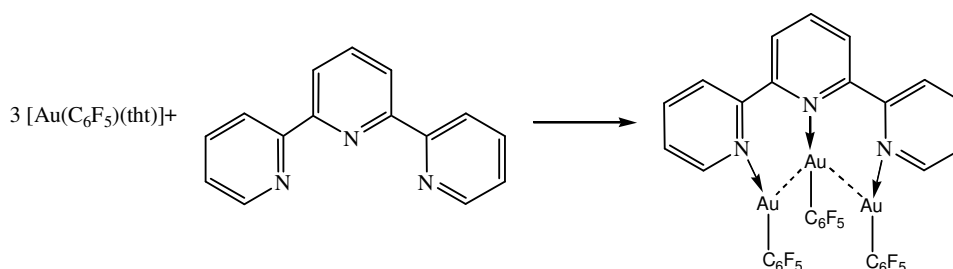
⁵ J.J. Guy, P.G. Jones, M.J. Mays and G.M. Sheldrick, *J. Chem. Soc., Dalton Trans.*, 1977, 8.

⁶ S. Cronje, H. G. Raubenheimer, H. S. C. Spies, C. Esterhuysen, H. Schmidbaur, A. Schier, G. J. Kruger, *Dalton Trans.*, 2003, **14**, 2859, and references cited therein.

In contrast, chloro(pyridine)gold(I) crystallises as a tetrameric salt $[\text{Au}(\text{py})_2]^+[\text{AuCl}_2]^-$ that is arranged in chains (Equation 3.3).⁷ The unprecedented $\eta^3\text{-M}_3$ coordination mode in a terpyridine ligand was recently reported as the first example of this ligand bonded to three different metals (Equation 3.4). The aurophilic interactions present in the molecule contribute to the overall stability of the system as confirmed with by DFT (density functional theory) calculations.⁸



Equation 3.3



Equation 3.4

In a study to elucidate the ligand preference of the $\text{C}_6\text{F}_5\text{Au}$ centre, Cronje and co-workers showed that the Au^+ soft acid centre, in a ligand substitution series, follows in order of decreasing preference: $>\text{C}=\text{S} > \text{R}_2\text{NH}$ (hard base) $> >\text{C}=\text{N}^-$ (borderline base) $> \text{RSR}$ (soft base), which is in disagreement to the conventional classification of hard and soft acids and bases by the order: $>\text{C}=\text{S} > \text{RSR}$ (soft base) $> >\text{C}=\text{N}^- > \text{R}_2\text{NH}$ (Equation 3.2 and 3.5).⁹ A salient feature in these compounds is the *trans* influence exerted on the stable Au-N coordination by the ligand in the *trans* position.¹⁰ When provided with a choice of borderline-hard or soft donor ligands, the pentafluorophenyl substituted gold(I) centre forms unexpected stable mononuclear imine complexes. Related compounds, chloro[1-methyl-2-(phenyl)imidazole]gold(I) and chloro[1-methyl-2-(2-pyridinyl)imidazole]

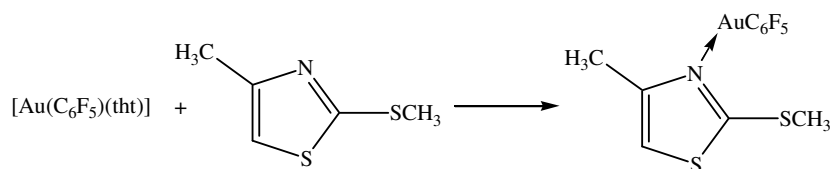
⁷ H.-N. Adams, W. Hiller and J. Strähle, *Z. Anorg. Allg. Chem.*, 1984, **512**, 169.

⁸ J. E. Aquado, M. J. Calhorda, M. Concepción Gimeno and A. Laguna, *Chem. Comm.*, 2005, 3355.

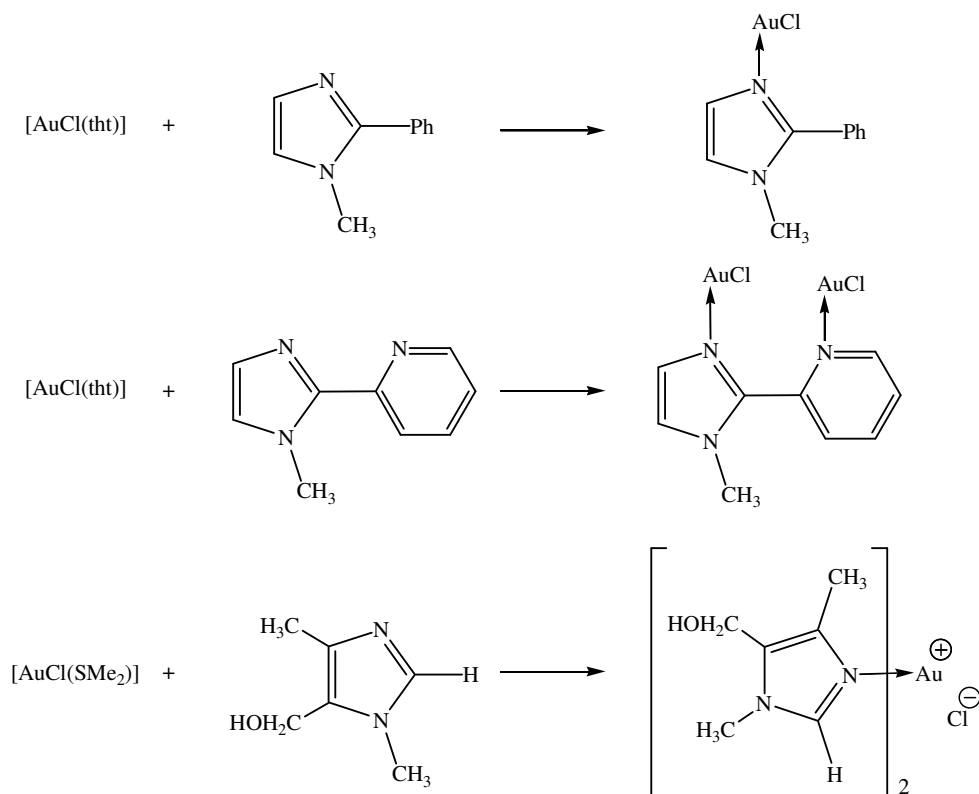
⁹ R. G. Pearson, *Inorg. Chim. Acta*, 1995, **240**, 93.

¹⁰ P. G. Jones and A. F. Williams, *J. Chem. Soc., Dalton Trans.* 1976, 1430

gold(I) appear thermodynamically unstable (Equation 3.6), and gold(I) complexes of the type $[\text{AuXL}]_2$ ($X = \text{Cl}$, $L = \text{N-methylimidazole}$, N-ethylimidazole)¹¹ and $[\text{AuL}_2]^-$ ($L = 4\text{-hydroxymethyl-1,5-dimethylimidazole}$) crystallise as metal salts.^{12, 13} This variance in stability can be ascribed to a greater *trans* influence that the C_6F_5 substituent has relative to the chloro group.



Equation 3.5



Equation 3.6

Gold(I) imine complexes notoriously form two coordinate, linear structures, although selective examples of threefold and fourfold coordinations have also been reported.¹⁴ In this regard additional stabilisation is provided by chelate-type ligands. An example, illustrating an expanded coordination centre, of the type $[\text{Au}(\text{L}^1\wedge\text{L}^2)\text{X}]$ (where $\text{L}^1\wedge\text{L}^2$ is a

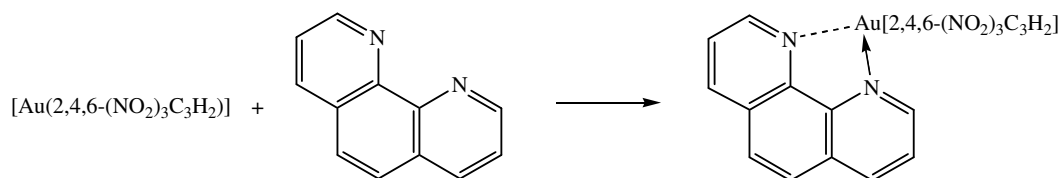
¹¹ M. Deetlefs, *PhD dissertation*, Stellenbosch University, 2001.

¹² Z. D. Matovic, D. J. Radanovic, G. Ponticelli, P. Scano and I. A. Efimenko, *Trans. Met. Chem.*, 1994, **19**, 461.

¹³ C. J. L. Lock and Z. Wang, *Acta Cryst.*, **C49**, 1993, 1330.

¹⁴ J. Vicente, A. Arcas, P.G. Jones and J. Lautner, *J. Chem. Soc., Dalton Trans.*, 1990, 451.

chelating ligand, and X a halide or pseudohalide) such as (2,9-dimethyl-1,10-phenanthroline)(2,4,6-trinitrophenyl)gold(I). An unsymmetrical chelate coordination is observed for the two N-donor atoms of the phenanthroline ligand, affording a distorted and near linear coordination about the N-Au-X axis (Equation 3.7).¹⁴



Equation 3.7

The preparation of neutral gold(I) complexes, derived from anionic nitrogen donor ligands, of the type $[\text{AuL}(\text{PR}_3)]$, where L represents various azolates, is well established and many complexes containing pyrazolate, imidazolate, triazolate and tetrazolate N-heterocycles have been described.^{15,3,16} A fascinating example of a photoluminescent neutral dinuclear amido complex, $[\{\text{Au}(\text{PPh}_3)\}_2](\mu\text{-bbzim})$ and its corresponding imine-amido tetranuclear analogue $[\{\text{Au}(\text{PPh}_3)\}_4](\mu\text{-bbzim})[\text{ClO}_4]_2$ (where bbzim = 2,2'-benzimidazolate) in which the imidazolate, bbzim⁻ anion acts as a bridging chelate ligand have been reported by Tzeng and co-workers¹⁷ (Equation 3.8). The photophysical properties of these complexes were ascribed to intraligand fluorescence and phosphorescence with gold(I) perturbation.

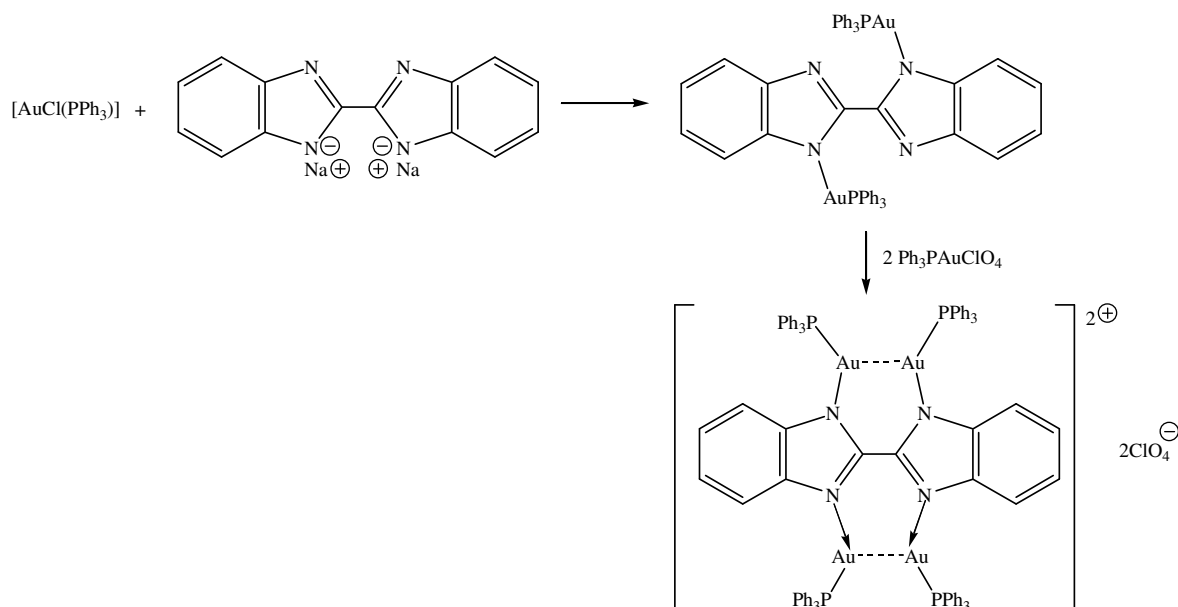
Mono and binuclear gold(I) amido complexes, derived from biologically active molecules such as purines, containing various bridging phosphine ligands, have recently been isolated in our laboratory.¹⁸ A detailed X-ray structural analysis of these complexes reveals that a coalescence of inter- and intramolecular aurophilic interactions and hydrogen bonding dictates the organisation within the crystalline forms.

¹⁵ G. Minghetti, G. Banditelli and F. Bonati, *Inorg. Chem.*, 1979, **18**, 658.

¹⁶ K. Nomiya, R. Noguchi and M. Oda, *Inorg. Chim. Acta*, 2000, **298**, 24.

¹⁷ B-C. Tzeng, D. Li, S-M. Peng and C-M. Che, *J. Chem. Soc., Dalton Trans.*, 1993, 2365.

¹⁸ U. E. I Horvath, S. Cronje, J. M. McKenzie, L. J. Barbour and H. G. Raubenheimer, *Z. Naturforsch.*, **59b**, 2004, 1605.



The potential medicinal application of tertiary phosphine complexes of gold(I) with amido ligands, remains a stimulating field of study.^{19,20,21} Metal complexes of various azoles (imidazole, triazoles, and tetrazoles) have been utilised as prototypes to investigate the relationship between medicinal efficiency and coordination properties to metal centres.²² Gold complexes in this regard have extensively been investigated due to their established activity against rheumatoid arthritis and more recently as anti-tumour agents.²³ This area of research is given further credence by recent findings in our laboratory, in which nitrogen-containing gold(I) trial compounds, have shown remarkable activity against HeLa cells (Human adenocarcinoma of the cervix). Furthermore, these compounds displayed a pronounced tumour selectivity with regard to resting and PHA-stimulated human lymphocytes.²⁴

In order to optimise efficacy and pharmacological activity of a potential lead clinical compound, a defined criterion has to be adhered to, which includes the synthesis of analogous compounds in order to establish structure activity relationship (SAR) trends. A favourable attribute to which gold(I) imine complexes adhere to, is their simple preparative procedure, chemical and *in vitro* stability and their solubility in biological

¹⁹ C. K. Mirabelli, D. T. Hill, L. F. Faucette, F. L. McCabe, G. R. Girard, D. B. Bryan, B. M. Sutton, J. O'Leary Bartus, S. T. Crooke and R. K. Johnson, *J. Med. Chem.*, 1987, **30**, 2181.

²⁰ K. Nomiya, R. Noguchi, K. Ohsawa, K. Tsuda and K. Oda, *J. Inorg. Biochem*, 2000, **78**, 363.

²¹ M. Navarro, F. Vásquez, R. A. Sánchez-Delgado, H. Pérez, V. Sinou and J. Schrével, *J. Med. Chem.*, 2004, **47**, 5204.

²² M. Bardaji, A. Laguna and M. Reyes Perez, *Organometallics*, 2002, **21**, 1877.

²³ E. R. T. Tiekink, *Gold Bull.*, 2003, **36/4**, 117.

²⁴ U. E. I Horvath, S. Cronje and H. G. Raubenheimer, unpublished results.

media. Stable N-coordinated pentafluorophenyl gold(I) complexes derived from neutralazole ligands, further retain the medicinally important acidic C²-proton rendering these molecule more water-soluble. In this regard the efficient synthesis of biologically relevant organic substrates, predominantly derived from N-rich heterocycles, becomes a crucial area of attention.

Burini and co-workers²⁵ have reported that mononuclear, trinuclear and polynuclear derivatives containing N- and C-bonded imidazole rings, show promising anticancer activity. More recent findings by Berners-Price co-workers²⁶ show that dinuclear gold(I)-carbene complexes that contain imidazole ligands, induce pronounced mitochondrial permeability in tumour cells. A similar gold(I) bridging coordination by a related 1,4-bis(imidazol-1-yl)butane ligand, without deprotonation of theazole proton and effected through the two imidazole donor functionalities, remain unexplored.

Bisthiazole and bisimidazole structures form the key components in bleomycines, a class of compounds that have potent tumour-killing properties, and which have widely been applied to cancer chemotherapy.²⁷ Tetrazoles as metabolically stable compounds and carboxylic acid mimics have found wide application as antibacterial, antiviral and anti-inflammatory agents.²⁸ Various coordination modes in substituted and unsubstituted tetrazoles have been explored and a number of metal-amido and metal-imine complexes are known.²⁹ However, gold(I) reactants of tetrazoles are limited to a few examples of anionic N-bonded tetrazolates, exocyclic thiolates and C-bonded tetrazolates.^{16,30,31} To our knowledge 1-substituted tetrazoles have never been successfully applied as a relatively soft N-donor ligands towards gold(I) imine coordination.

The preparation of tetrazoles from the cycloaddition reactions between an azide and a nitrile is well documented. However, only limited reports on the synthesis of pyridyl C- and N-tetrazoles from pyridyl carbonitriles or amines are available. The methodology reported therein requires heating at high temperatures for an extended period of time (up to 108 h.), resulting in impure products whose formation is accompanied by solvent

²⁵ A. Burini, B. R. Pietroni, R. Galassi, G. Valle and S. Calogero, *Inorg. Chim. Acta*, 1995, **229**, 299

²⁶ P. J. Barnard, M. V. Baker, S. J. Berners-Price and D. A. Day, *J. Inorg. Biochem.*, 2004, **98**, 1642.

²⁷ J. Hay, S. Shahzeidi and G. Laurent, *Archives of Toxicology*, 1991, **65**, 81.

²⁸ A. Rajasekaran and P. P. Thampi, *Eur. J. Med. Chem.* 2004, **39**, 273, and references cited therein.

²⁹ A. Fachetti, A. Abbotto, L. Beverina, S. Bradamante, P. Mariani, C.L. Stern, T.J. Marks, A. Vacca and G. A. Pagani, *Chem. Comm.*, 2004, 1770.

³⁰ H. Noth, W. Beck and K. Burger, *Eur. J. Inorg. Chem.*, 1998, 93.

³¹ W. Beck, K. Burger and W. P. Fehlhammer, *Chem. Ber.* 1971, **104**, 1816.

(DMF) degradation.³² A microwave-enhanced reaction could provide a fast and efficient alternative to these simple reactions. High through-put microwave-assisted synthesis of pharmacologically active heterocycles has been an important contribution to combinatorial chemistry, regarding the generation of various libraries for biological screening.³³

To compliment the preparation of gold(I) complexes containing phosphines derived from natural azoles in Chapter 2, and to further elaborate on the stable gold(I) imine coordination complexes illustrated therein (complexes **12-14**), we report in this chapter the preparation, and complete structural characterisation of simple mononuclear and dinuclear gold(I) complexes comprised of imine and amido donor ligands derived from N-rich heterocycles, such as imidazoles and tetrazoles. Our investigations also include other natural azoles, such as thiazoles. The preparation of various gold(I) complexes derived from thiazoles has been a focus area within our research group.³⁴ Cronje and co-workers⁶ have illustrated that when a soft gold(I) centre is provided with a choice between marginal hard or soft-imine ligands and soft endo- or exo-cyclic thioether ligands, the imine coordination is favoured. Structural analysis of the obtained product, in this regard could further indicate whether the sulphur atom, which remained unreactive in (thiazole)gold(I) imine complexes reported in the literature, plays a role in stabilising the crystalline material.

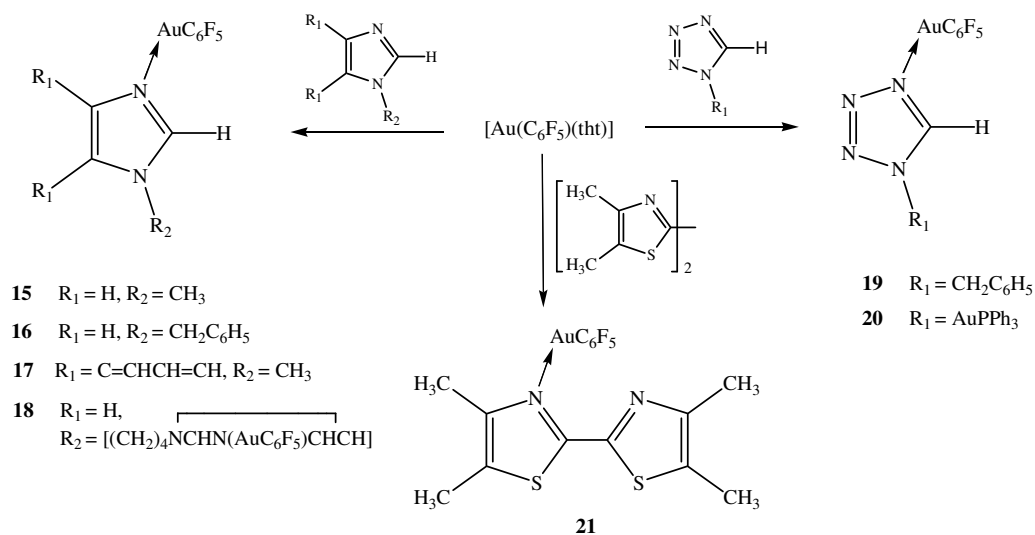
3.2 Results and discussion

Scheme 3.1, shows our approach to the preparation of various gold(I) imine complexes. A thorough X-ray structure analysis study, of these remarkably stable complexes, provides some insight to their stability in crystalline forms. This will be compared to the analogous chloro complexes, which contain overtly stabilising secondary interactions in their molecular organisation. A first-time preparation of an imine-coordinated tetrazole gold(I) complex and derivatives thereof will be illustrated. The preparation of a novel neutral gold(I) complex derived from an anionic tetrazolate ligand, will contribute to the limited number of gold(I) complexes known, with this class of heterocycles as ligands (Scheme 3.2).

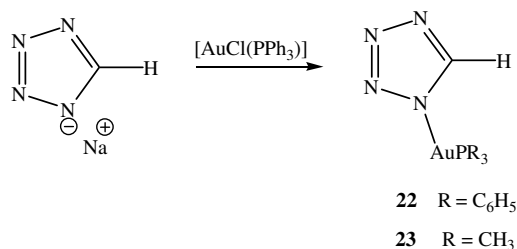
³² C. M. Grunert, P. Weinberger, J. Schweifer, C. Hampel, A. F. Stassen, K. Mereiter and W. Linert, *J. Mol. Struct.*, 2005, **733**, 41.

³³ N. Kaval, D. Ermolate'ev, P. Appukkuttan, W. Dehaen, C. Kappe and E. Van der Eycken, *J. Comb. Chem.*, 2005, **7**, 490.

³⁴ H. G. Raubenheimer, F. Scott, G. J. Kruger, J. G. Toerien, R. Otte, W. van Zyl, I. Taljaard, P. Olivier and L. Linford, *J. Chem. Soc., Dalton Trans.*, 1994, 2091.



Scheme 3.1 A general synthetic route towards gold(I)-imine complexes derived from biologically relevant azoles.



Scheme 3.2 The synthetic route towards gold(I) azolate complexes.

This study also comprises a brief molecular structure and ^{15}N NMR investigation with regards to N-donor capability of tetrazoles. The facile functionalisation of a pyridyl ring by tetrazoles, using microwave-induced reaction methodology, provides an access route to numerous nitrogen rich substrates for metal coordination. An interesting example of a self-assembly, compliment the study of soft gold(I) interactions towards N-donor ligands.

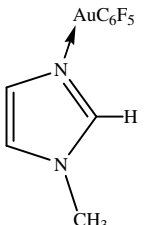
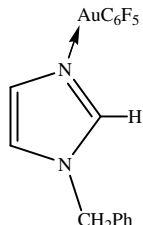
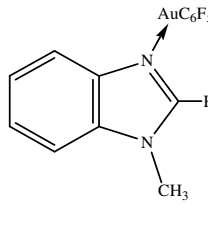
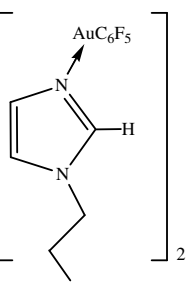
3.2.1 Mono- and dinuclear gold(I) imine complexes derived from imidazoles.

A. Preparation of 1-methylimidazole(pentafluorophenyl)gold(I), **15**, 1-benzylimidazole(pentafluorophenyl)gold(I), **16**, 1-methylbenzimidazole(pentafluorophenyl)gold(I), **17** and [1,4-bis(imidazol-1-yl)butane]bis[(pentafluorophenyl)gold(I)], **18**.

The treatment of equimolar amounts of the starting gold(I) complex, $[\text{Au}(\text{C}_6\text{F}_5)(\text{tht})]$, with 1-benzylimidazole, 1-methylbenzimidazole and 1,4-bis(imidazol-1-yl)butane readily effected substitution of the tht ligand to produce colourless neutral N-coordinated complexes **15-18** (Scheme 1). The reaction mixtures were all filtered through MgSO_4 , to remove any solid contaminants, and evaporated to complete dryness. The resultant complexes are soluble in polar organic solvents and can be obtained in analytically pure form by recrystallisation from solutions of dichloromethane (**15-17**) and tetrahydrofuran

(thf) (**18**) layered with *n*-hexane, at -20 °C. Complex **18** is stable at room temperature and under inert conditions for prolonged periods, but is more air and moisture sensitive than **15-17**. X-ray quality crystals of **15-17** could be obtained, and the resultant structural determination confirmed the molecular structure of these compounds. It is noteworthy that no homoleptic rearranged by-products of **15-17** in various solvents were identified during analysis or crystallisation. Lock and co-workers¹³ isolated the rearranged bis(4-hydroxymethyl-1,5-dimethylimidazole)gold(I) chloride by reacting [AuCl(SMe₂)] with an equimolar amount of 4-hydroxymethyl-1,5-dimethylimidazole. This complex appears unstable in solutions, and revealed metal deposition after prolonged storage as a solid. The free ligand of complexes **17** and **18** were prepared by slight modifications of literature methods.^{35,36} The analytical data for complexes **15-18** are summarised in Table 3.1.

Table 3.1 Analytical data for complexes **15-18**

Complex				
	15	16	17	18
M.p.(°C)	136	120-122	233(decomp.)	148(decomp.)
Colour	colourless	colourless	colourless	colourless
Yield(%)	89	93	90	83
<i>M_r</i>	446.01	522.04	496.03	918.04
Analysis(%) [*]	C ₁₀ H ₆ AuF ₅ N ₂	C ₁₆ H ₁₀ AuF ₅ N ₂	C ₁₄ H ₈ AuF ₅ N ₂	C ₂₂ H ₁₄ N ₄ F ₁₀ Au ₂
C	26.58 (26.92)	36.91 (36.80)	33.60 (33.89)	28.86 (28.78)
H	1.41 (1.36)	1.90 (1.93)	1.51 (1.63)	1.51 (1.54)
N	6.22 (6.28)	5.71 (5.36)	5.82 (5.65)	6.15 (6.10)

* Required calculated values given in parenthesis.

B. Spectroscopic characterisation of complexes **15-18**.

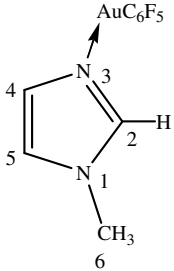
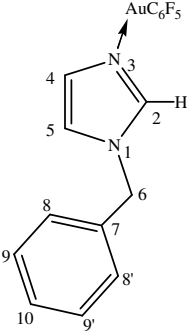
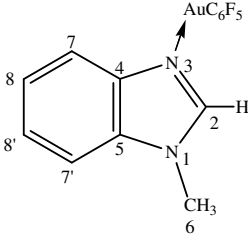
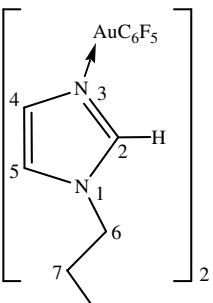
Nuclear magnetic resonance spectroscopy

The ¹H, ¹³C{¹H}, ³¹P{¹H} NMR and ¹⁵N NMR spectroscopic data for complexes **15-18** are summarised in Table 3.2.

³⁵ J-F. Ma, J. Yang, G-L. Zheng, L. Li and J-F. Liu, *Inorg. Chem.*, 2003, **42**, 7531.

³⁶ L. J. Mathias and D. Burkett, *Tetrahedron Lett.*, 1979, **49**, 4709.

Table 3.2 ^1H , $^{13}\text{C}\{^1\text{H}\}$, ^{15}N and ^{19}F NMR spectroscopic data for complexes **15-18**

Complex	 15	 16	 17	 18
Solvent	CD_2Cl_2	$(\text{CD}_3)_2\text{CO}$	$(\text{CD}_3)_2\text{CO}$	$(\text{CD}_3)_2\text{SO}$
Temperature ($^\circ\text{C}$)	25	25	25	25
^1H NMR	H^2	H^2	H^2	H^2
(15, 17 at 300 MHz)	7.78 (s, 1H)	8.46 (m, 1H)	8.82 (s, 1H)	8.48 (dd, 2H, $^3J = 2.6$ Hz, $^4J = 0.2$ Hz)
(16, 18 at 600 MHz)	H^4	7.29 (m, 1H)		7.29 (dd, 2H, $^3J = 2.8$ Hz, $^4J = 0.4$ Hz)
	H^5	7.60 (td, 1H, $^3J = 3.0$ Hz, $^4J = 0.6$ Hz, $^4J = 0.3$ Hz)		7.64 (dd, 2H, $^3J = 3.0$ Hz, $^4J = 0.3$ Hz)
	H^6	5.47 (bs, 2H)	4.15 (s, 3H)	4.12 (t, 4H, $^3J = 5.0$ Hz)
	$\text{H}^7, \text{H}^{7'}$	7.36-7.45 (m, 5H)	7.53 (m, 2H)	1.75 (q, 4H, $^3J = 2.8$ Hz)
	$\text{H}^8, \text{H}^{10}$	141.5 (s)	7.96 (m, 1H) and 7.83 (m, 1H)	139.7 (s)
$^{13}\text{C}\{^1\text{H}\}$ NMR	C^2	130.7 (s)	148.6 (s)	128.2 (s)
(15, 17 at 75 MHz)	C^4	122.9 (s)	142.4 (s)	121.0 (s)
(16, 18 at 150 MHz)	C^5	53.4 (s)	135.6 (s)	46.7 (s)
	C^6	129.4 (s)	33.6 (s)	26.7 (s)
	$\text{C}^7, \text{C}^{7'}$	130.9 (s)	113.8 / 120.1 (s)	
	$\text{C}^8, \text{C}^{8'}$	129.9 (s)	126.4 / 127.2 (s)	
	$\text{C}^9, \text{C}^{9'}$	130.4 (s)		
	C^{10}	119.2 (tm, $J_{\text{CF}} = 54.1$ Hz)	117.7 (m)	118.8 (t, $J_{\text{CF}} = 53.2$ Hz)
	$\text{C}_6\text{F}_5\text{-C}^{\text{ipso}}$	150.3 (ddm, $J_{\text{CF}} = 227.2$ Hz, $J_{\text{CF}} = 24.2$ Hz)	151.7 (ddm, $J_{\text{CF}} = 227.6$ Hz, $J_{\text{CF}} = 24.1$ Hz)	148.6 (ddm, $J_{\text{CF}} = 228.6$ Hz, $J_{\text{CF}} = 23.8$ Hz)
	$\text{C}_6\text{F}_5\text{-C}^{\text{ortho}}$	135.3 (dm, $J_{\text{CF}} = 251.4$ Hz)	138.7 (dm, $J_{\text{CF}} = 242.8$ Hz)	137.4 (dm, $J_{\text{CF}} = 243.9$ Hz)
	$\text{C}_6\text{F}_5\text{-C}^{\text{meta}}$	139.4 (dm, $J_{\text{CF}} = 243.6$ Hz)	140.4 (dm, $J_{\text{CF}} = 244.5$ Hz)	136.0 (dm, $J_{\text{CF}} = 249.8$ Hz)
	$\text{C}_6\text{F}_5\text{-C}^{\text{para}}$	-217.7 (s)		-200.7 (s)
^{15}N NMR (61 MHz)	N^1	-166.3 (s)		-168.4 (s)
	N^3			-116.2 (m)
^{19}F NMR (376 MHz)	F^{ortho}	-115.7 (m)	-115.8 (m)	-116.2 (m)
	F^{meta}	-161.7 (t, $J_{\text{FF}} = 19.5$ Hz)	-157.1 (t, $J_{\text{FF}} = 19.3$ Hz)	-161.3 (t, $J_{\text{FF}} = 21.2$ Hz)
	F^{para}	-164.3 (m)	-161.3 (m)	-164.0 (m)

The ^1H and ^{13}C NMR spectra of the complexes provide limited information as to the structure of the coordinated complexes. The resonances of the atoms in the complexes are shifted consistently downfield ($\Delta\delta_{\text{H}}$ 0.3 and $\Delta\delta_{\text{C}}$ 4.0) from their positions in the spectra of the free ligands. The most notable changes occur in the proton resonances of the acidic CH's, which show a more significant downfield shift ($\Delta\delta$ 1.0) relative to the free ligands. High resolution ^{13}C and ^{19}F NMR spectra of complexes **15-19** confirm the presence of AuC_6F_5 moieties in the noted distinctive C-F and F-F coupling patterns of the signals. To determine whether coordination occurs on both imine donor sites in **18**, we relied on ^{15}N NMR spectra as no crystals of suitable dimension for crystal structure determination could be obtained. A general upfield shift, with a pronounced shift ($\Delta\delta$ 52) in the case of the nitrogen atoms in the 3-position of the imidazole ring compared to the signal in the free ligand upon coordination, provides sufficient evidence that gold(I) coordination to the donor atom in the 3-position had indeed taken place.

Mass spectrometry

The EI-(**15-17**) and positive-ion FAB(**18**)-mass spectrometric data are summarised in Table 3.3. The molecular ions of **15** (m/z 446), **16** (m/z 522), **17** (m/z 496) are observed in the electron impact mass spectra, whereas the molecular ion peak of **18** (m/z 918) was only obtained by the softer FAB ionisation. Diagnostic fragmentation patterns include successive division of C_6F_5^- and AuC_6F_5^- -moieties from the molecular ion.

Table 3.3 Mass spectrometric data for **15-18**

Fragment	m/z (%)			
	15	16	17	18
$[M]^+$	446 (9)	522 (25)	496 (2)	918 (2)
$\{[M]-\text{C}_6\text{F}_5\}^+$	279 (5)	355 (2)	-	751 (13)
$\{[M]-\text{AuC}_6\text{F}_5\}^+$	82 (28)	158 (100)	132 (100)	555 (12)
$\{[M]-\text{Au}(\text{C}_6\text{F}_5)_2\}^+$				387 (12)
$\{[M]-[\text{Au}(\text{C}_6\text{F}_5)_2]_2\}^+$				191 (15)
$\{\text{AuC}_6\text{F}_5\}^+$	364 (2)	364 (6)	-	-
$\{\text{C}_{12}\text{F}_{10}\}^+$	334 (100)	334 (62)	334 (100)	-
$\{\text{C}_{12}\text{F}_{10}-\text{CF}_3\}^+$	265 (36)	265 (22)	265 (55)	-

C. X-ray structure determination of complexes **15**, **16** and **18**.

The crystal and molecular structures of compounds **15**, **16** and **18** were determined by single crystal X-ray diffraction. The molecular structure of **15** is depicted in Figure 3.1 and selected bond lengths and bond angles are summarised in Table 3.4, numbered according to the figure. Compound **15** crystallises in the triclinic space group $\bar{P}1$ as colourless needles. The molecular units consist of two-coordinate gold(I) atoms bonded to

a C₆F₅-group and to the imine N-atom of the imidazole ring. The coordination about the metal centre approaches linearity [C(11)-Au(1)-N(1) 177.08°]. The Au-C [2.001(4) Å] and Au-N [2.044(3) Å] bond lengths are consistent with those reported in analogous imine(pentafluorophenyl)gold(I) complexes reported later and in the literature.^{6,8,37} The neutral molecules are paired in the crystal lattice by weak hydrogen bonds involving the acidic azole hydrogen and a phenyl fluorine atom (Figure 3.2). It is striking that no intermolecular aurophilic interactions occur in this simple gold(I) complex derived from non-bulky ligands (compare complexes **16** and **17**), especially considering the remarkable stability of the complex in crystalline form. It appears that the absence of a co-planar arrangement of the ligands prohibit metal separations smaller than 4.790 Å.

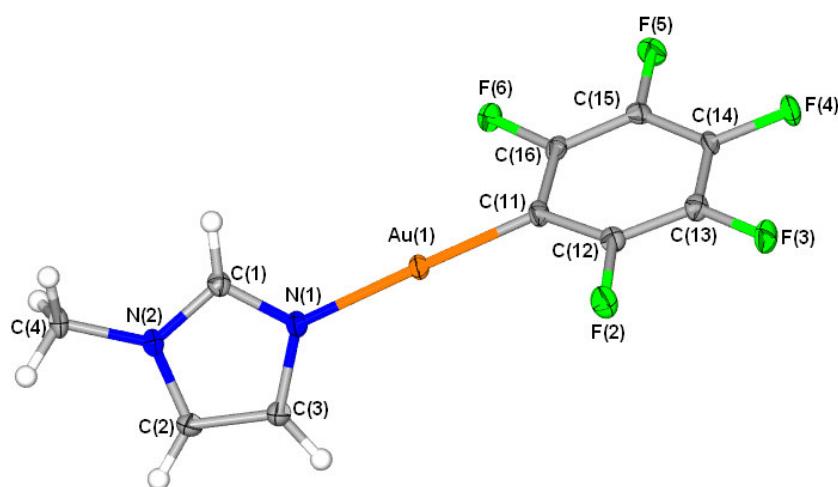


Figure 3.1 Molecular structure of **15** showing the numbering scheme.

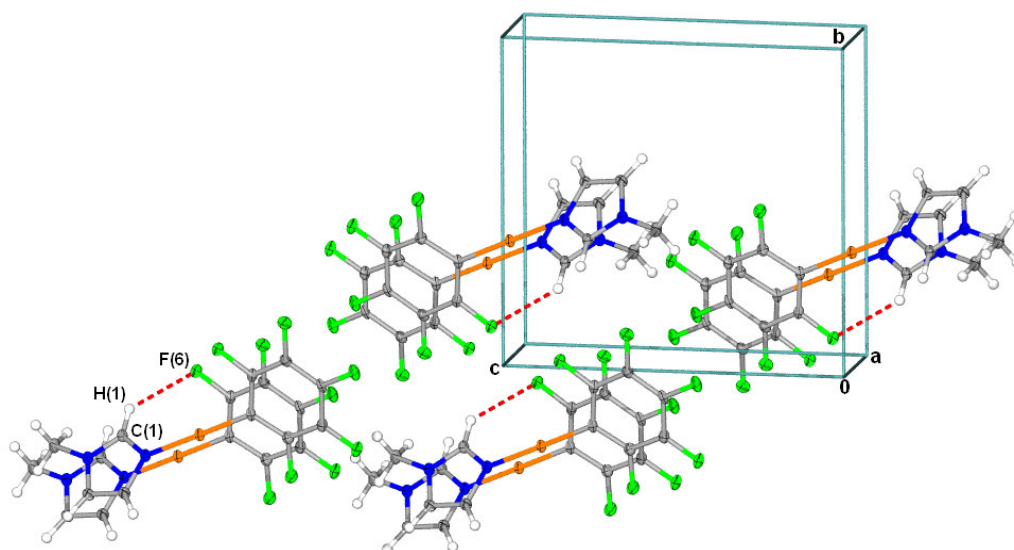


Figure 3.2 Unit cell and packing pattern in the crystal lattice of **15** viewed along the a-axis, showing the non-specific H-bonds involving the azole hydrogen [F(6)...C(1)-H(1) 2.608 Å].

³⁷ E. M. Barranco, O. Crespo, M. C. Gimeno, P. G. Jones, A. Laguna and M. D. Villacampa, *J. Organomet. Chem.*, 1999, **592**, 258.

Table 3.4 Selected bond lengths (Å) and angles (°) for complex **15** with e.s.d.s in parenthesis

Bond lengths		Bond angles	
Au(1)-C(11)	2.001(4)	C(11)-Au(1)-N(1)	177.1(1)
Au(1)-N(1)	2.044(3)	C(1)-N(1)-C(3)	106.2(3)
N(1)-C(1)	1.334(4)	C(1)-N(1)-Au(1)	127.7(3)
N(1)-C(3)	1.387(5)	C(3)-N(1)-Au(1)	126.0(2)
N(2)-C(1)	1.340(5)	C(1)-N(2)-C(4)	126.2(3)
N(2)-C(2)	1.370(5)	C(16)-C(11)-Au(1)	122.1(3)
N(2)-C(4)	1.461(4)	C(12)-C(11)-Au(1)	124.3(3)
C(2)-C(3)	1.361(5)		

The molecular structure of **16** is depicted in Figure 3.3 and selected bond lengths and bond angles in Table 3.5, numbered according to the figure. Compound **16** crystallises in the triclinic space group $P\bar{1}$ as colourless needles. The molecular structure can be described as two discrete linear two coordinate molecules, which assemble in the unit cell as dimeric units. The Au-C [1.996(5) Å and 2.000(5) Å] and Au-N [2.049(4) Å] bond lengths are similar to those found in other imine(pentafluorophenyl)gold(I) complexes reported here and in the literature.^{6,8,37} The two-coordinative centres approach linearity, with the N-Au-C angle, at 179.0(2)° and 177.6(2)°. Weak aurophilic interactions between the gold centres [Au(1)-Au(2) 3.2237(3) Å] are attained by a staggered conformation about the metallic bond plane. This places the planes through the pentafluorophenyl substituents parallel to each other, whilst the planes through the imidazole rings are at an angle. The empirical plane through the coordination centre of the two parts of the dimer approach each other in a characteristic, almost-perpendicular fashion [torsion angle N(11)-Au(1)-Au(2)-N(21) 74.2(2)° and C(31)-Au(1)-Au(2)-C(41) 73.3(2)°]. The spatial separation of the hydrogen bearing C(11) and F(25) is at 3.260 Å [C(21)...F(15) 3.290 Å], approximately the sum of the carbon and fluorine van der Waals radii, which implies a further stabilisation of these dimeric units by weak hydrogen bonding (Figure 3.4).

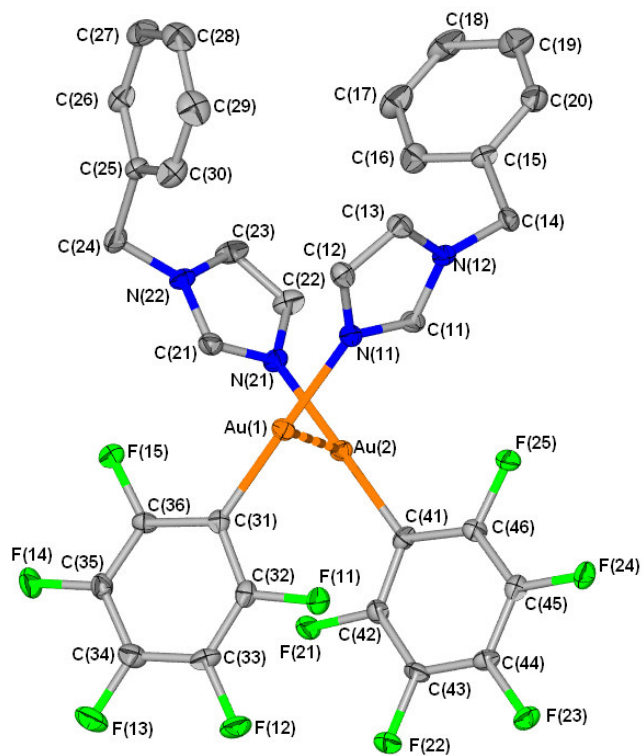


Figure 3.3 Molecular structure of **16** showing the numbering scheme.

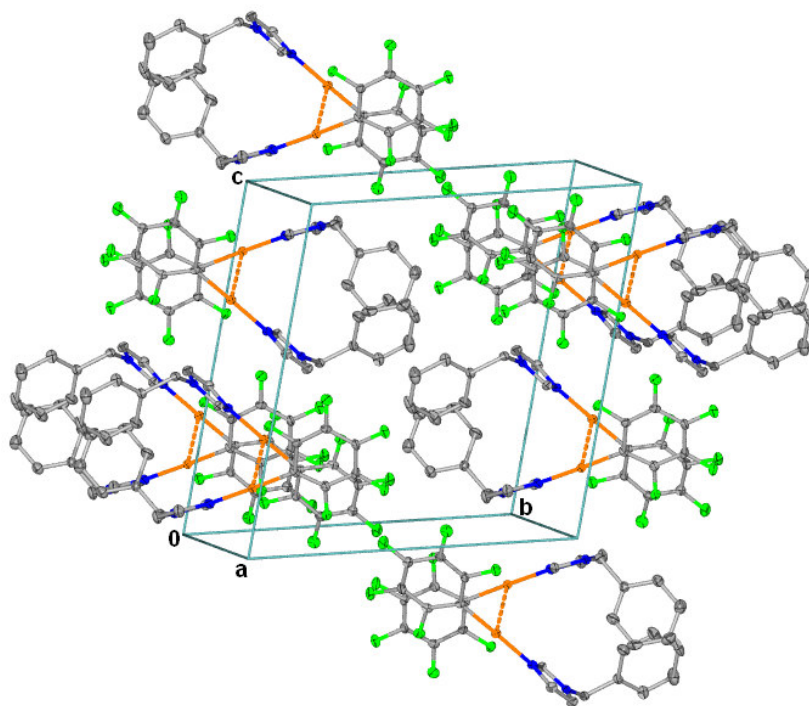
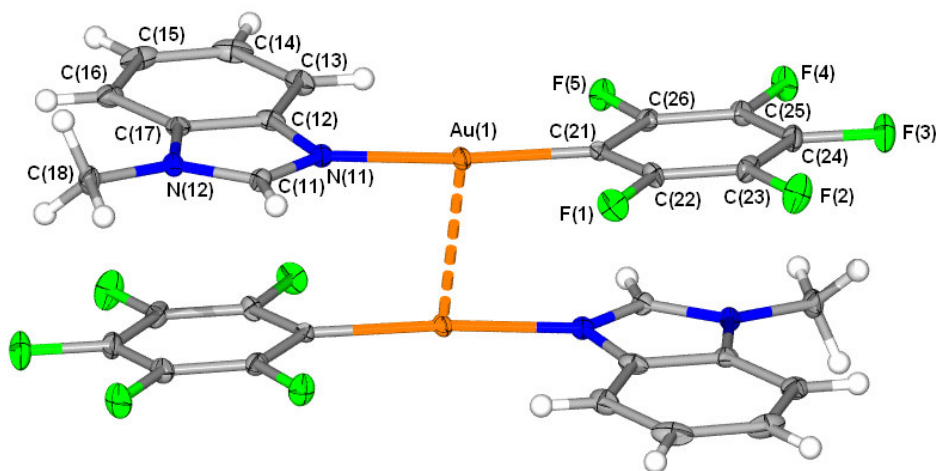


Figure 3.4 Unit cell and packing pattern in the crystal lattice of **16** viewed along the a-axis, showing the paired arrangements.

Table 3.5 Selected bond lengths (Å) and angles (°) for complex **16** with e.s.d.s in parenthesis

Bond lengths		Bond angles	
Au(1)-C(31)	1.996(5)	C(31)-Au(1)-N(11)	179.0(2)
Au(1)-N(11)	2.049(4)	C(41)-Au(2)-N(21)	177.6(6)
Au(2)-C(41)	2.000(5)	C(31)-Au(1)-Au(2)	89.9(1)
Au(2)-N(21)	2.049(4)	C(41)-Au(2)-Au(1)	89.3(1)
N(11)-C(11)	1.327(6)	N(11)-Au(1)-Au(2)	90.7(1)
N(11)-C(12)	1.378(6)	N(21)-Au(2)-Au(1)	88.3(1)
C(11)-N(12)	1.342(6)	C(11)-N(11)-C(12)	105.8(4)
N(12)-C(13)	1.368(6)	C(11)-N(11)-Au(1)	124.9(3)
N(12)-C(14)	1.457(6)	C(12)-N(11)-Au(1)	129.3(3)
C(12)-C(13)	1.347(7)	N(11)-C(11)-N(12)	111.2(4)
Au(1)-Au(2)	3.2237(3)	C(11)-N(12)-C(14)	126.1(4)
		N(12)-C(14)-C(15)	111.8(4)
		C(36)-C(31)-Au(1)	125.6(4)
		C(32)-C(31)-Au(1)	121.8(3)

The molecular structure of **17**, is depicted in Figure 3.5 and selected bond lengths and bond angles are summarised in Table 3.6, numbered according to the figure. Compound **17** crystallises in the monoclinic space group $P2_1/c$, as colourless needles. The two-coordinated gold(I) centre is bonded to the imine N-atom of the benzimidazole and a pentafluorophenyl ligand, and the geometry of the gold atom is slightly distorted from linearity [with C(21)-Au(1)-N(11) 175.6(1) °]. Furthermore, central bonds about the metal centre, Au(1)-C(21) and Au(1)-N(11), appear normal at 2.008(4) Å and 2.046(3) Å, respectively in agreement with similar compounds reported here and in literature.^{6,8,37} The simple linear complex is involved in aurophilic interactions [Au...Au at 3.2896(3) Å] with a neighbouring molecule across an inversion centre, and the dimers are arranged in a head to toe configuration.

**Figure 3.5.** Molecular structure of **17** showing the numbering scheme.

In addition, the C₆F₅ and imine substituent are co-planar and as a result of weak π -stacking interaction between pentafluorophenyl and the 5-membered ring of benzimidazole (distance between centroids 3.484 Å) of the paired units allows for efficient packing in the crystal lattice (Figure 3.6).

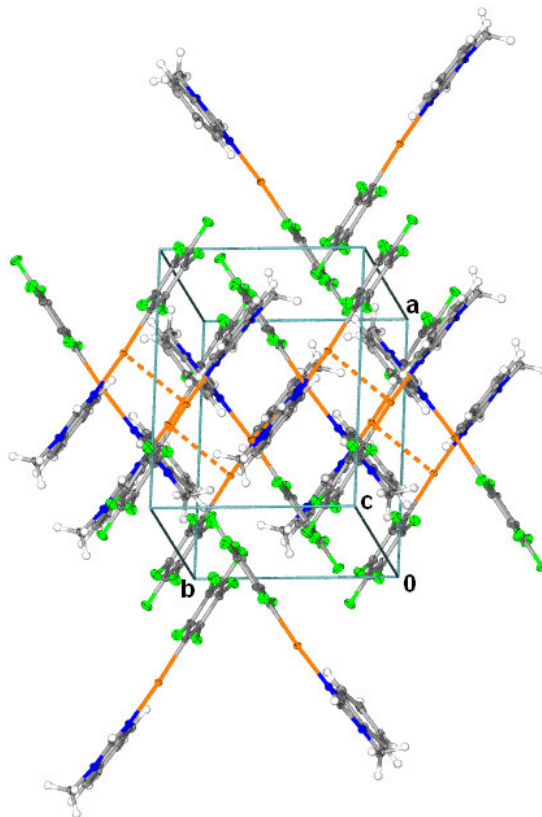


Figure 3.6 Unit cell and packing pattern in the crystal lattice of **17** viewed along the c-axis, showing the head-to-toe organization of the paired molecules.

Table 3.6 Selected bond lengths (Å) and angles (°) for complex **17** with e.s.d.s in parenthesis

Bond lengths		Bond angles	
Au(1)-C(21)	2.008(4)	C(21)-Au(1)-N(11)	175.6(1)
Au(1)-N(11)	2.046(3)	C(21)-Au(1)-Au(1)	98.1(1)
N(11)-C(11)	1.316(5)	N(11)-Au(1)-Au(1)	84.32(9)
N(11)-C(12)	1.404(5)	C(11)-N(11)-C(12)	105.7(3)
C(11)-N(12)	1.351(5)	C(11)-N(11)-Au(1)	129.6(3)
N(12)-C(17)	1.384(5)	C(12)-N(11)-Au(1)	124.6(3)
N(12)-C(18)	1.461(4)	N(11)-C(11)-N(12)	112.5(3)
C(12)-C(17)	1.388(5)	C(11)-N(12)-C(17)	107.2(3)
C(12)-C(13)	1.398(6)	C(11)-N(12)-C(18)	127.1(3)
C(16)-C(17)	1.392(5)	C(17)-N(12)-C(18)	125.7(3)
Au(1)-Au(1)	3.2896(3)	C(17)-C(12)-C(13)	121.1(4)
		C(17)-C(12)-N(11)	108.6(3)
		C(13)-C(12)-N(11)	130.4(4)
		N(12)-C(17)-C(16)	131.3(3)
		C(26)-C(21)-Au(1)	120.8(3)
		C(22)-C(21)-Au(1)	125.0(3)

3.2.2 Mono- and dinuclear gold(I) imine complexes derived from tetrazoles.

A. Preparation of 1-benzyltetrazole(pentafluorophenyl)gold(I), **19**, [(triphenylphosphine)(tetrazol-1-yl)gold(I)][pentafluorophenyl]gold(I), **20** and the formation of a bis(pentafluorophenyl)gold(I) lithium salt, **21**.

Numerous metal complexes of tetrazoles with mono- and bi-dentate coordination of the N¹, N² and N³ nitrogen atoms have been described in the literature. These include predominantly coordination to hard metal centres, e.g. Cu(II), Fe(II), Ni(II) and Tl(I).^{38,39,40,,41,42} To the best of our knowledge, there are no reports in literature describing imine coordination of any tetrazole to a gold(I) metal centre. This first-time preparation of an imine-coordinated tetrazole gold complex, **19**, was carried out in a similar manner to the analogous imidazole-imine complexes. Whereas imine-coordination with imidazole substrates led to immediate product formation, the related tetrazole coordination required prolonged reaction periods and were incomplete. This afforded compound **19** as a colourless solid that is both air and moisture sensitive. Recrystallisation of **19** from dichloromethane layered with *n*-pentane at -20 °C afforded colourless needles of the targeted complex and a co-crystallised free ligand. Subsequent extraction of the crystalline product with diethyl ether afforded **19** in pure form.

Using a similar approach described previously (Section 2.2.3.2) towards the synthesis of multinuclear complexes (**12-14**), complex **24** (preparation described in Section 3.2.4, *vide infra*). was employed as a bifunctional secondary ligand towards further metal coordination. The bimetallic imine-amido complex, **20**, was obtained by following the exact procedure, from the (triphenylphosphine)(tetrazol-1-yl)gold(I) substrate **24**. A complicating reaction occurred during this preparation affording (triphenylphosphine)(pentafluorophenyl)gold(I), [Au(C₆F₅)(PPh₃)]. This result is similar to our attempted metallation of an azolyl(pentafluorophenyl)aurate complex, with (nitrate)(triphenylphosphine)gold(I), [Au(NO₃)(PPh₃)], that afforded the same rearranged by-product (Chapter 4). This rearrangement is reproducible. Complex **20** could thus not be isolated in pure form, and numerous attempts at obtaining X-ray quality crystals only

³⁸ A. F. Stassen, M. Grunert, A. M. Mills and A. L. Spek, J. G. Haasnoot, J. Reedijk and W. Linert, *Dalton Trans.*, 2003, 3628.

³⁹ R. Hinek, H. Spiering, D. Schollmeyer, P. Gutlich and A. Hauser., *Eur. J. Chem.*, 1996, **2**, 1427.

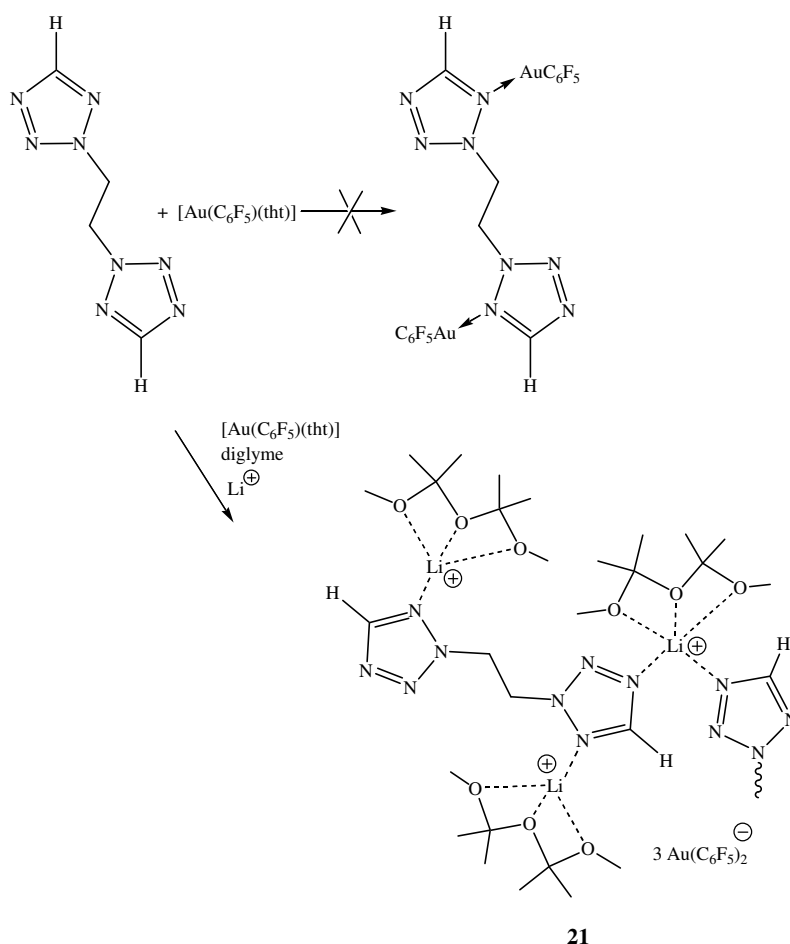
⁴⁰ Z. G. Aliev, T. K. Goncharov, V. P. Grachev and S. V. Kurmaz and V. P. Roschchupkin, *Coord. Chem.*, 1991, **17**, 1101.

⁴¹ A. F. Stassen, O. Roubeau, I. F. Gramage, J. Linares, F. Varret, I. Mutikainen, U. Turpeinen, J.G. Haasnoot and J. Reedijk, *Polyhedron.*, 2001, **20**, 1699.

⁴² S. Bhandari, M. F. Mahon, K. C. Molloy, J. S. Palmer and S. F. Sayers, *J. Chem. Soc., Dalton Trans.*, 2000, 1053.

yielded very stable crystalline forms of $[\text{Au}(\text{C}_6\text{F}_5)(\text{PPh}_3)]$.

The preparation of a dinuclear tetrazolyl imine complex from 1,2-di(tetrazol-2-yl)ethane (ebtz), was attempted in much the same way as the synthesis of the dinuclear imidazole complex **18**. However, residual lithium ions (from the preparation of $[\text{Au}(\text{C}_6\text{F}_5)(\text{tht})]$), stabilised in a 1:1 ratio by diethylene glycol dimethyl ether (diglyme, left over from the preparation of ebtz), effected coordination with the free ligand, that resulted in the formation of a coordination polymer (Scheme 3.3). The polymeric salt contains a free imine coordination site on the N^1 atoms of the terminal ring, but otherwise is derivitised on the N^1 and coordinated on the N^4 positions. Bis(tetrazolyl) units are associated by 4,4'-chelation of the lithium ion.

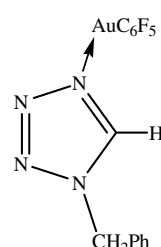
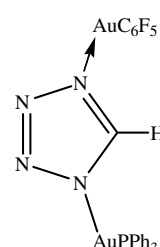
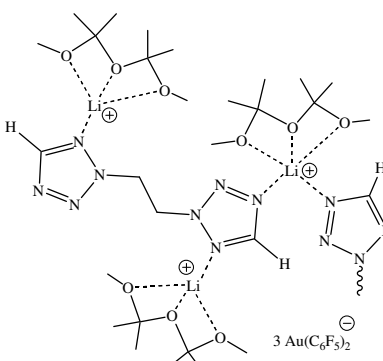


Scheme 3.3 The formation of a lithium(diglyme)-bridged coordination polymeric salt.

These charged aggregates either prevented the coordination of gold(I) to the imine sites of the tetrazole rings, or promoted a metal substitution reaction followed by a homoleptic rearrangement to form the bis(pentafluorophenyl)aurate serving as counterion in **21**. The spontaneous formation of bis(pentafluorophenyl)aurate salts have been reported in

literature, and almost exclusively occurs with stable cations.^{43,44} In addition, the formation of [bis(pentafluorophenyl) gold(I)][(dimethylamine-ethylene)trimethylammonium] will be discussed in Chapter 4 of this dissertation. The salt, **21**, is a yellow crystalline solid, stable at room temperature and in air. Recrystallisation from a concentrated dichloromethane solution layered with *n*-hexane afforded **21** in pure form at -20 °C. The analytical data for complexes **19-21** are summarised in Table 3.7.

Table 3.7 Analytical data for complexes **19-21**

Complex			
	19	20	21
M.p.(°C)	121(decomp.)	57(decomp.)	104(decomp.)
Colour	colourless	colourless	colourless
Yield(%)	62	63	57
M_r	524.03	892.04	1566.26
Analysis(%)*	C ₁₄ H ₈ AuF ₅ N ₄	C ₂₅ H ₁₆ Au ₂ F ₅ N ₄ P	not analysed
C	32.24 (32.08)	33.55 (33.65)	
H	1.51 (1.54)	1.77 (1.81)	
N	10.78 (10.69)	6.20 (6.28)	

* Required calculated values given in parenthesis.

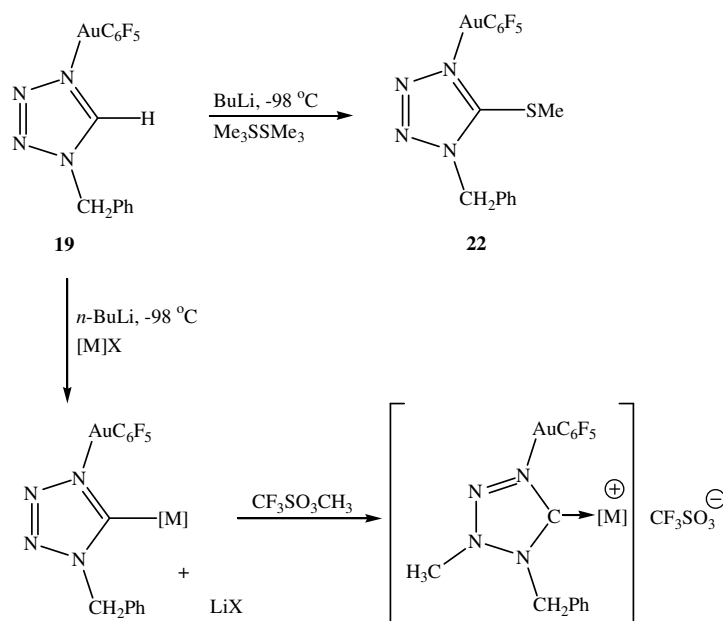
B. Preparation of 1-benzyl-5-methylsulfidotetrazole(pentafluorophenyl) gold(I), **22**.

In order to investigate the effect of C⁵ deprotonation on the stability of complex **19**, the compound was derivitised (Scheme 3.4). Lithiation at low temperature (-98 °C) followed by quenching with dimethyldisulphide afforded **22** as a yellow amorphous solid. During the reaction no decomposition with regard to ring fragmentation or metal deposition was noted. However, when left in common organic solvents, **22** was thermodynamically

⁴³ R. Uson, A. Laguna, J. Vicente, J. Garcia, P. G. Jones, G. M. Sheldrick, *J. Chem. Soc., Dalton. Trans.*, 1981, 655.

⁴⁴ P. G. Jones, *Z. Kristallogr.*, 1993, **208**, 347.

unstable which excluded the formation of X-ray quality crystals. The ^1H , ^{13}C NMR spectroscopic and FAB mass spectrometric data for **22** are summarised in Tables 3.8 and 3.9, respectively. From the successful preparation of complex **19**, emanates a future study towards the synthesis of a potential bimetallic imine-carbene complex by a remote N-alkylation (Scheme 3.4). Further discussion regarding tetrazolyl carbene complexes of gold(I) is reserved for Chapter 4.



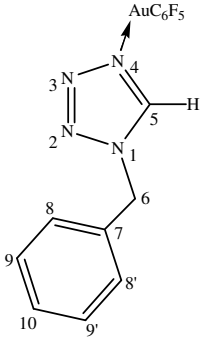
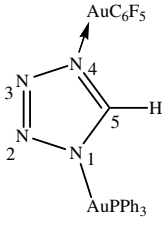
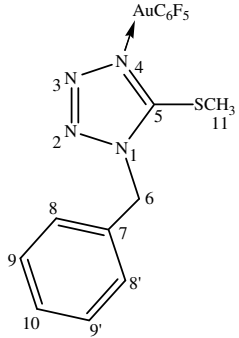
Scheme 3.4 The synthetic route towards C^5 derivatisation of complex **19** (where $[\text{M}]\text{X} = (\text{CO})_5\text{WCl}$ or $\text{Cp}(\text{CO})_2\text{FeCl}$).

C. Spectroscopic characterisation of complexes **19**, **20** and **22**.

Nuclear magnetic resonance spectroscopy

The ^1H , $^{13}\text{C}\{^1\text{H}\}$, $^{31}\text{P}\{^1\text{H}\}$ NMR and ^{15}N NMR spectroscopic data for compounds **19**, **20** and **22** are summarised in Table 3.8. The ^1H and ^{13}C NMR spectra of complexes **19** and **20** provide only partial evidence for the formation of the coordinated complexes. The resonances of complexes **19** and **20** are shifted consistently downfield ($\Delta\delta_{\text{H}}$ 0.3-0.6 for **19** and $\Delta\delta_{\text{C}}$ 3.0 for **20**) compared to 1-benzyltetrazole. The most notable change occurs in the proton resonances of the acidic CH ($\Delta\delta$ 0.6) for both complexes relative to the free ligand.

Table 3.8 ^1H , $^{13}\text{C}\{^1\text{H}\}$, ^{15}N , ^{19}F and ^{31}P NMR spectroscopic data for complexes **19**, **20** and **22**

Complex	 19	 20	 22
Solvent Temperature (°C) ^1H NMR (300 MHz) $^{13}\text{C}\{^1\text{H}\}$ NMR (75 MHz) $^{31}\text{P}\{^1\text{H}\}$ NMR (121 MHz) ^{15}N NMR (61 MHz) ^{19}F NMR (376 MHz)	(CD ₃) ₂ CO 25 H ⁵ 9.24 (s, 1H) H ⁶ 5.80 (s, 2H) H ⁸ -H ¹⁰ 7.40-7.46 (m, 5H) H ¹¹ PPh C ⁵ 145.6 (s) C ⁶ 53.2 (s) C ⁷ 137.2 (s) C ⁸ , C ^{8'} 131.2 (s) C ⁹ , C ^{9'} 130.5 (s) C ₁₀ 130.8 (s) C ₁₁ PPh-C ^{ipso} PPh-C ^{ortho} PPh-C ^{meta} PPh-C ^{para} C ₆ F ₅ -C ^{ipso} 118.7 (tm, $J_{\text{CF}} = 56.8$ Hz) C ₆ F ₅ -C ^{ortho} 150.1 (ddm, $J_{\text{CF}} = 223.9$ Hz, $J_{\text{CF}} = 26.9$ Hz) C ₆ F ₅ -C ^{meta} 139.9 (dm, $J_{\text{CF}} = 245.4$ Hz) C ₆ F ₅ -C ^{para} 141.3 (dm, $J_{\text{CF}} = 250.7$ Hz)	(CD ₃) ₂ CO 25 9.32 (s) 7.60-7.70 (m, 15H) 151.7 (s) 132.0 (d, $^1J = 61.8$ Hz) 136.4 (d, $^2J = 13.8$ Hz) 131.8 (d, $^3J = 12.6$ Hz) 134.5 (d, $^4J = 1.5$ Hz) 119.9 (tm, $J_{\text{CF}} = 57.7$ Hz) 151.8 (ddm, $J_{\text{CF}} = 231.6$ Hz, $J_{\text{CF}} = 22.7$ Hz) 138.5 (dm, $J_{\text{CF}} = 249.7$ Hz) 140.4 (dm, $J_{\text{CF}} = 244.7$ Hz) 34.7 (s) } not detected -117.0 (m) -160.8 (t, $J_{\text{FF}} = 19.2$ Hz) -164.3 (m)	(CD ₃) ₂ CO 25 5.54 (s, 2H) 7.51-7.56 (m, 5H) 2.75 (s, 3H) 186.1 (bs) 52.1 (s) 135.9 (s) 130.8 (s) 130.4 (s) 129.9 (s) 36.7 (s) 118.9 (tm) 150.8 (ddm, $J_{\text{CF}} = 225.1$ Hz, $J_{\text{CF}} = 22.2$ Hz) 139.5 (dm, $J_{\text{CF}} = 242.2$ Hz) 138.4 (dm, $J_{\text{CF}} = 262.4$ Hz)

In both the ^1H and ^{13}C NMR spectra of **20**, tetrahydrothiophene was notably absent indicating that this has been substituted by the imine ligand. High resolution ^{13}C and ^{19}F NMR spectra of complexes **19** and **20** confirm the presence of AuC₆F₅ moieties in that the noted distinctive C-F and F-F coupling patterns, were observed. A pronounced downfield shift ($\Delta\delta$ 49) of the resonance for N⁴ in the ^{15}N NMR spectrum of **19** compared to that of 1-benzyltetrazole, provides unambiguous evidence for the coordination of gold(I) centre to the nitrogen atom. A similar two dimensional ^1H , ^{15}N gHMQC experiment of **20** failed

due to the difficulty of correlating the acidic azole proton and nitrogen atom resonance. The ^{31}P NMR spectrum contains two signals, a broad singlet at δ 34.7 assigned to complex **20**, representing an insignificant downfield shift ($\Delta\delta$ 2.0) relative to complex **24** (*vide infra*), and a sharp singlet at δ 43.5 assigned to $[\text{Au}(\text{C}_6\text{F}_5)(\text{PPh}_3)]$.

The signals in the ^1H NMR spectrum of the thioether complex **22**, are shifted no more than 0.3 ppm from the corresponding signals in **20**. However, the presence of a sharp singlet corresponding to three protons at δ 2.75 and the absence of an acidic CH resonance establishes the formation of the sulphide derivative. Diagnostic signals in the ^{13}C NMR include the SMe resonance at δ 36.6 and a prominent downfield shift ($\Delta\delta$ 41.0) for the substituted C5 carbon to δ 181.1.

Mass spectrometry

The molecular ions of complexes **19**, **22** (EI) and **20** (FAB) were observed in the respective mass spectra. A conspicuous omission from the fragmentation pattern of the imine complexes **19**, **20** and **22** is the initial loss of dinitrogen that is characteristic in the ionisation of free 1- and 5-substituted tetrazoles (Section 3.2.5), 1-benzyltetrazol-2-yl(diphenyl)phosphines and gold(I) complexes thereof (Section 2.2.2), various tetrazol-5-ylidene-gold(I) complexes (Chapter 4) and trialkylphosphine(tetrazol-1-yl)gold(I) complexes (Section 3.2.4). The N^4 -imine coordination to gold(I) appears to stabilise the ring fragmentation that is prevalent in this class of compounds.

Table 3.9 Mass spectrometric data for **19-22**

Fragment	<i>m/z</i> (%)		
	19	20	22
$[\text{M}]^+$	524 (3)	892 (7)	570 (1)
$\{[\text{M}]-\text{S}\}^+$			538 (6)
$\{[\text{M}]-\text{AuC}_6\text{F}_5\}^+$	-	528 (3)	-
$\{\text{AuC}_6\text{F}_5\}^+$	364 (2)	-	364 (4)
$\{\text{C}_{12}\text{F}_{10}\}^+$	334 (100)	-	334 (75)
$\{\text{C}_{12}\text{F}_{10}-\text{CF}_3\}^+$	265 (40)	-	265 (37)
$\{\text{Au}(\text{PPh}_3)_2\}^+$		720 (52)	
$\{\text{AuPPh}_3\}^+$		459 (100)	

D. X-ray structure determination of complexes **19** and **21**.

The crystal and molecular structures of compounds **19** and **21** were determined by single crystal X-ray diffraction. The molecular structure of **19** is depicted in Figure 3.8 and selected bond lengths and bond angles are summarised in Table 3.10. Compound **19** co-crystallises with a molecule of free ligand, 1-benzyltetrazole in the monoclinic space

group $P2_1/c$. The molecular structure can best be described as a discrete monomer consisting of C_6F_5Au unit, coordinated to the neutral imine tetrazole creating an almost linear geometry about the gold(I) atom [C(31)-Au(1)-N(11) 177.5(2) Å]. Of the three unsubstituted nitrogen atoms, only N(14) (N^4 in Table 3.8) is involved in the coordination to the gold centre. It is worth mentioning that the Au(1)-N(11) [2.050(5) Å], adjacent N(11)-N(12) [1.368(7) Å] and C(10)-N(11) [1.310(7) Å] bond lengths in the tetrazole imine complex are consistent with Au-N [2.043(5) Å], N-N [1.336(6) Å] and C-N [1.306(7) Å] bond lengths in the related triphenylphosphine(tetrazol-1-yl)gold(I) amine complex (the only entry of a gold(I) ring substituted tetrazole complex in the Cambridge Crystallographic database).¹⁶ Furthermore, the Au-N distances are probably shorter than the reported gold(I) amine complex, AuCl[NH(CH₂)₄CH₂] [2.07(2) Å] and a gold(I) imine compound, Au(NC₅H₄CH₃-3)(C₆F₅) [2.07(5) Å].⁶ It is similar to the other imines of gold(I) reported in this study, **15** [2.044(3) Å], **16** [2.049(4) Å], **17** [2.046(3) Å], but longer than in the amide gold(I) complex, Au(NNC₃H₃)PPh₃ [2.02(7) Å]. Similarly, the observed Au(1)-C(31) [2.004(6) Å] bond length in **19** is consistent with corresponding lengths in **15** [2.001(4) Å], **16** [1.996(5) Å] and **17** [2.008(4) Å]. The coordination of gold(I) to 1-benzyl tetrazole has to have little effect on the bond lengths and angles of the free ligand. The free ligand in the unit cell associates with the gold(I) complex through weak fluorine and hydrogen interactions. No aurophilic interaction is observed in the crystal lattice of **19**; apart from additional fluorine and hydrogen interaction, π -stacking interactions of the phenyl rings govern the lattice organisation (Figure 3.8).

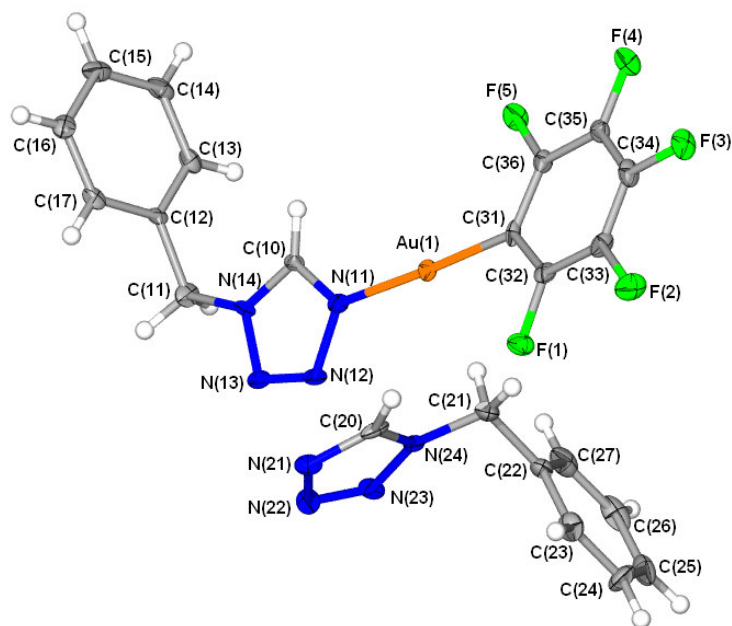


Figure 3.7 Molecular structure of **19** showing the numbering scheme and the presence of a free ligand in the unit cell.

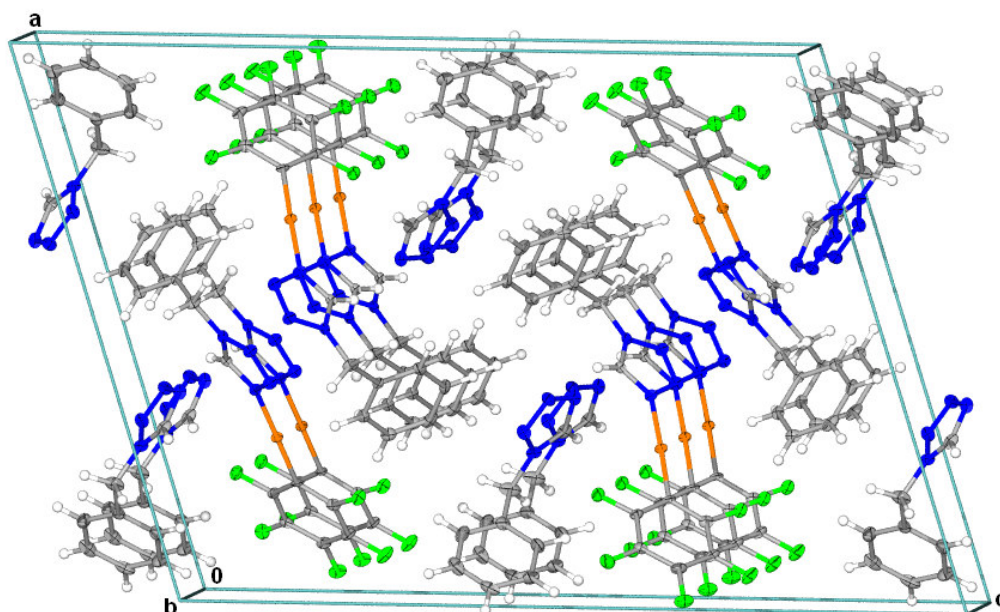


Figure 3.8 Unit cell and packing pattern in the crystal lattice of **19** viewed along the b-axis.

Table 3.10 Selected bond lengths (Å) and angles (°) for complex **19** and 1-benzyltetrazole with e.s.d.s in parenthesis

Bond lengths		Bond angles	
Au(1)-C(31)	2.004(6)	C(31)-Au(1)-N(11)	177.5(2)
Au(1)-N(11)	2.050(5)	C(10)-N(11)-Au(1)	128.9(4)
C(10)-N(11)	1.310(7)	N(12)-N(11)-Au(1)	123.4(4)
C(10)-N(14)	1.334(7)	N(11)-C(10)-N(14)	107.4(5)
N(11)-N(12)	1.368(7)	C(10)-N(11)-N(12)	107.7(5)
N(12)-N(13)	1.283(7)	N(14)-C(11)-C(12)	113.4(5)
N(13)-N(14)	1.349(7)	N(13)-N(12)-N(11)	108.7(5)
C(11)-N(14)	1.478(8)	N(12)-N(13)-N(14)	107.7(5)
		C(10)-N(14)-N(13)	108.5(5)
		C(10)-N(14)-C(11)	131.3(5)
		N(13)-N(14)-C(11)	119.9(5)
1-benzyltetrazole		1-benzyltetrazole	
C(20)-N(21)	1.315(8)	N(21)-C(20)-N(24)	110.7(6)
C(20)-N(24)	1.318(8)	C(20)-N(21)-N(22)	104.5(5)
N(21)-N(22)	1.366(7)	N(24)-C(21)-C(22)	115.0(5)
N(22)-N(23)	1.307(7)	N(23)-N(22)-N(21)	110.5(5)
N(23)-N(24)	1.346(7)	N(22)-N(23)-N(24)	106.4(5)
C(21)-N(24)	1.470(8)	C(20)-N(24)-N(23)	107.9(5)
		C(20)-N(24)-C(21)	129.6(6)
		N(23)-N(24)-C(21)	122.2(5)
		C(32)-C(31)-Au(1)	124.5(5)
		C(36)-C(31)-Au(1)	120.9(4)

The molecular structure of **21**, is depicted in Figure 3.9 and selected bond lengths and bond angles are summarised in Table 3.11, numbered according to the figure. Compound **21** crystallises in the monoclinic space group $P2_1/m$. The single-crystal X-ray diffraction analysis reveals that the complex is composed of non-interacting $\text{Au}(\text{C}_6\text{F}_5)_2^-$ anions and

$\{[\text{Li}(\text{diglyme})_{2.5}(\text{ebtz})]\}_{\infty}^{+}$ cations. Figure 3.9 shows a section of the cation in which two lithium ions each (stabilised by a molecule of diglyme) are coordinated independently to the N(1) and N(5) atoms of the ligand. The coordination of the Li^{+} cations to the diglyme molecule occurs through all three oxygen atoms. The remaining coordination position on Li(1) is filled by a molecule carbonyl-coordinated acetone (not shown). The monomeric units are linked by Li(1) that is bridge-coordinated to the N(8) atom on the first ligand and N(1) of the adjacent molecule (Figure 3.10). The remaining coordination position in Li(1) is equally occupied by a tridentate coordination to a diglyme molecule, to afford a 5-coordinate distorted square pyramidal geometry about both alkali metals. The polymeric cations appear to dictate the ordering of the crystal lattice, and the loosely associative aurate molecules are ordered in parallel rows along the a-axis, flanking the network of cations. The organisation is devoid of intermolecular aurophilic interactions or notable secondary interactions. The angle between the planes of the pentafluorophenyl substituents approaches co-planarity [torsion angles C(41)-Au(1)-C(31)-C(32) and C(41)-Au(1)-C(31)-C(36) of $151(6)^{\circ}$ and $-29(7)^{\circ}$, respectively], which differs from the angle between the aryl planes of the homoleptic rearranged products in bis(*o*-phenylene-bis(dimethylarsine)gold(I), bis(pentafluorophenyl)gold(I) ($\sim 0^{\circ}$) and tetra-*N*-butylammoniumbis(pentafluorophenyl)gold(I) [$81.1(4)^{\circ}$].^{43,44} The near linear molecules of bis(pentafluorophenyl)gold(I) [C(31)-Au(1)-C(41) $177.8(2)^{\circ}$] contain typical Au-C bonds [Au(1)-C(31) and Au(1)-C(41) at $2.047(7)^{\text{\AA}}$ and $2.057(7)^{\text{\AA}}$, respectively](also compare related complexes **16-19**).^{43,44}

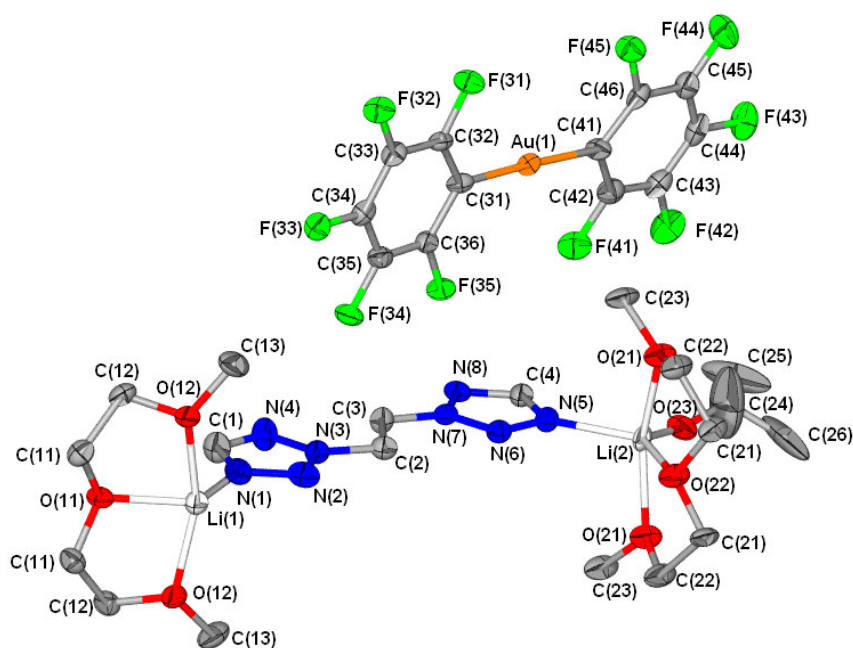


Figure 3.9 Molecular structure of **21** showing the numbering scheme.

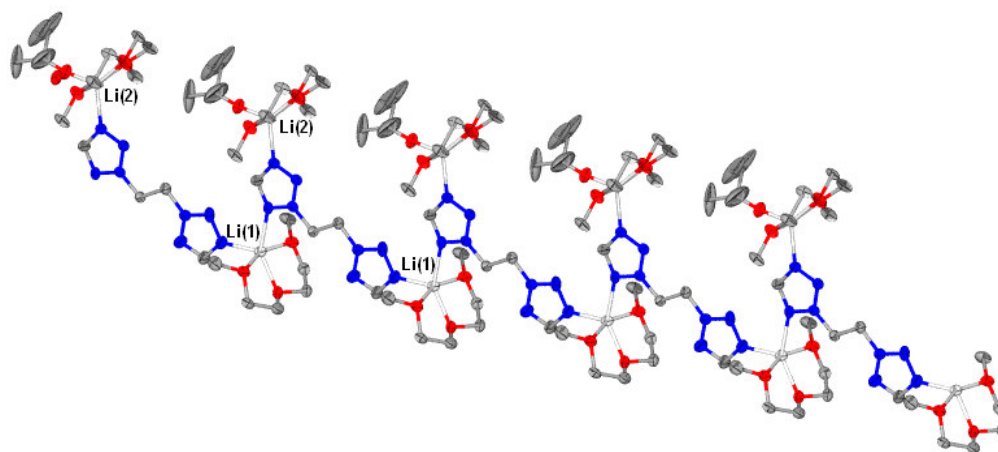


Figure 3.10 Molecular structure of **21** showing the lithium(diglyme)-bridged polymeric chain of bis(tetrazoly)ethane ligands; the $\text{Au}(\text{C}_6\text{F}_5)_2^-$ units are omitted for clarity.

Table 3.11 Selected bond lengths (Å) and angles (°) for complex **21** with e.s.d.s in parenthesis

Bond lengths		Bond angles	
Au(1)-C(31)	2.047(7)	C(31)-Au(1)-C(41)	177.8(2)
Au(1)-C(41)	2.057(7)	C(1)-N(1)-N(2)	107.3(9)
N(1)-C(1)	1.33(1)	C(1)-N(1)-Li(1)	135(1)
N(1)-N(2)	1.36(1)	N(2)-N(1)-Li(1)	117.5(9)
N(2)-N(3)	1.33(1)	N(1)-C(1)-N(4)	113(1)
N(3)-N(4)	1.35(1)	O(11)-Li(1)-N(1)	116.7(9)
C(2)-N(3)	1.47(1)	N(1)-Li(1)-O(12)	100.9(6)
C(2)-C(3)	1.52(1)	O(12)-Li(1)-O(12)	156(1)
C(3)-N(7)	1.44(1)	O(11)-Li(1)-N(8)	141(1)
N(1)-Li(1)	2.06(2)	N(1)-Li(1)-N(8)	101.5(9)
Li(1)-O(11)	2.00(2)	O(12)-Li(1)-N(8)	92.6(5)
Li(1)-O(12)	2.060(7)	O(21)-Li(2)-O(21)	155.1(9)
Li(1)-N(8)	2.23(2)	O(22)-Li(2)-N(5)	127(1)
Li(2)-O(22)	2.06(2)	O(21)-Li(2)-N(5)	99.3(5)
Li(2)-O(21)	2.090(6)	N(3)-N(2)-N(1)	104.4(9)
Li(2)-N(5)	2.10(2)	N(3)-C(2)-C(3)	107.1(9)
		N(2)-N(3)-N(4)	114.2(9)
		N(2)-N(3)-C(2)	120.7(9)
		C(1)-N(4)-N(3)	101.4(9)
		N(4)-N(3)-C(2)	125.2(9)
		N(7)-C(3)-C(2)	111.1(9)
		N(8)-C(4)-N(5)	112(1)
		C(4)-N(5)-Li(2)	132.1(9)
		C(32)-C(31)-Au(1)	125.8(5)
		C(36)-C(31)-Au(1)	121.8(5)

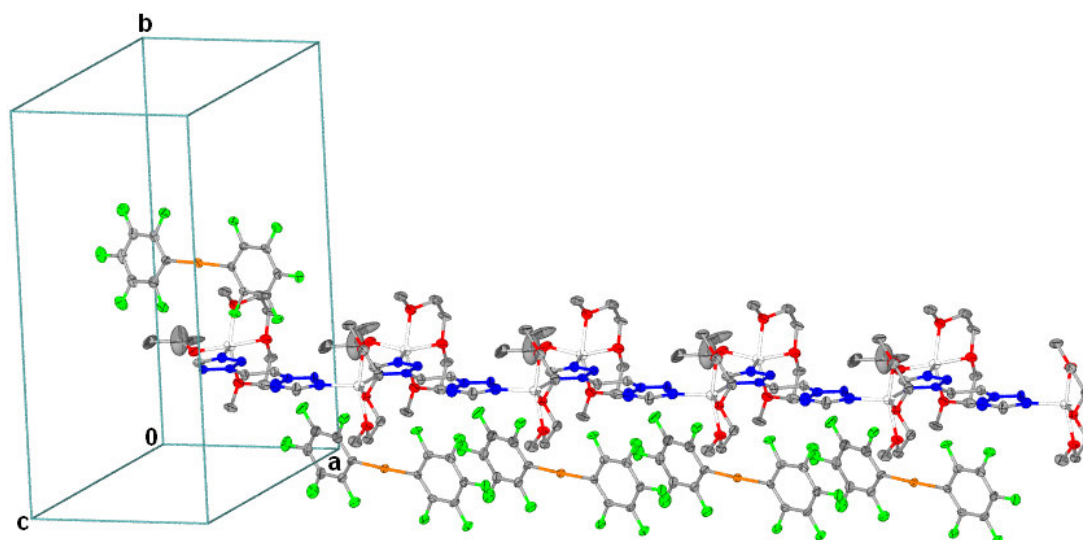


Figure 3.11 Unit cell and packing pattern in the crystal lattice of **21** viewed along the a-axis.

E. ^{15}N NMR and a molecular structure analysis study of the imine coordination potential of tetrazole ligands

From the preceding discussion and examples from the literature it is clear, imidazoles almost without exception form neutral gold(I) imine complexes when reacted with $[\text{Au}(\text{C}_6\text{F}_5)(\text{tht})]$. In contrast the imine coordination potential of tetrazoles is delicately balanced by ring substituents. Molecular orbital calculations on three neutral 5-substituted tetrazoles ($\text{R} = \text{NH}_2$, H and CF_3) confirm that the electron density on the nitrogens of the tetrazole ring decreases as R becomes more electronegative.⁴⁵ More recently density functional theory (DFT) calculations have shown that the thermodynamic stability of tetrazoles are determined by the ring substituents.⁴⁶ The preparation of imine complexes of gold from 1-*H* tetrazole, 5-chloro-1-phenyltetrazole, 1-benzyltetrazolyl(diphenyl) phosphines (described in Section 2.2.3.2), pyridyl and imidazolyl-tetrazoles (described in Section 3.2.5) were all unsuccessful, even in the presence of large excesses of ligand and higher reaction temperatures. This prompted a ^{15}N NMR- and a molecular-structure-analysis-based investigation of 1-benzyltetrazole and 5-chloro-1-phenyltetrazole ligands (see Figure 3.7 and Figure 3.12, respectively) in an attempt to ultimately relate the structural parameters to reactivity.

^{15}N NMR analysis

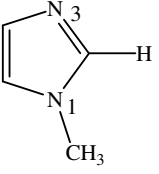
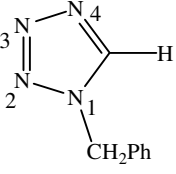
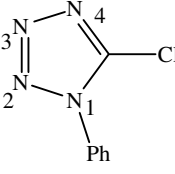
The mapping of ^{15}N -resonances for different N-heterocyclic ligands and coordinated complexes gives us an insight into the reactive moieties present in the relevant molecules.

⁴⁵ J. H. Corrington, H. S. Aldrich, C. W. McCurdy and L. C. Cusachs, *Int. J. Quantum Chem.*, 1971, **5S**, 307.

⁴⁶ A. Skancke and J. F. Liebman, *J. Mol. Struct.*, 2001, **567-568**, 59.

As expected the N¹ nucleus (ca. sp³ hybridised) of N-heterocycles appears at the highest field in the ¹⁵N-spectrum compared to resonance peaks for N², N³ and N⁴ (Table 3.12), due to less shielding by the latter electrons (compare sp³, sp² carbons). The chemical shifts of N¹ in 1-methylimidazole, at δ -220 appears at much higher field strength than the N³ imine nitrogen, at δ -122. Gold(I) coordination to N³ causes an upfield shift of 42 ppm. The same holds true for the 1-benzyltetrazole compound where the N¹ appears at δ -143 compared to the chemical shifts for N² (δ -13), N³ (δ 12) and N⁴ (δ -51). The N¹-N⁴ resonances were unambiguously assigned using gradient heteronuclear multiple quantum coherence (gHMQC) experiments.

Table 3.12 Comparative ¹⁵N NMR spectroscopic data for compounds: 1-methyl-imidazole, 1-benzyltetrazole and 5-chloro-1-phenyltetrazole

Ligand			
¹⁵ N NMR (CD ₂ Cl ₂ , 61 MHz)			
N ¹	-220	-143	-141
N ²		-13	-5
N ³	-122	12	13
N ⁴		-51	-56

The marked difference ($\Delta\delta$ 77) between the N¹ chemical shifts of 1-methylimidazole and 1-benzyltetrazole, can be ascribed to the higher electronegativity of the nitrogen in methylimidazole compared to the nitrogen (ca. sp²) in the instance of 1-benzyltetrazole. This is brought about in part by the carbon substituent (C⁵) to N¹ in the case of methylimidazole compared to a nitrogen substituent in the instance of benzyltetrazole. In 5-chloro-1-phenyltetrazole the phenyl and adjacent electropositive carbon substituent have little effect on the chemical shift of N¹; δ -141 compared to δ -143 in 1-benzyltetrazole. In this instance the magnetic anisotropic effect of the heterocyclic ring rather than the deshielding of the electronegative ring substituents largely determine the magnetic environment of the nitrogen nuclei. It is thus apparent that no significant difference exists in the ¹⁵N chemical shifts of the two heterocyclic systems.

X-ray structure analysis

The bond lengths in the heterocyclic rings provide an insight into the nature of the bonds between neighbouring atoms (Table 3.13). The single bond lengths in 1-benzyltetrazole [N(21)-N(22), N(23)-N(24), N(24)-C(20)] and 5-chloro-1-phenyltetrazole [N(4)-N(3),

N(2)-N(1), N(1)-C(1)] are consistently longer than the double bond lengths [N(22)-N(23), N(21)-C(20)] and [C(1)-N(4), N(3)-N(2)] in the respective molecules. Furthermore, no significant differences exist in the relevant bond lengths of the two molecules. The equivalent nature of the three (ca. sp^2) nitrogen atoms in the tetrazole rings are substantiated by no notable difference in the lengths of N(21)-N(22), N(22)-N(23) and N(23)-N(24) in 1-benzyltetrazole (Figure 3.12). Similarly, no significant difference exist in the bonds N(1)-N(2), N(2)-N(3) and N(3)-N(4) of 5-chloro-1-phenyltetrazole.

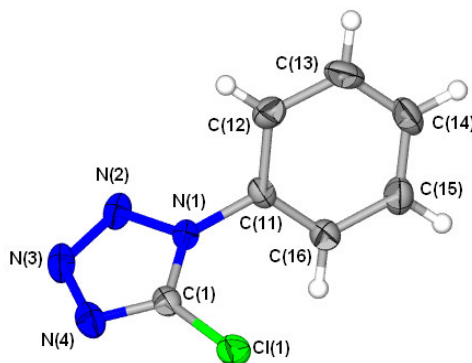


Figure 3.12 Molecular structure of 5-chloro-1-phenyltetrazole showing the numbering scheme.

Table 3.15 Selected bond lengths (Å) for 1-benzyltetrazole and 5-chloro-1-phenyltetrazole with e.s.d.s in parenthesis

1-benzyltetrazole		5-chloro-1-phenyltetrazole	
C(20)-N(21)	1.315(8)	C(1)-N(2)	1.310(3)
C(20)-N(24)	1.318(8)	N(1)-C(1)	1.342(3)
N(21)-N(22)	1.366(7)	N(1)-N(2)	1.358(2)
N(22)-N(23)	1.307(7)	N(2)-N(3)	1.301(3)
N(23)-N(24)	1.346(7)	N(3)-N(4)	1.358(3)

To elucidate the possible role that the chlorine atom plays in deactivating the tetrazole ring towards imine coordination, a more appropriate compound, e.g. 1-phenyltetrazole can be employed as ligand. The application of compounds with strong -I (inductive) and -R (resonance) effects, e.g. 5-nitrotetrazole could be used to establish whether the chlorine (strong -I and weak +R) plays a role in the gold(I) coordination potential of this class of heterocycles.

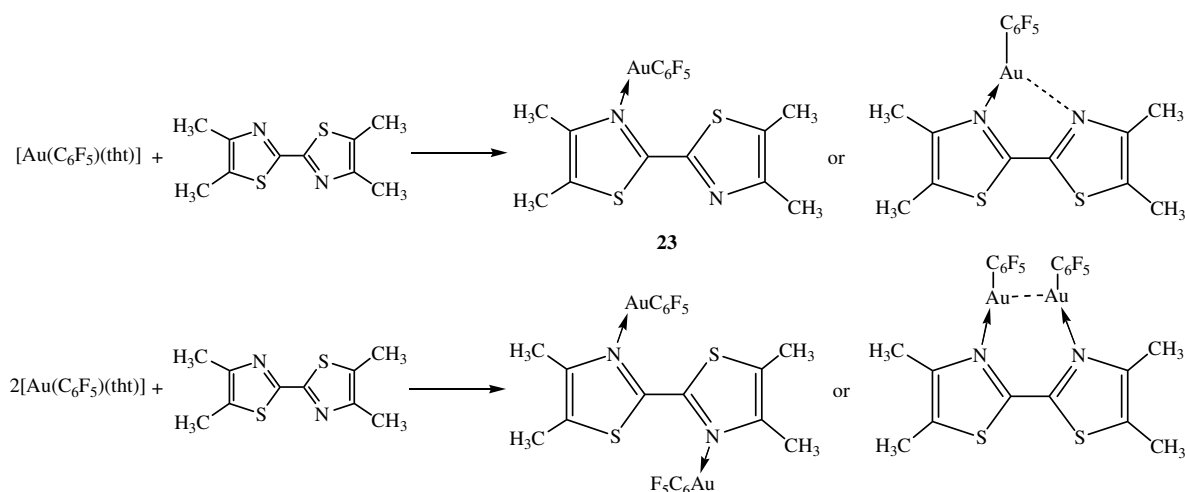
3.2.3 Attempted synthesis of a dinuclear gold(I) imine complex derived from bis(thiazole).

A. Formation of [2,2-bis(4,5-dimethylthiazol-2-yl)](pentafluorophenyl)gold(I) 23.

Using an identical approach to the synthesis of related imidazole and tetrazole complexes **15-20**, the preparation of gold(I) imine derivatives of 2,2'-bis(4,5-dimethylthiazole) was

attempted. This ligand provides a number of potential coordination modes that could occur (Scheme 3.5). Reacting equimolar amounts of ligand and starting complex, could potentially afford mono-nuclear imine complexes with or without additional N-interactions. With an excess of $[\text{Au}(\text{C}_6\text{F}_5)(\text{tht})]$, η^2 -coordination could result, which could allow for intramolecular aurophilic interactions within a 6-membered metallocycle.

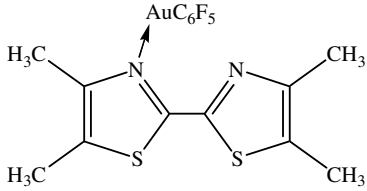
What ensued was the rapid formation of the highly insoluble mono-imine complex 2,2-bis(4,5-dimethylthiazol-2-yl)(pentafluorophenyl)gold(I), **23** (Scheme 3.5). The result was further confirmed, when the ligand was reacted in an equimolar and an excess amount of ligand relative to $[\text{Au}(\text{C}_6\text{F}_5)(\text{tht})]$. In all three attempts the immediate formation of a similar hair-fine needle-like product resulted.



Scheme 3.5 The synthetic route towards (thiazole)gold(I) imine complexes, highlighting possible coordination modes.

The microcrystalline complex is insoluble in most polar and apolar organic solvents, and characterisation by NMR was impossible. In this light, a molecular structure analysis by X-ray diffraction was crucial and will be discussed in part C of this section. In order to obtain crystals suitable for a crystal structure determination, we set out to slow down the reaction and thus the immediate formation of the microcrystalline product. Crystals of suitable dimension were obtained by carefully layering a solution of $[\text{Au}(\text{C}_6\text{F}_5)(\text{tht})]$ (0.02 mg, 0.03 mmol) in thf (1 ml) in a crystallisation tube, with diethyl ether (1 ml) followed by a solution of bisthiazole (0.01 g, 0.03 mmol) in *n*-pentane(1 ml). Leaving the reaction at $-20\text{ }^\circ\text{C}$, the first crystalline product formed within hours at the contact point between the reagent solutions. The highly stable (at room temperature and in air) and insoluble nature of complex **21** could explain in part why the desired dinuclear complexes could not be obtained. Additional analytical data are summarised in Table 3.14.

Table 3.14 Analytical data for complex **23**

Complex	 <p style="text-align: center;">23</p>
M.p.(°C)	182(decomp.)
Colour	yellow
Yield(%)	93
M_r	588.00
Analysis(%)*	$C_{16}H_{12}AuF_5N_2S_2$
C	(32.78) (32.66)
H	(2.09) (2.06)
N	(4.91) (4.76)

*Required calculated values given in parenthesis.

B. Mass spectrometric characterisation of complex **23**.

The electron impact mass spectrometric data for **23** show the molecular ion peak at m/z 588 and a fragmentation peak at m/z 224 ($\{M-AuC_6F_5\}^+$, base peak). Characteristic signals assigned to the fragmentation and rearrangement of the pentafluorophenyl moiety are also noted at m/z 334 ($\{C_{12}F_{10}\}^+$) and 265 ($\{C_{12}F_{10}-CF_3\}^+$).

C. X-ray structure determination of complexes of **23**.

The crystal and molecular structures of compounds **23** were determined by single crystal X-ray diffraction. The molecular structure of **23**, is shown in Figure 3.13 and selected bond lengths and angles are summarised in Table 3.15, numbered according to the figure. Compound **23** crystallises in the triclinic space group $P\bar{1}$ as yellowish needles. The simple two-coordinate gold(I) centre is bonded to a C_6F_5 -group and to only one of the imine N-atoms of the bisthiazole ligand, in an approximately linear coordination geometry [C(31)-Au(2)-N(11) at $178.4(2)^\circ$]. The bonds about the gold(I) centre, Au(1)-C(21) and Au(1)-N(11) appear normal at $2.014(7)$ Å and $2.061(6)$ Å, respectively, in agreement with results for similar compounds reported in this work and in the literature.⁶

The planes of the two thiazole rings that constitute the ligand are almost co-planar [torsion angles N(11)-C(11)-C(21)-N(21) and S(11)-C(11)-C(21)-N(21) at $171.5(7)$ and $-8.6(9)$,

respectively]. The bond lengths in the coordinated ring [N(11)-C(11) 1.329(9) Å and N(11)-C(13) 1.408(9) Å] remain largely unchanged compared with bond lengths in the uncoordinated ring [N(21)-C(21) 1.321(9) Å and N(21)-C(23) 1.375(9)Å].

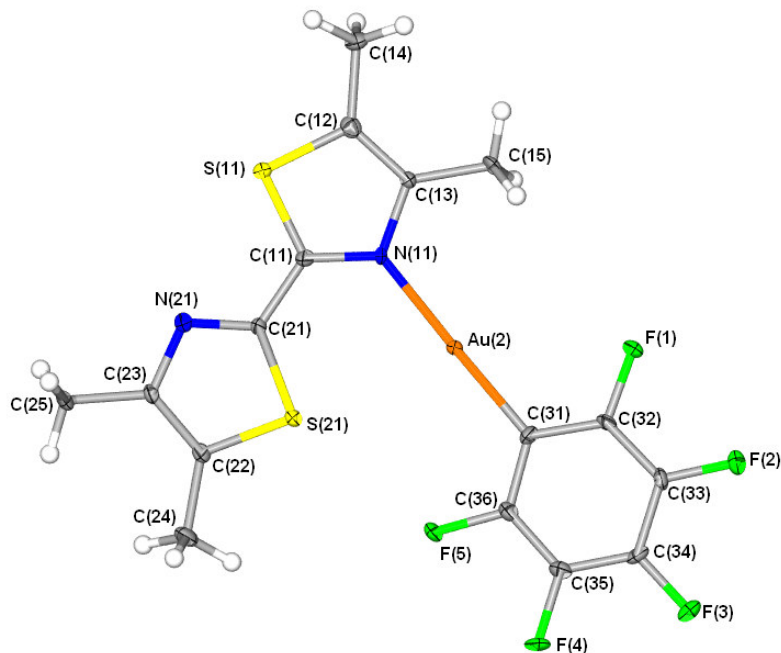


Figure 3.13 Molecular structure of **23** showing the numbering scheme.

A possible electron charge delocalisation from N(21), effected by the gold(I) coordination to N(11), which would rationalise the mono-substitution, remains unsubstantiated, due to a typical single bond character of C(21)-C(11) [1.447(10) Å]. This bond length is in agreement with the reported lengths in literature for single bond trigonally bound carbon atoms [2,2'-bis(4-methylthiazole) 1.468(6) Å and 2,2'-bis(4,5-tetraphenylthiazole) 1.452(4) Å], and inconsistent with the values reported for a double bond [2,2'-bis(3,4,5-trimethylthiazol-2-ylidene) 1.340(6) Å] in a related compound.^{47,48,49}

⁴⁷ A. Bolognesi, M. Catellani, S. Destri and W. Porzio, *Acta. Cryst.*, **C43**, 1987, 1171.

⁴⁸ A. R. Mahjoub, A. Morsali, M. R. Poorheravi and E. Shams, *Z. Kristallogr. New Cryst. Struct.*, 2002, **217**, 97.

⁴⁹ A. J. Arduengo III, J. R. Goerlich and W. J. Marshall, *Liebigs Ann.*, 1997, 365.

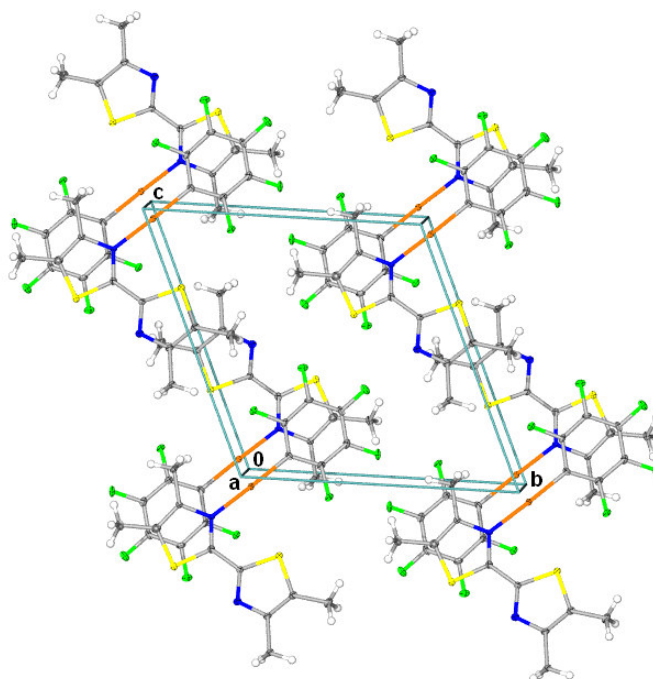


Figure 3.14 Unit cell and packing pattern in the crystal lattice of **23** viewed along the a-axis.

Table 3.15 Selected bond lengths (Å) and angles (°) for complex **23** with e.s.d.s in parenthesis

Bond lengths		Bond angles	
Au(2)-C(31)	2.014(7)	C(31)-Au(2)-N(11)	178.4(2)
Au(2)-N(11)	2.061(6)	C(11)-N(11)-Au(2)	127.0(5)
N(11)-C(11)	1.329(9)	C(13)-N(11)-Au(2)	121.5(4)
N(11)-C(13)	1.408(9)	C(11)-N(11)-C(13)	111.5(6)
S(11)-C(11)	1.699(7)	C(11)-S(11)-C(12)	90.2(4)
S(11)-C(12)	1.724(8)	N(11)-C(11)-C(21)	126.0(7)
C(12)-C(13)	1.36(1)	N(11)-C(11)-S(11)	114.3(5)
C(11)-C(21)	1.45(1)	C(21)-C(11)-S(11)	119.8(5)
C(12)-C(14)	1.51(1)	C(13)-C(12)-S(11)	111.1(6)
C(13)-C(15)	1.49(1)	N(11)-C(13)-C(15)	119.6(6)
S(21)-C(22)	1.724(7)	N(21)-C(21)-C(11)	121.0(7)
S(21)-C(21)	1.733(7)	C(21)-N(21)-C(23)	110.7(6)
N(21)-C(21)	1.321(9)	N(21)-C(23)-C(25)	117.9(6)
N(21)-C(23)	1.375(9)	C(32)-C(31)-Au(2)	120.8(6)
C(22)-C(23)	1.37(1)	C(36)-C(31)-Au(2)	124.7(5)
C(22)-C(24)	1.50(1)		
C(23)-C(25)	1.52(1)		

Molecules in the crystal lattice are organised in closely knitted sheets in the bc plane that stack upon one another along the a-axis by translation (Figure 3.14). Molecules arrange across the gold centres, with C₆F₅ moieties in a *trans* configuration about the coordinative axis of adjacent molecules. The structure is devoid of sulphur-Au(I) contacts [3.10(5) Å] or aurophilic interactions. The intermolecular interactions are limited to π -stacking between the thiazole and pentafluorophenyl ring (distance between centroids 3.554 Å),

which brings the non-interactive gold(I) centres in the closest possible separation at 3.679 Å.

3.2.4 Neutral phosphine gold(I) amido complexes derived from tetrazoles.

A. Preparation of (triphenylphosphine)(tetrazol-1-yl)gold(I), **24**, (trimethylphosphine)(tetrazol-1-yl)gold(I), **25**.

Kieft and co-workers were first to prepare a series of complexes of gold(I) and 5-substituted tetrazoles.⁵⁰ By reaction of aceto(triphenylphosphine)gold(I), [Au(OAc)(PPh₃)] with 1*H*-tetrazole, the complex is obtained in moderate yield. An alternative approach towards N-derivitised gold(I) tetrazoles, involves 1,3-dipolar cycloaddition of highly reactive azido(triphenylphosphine)gold(I), [Au(N₃)(PPh₃)] with carbonitriles.⁵¹ However, drawbacks of this method include the handling of potentially explosive metal azides and extremely hazardous hydrogen cyanide.⁵² Nomiya and co-workers employed [AuCl(PPh₃)] as starting material and isolated the (triphenylphosphine)gold(I) amido complex **24**, as stable colourless needle-like crystals, from a reaction in acetone with 1-*H*-tetrazole in the presence of aqueous NaOH.¹⁶ Apart from a full structural characterisation, including single-crystal X-ray diffraction, the anti-bacterial activity against Gram-positive bacteria (*B.subtilis* and *S.aureus*) was also assessed.

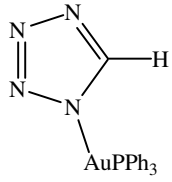
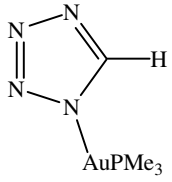
We now continued this work and prepared complex **24** as well as the novel (trimethylphosphine)(tetrazol-1-yl)gold(I) complex **25**, using essentially the same procedure. Not only were these complexes used as starting substrates for secondary imine complexes (complex **20**), but similar motifs were used in the attempted synthesis of binuclear gold(I) amido complexes from pyridyl tetrazole ligands (section 3.2.5). The colourless solids are moisture and air stable, however in agreement to the findings of Kieft *et al.*, **24** appeared prone to contamination when suspended in halogenated solvents (chloroform, dichloromethane). Analytical data for complexes **24** and **25** are summarised in Table 3.16.

⁵⁰ R. L. Kieft, W. M. Peterson, G. L. Blundell, S. Horton, R. A. Henry and H. B. Jonassen, *Inorg. Chem.*, 1976, **15**, 7.

⁵¹ F. A. Mautner, C. Gaspan, K. Gatterer, M. A. S. Abu-Youssef, E. Bucher and W. Sitte, *Polyhedron*, 2004, **23**, 1217.

⁵² W. Beck, K. Burger and W.P. Fehlhammer, *Chem. Ber.*, 1971, **104**, 1816.

Table 3.16 Analytical data for complexes **24** and **25**

Complex	 24	 25
M.p.(°C)	190(decomp.)	154(decomp.)
Colour	colourless	colourless
Yield(%)	34	74
M_r	528.08	342.03
Analysis(%)*	$C_{19}H_{16}AuN_4P$	$C_4H_{10}AuN_4P$
C	(43.52) (43.20)	(14.31) (14.04)
H	(2.95) (3.05)	(2.72) (2.95)
N	(10.23) (10.60)	(16.10) (16.38)

* Required calculated values given in parenthesis.

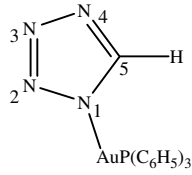
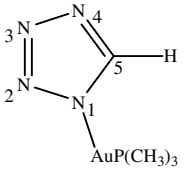
B. Spectroscopic characterisation of complexes **24** and **25**.

Nuclear magnetic resonance spectroscopy

The 1H , $^{13}C\{^1H\}$, $^{31}P\{^1H\}$ NMR spectroscopic data for compounds **24** and **25** are summarised in Table 3.17. In the 1H NMR spectra of **24** and **25**, singlet resonances appear at δ 8.56 (lit. δ 8.55) and δ 7.95 pertaining to the acidic azole proton.¹⁶ A broad multiplet in the range δ 7.48-7.64 (lit. δ 7.54), is assigned to 15 protons of the phenyl groups in **24**, whereas a sharp doublet resonance at δ 0.87 ($^1J = 12.0$ Hz) is due to 9 methyl protons in the phosphine substituent of **25**.

In the ^{13}C NMR spectra of **24** the C⁵-atom resonates at δ 149.3 (δ 149.1), approximately 9 ppm downfield compared to the corresponding resonance in **25** (δ 140.7). Characteristic carbon-phosphorous coupling patterns are present for all the non-equivalent carbon atoms of the phenyl ring in **24** as well as the methyl carbon atoms in **25** at δ 5.4 ($^1J_{CP} = 42$ Hz).

Table 3.17 ^1H , $^{13}\text{C}\{^1\text{H}\}$, $^{31}\text{P}\{^1\text{H}\}$ NMR spectroscopic data for **24** and **25**

Complex		
Solvent	CD_2Cl_2	$(\text{CD}_3)\text{SO}$
Temperature ($^\circ\text{C}$)	25	25
^1H NMR (300 MHz)	H^5 8.56 (s, 1H) PCH ₃ 7.48-7.64 (m, 15H)	7.95 (s, 1H) 0.87 (d, 9H, $^1J = 12.0$ Hz)
$^{13}\text{C}\{^1\text{H}\}$ NMR (75 MHz)	PPh C ⁵ 149.3 (s) PCH ₃ - PPh-C ^{ipso} 129.2 (d, $^1J = 57.2$ Hz) PPh-C ^{ortho} 134.7 (d, $^2J = 13.5$ Hz) PPh-C ^{meta} 129.9 (d, $^3J = 12.0$ Hz) PPh-C ^{para} 132.7 (d, $^4J = 2.4$ Hz)	- 140.7 (bs) 5.4 (d, $^1J = 42.1$ Hz)
$^{31}\text{P}\{^1\text{H}\}$ NMR (121MHz)	P 33.0 (bs)	-10.1 (s)

The resonance in the ^{31}P NMR spectrum of **24** appear as a broad singlet signal at δ 33.0 (lit. δ 31.0).¹⁶ The phosphorus resonance in **25** is observed as a sharp singlet at δ -10.1, in agreement with the resonance found for the related compound, $[\text{AuCl}(\text{PMe}_3)]$ at δ - 4.4.

Mass spectrometry

EI-(**24**) and FAB(**25**)-mass spectrometric data are summarised in Table 3.18. The molecular ion peaks are observed for both complexes at m/z 528 and 342 for **24** and **25**, respectively. Diagnostic fragmentation peaks include expulsion of a molecule of nitrogen as shown by the peaks at m/z 500 and 314 for complex **24** and **25**.

Table 3.18 Mass spectrometric data for **24** and **25**

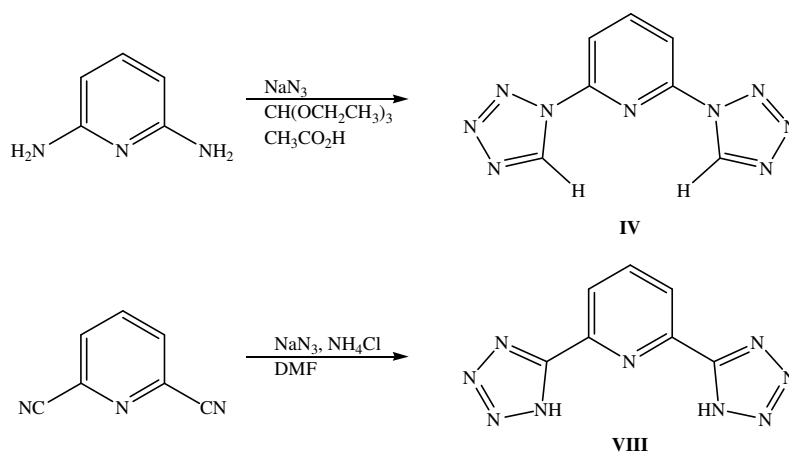
Fragment	m/z (%)	
	24	25
$\{[\text{M}]\}^+$	528 (9)	342 (72)
$\{[\text{M}]-\text{N}_2\}^+$	500 (2)	314 (4)
$\{[\text{M}]-\text{CHN}_4\}^+$	459 (39)	273 (100)
$\{\text{Au}(\text{PPh}_3)_2\}^+$	721 (100)	
$\{\text{Au}(\text{PMe}_3)_2\}^+$		349 (15)

The expected fragmentation and rearrangement peaks of the (trialkylphosphine)gold(I) moiety, $\{\text{Ph}_3\text{PAu}\}^+$ (m/z 459) and $\{(\text{Ph}_3\text{P})_2\text{Au}\}^+$ (m/z 721; see **24**) and $\{\text{Me}_3\text{PAu}\}^+$ (m/z 273) and $\{(\text{Me}_3\text{P})_2\text{Au}\}^+$ (m/z 349; see **25**), are also noted.

3.2.5 Attempted complexation reaction of gold(I) to pyridine and imidazole ligands containing C- and N-tetrazolyl substituents.

A. A microwave assisted synthesis of pyridine and imidazole ligands containing C- and N-tetrazolyl substituents.

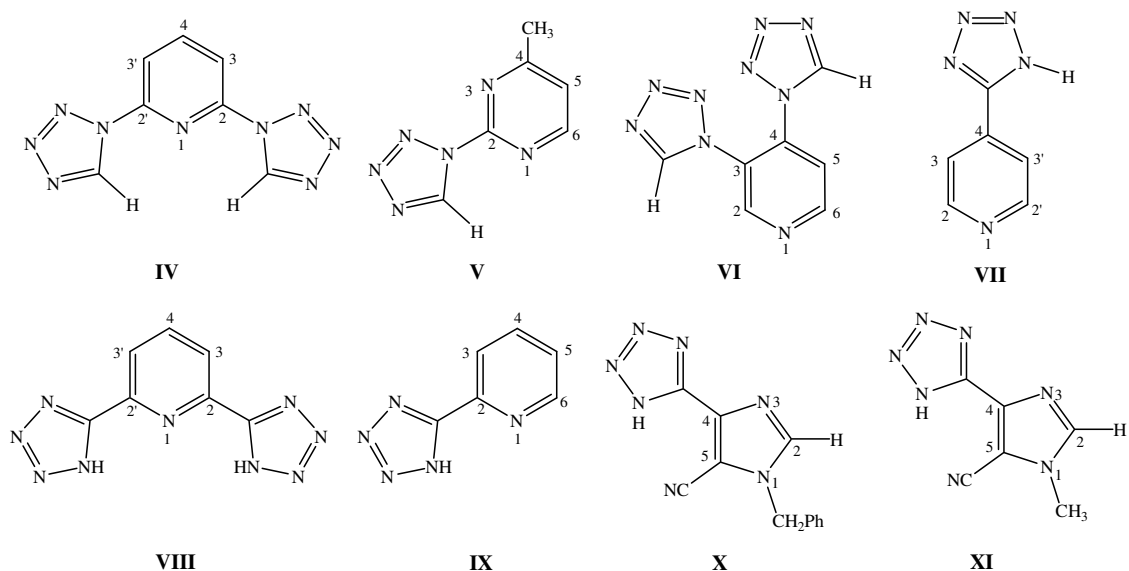
Reactions activated by microwave (Mw)-irradiation have received much attention due to their enhanced reaction rates as well as higher yields and purities compared to conventional synthetic methods at high temperatures.⁵³ Applying this synthetic approach to the simple 2,3-cycloaddition reaction of azide to a pyridyl nitrile or amino functionality (Scheme 3.5) the desired tetrazole derivatives can be isolated in pure form without the excess handling of potentially hazardous organic azides. Furthermore, reaction times are dramatically decreased from hours to minutes. The insoluble nature of the products allows for easy isolation by crystallisation.



Scheme 3.5 The synthetic route towards C- and N-bonded tetrazolylpyridine ligands.

Various aromatic nitrogen heterocycles were synthesised that could be utilised as metal-chelating and polytopic ligands. Both carbon and nitrogen-bonded tetrazolylpyridine compounds were prepared – mono- and disubstituted in the 2, 3, 4- and 6-positions on the pyridine ring (Scheme 3.6). This includes 2,6-bis(tetrazol-5-yl)pyridine, **IV**, 4-methyl-2-tetrazol-1-ylpyrimidine, **V**, 3,4-bis(tetrazol-1-yl)pyridine, **VI**, 4-(1H-tetrazol-5-yl)pyridine, **VII**, 2,6-bis(1H-tetrazol-5-yl)pyridine, **VIII**, and 2-(1H-tetrazol-5-yl)pyridine, **IX**. Related imidazole ligands, 1-benzyl-5-cyano-4-(1H-tetrazol-5-yl)imidazole, **X**, and 5-cyano-1-methyl-4-(1H-tetrazol-5-yl)imidazole, **XI**, were also prepared.

⁵³ N. Kaval, B. Halasz-Dajka, G. Vo-Thanh, W. Dehaen, J. Van der Eycken, P. Mátyus, A. Loupy and E. Van der Eycken, *Tetrahedron*, 2005, **61**, 9052.



Scheme 3.6 Di and tricyclic nitrogen rich heterocycles as ligands for metal complexation.

The traditional preparation involved the corresponding amino-substituted pyridine compounds, sodium azide and triethylorthoformate in glacial acetic acid under reflux conditions for prolonged periods of time (Table 3.19).

Table 3.19 Synthesis of ligands **IV-XI** under conventional heating (Δ) and microwave-assisted irradiation (Mw)

Compound (M.p. °C)	Method activation	Solvent	Temp(°C)/time	Yields* (%)
IV (196-198)	Δ	CH ₃ CO ₂ H	105/15 h	25
	Mw	CH ₃ CO ₂ H	115/15 min	87
V (75-77)	Δ	CH ₃ CO ₂ H	100/18 h	29
	Mw	CH ₃ CO ₂ H	115/20 min	91
VI (201-202 decomp.)	Δ	CH ₃ CO ₂ H	100/72 h	22
	Mw	-	-	-
VII (206-208)	Δ	-	-	-
	Mw	DMF	150/20 min	96
VIII (290-291 decomp.)	Δ	DMF	100/18 h	34
	Mw	DMF	150/20 min	90
IX (215-218)	Δ	-	-	-
	Mw	DMF	150/20 min	89
X (158-159)	Δ	DMF	100/21 h	39
	Mw	DMF	150/15 min	94
XI (238)	Δ	DMF	100/6 h	36
	Mw	DMF	150/15 min	88

*Reactions not optimised.

After the removal by evaporation of the solvent, the crystalline residue was suspended in water and extracted with ethyl acetate. Aqueous washing of the organic phase removed any trace amounts of unreacted amino-pyridine substrate and excess inorganic salts. Under microwave irradiation conditions the preparation of these compounds was dramatically

improved and required limited work-up procedures (Table 3.19). The reactions were carried out on preparative scale (10-20 mmol) in a total solvent volume of 30 ml, at 115°C at 500 W for 20 min.

In a related approach C-tetrazolypyridine ligands **VII-IX** were prepared from the parent carbonitrile-substituted pyridine compounds, sodium azide and ammonium chloride in DMF (*N,N'*-dimethylformamide) under reflux conditions for prolonged periods of time (Table 3.19). The solid tetrazole derivatives were isolated by acidifying an aqueous suspension of the reaction mixture with cooling. Recrystallisation from DMF solutions layered by diethyl ether afforded ligands in analytically pure form. Microwave irradiation of these reaction mixtures noticeably improved the ease of work up and purity of the desired products (Table 3.19). The reactions were carried out on preparative scale (10-20 mmol) in a total solvent volume of 10 ml, at 150°C at 500 W for 20 min.

The analogous C-tetrazylimidazole ligands **X** and **XI**, substituted in the 4 position of the imidazole ring were prepared in a similar manner from parent 4, 5-dicyano imidazole. By using microwave heating at 150 °C for 15 min both products were obtained in considerable higher yields compared to using conventional heating (Table 3.19). Careful assessment of NMR, MS and IR spectra confirmed that the derivatisation of the 4-cyano substituent is favoured. Nevertheless signals assignable to the 4,5-ditetrazolyl derivative were confirmed by weak signals in the ¹H and ¹³C NMR spectra.

B. Spectroscopic characterisation of ligands IV-XI.

Nuclear magnetic resonance spectroscopy

The ¹H, ¹³C{¹H} NMR and IR-spectroscopic data and EI mass spectrometric data for ligands **IV-XI** are summarised in Table 3.20. NMR spectroscopic data were compared to related compounds reported in the literature.

Table 3.20 ^1H , $^{13}\text{C}\{^1\text{H}\}$ NMR, IR and EI-MS data for ligands **IV-XI**

Compound		IV	V	VI	VII	VIII	IX	X	XI
Solvent		(CD ₃) ₂ SO	CDCl ₃	(CD ₃) ₂ SO	(CD ₃) ₂ SO	(CD ₃) ₂ SO	(CD ₃) ₂ SO	(CD ₃) ₂ SO	(CD ₃) ₂ SO
Temperature (°C)		25	25	25	25	25	25	25	25
^1H NMR (300 MHz)	H ² ,H ^{2'}			8.15 (s, 1H)	8.84 (dd, 2H, ³ J = 4.5 Hz, ⁴ J = 1.3 Hz)			8.39 (s, 1H)	8.14 (s)
	H ³ ,H ^{3'}	8.22 (d, 2H, ³ J = 8.10 Hz)			8.07 (dd, 2H, ³ J = 4.21 Hz, ⁴ J = 1.52 Hz)	8.28 (m, 2H)	8.21 (ddd, 1H, ³ J = 7.92 Hz, ⁴ J = 1.4 Hz, ⁵ J = 0.81 Hz)		
	H ⁴	8.50 (dd, 1H, ³ J = 7.80, 7.80 Hz,)				7.92 (m, 1H)	8.04 (td, 1H, ³ J = 7.82 Hz, ⁴ J = 1.81 Hz)		
	H ⁵		7.35 (dq, 1H, ³ J = 5.12 Hz, ⁴ J = 0.50 Hz)	8.04 (bs, 1H)			7.59 (ddd, 1H, ³ J = 4.91 Hz, ³ J = 4.82 Hz, ⁴ J = 0.92 Hz)		
	H ⁶		8.73 (d, 1H, ³ J = 5.12 Hz)	8.16 (bs, 1H)			8.76 (ddd, 1H, ³ J = 4.81 Hz, ⁴ J = 0.91 Hz, ⁵ J = 0.80 Hz)		
	N ₄ CH	10.49(s, 1H)	9.59 (s, 1H)	9.06 (s, 1H)	9.25 (s, 1H)			8.85-9.12 (bs, 1H)	5.70-7.03 (s, 1H)
	CH ₃		2.65 (d, 3H, ⁴ J = 0.41 Hz)						3.96 (s, 3H)
	CH ₂ Ph							5.72 (s, 2H)	
$^{13}\text{C}\{^1\text{H}\}$ NMR (75 MHz)	Ph C ² ,C ^{2'}	145.1 (s)	171.1 (s)	153.9 (s)	149.8 (s)	144.2 (s)	143.6 (s)	7.04-7.21 (m, 5H)	142.9 (s)
	C ³ ,C ^{3'}	114.8 (s)	-	122.4 (s)	121.1 (s)	124.1 (s)	126.1 (s)	-	-
	C ⁴	142.0 (s)	152.4 (s)	132.6 (s)	133.4 (s)	140.3 (s)	138.2 (s)	135.9 (s)	127.6 (s)
	C ⁵ ,C ^{5'}		121.4 (s)	115.8 (s)	121.1 (s)		122.6 (s)	114.0 (s)	113.4 (s)
	C ⁶		158.8 (s)	154.8 (s)	149.8 (s)		150.0 (s)	-	-
	CHN ₄	144.9 (s)	141.6 (s)	152.1 (s)	155.1 (s)	155.1 (s)	154.8 (s)	151.2 (s)	151.3 (s)
	CN							114.5 (s)	114.7 (s)
	CH ₃		24.1 (s)						34.4 (s)
	CH ₂ Ph							49.8 (s)	
	Ph							127.0 (s), 128.0 (s), 128.7 (s)	
IR (cm ⁻¹)	ν N-H				3073 (s)	3079 (s)	3083 (s)	3130 (s)	3123 (s)
	ν C≡N				-	-	-	2229 (s)	2245 (s)
EI-MS (<i>m/z</i>)	{M+H} ⁺	216 (10)	163 (100)	216 (19)	148 (23)	216 (3)	148 (14)	252 (100)	176 (14)
	{M-N ₂ } ⁺	188 (5)	135 (25)	188 (7)	119 (12)	-	-	223 (5)	147 (9)
	{M-2N ₂ } ⁺	160 (15)		160 (23)		-	-	-	-

Mass spectrometry

Low resolution electron impact mass spectrometric data for ligands **IV-XI** are summarised in Table 3.20. The molecular ion peaks for all the ligands were observed, together with characteristic fragmentation peaks thereof.

Infrared spectroscopy

The IR spectra of the crystalline ligands **VII-XI** were recorded directly by ATR, and are summarised in Table 3.20. Diagnostic $\nu(\text{NH})$ and $\nu(\text{CN})$ absorption peaks occur in the typical range reported in literature for related compounds.^{54,55}

C. X-ray structure determination of ligand **VIII**.

The crystal and molecular structures of ligand **VIII** were determined by single crystal X-ray diffraction. The molecular structure of **VIII**, is depicted in Figure 3.15 and selected bond lengths and bond angles are summarised in Table 3.21, numbered according to the figure. Compound **VIII** crystallises in the monoclinic space group $P2_1/c$ as colourless needle-like crystals. The asymmetric unit of **VIII** consists of a tricyclic molecule, composed of a central pyridine molecule substituted in the 2- and 6-position with a C-bonded tetrazole. Each ligand is associated to a crystallisation solvent molecule, DMF, *via* hydrogen bonding through both N-H groups.

The two hydrogen atoms are localised on the N^1 nitrogens of the tetrazole rings, and in contrast to the migratory nature of hydrogens around these heterocycles in related compounds.⁵⁶ The pattern of N-N bonds is consistent in the two rings, with N=N double bonds localised between N^3 and N^2 [$\text{N}(13)\text{-N}(14)$ 1.304 Å and $\text{N}(23)\text{-N}(24)$ 1.298 Å].³² The tetrazole rings are planar and co-planar with respect to the central pyridyl ring [torsion angle $\text{N}(12)\text{-C}(11)\text{-C}(2)\text{-N}(1)$ -1.0° , $\text{N}(22)\text{-C}(21)\text{-C}(6)\text{-N}(1)$ -0.9°], in agreement with 1,3,5-tri(tetrazol-5-yl)benzene [torsion angles 5.0° , 3.4° , 6.9°] but in contrast to sterically hindered compounds 1,3,5-[2-(tributylstannyl)tetrazole-5-yl]benzene [torsion angles 0° and 21°], and 1,2-bi(tetrazol-5-yl)benzene [torsion angles 34.1° and 34.8°].^{57,58}

⁵⁴ R. Bronisz, *Inorg. Chim. Acta*, 2002, **340**, 215.

⁵⁵ A. J. Downard, P.J. Steel and J. Steenwijk, *Aust. J. Chem.*, 1995, **48**, 1625.

⁵⁶ H. Gallardo, E. Meyer, A. J. Bartoluzzi, F. Molin and A. S. Mangrich, *Inorg. Chim. Acta*, 2004, **357**, 505.

⁵⁷ C. A. K. Diop, M. F. Mahon, K. C. Molloy, L. Ooi, P. R. Raithby, M. M. Venter and S. J. Teat, *CrystEngComm.*, 2002, **4**, 462.

⁵⁸ P. A. Bethel, M. S. Hill, F. Mahon and K. Molloy, *J. Chem. Soc., Perkin Trans. 1*, 1999, 3507.

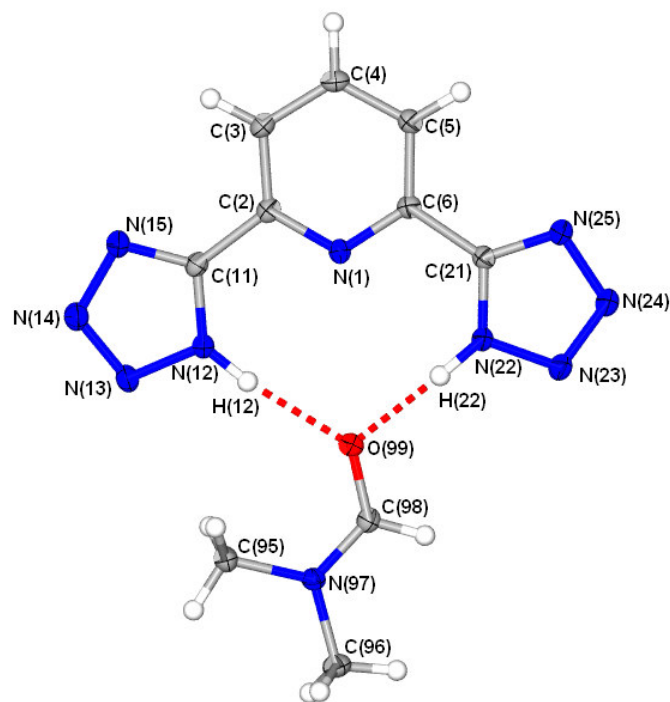


Figure 3.15 Molecular structure of **VIII** showing the numbering scheme; an equimolar amount of DMF co-crystallised and associated with **VIII** *via* hydrogen bonds.

N-Unsubstituted tetrazoles are often solvated and the geometry of the rings adapts to suit the most efficient hydrogen bonding to solvent molecules.⁵⁷ In this regard, the remarkable co-planar configuration of tetrazole rings effects an unprecedented unsymmetrical dihydrogen bond [H(12)...O(99) 1.980 Å, H(22)...O(99) 1.843 Å] to a carbonyl oxygen atom of the DMF molecule. The lattice construction is completed by the stacking of solvated molecules in rows along the b-axis (Figure 3.16). Rows in the centre and on the perimeters of the unit cells are related by a two-fold screw axis parallel to the a-axis.

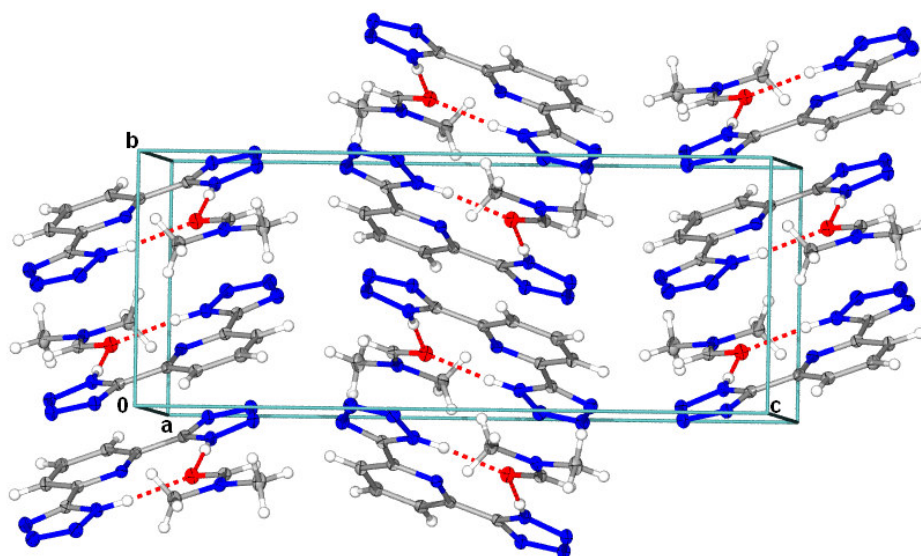


Figure 3.16 Unit cell and packing pattern in the crystal lattice of **VIII** viewed along the a-axis.

Table 3.21 Selected bond lengths (Å) and angles (°) for **IV** with e.s.d.s in parenthesis

Bond lengths			Bond angles		
N(1)-C(2)	1.337(2)		C(2)-N(1)-C(6)	117.3(1)	
N(1)-C(6)	1.340(2)		N(1)-C(2)-C(11)	112.9(1)	
C(2)-C(11)	1.467(2)		N(1)-C(6)-C(21)	113.2(1)	
C(6)-C(21)	1.469(2)		N(12)-C(11)-C(2)	122.8(1)	
C(11)-N(12)	1.336(2)		N(15)-C(11)-C(2)	128.3(1)	
C(11)-N(15)	1.322(2)		N(25)-C(21)-C(6)	127.8(1)	
N(12)-N(13)	1.344(2)		N(15)-C(11)-N(12)	109.0(1)	
N(13)-N(14)	1.304(2)		N(25)-C(21)-N(22)	109.1(1)	
N(14)-N(15)	1.367(2)		C(11)-N(12)-N(13)	108.8(1)	
C(21)-N(22)	1.331(2)		C(21)-N(22)-N(23)	108.7(1)	
C(21)-N(25)	1.321(2)				
N(22)-N(23)	1.345(2)				
N(23)-N(24)	1.298(2)				
N(24)-N(25)	1.367(2)				
Significant hydrogen bond distances (Å) and angles (°)					
D-H	<i>d</i> (D-H)	<i>d</i> (H-A)	∠DHA	<i>d</i> (D...A)	A
N(12)-H(12)	0.92(2)	1.98(2)	172(2)	2.895(2)	O(99)
N(22)-H(22)	0.91(2)	1.84(2)	176(2)	2.751(2)	O(99)

D. Reactions of ligands IV, V, VIII, X and XI with gold(I) substrates.

The utilisation of the ligands described in the preceding discussion towards the synthesis of (pentafluorophenyl)gold(I) imine, cationic (phosphine)gold(I) imine and (phosphine)gold(I) amide complexes, will be described in Addendum 1.

3.3 Conclusion

Against the conventional belief that gold(I) only exhibits a moderate affinity towards nitrogen atoms we have successfully prepared and characterised various stable gold(I) imine and amine complexes derived from nitrogen rich heterocycles. We have illustrated that by employing a simple methodology, stable forms of mono- and dinuclear N-coordinated (pentafluorophenyl)gold(I) imine complexes derived from imidazoles, complexes **15-18**, can be obtained. The remarkable stability of these new complexes differ significantly from the thermodynamical unstability of comparable chloro-substituted compounds. Structural analysis by single crystal X-ray diffraction reveals that intermolecular aurophilic interactions aggregate and stabilise the crystalline forms as dimers. Nevertheless, the bond distances between imines and a neutral gold fragment are intermediate between those of amides with a cationic fragment and amines bonded to a neutral one – the latter being the shorter. Crystal and molecular structural data reveal that the gold(I)-N bond is relatively insensitive to the type of nitrogen involved.

The unprecedented imine-coordination of a tetrazole ring to a gold(I) centre has been successfully demonstrated in the synthesis, characterisation and single crystal X-ray analysis of 1-benzyltetrazole(pentafluorophenyl)gold(I), **19**. Prepared derivatives of this compound include a binuclear imine-amido complex **20** and the C⁵-functionalised thiolate complex **22**. From the successful preparation of complex **22** emanates a future study towards the synthesis of a bimetallic imine-carbene complex by a remote N-alkylation. The attempted synthesis of a dinuclear (tetrazolyl)gold(I) imine complex from 1,2-di(tetrazol-2-yl)ethane, has resulted in a unique self assembly and formation of a polymeric lithium(tetrazolyl) aurate salt, **21**. To further expand the limited number of gold(I) amido complexes derived from tetrazoles, complexes **24** and **25** were prepared using sodium tetrazolate and the corresponding phosphinegold(I) halide.

¹⁵N NMR- and molecular-structure-analysis-based study of simple tetrazole ligands, 1-benzyltetrazole and 5-chloro-1-phenyltetrazole, allows prediction of imine coordination potential of a given ligand to a neutral (C₆F₅)Au moiety.

Reaction of 2,2'-bis(4,5-dimethylthiazole) with different concentrations of [Au(C₆F₅)(tht)] only affects the formation of mono-substituted product, [2,2-bis(4,5-dimethylthiazol-2-yl)](pentafluorophenyl)gold(I), **23**.

The well documented preparation of tetrazoles by a 2,3-cycloaddition reaction of inorganic azides and carbonitriles or amines has been revisited in a first-time microwave-assisted synthesis of pyridine and imidazole ligands containing C- and N-tetrazolyl substituents. An assessment of microwave irradiation compared to conventional heating reveals that a dramatic reduction in reaction times, increased production yields and purity can be obtained using microwave assisted reactions, under very green conditions.

3.4 Experimental

3.4.1 General procedures and instruments

Reactions were carried out under argon using standard Schlenk and vacuum-line techniques. Tetrahydrofuran (thf), *n*-hexane, *n*-pentane and diethyl ether were distilled under N₂ from sodium benzophenone ketyl, dichloromethane and N,N'-dimethylformamide (DMF) from CaH₂, ethanol and methanol from magnesium. 1-Methylimidazole, 1-benzylimidazole, 2,6-diaminopyridine, 3,4-diaminopyridine, 2-amino-4-methylpyrimidine, 2-cyanopyridine, 2,6-dicyanopyridine, 4-cyanopyridine, sodium

azide and ammonium chloride were purchased from Aldrich. Butyllithium (1.6 M solution *n*-hexane), sodium hydride, dimethyldisulphide, triethyl orthoformate and glacial acetic acid were purchased from Merck. Literature methods were used to prepare 1-*H*-tetrazole,⁵⁴ 1-benzyltetrazole,⁵⁹ 5-chloro-1-phenyltetrazole,⁶⁰ 1-methylbenzimidazole,³⁶ 1,4-bis(imidazol-1-yl)butane,³⁵ 1,2-di(tetrazol-2-yl)ethane,⁵⁴ 2,2'-bis(4,5-dimethylthiazole),⁶¹ [AuCl(tht)],⁶² [Au(C₆F₅)(tht)],⁶³ [AuCl(PPh₃)],⁶⁴ [AuCl(PMe₃)] and {[AuPMe₂Cl]₂en} from [AuCl(tht)] and appropriate phosphine.⁶²

Melting points were determined on a Stuart SMP3 apparatus and are uncorrected. Mass spectra were recorded on an AMD 604 (EI, 70 eV), VG Quattro (ESI, 70 eV methanol, acetonitrile) or VG 70 SEQ (FAB, 70 eV) instruments. In the instance of EI and FAB MS the isotopic distribution patterns was checked against the theoretical distribution. All NMR spectra were recorded on a Varian 300 FT or INOVA 600 MHz spectrometer (¹H NMR at 300/600 MHz, ¹³C{¹H} NMR at 75/150 MHz, ³¹P{¹H} NMR at 121/243 MHz, ¹⁵N NMR at 60.8 MHz, ¹⁹F NMR at 376 MHz) except for spectra of compounds **IV-XI** which were recorded on a Bruker Avance 300 MHz spectrometer (¹H NMR at 300, ¹³C{¹H} and DEPT 135 NMR at 75/150 MHz). Chemical shift (δ) is reported relative to solvent resonance or external reference of 85 % H₃PO₄ (³¹P), NH₃NO₂ (¹⁵N) and CFC₃ (¹⁹F). Infrared spectra were recorded on a Thermo Nicolet Avatar 330FT-IR with Smart OMNI ATR (attenuated total reflectance) sampler. Elemental analysis were carried out at the School of Chemistry, University of the Witwatersrand. An Ethos MicroSynth Microwave reactor was used in the standard configuration, including Milestone easyWave software. Certain characterisation data (elemental analysis, melting point and also yields) are given in the main text. For elemental analysis, products were evacuated under high vacuum for 10 h.

3.4.2 Preparations and procedures

3.4.2.1 Preparation of 1-methylimidazole(pentafluorophenyl)gold(I), **15**.

The addition of a solution of 1-methylimidazole (0.17 g, 2.1 mmol) in diethyl ether (20 ml) to a solution of freshly prepared [Au(C₆F₅)(tht)] (0.95 g, 2.1 mmol) in diethyl ether

⁵⁹ Y. Satoh, N. Marcopulos, *Tet. Lett.*, 1995, **36**(1), 1759.

⁶⁰ J. A. C. Alves and A.W. Johnstone, *Synth. Comm.*, 1997, **27**(15), 2645.

⁶¹ R. Mostaghim and Y. A. Beni, *Indian. J. Chem.*, 2001, **40B**, 498.

⁶² R. Usòn and A. Laguna, in *Organometallic Synthesis*, eds. R. B. Lang and J. J. Eisch, Elsevier, Amsterdam, 1986, vol. 3, p. 325.

⁶³ R. Usòn and A. Laguna, in *Organometallic Synthesis*, eds. R. B. Lang and J. J. Eisch, Elsevier, Amsterdam, 1986, vol. 3, p. 326.

⁶⁴ M.I. Bruce, B.K. Nicholson, O. Bin Shawkataly, *Inorg. Synth*, 1989, 324.

(20 ml) produces a cloudy solution. The mixture was stirred for 1.5 h at room temperature upon which the solution was reduced to dryness *in vacuo*. The white residue was extracted with diethyl ether, filtered through anhydrous MgSO₄ and the filtrate concentrated *in vacuo* to yield a white microcrystalline material. Recrystallisation of the white solid by layering a dichloromethane solution with *n*-hexane produced colourless needles, **15** (0.83 g, 89 %) at -20 °C.

3.4.2.2 Preparation of 1-benzylimidazole(pentafluorophenyl)gold(I), 16.

This product was prepared in a similar fashion as **15** from 1-benzylimidazole (0.04 g, 0.3 mmol) and [Au(C₆F₅)(tht)] (0.12 g, 0.27 mmol). Colourless crystals of **16** (0.13 g, 93 %) were obtained, from a dichloromethane solution layered with *n*-hexane, at -20 °C.

3.4.2.3 Preparation of 1-methylbenzimidazole(pentafluorophenyl)gold(I), 17.

This product was prepared in a similar manner as **15** from 1-methylbenzimidazole (0.04 g, 0.3 mmol) and [Au(C₆F₅)(tht)] (0.12 g, 0.27 mmol). Colourless crystals of **17** (0.12 g, 90 %) were obtained, from a dichloromethane solution layered with *n*-hexane, at -20 °C.

3.4.2.4 Preparation of [1,4-bis(imidazol-1-yl)butane]bis[(pentafluorophenyl)gold(I)], 18.

This product was prepared in a similar fashion as **15** from 1,4-bis(imidazol-1-yl)butane (0.05 g, 0.3 mmol) in methanol (10 ml) and [Au(C₆F₅)(tht)] (0.23 g, 0.50 mmol) in thf/methanol (10:1, 10 ml). Colourless microcrystalline material of **18** (0.19 g, 83 %) was obtained, from a thf solution layered with *n*-hexane, at -20 °C.

3.4.2.5 Preparation of 1-benzyltetrazole(pentafluorophenyl)gold(I), 19.

This product was prepared in a similar manner as **15** from 1-benzyltetrazole (0.39 g, 2.4 mmol) and [Au(C₆F₅)(tht)] (1.10 g, 2.43 mmol). An *n*-hexane extract of the dried product residue, was recrystallised and afforded colourless crystals of **19** (0.79 g, 62 %), from a dichloromethane solution layered with diethyl ether, at -20 °C.

3.4.2.6 Preparation of [(triphenylphosphine)(tetrazol-1-yl)gold(I)][pentafluorophenyl]gold(I), 20.

This product was prepared in a similar manner as **15** from **22** (0.16 g, 0.30 mmol) in dichloromethane (10 ml) and [Au(C₆F₅)(tht)] (0.14 g, 0.30 mmol) in dichloromethane (10

ml). Colourless microcrystalline material of **20** (0.16 g, 63 %) was obtained, from a dichloromethane solution layered with *n*-hexane, at -20 °C.

3.4.2.7 *Attempted synthesis of [1,2-di(tetrazol-2-yl)ethane]-bis[(pentafluorophenyl)gold(I)], and the formation of 21.*

The solution of 1,2-di(tetrazol-2-yl)ethane (0.05 g, 0.3 mmol) in thf/methanol (5:1, 10 ml) was added to [Au(C₆F₅)(tht)] (0.27 g, 0.60 mmol) in thf (10 ml). The resultant cloudy solution was stirred for 2 h at room temperature, whereafter the mixture was concentrated *in vacuo* to yield a white solid residue. The residue was resuspended in dichloromethane (20 ml), filtered through anhydrous MgSO₄, and concentrated *in vacuo* to afford a colourless crystalline material. Colourless crystals of **21** (0.27 g, 57 %) were obtained, from a dichloromethane solution layered with *n*-hexane, at -20 °C. Note that trace amounts of lithium chloride (from the synthesis of [Au(C₆F₅)(tht)]) and diglyme (from freshly distilled *n*-hexane) affected the formation of **21**.

3.4.2.8 *Preparation of 1-benzyl-5-methylsulphidetetrazol(pentafluorophenyl)gold(I), 22.*

A solution of **19** (0.10 g, 0.19 mmol) in thf (10 ml) was treated with *n*-butyllithium in *n*-hexane (0.13 ml, 0.19 mmol) at -98 °C. The light yellow solution turned a bright orange almost immediately. After 30 min. of stirring the solution was treated with, dimethyldisulphide (0.02 ml, 0.2 mmol) and the reaction mixture was stirred for a further 2 h at -78 °C. The resultant colourless solution was allowed to warm to room temperature and concentrated *in vacuo* to yield a white oily residue. The residue was extracted with diethyl ether (20 ml), filtered through anhydrous MgSO₄, and concentrated *in vacuo* to afford a colourless oily substance, which contained predominantly complex **22** and trace amounts of 1-benzyltetrazole-5-methylsulphide.

3.4.2.9 *Preparation of [2,2-bis(4,5-dimethylthiazol-2-yl)](pentafluorophenyl)gold(I), 23.*

The addition of a solution of 2,2'-bis(4,5-dimethylthiazole) (0.03 g, 0.2 mmol) in diethyl ether (10 ml) to [Au(C₆F₅)(tht)] (0.14 g, 0.30 mmol) in diethyl ether (10 ml), produced an immediate thick precipitate. The resultant suspension was stirred at room temperature for 1 h, filtered and washed sequentially with diethyl ether (10 ml) and dichloromethane (10 ml), to afford a highly insoluble off-white microcrystalline material of **23** (0.08 g, 93 %). Repetition of the reaction with equimolar amounts of [Au(C₆F₅)(tht)] and the bisthiazole effected the same result. Crystals suitable for a crystal structure determination were

obtained at -20 °C from a solution of [Au(C₆F₅)(tht)] (0.02 g, 0.03 mmol) in thf (1 ml) in a crystallisation tube, layered with a solution of bisthiazole (0.01 g, 0.03 mmol) in *n*-pentane (1 ml) and separated by a diethyl ether layer (1 ml) to allow for slow solvent diffusion.

3.4.2.10 The preparation of (triphenylphosphine)(tetrazol-1-yl)gold(I), 24.

As described by Nomiya *et al.*,¹⁶ [AuCl(PPh₃)] (0.50 g, 1.0 mmol) and 1-*H* tetrazole (0.07 g, 1.0 mmol) were dissolved in acetone (80 ml). The clear solution was treated with 1.0 M aqueous NaOH (1.0 ml, 1.0 mmol). An immediate white precipitate formed and after 4 h of stirring, the resultant NaCl (that formed) was filtered off. The clear solution was evaporated to dryness, resuspended in benzene (30 ml) and added drop wise to *n*-hexane (150 ml). The white precipitate that formed was filtered and washed with *n*-hexane. The white solid was crystallised from benzene/*n*-hexane mixture (1:3) to yield colourless needles, **24** (0.18 g, 34 %).

3.4.2.11 The preparation of (trimethylphosphine)(tetrazol-1-yl)gold(I), 25.

This product was prepared in a similar manner as **22** from [AuCl(PMe₃)] (0.56 g, 1.8 mmol) and 1-*H* tetrazole (0.13 g, 1.8 mmol) in acetone (60 ml), treated with 1.0 M aqueous NaOH (1.8 ml, 1.8 mmol). Colourless microcrystalline material of **25** (0.46 g, 74 %) was obtained, from a methanol solution layered with *n*-pentane, at -20 °C.

3.4.2.12 Representative preparation procedure for ligands IV-VI.

Using conventional heating

A mixture of the parent aminopyridine (23 mmol), sodium azide (70 mmol) and triethyl orthoformate (75 mmol) in glacial acetic acid (60 ml) was reacted at 100-150°C for 6-21 h (Table 3.19). The bright yellow suspensions turned to a golden-brown solution over this period. Upon completion of the reaction the mixture was cooled to room temperature, and the volatile materials removed *in vacuo*. The residue was diluted with distilled water (40 ml) and extracted twice with ethyl acetate (60 ml). The combined organic extracts were washed successively with 1 N HCl, water, saturated NaHCO₃, and saturated NaCl, dried over MgSO₄, filtered and the filtrate concentrated *in vacuo*. The residue was recrystallised from DMF layered with diethyl ether, at -20 °C.

Using microwave irradiation

A microwave Teflon TFMTM reactor, equipped with temperature/pressure sensors and a magnetic stirring bar, was charged with a mixture of aminopyridine (11.52 mmol), sodium azide (35.01 mmol) and triethyl orthoformate (37.51 mmol) in glacial acetic acid (30 ml) and irradiated at 500 W power for the time and at the temperature indicated in Table 3.19. After the completion of the reaction, the reactor was cooled to 50 °C with air jet cooling over a 30 min ventilation period. A similar work-up procedure was followed as described previously.

3.4.2.13 Representative preparation procedure for ligands VII-XI.

Using conventional heating

A mixture of the parent cyanopyridine or cyanoimidazole (3.10 mmol), sodium azide (7.60 mmol) and ammonium chloride (1.21 mmol) in anhydrous DMF (10-15 ml) were reacted at 100-150 °C at 6-21 h (Table 3.19). After cooling, the inorganic salts were separated by filtration and the solvent was removed *in vacuo*. The oily residue was taken up in water and acidified with HCl (0.1 M) to pH 1. The formed solid was collected by filtration, and recrystallised from DMF layered with diethyl ether, at -20 °C.

Using microwave irradiation

A microwave Teflon TFMTM reactor, equipped with temperature/pressure sensors and a magnetic stirring bar, was charged with a mixture of cyanoimidazole (7.72 mmol), sodium azide (18.96 mmol), ammonium chloride (2.92 mmol) in anhydrous DMF (10 ml), and irradiated at 500 W power for the time and at the temperature indicated in Table 3.19. After the completion of the reaction, the reactor was cooled to 50 °C *via* air jet cooling over a 30 min. ventilation period. A similar work-up procedure was followed as described previously (section 3.4.2.12).

3.4.2.14 X-ray crystal structure determinations.

Crystal data collection and refinement details for complexes **15**, **16**, **17**, **19**, **21**, **23**, **VIII** and 5-chloro1-phenyltetrazole are summarised in Tables 3.22-3.25. Data sets for 5-chloro1-phenyltetrazole were collected on an Enraf-Nonius Kappa CCD diffractometer⁶⁵ and all other data sets collected on a Bruker SMART Apex CCD diffractometer⁶⁶ with

⁶⁵ COLLECT Data Collection Software, Nonius BV Delft, The Netherlands, 1998.

⁶⁶ SMART Data Collection Software, Version 5.629, Bruker AXS Inc., Madison, WI, 2003.

graphite monochromated Mo-K α radiation ($\lambda = 0.71073 \text{ \AA}$). Data reduction was carried out with standard methods from the software package Bruker SAINT.⁶⁷ Empirical corrections were performed using SCALEPACK⁶⁸ and data were treated with SADABS.^{69,70}

All the structures were solved in collaboration with Dr S. Nogai, using direct methods or interpretation of a Patterson synthesis which yielded the position of the metal atoms, and conventional difference Fourier methods. All non-hydrogen atoms were refined anisotropically by full-matrix least squares calculations on F^2 using SHELX-97⁷¹ within the X-seed environment.⁷² The hydrogen atoms were fixed in calculated positions. Figures were generated with X-seed⁷² and POV Ray for Windows, with the displacement ellipsoids at 50% probability level. Further information is available from Prof. H.G. Raubenheimer at the Department of Chemistry and Polymer Science, Stellenbosch University.

X-ray quality single crystals of **24** were obtained by slow solvent diffusion of diethyl ether in a concentrated dimethylformamide solution at $-20 \text{ }^\circ\text{C}$. X-ray quality single crystals of 5-chloro-1-phenyltetrazole were obtained from a concentrated toluene solution at $-20 \text{ }^\circ\text{C}$. Crystallisation procedures for other complexes, are described in the preparation and procedure part of section 3.4.2.

⁶⁷ SAINT, Data Reduction Software, Version 6.45, Bruker AXS Inc., Madison, WI, 2003.

⁶⁸ L. J. Ferrugia, *J. Appl. Crystallogr.*, 1999, **32**, 837.

⁶⁹ R. H. Blessing, *Acta Cryst.*, 1995, **A51**, 33.

⁷⁰ SADABS, Version 2.05, Bruker AXS Inc., Madison, WI, 2002.

⁷¹ G. M. Shelrick, SHELX-97. Program for Crystal Structure Analysis, University of Göttingen, Germany, 1997.

⁷² L. J. Barbour, *J. Supramol. Chem.* 2001, **1**, 189.

Table 3.22 Crystallographic data for **15** and **16**

	15	16
Empirical formula	C ₁₀ H ₆ AuF ₅ N ₂	C ₁₆ H ₁₀ AuF ₅ N ₂
<i>M_r</i>	446.13	522.23
Temp. (K)	100(2)	100(2)
Wavelength (Å)	0.71073 Å	0.71073
Crystal system	Triclinic	Triclinic
Space group	P $\bar{1}$	P $\bar{1}$
a (Å)	4.7900(3)	8.1714(8)
b (Å)	10.3738(6)	13.4065(13)
c (Å)	11.0755(7)	14.5984(13)
α (°)	88.0840(10)	77.470(2)
β (°)	86.0360(10)	86.845(2)
γ (°)	82.6480(10)	79.489(2)
Volume (Å ³)	544.35(6)	1534.8(3)
Z	2	4
<i>d</i> _{calcd} (g/cm ³)	2.722	2.260
Absorption coefficient (μ , mm ⁻¹)	13.563	9.640
Absorption correction	Semi-empirical from equivalents	Semi-empirical from equivalents
F(000)	408	976
Crystal size (mm ³)	0.30 x 0.20 x 0.20	0.30 x 0.20 x 0.15
θ -range for data collection (°)	1.84 to 28.24	1.89 to 25.68
Index range	-6 ≤ h ≤ 6 -13 ≤ k ≤ 13 -14 ≤ l ≤ 14	-9 ≤ h ≤ 9 -16 ≤ k ≤ 15 -10 ≤ l ≤ 17
No. of reflections collected	6256	8529
No. independent reflections	2494 (R _{int} = 0.0235)	5710 (R _{int} = 0.0176)
Max. and min. transmission	0.2355 and 0.1318	0.3258 and 0.2133
Refinement method	Full-matrix least-squares on F ²	Full-matrix least-squares on F ²
Data/restraints/parameters	2494 / 0 / 165	5710 / 0 / 433
Goof on F ²	1.056	1.025
Final R-indices [I > 2σ >(I)]	R ₁ = 0.0194 wR ₂ = 0.0444	R ₁ = 0.0263 wR ₂ = 0.0635
R indices (all data)	R ₁ = 0.0209 wR ₂ = 0.0451	R ₁ = 0.0308 wR ₂ = 0.0656
Largest diff. peak and hole (e.Å ⁻³)	1.487 and -0.566	1.952 and -0.641
Weighing scheme	a = 0.0221 / b = 0.2729	a = 0.0384

Table 3.23 Crystallographic data for **17** and **19**

	17	19
Empirical formula	C ₁₄ H ₈ AuF ₅ N ₂	C ₂₂ H ₁₆ AuF ₅ N ₈
<i>M_r</i>	496.19	684.39
Temp. (K)	100(2)	100(2)
Wavelength (Å)	0.71073	0.71073
Crystal system	Monoclinic	Monoclinic
Space group	P2 ₁ /c	P2 ₁ /c
a (Å)	11.0548(11)	18.4500(13)
b (Å)	8.1204(8)	5.0734(4)
c (Å)	15.1295(16)	25.1579(17)
α (°)	90	90
β (°)	101.383(2)	107.5310(10)
γ (°)	90	90
Volume (Å ³)	1331.5(2)	2245.5(3)
Z	4	4
<i>d</i> _{calcd} (g/cm ³)	2.475	2.024
Absorption coefficient (μ, mm ⁻¹)	11.104	6.623
Absorption correction	Semi-empirical from equivalents	Semi-empirical from equivalents
F(000)	920	1312
Crystal size (mm ³)	0.20 x 0.20 x 0.10	0.20 x 0.10 x 0.10
θ-range for data collection (°)	1.88 to 26.37	1.70 to 26.73
Index range	-11 ≤ h ≤ 13 -10 ≤ k ≤ 9 -18 ≤ l ≤ 15	-23 ≤ h ≤ 22 -6 ≤ k ≤ 6 -26 ≤ l ≤ 31
No. of reflections collected	7396	12484
No. independent reflections	2707 (R _{int} = 0.0220)	4727 (R _{int} = 0.0404)
Max. and min. transmission	0.4031 and 0.2039	0.5572 and 0.4477
Refinement method	Full-matrix least-squares on F ²	Full-matrix least-squares on F ²
Data/restraints/parameters	2707 / 0 / 200	4727 / 0 / 325
Goof on F ²	1.059	1.057
Final R-indices [I > 2σ >(I)]	R ₁ = 0.0221 wR ₂ = 0.0520	R ₁ = 0.0391 wR ₂ = 0.0851
R indices (all data)	R ₁ = 0.0244 wR ₂ = 0.0531	R ₁ = 0.0502 wR ₂ = 0.0894
Largest diff. peak and hole (e.Å ⁻³)	1.557 and -1.283	2.977 and -1.524
Weighing scheme	a = 0.0312 / b = 0.9283	a = 0.0490

Table 3.24 Crystallographic data for **19** and **21**

	21	23
Empirical formula	C ₄₃ H ₄₀ Au ₂ F ₂₀ Li ₂ N ₈ O ₇	C ₁₆ H ₁₂ AuF ₅ N ₂ S ₂
M_r	1568.64	588.36
Temp. (K)	173(2)	100(2)
Wavelength (Å)	0.71073	0.71073
Crystal system	Monoclinic	Triclinic
Space group	P2 ₁ /m	P $\bar{1}$
a (Å)	9.157(10)	6.875(4)
b (Å)	21.270(18)	11.536(6)
c (Å)	14.064(15)	11.747(6)
α (°)	90	112.809(7)
β (°)	103.34(3)	94.191(8)
γ (°)	90	99.105(8)
Volume (Å ³)	2665(5)	838.7(8)
Z	2	2
d_{calcd} (g/cm ³)	1.955	2.330
Absorption coefficient (μ , mm ⁻¹)	5.623	9.074
Absorption correction	Semi-empirical from equivalents	Semi-empirical from equivalents
F(000)	1508	556
Crystal size (mm ³)	0.20 x 0.10 x 0.10	0.30 x 0.10 x 0.05
θ -range for data collection (°)	2.42 to 25.68	1.90 to 25.68
Index range	-11 \leq h \leq 10 -25 \leq k \leq 20 -17 \leq l \leq 16	-8 \leq h \leq 8 -7 \leq k \leq 14 -14 \leq l \leq 14
No. of reflections collected	12711	4412
No. independent reflections	5090 ($R_{\text{int}} = 0.0338$)	3081 ($R_{\text{int}} = 0.0277$)
Max. and min. transmission	0.6032 and 0.4861	0.6597 and 0.2428
Refinement method	Full-matrix least-squares on F ²	Full-matrix least-squares on F ²
Data/restraints/parameters	5090 / 1 / 408	3081 / 0 / 239
Goof on F ²	1.029	1.064
Final R-indices [$I > 2\sigma > (I)$]	$R_1 = 0.0351$ $wR_2 = 0.0761$	$R_1 = 0.0355$ $wR_2 = 0.0909$
R indices (all data)	$R_1 = 0.0727$ $wR_2 = 0.0901$	$R_1 = 0.0393$ $wR_2 = 0.0931$
Largest diff. peak and hole (e.Å ⁻³)	1.644 and -0.634	3.027 and -2.290
Weighing scheme	a = 0.0388 / b = 5.9665	a = 0.0586

Table 3.25 Crystallographic data for **VIII** and 5-chloro-1-phenyltetrazole

	VIII	5-chloro-1-phenyltetrazole
Empirical formula	C ₁₀ H ₁₂ N ₁₀ O	C ₇ H ₅ C ₁₁ N ₄
<i>M_r</i>	288.30	180.60
Temp. (K)	100(2)	203
Wavelength (Å)	0.71073	0.71073
Crystal system	Monoclinic	monoclinic
Space group	P2 ₁ /c	P2 ₁ /n
a (Å)	9.6613(17)	7.0246(2)
b (Å)	7.2879(13)	6.3305(2)
c (Å)	18.253(3)	17.5412(4)
α (°)	90	90
β (°)	93.061(3)	96.6007(14)
γ (°)	90	90
Volume (Å ³)	1283.4(4)	774.87(4)
Z	4	4
<i>d</i> _{calcd} (g/cm ³)	1.492	
Absorption coefficient (μ, mm ⁻¹)	0.109	0.434
Absorption correction	Semi-empirical from equivalents	Semi-empirical from equivalents
F(000)	600	368
Crystal size (mm ³)	0.3 x 0.15 x 0.15	0.3 x 0.15 x 0.15
θ-range for data collection (°)	2.11 to 25.71	3.02 to 25.00
Index range	-6 ≤ h ≤ 11 -8 ≤ k ≤ 8 -22 ≤ l ≤ 22	-8 ≤ h ≤ 8 -7 ≤ k ≤ 7 -20 ≤ l ≤ 20
No. of reflections collected	5669	2595
No. independent reflections	2413 [R(int) = 0.0317]	1364 [R(int) = 0.0207]
Max. and min. transmission	0.6032 and 0.4861	
Refinement method	Full-matrix least-squares on F ²	Full-matrix least-squares on F ²
Data/restraints/parameters	2413 / 0 / 200	1364 / 0 / 110
Goof on F ²	0.957	1.030
Final R-indices [I > 2σ > (I)]	R ₁ = 0.0361 wR ₂ = 0.0867	R ₁ = 0.0313 wR ₂ = 0.0906
R indices (all data)	R ₁ = 0.0489 wR ₂ = 0.0915	R ₁ = 0.0396 wR ₂ = 0.0969
Largest diff. peak and hole (e.Å ⁻³)	0.200 and -0.178	0.381 and -0.174
Weighing scheme	a = 0.0523	a = 0.044

CHAPTER 4

Preparation and characterisation of novel gold(I) N-heterocyclic carbene (NHC) and acyclic carbene complexes, derived from lithiated and isocyanide precursors.

Abstract

Neutral and cationic tetrazolyl and (tetrazolylidene)gold(I) complexes have been prepared using two different methodologies; firstly, by sequential lithiation of 1-benzyltetrazole, transmetalation with $[\text{AuCl}(\text{PPh}_3)]$, $[\text{AuCl}(\text{tht})]$ or $[\text{Au}(\text{C}_6\text{F}_5)(\text{tht})]$, and alkylation. The cationic mono(carbene) complex, (1-benzyl-4-methyltetrazol-5-ylidene)(triphenylphosphine)gold(I), **28**, is unstable in solution and undergoes spontaneous homoleptic rearrangement. The neutral mono(carbene) complex, (1-benzyl-4-methyltetrazol-5-ylidene)(pentafluorophenyl)gold(I), **29**, and the cationic bis(carbene) complex, bis(1-benzyl-4-methyltetrazol-5-ylidene)gold(I), **30**, are both stable isolable crystalline complexes. The molecular and crystal structure of **30** has been determined by single crystal X-ray diffraction. The addition of a 10% TMEDA (tetramethylenediamine) in a thf solution to lithiated 1-benzyltetrazole, followed by reaction with $[\text{Au}(\text{C}_6\text{F}_5)(\text{tht})]$, and alkylation, affords the homoleptic rearranged product $[\text{Au}(\text{C}_6\text{F}_5)_2]\text{TMEDAME}$, **31**. Additionally, two unique Li^+ triflate coordination compounds, **32** and **33**, crystallise from these reaction mixtures and show common coordination and crystallisation behaviour.

A series of C-tetrazolyl and tetrazolylidene complexes of gold(I), i.e. [1-(2,6-dimethylphenyl)tetrazol-5-yl](triphenylphosphine)gold(I), **37**, [1-(2,6-dimethylphenyl)-4-methyltetrazol-5-ylidene](triphenylphosphine)gold(I), **38**, [1-(*tert*-butyl)tetrazol-5-yl](triphenylphosphine)gold(I), **39**, [1-(cyclohexyl)tetrazol-5-yl](triphenylphosphine)gold(I), **40**, have been prepared from the reaction of $[\text{Au}(\text{N}_3)(\text{PPh}_3)]$ with various isocyanides. The molecular and crystal structures of **36** and **37** reveal an exclusive N^4 alkylation to afford carbene complexes. A luminescent (isocyanide)(pentafluorophenyl)gold(I) complex, **41**, converts into acyclic di(amino)carbene complex, **42** by the addition of 1,2,4-triazol-3-ylamine. An amino(ethoxy)carbene complex, **43**, and a di(amino)carbenegold(I) complex, **44**, can be prepared from a (isocyanide)(tetrazol-5-yl)gold(I) complex, spontaneously assemble and co-crystallise due to aurophillic interaction.

4.1 Introduction

The study of N-heterocyclic carbene (NHC) complexes of various metals remains a topical field of research in inorganic chemistry. Since the first isolable NHC was characterised more than a decade ago, dedicated effort has been made to develop transition

metal derivatives of such compounds.¹ N-Heterocyclic carbenes constitute a class of strongly coordinating ligands that have often been compared to phosphines with regard to their chemical bonding and the complex synthetic methodologies from which they are derived.² The emerging interest in NHC's as surrogates for phosphines in organometallic catalysis, is testimony to the remarkable stability and versatility observed for such transition metal complexes. In particular, imidazol-2-ylidenes of rhodium and palladium have shown excellent catalytic properties for Heck-olefination, hydroformylation and isomerisation.^{3,4} NHC ligands share electronic similarities with trialkylphosphines but appear as stronger coordinating ligands which show non-dissociative behaviour in solution.⁵ Herrmann and co-workers⁵ elegantly merged the best attributes of both these ligand systems, in the preparation of mixed palladium(II) complexes of NHCs and phosphines, i.e. combining the high stability of the NHC-palladium bond with the facile dissociation of the phosphine ligand. In a number of instances substitution of phosphine ligands by NHC has led to enhanced catalytic activity and thermodynamic stability of the obtained carbene complexes. A plausible explanation is that due to the more powerful σ -donation of NHC's, and subsequent stronger bonding compared to closely related phosphines, more active, electron rich metal centres are effected.⁶

The strong stabilising effect of N-heterocyclic carbenes has also found relevance in gold(I) chemistry. Liao and co-workers⁷ have recently isolated terminal acetylides, as gold(I) ethynyl complexes of the type, LAuC \equiv CH (L = MePH₂, Me₃P). A determining factor in the assembly of these compounds is the employment of an appropriate phosphine ligand in stabilising such compounds. Due to their predictable aurophilic interactions, these linear complexes can be used as reliable synthons in crystal engineering. Exploiting the expanding use of sterically hindered NHC gold(I) complexes as synthons for further facile functionalisation, Singh and co-workers⁸ demonstrate the preparation of the equally stable

¹ A. J. Arduengo III, R. L. Harlow and M. Kline, *J. Am. Chem. Soc.*, 1991, **113**, 361.

² W. A. Herrmann, *Angew. Chem., Int. Ed.*, 2002, **41**, 1291.

³ W. A. Herrmann, L. J. Goosen, C. Köcher and G. R. J. Artus, *Angew. Chem., Int. Ed. Engl.*, 1996, **35**, 2805.

⁴ W. A. Herrmann, L. J. Goosen and M. Spiegler, *Organometallics*, 1998, **17**, 2162, and references cited therein.

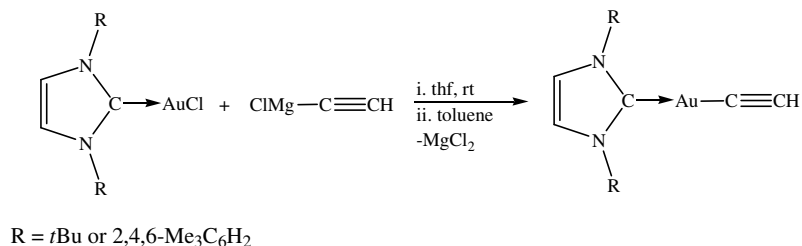
⁵ W. A. Herrmann, V. P. W. Böhm, C. W. K. Gstöttmayr, M. Grosche, C-P Reisinger and T. Weskamp, *J. Organomet. Chem.*, 2001, **617-618**, 616.

⁶ S. Grundemann, M. Albrecht, J. A. Loch, J. W. Faller and R. H. Crabtree, *Organometallics*, 2001, **20**, 5485.

⁷ R.-Y. Liao, A. Schier and H. Schmidbaur, *Organometallics*, 2003, **22**, 3199.

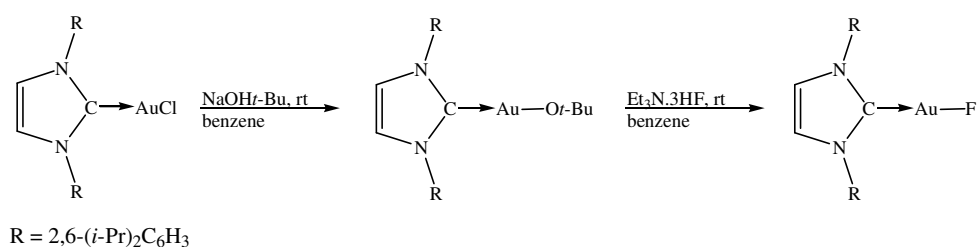
⁸ S. Singh, S. S. Kumar, V. Jancik, H. W. Roesky, H-G. Schmidt and M. Noltemeyer, *Eur. J. Inorg. Chem.*, 2005, 3057.

terminal acetylide of the type $\text{LAuC}\equiv\text{CH}$ ($\text{L} = \text{NHC}$, e.g. 1,3-di(*tert*-butyl)imidazol-2-ylidene) from (NHC)gold(I) chlorides (Equation 4.1).



Equation 4.1

The remarkable stabilising effect inherent in NHC is best illustrated in the preparation of the first isolable gold(I) fluoride complex (Equation 4.2) as a two-coordinate monomer.⁹ Late transition metal complexes of fluoride are rare and display unpredictable reactivity. According to the usual classification of hard and soft acids and bases, the fluoride ion is mismatched with the cations afforded by these transition metals in low oxidation states;¹⁰ the strong π -donating ability of F^- destabilises the filled d-orbitals of the metals, affording a labile reactive metal-fluorine bond.¹¹ In this regard, gold(I) fluorides would be expected to appear as very unstable complexes. However, Laiter and co-workers⁹ reported that stable forms of these complexes can be prepared by the addition of triethylamine tris(hydrofluoride) ($\text{Et}_3\text{N}\cdot 3\text{HF}$) to an (NHC)gold(I) alkoxide. Subsequent DFT calculations find a slight lengthening of the Au-F bond, and a large partial negative charge on the fluorine atom due to electrostatic $p\pi/d\pi$ repulsive interactions.



Equation 4.2

The nature and indeed the stability of the metal-carbene bond has been a subject of much discussion.¹² The preparation, in recent times, of numerous metal NHC complexes complemented by the advent of readily available single crystal X-ray diffraction analysis, has provided access to structural parameters and insight into the nature of various

⁹ D. S. Laiter, P. Müller, T. G. Gray and J. P. Sadighi, *Organometallics*, 2005, **24**, 4503.

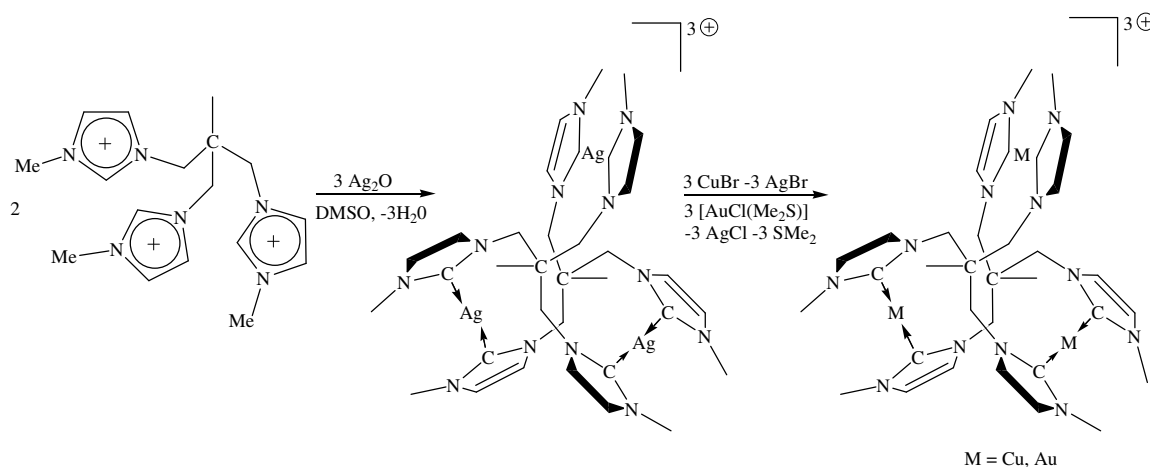
¹⁰ K. Fagnou and M. Lautens, *Angew. Chem., Int. Ed.*, 2002, **41**, 26.

¹¹ A. Yahav, I. Goldberg and A. Vigalok, *J. Am. Chem. Soc.*, 2003, **125**, 13634.

¹² D. Nemcsok, K. Wichmann and G. Frenking, *Organometallics*, 2004, **23**, 3640.

coordination complexes. However, the denotation of many M-C bonds as single bonds, based on determined bond distances, has led to the assumption that NHC are pure σ -donor ligands. In order to establish whether a secondary bond contribution to the metal-carbene bond, i.e. by π -back bonding from the metal to the π^* orbitals of the NHC (often considered negligible), is of importance, careful consideration should be taken of other factors. A more instructive approach could be a comparison of metric parameters of heterocyclic rings in a range of isostructural NHC complexes containing varying electronic metal centres.¹³ For example π -back donation from an electron rich metal centre will be manifested by an increase in C-N bond lengths due to the decrease of nitrogen to carbene π -bonding. In this regard the synthesis and structural characterisation of simple linear NHC gold(I) complexes becomes a salient feature. Various methodologies have recently been developed towards the easy access of not only NHC gold(I) complexes but also their now, readily obtainable derivatives.

Meyer and co-workers¹³ have reported that by examination of the electronic structures solved by means of molecular orbital analysis by DFT calculation, an unambiguous insight can be gained into the nature of such transition metal coordination. For a series of isostructural metal complexes of a tripodal NHC ligand, 1,1,1-tris[(3-methylimidazol-2-ylidene)ethane] (TIME^{Me}) of the type, [(TIME^{Me})₂M₃] (PF₆)₃ (M = Cu, Ag and Au), it follows that apart from the major contributing σ -type interaction an additional non-negligible π interaction between the electron rich metal centres and the carbene π -p orbitals contributes 15-30% of the total orbital interaction energy (Equation 4.3).

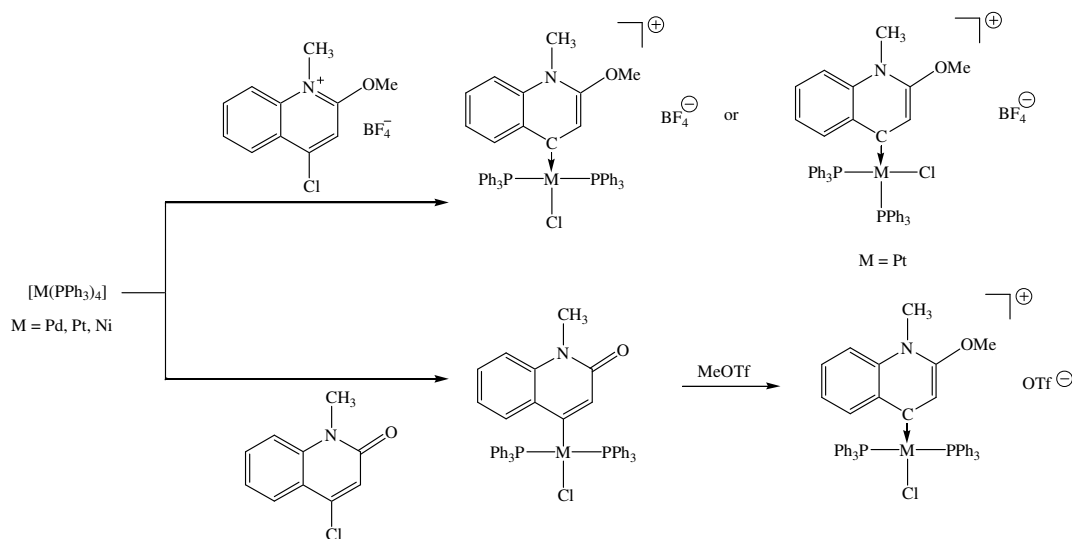


Equation 4.3

¹³ X. Hu, I. Castro-Rodriguez, K. Olsen and K. Meyer, *Organometallics*, 2004, **23**, 755.

Frenking and co-workers¹⁴ however emphasise that energy contributions of σ and π orbitals should be addressed quantitatively using energy decomposition analysis (EDA). The advantage of using this method is that it not only provides information regarding the strength of the covalent (orbital) interactions but also about the electrostatic (Coulomb) contribution.¹²

A new class of NHCs recently developed in our laboratory, are the remote N-heteroatomic carbene (*r*NHC) complexes. These complexes feature, in contrast to the conventional Öfele-Wanzlick-type^{15, 16} heterocyclic carbene complexes that contain at least one heteroatom adjacent (α) to the carbene carbon, no heteroatom in these positions. It is now possible to obtain carbene complexes of Pd(II), Pt(II) and Ni(II) by the oxidative addition of neutral chloro-quinolinone and cationic chloro-quinolinium precursors to Pd(0), Pt(0) and Ni(0) tetrakis (triphenylphosphine) starting compounds (Scheme 4.1).¹⁷ Similar products are obtained by electrophilic attack before or after metal coordination.



Scheme 4.1 The synthetic route towards *r*NHC of Pd(II), Pt(II) and Ni(II).

This is an especially elegant route to Ni-carbene complexes, and also the first examples of remote heterocyclic carbene complexes prepared from precursors in which the nucleophilic heteroatoms are located three bonds away from the carbene carbon. However, the most startling attribute of these complexes is their exceptional stability in solution,

¹⁴ G. Frenking, K. Wichmann, N. Frohlich, C. Loschen, M. Lein, J. Frunzke and V. M. Rayon, *Coord. Chem. Rev.*, 2003, **238**, 55.

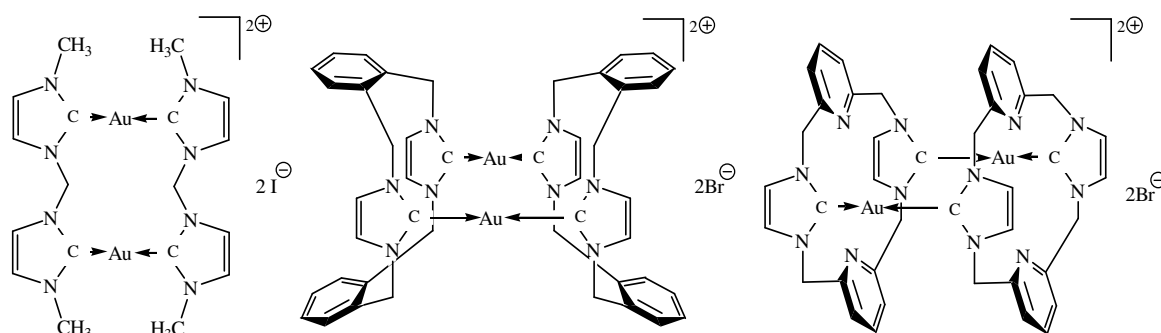
¹⁵ K. Öfele, *J. Organomet. Chem.*, 1968, **12**, 42.

¹⁶ H. W. Wanzlick and H. J. Schönherr, *Angew. Chem.*, 1968, **80**, 154.

¹⁷ W. H. Meyer, M. Deetlefs, M. Pohlmann, R. Scholtz, M. W. Esterhuysen, G. R. Julius and H. G. Raubenheimer, *Dalton Trans.*, 2004, 413.

which prompted a comparative quantum mechanical study of related compounds to determine the role the remote heteroatom plays in rendering the structures stable and, eventually in their potential use as precatalysts.¹⁸ The latter aspect of this ongoing study is illustrated in comparative Mizorocki-Heck and Suzuki-Miyaura C-C coupling reactions that involve a number of phosphines, NHC complexes and *r*NHC of Pd. Results indicate that the carbene-type ligand with no heteroatom in the immediate vicinity of the carbon donor atom activates the metal centre significantly more than comparable N-heterocyclic carbene ligands. It follows further from EDA results that the metal-carbene interactions in the *r*NHC complex, is notably stronger ($\Delta E_{\text{int}} = -107.6$ kcal/mol) than for a related NHC complex ($\Delta E_{\text{int}} = -85.5$ kcal/mol). Furthermore, in both cases the bulk (ca. 70 %) of the metal-carbene bonding attractive force is made up of electrostatic interactions. Interestingly, in both complexes, 15-17% of the orbital interaction is due to π -bonding.

NHC's have also replaced phosphines lately in chrysotherapy and the use of gold(I) as anti-tumour agents. Berners-Price and co-workers¹⁹ have used NHCs as alternatives to phosphines in the preparation of new, potent gold(I) anti-tumour agents. It is known that in bis-chelated gold(I) and silver(I) equivalents of $[\text{Au}(\text{dppe})_2]^+$, a selectivity for tumour cells over healthy cells is gained by the fine-tuning of the hydrophilic-lipophilic balance of the ligand. However, the extent of application of this method is limited by the ease of synthesis of the relevant phosphine. In this regard, bidentate NHCs provide an efficient alternative because a series of N-functionalised and structurally similar complexes can readily be obtained (Equation.4.4).²⁰



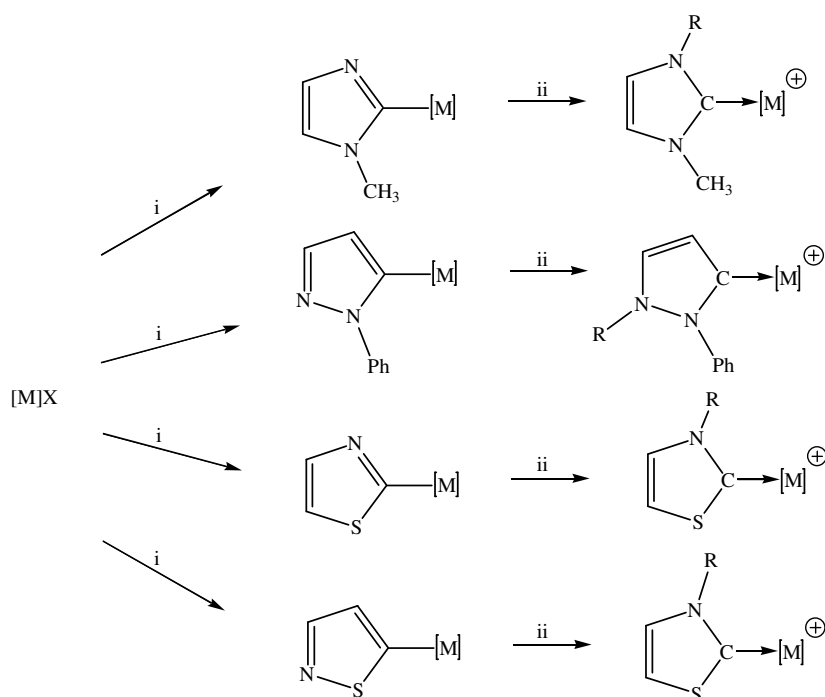
Equation 4.4

¹⁸ S. K. Schneider, P. Roembke, G. R. Julius, C. Loschen, H. G. Raubenheimer, G. Frenking and W. A. Herrmann, *J. Eur. Chem.*, 2005, 2973.

¹⁹ M. W. Baker, P. J. Barnard, S. J. Berners-Price, S. K. Brayshaw, J. L. Hickey, B. W. Skelton and A. H. White, *J. Organomet. Chem.*, 2005, **690**, 5625.

²⁰ P. J. Barnard, M. V. Baker, S. J. Berners-Price, B. W. Skelton and A. H. White, *Dalton Trans.*, 2004, 1038.

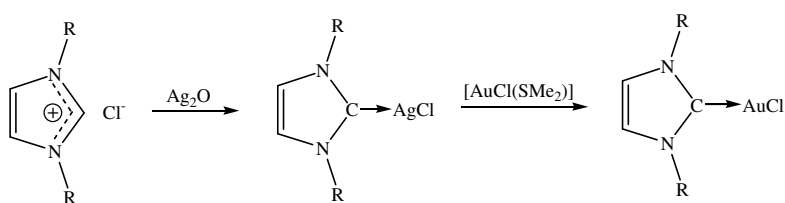
Several methods have recently been developed to prepare gold(I) NHC complexes. The synthesis of (NHC)gold(I) complexes *via* the sequential lithiation of an imidazole substrate, transmetalation to a gold(I) substrate, followed by the alkylation or protonation, has been developed in our laboratory and provides an access route to a variety of this class of gold(I) carbenes (Scheme 4.2).²¹



[M]X = [AuCl(PPh₃)], [AuCl(tht)] or [Au(C₆F₅)(tht)], R = CH₃ or H
 i) lithiated azoles ii) acid or alkylating agent

Scheme 4.2 The synthetic route towards NHC of gold(I) from lithiated azoles.

The use of silver(I) NHC complexes as carbene-transfer reagents, towards the synthesis of gold(I) NHC complexes is due to Lin and co-workers²² (Equation 4.5). Apart from neutral (NHC)gold(I) complexes, cationic imidazolium- and benzimidazolium-derived carbene complexes have been prepared.



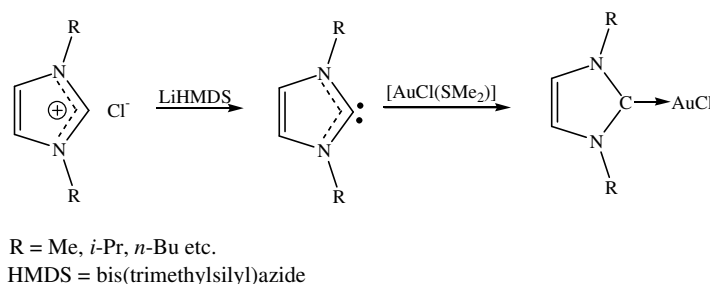
R = Me, *i*-Pr, *n*-Bu etc.

Equation 4.5

²¹ H. G. Raubenheimer and S. Cronje, *J. Organomet. Chem.*, 2001, **617-618**, 170

²² H. M. J. Wang and I. J. B. Lin, *Organometallics*, 1998, **17**, 972.

Barnard and co-workers²⁰ have illustrated that the addition of carboxylate salts, such as sodium acetate, lithium acetate or lithium butyrate to DMF mixtures of imidazolium salts and $[\text{AuCl}(\text{SMe}_2)]$, readily affords cationic (NHC)gold(I) complexes as precipitates from reaction mixtures. Related reactions can also be conducted in the presence of strong bases which effect the *in situ* formation of the NHC from imidazolium salts and substitution of a labile ligand from suitable gold(I) substrates.²³ Using a similar approach, Baker and co-workers²⁴ however, found that the desired (NHC)gold(I) complexes were only isolated in moderate yields, owing to the formation of cationic bis(NHC)gold(I) by-products (Equation 4.6).



Equation 4.6

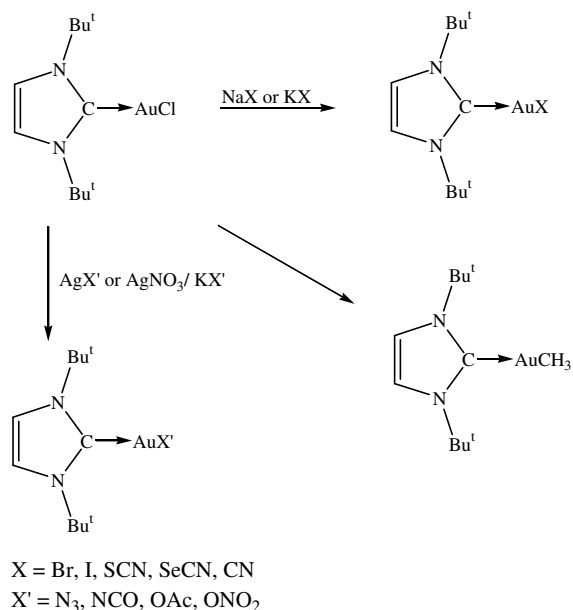
This result was corroborated by very recent findings of de Fremont,²⁵ which indicate that the straightforward reactions between equimolar amounts of AuCl and free NHC produces unsatisfactory yields of (NHC)gold(I) chlorides due to the formation of metallic gold deposition and similar homoleptic by-products. However, in contrast to the findings of Baker *et al.*,²⁴ reactions of $[\text{AuCl}(\text{SMe}_2)]$ and thf-solutions of free NHCs, e.g. 1,3-bis(2,4,6-trimethylphenyl)imidazol-2-ylidene, afford gold(I) carbene complexes in high yields. The application of chloro(NHC)gold(I) complexes as useful synthons towards functionalisation, is well evident in the array of recently prepared novel gold(I) carbene complexes (Scheme 4.3; see also Equations 4.1 and 4.2).²⁴

In this investigation, the facile preparation and structural characterisation of a series of N-heterocyclic carbene complexes allows an insight into the nature of the metal-carbene bond (*vide supra*), i.e. by using spectroscopic data, e.g. ^{13}C NMR chemical shifts of carbene carbon resonances, the trans-effects of NHC on ancillary ligands as well as the correlation of structural parameters to reactivity of complexes.

²³ R. Frankel, J. Kniczek, W. Ponikwar, H. Noth, K. Polborn and W.P. Fehlhammer, *Inorg. Chim. Acta*, 2001, **312**, 23.

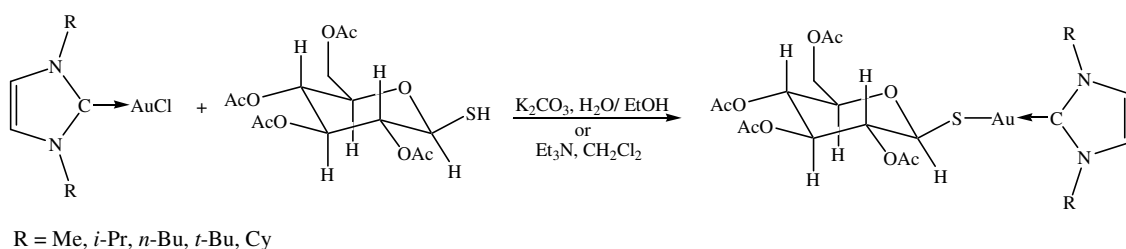
²⁴ M. V. Baker, P. J. Barnard, S. K. Brayshaw, J. L. Hickey, B. W. Skelton and A. H. White, *Dalton Trans.*, 2005, 37.

²⁵ P. de Fremont, N. M. Scott, E. D. Stevens and S. P. Nolan, *Organometallics*, 2005, **24**, 2411.



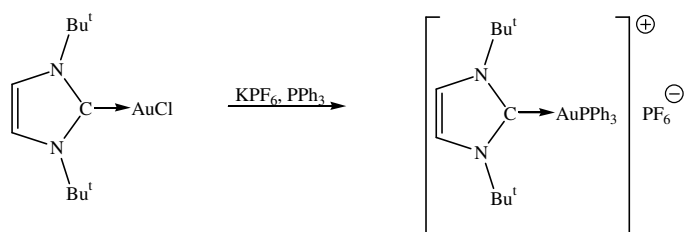
Scheme 4.3 The functionalisation of chloro(NHC)gold(I).

The versatility of (NHC)gold(I) complexes as starting material is also evident in the preparation of useful and biologically active substrates, e.g. Auranofin (equation 4.7), which allows for screening, and the establishment of SAR trends of these complexes.¹⁹



Equation 4.7

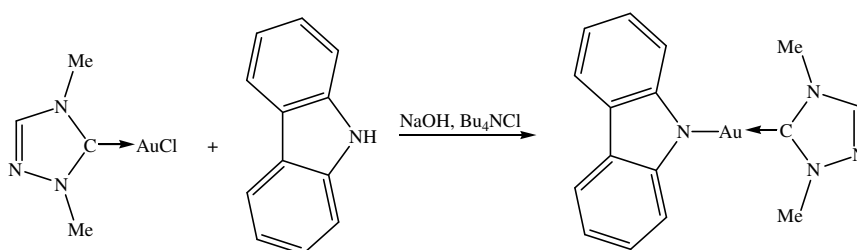
Bulky (NHC)gold(I) chloride complexes are also ideally suited for the preparation mono(NHC)gold(I) complexes containing relatively labile phosphine ligands which have previously been reported to be prone to homoleptic rearrangements (Equation 4.8).²⁶



Equation 4.8

²⁶ H. G. Raubenheimer, L. Lindeque and S. Cronje, *J. Organomet. Chem.*, 1996, **511**, 177.

Wang and co-workers²⁷ have very recently attempted to coalesce the well-documented photoluminescent properties displayed by certain gold(I) phosphines, and the photophysical chromophoric behaviour of carbazole. In view of the parallels between phosphines and NHC ligands it was envisaged that a similar type of photophysical behaviour would be exhibited by (NHC)gold(I) complexes in the presence of carbazole. By simple functionalisation of (NHC)gold(I) chloride, (carbazol-1-yl)(1,3-dimethyltriazol-2-ylidene)gold(I), can be isolated as yellow luminescent solids. For a series of carbazolate complexes, all the compounds exhibit high-energy emission bands at ~ 400 nm (Equation 4.9). Low energy emission bands appear at 584-592 nm and are ascribed to the carbazolate tuning by the metal centre.



Equation 4.9

A glaring omission from the range of simple (NHC)gold(I) complexes prepared to date are those of tetrazoles. Both mono and bis(carbene) complexes of gold(I) derived from lithiated pyridine have been prepared and structurally characterised.²⁸ Furthermore, numerous imidazolyl and triazolyl gold(I) carbene complexes are obtainable from routes and methods described in the preceding discussion. The only remaining class of simple C-bonded or carbene-bonded N-heterocyclic gold(I) complexes to be prepared are those that contain tetrazole rings. To the best of our knowledge, the only reports of C-bonded tetrazolyl gold(I) complexes are of the type (RNC)(RN₄C)Au(I) (R = methyl, cyclohexyl, phenyl) that have been prepared in the group of Beck and Fehlhammer.²⁹ Although, these complexes can be isolated as crystalline solids, the rapid decomposition in the X-ray beam of almost all these crystals, impedes their structural characterisation. A search in the Cambridge Crystallographic database shows a solitary entry of a tetrakis(tetrazol-5-yl)gold(III) complex prepared by the same research group.³⁰ Although, the preparation of the corresponding carbene complex by protonation of the tetrazolyl precursor is reported,

²⁷ H. M. J. Wang, C. S. Vasam, T. Y. R. Tsai, S-H. Chen, A. H. H. Chang and I. J. B. Lin, *Organometallics*, 2005, **24**, 486.

²⁸ H. G. Raubenheimer, J. G. Toerien, G. J. Kruger, R. Otte, W. van Zyl and P. Olivier, *J. Organomet. Chem.*, 1994, **466**, 291.

²⁹ W. Beck, K. Burger and W. P. Fehlhammer, *Chem. Ber.* 1971, **104**, 1816.

³⁰ M. Wehlan, R. Thiel, J. Fuchs, W. Beck and W. P. Fehlhammer, *J. Organomet. Chem.*, 2000, 159.

the authors acknowledge that no unambiguous proof exists to confirm that such a reaction had indeed taken place. The synthesis of tetrazole-derived NHC complexes of gold(I) poses, from a structural point of view, certain challenges. Firstly, due to the fact that lithiated tetrazoles are innately unstable and readily lose molecular nitrogen to form cyanamide byproducts³¹ and, secondly, although alkylation should be favoured on the more nucleophilic adjacent α nitrogen in (tetrazolyl)aurates, electrophilic additions in theory could also occur at the remote nitrogen, β with regard to the coordinated carbon owing to the resonance of delocalised electronic charge around the ring. The procedure of 1,3-dipolar cycloaddition of organic isocyanides to metal azides, in this regard provides an elegant alternative towards various C-coordinated tetrazolyl gold(I) complexes. In contrast to the widely applied and related cycloaddition reaction of nitriles and coordinated azides which afford N-coordinated tetrazolate complexes, the carbon-metal variety is limited to only a few reports.^{32,33}

Ironically, the structural motifs found in these complexes, i.e. metal-coordinated isocyanides, are representatives of the first gold(I) carbene precursor functionalities. A well established methodology to functionalise these “masked carbenes”, i.e. by the nucleophilic additions of alcohols and amines, to acyclic (diamino)- and (alkoxy)(amino)carbenegold(I) complexes, exists.^{34,35} In recent times these gold(I) carbene types, have often been reported to display interesting photoluminescent properties both in the solid state and in solution. Numerous reports have ascribed such unique photophysical property to the self-association of fragments initiated by strong aurophilic interactions. White-Morris,³⁶ reported that the extent of luminescence is directly related to the degree of self-association that occurs in solution between cationic $[\text{Au}\{\text{C}(\text{NHMe})_2\}_2]^+$ species, as dimers and extended oligomers. Balch and co-workers³⁷ illustrated that the hydrogen bonding between cations and cyano-groups in various $[\text{Au}(\text{CN})_2]$ salts mediates the formation of the crystalline organisation containing strong Au...Au interactions.

This addresses some molecular reactivities that are topical to gold(I) complexes that contain carbene ligands. It also complements the preceding chapters, in that it relates

³¹ L. L. Garber and C. H. Brubaker, Jr, *J. Am. Chem. Soc.*, 1966, **88**, 4266.

³² Y-J. Kim, Y-S. Kwak, Y-S. Joo and S-W. Lee, *J. Chem. Soc., Dalton Trans.*, 2002, 144.

³³ Y-J. Kim, Y-S. Joo, J-T Han, W. S. Han and S-W. Lee, *J. Chem. Soc., Dalton Trans.*, 2002, 3611.

³⁴ F. Bonati and G. Minghetti, *Gazz. Chim. Ital.*, 1973, **103(3)**, 373.

³⁵ R. Usón, A. Laguna, J. Vicente, J. García and B. Bergareche, *J. Organomet. Chem.*, 1979, **173**, 349.

³⁶ R. L. White-Morris, M. M. Olstead, F. Jiang and A.L. Balch, *Inorg. Chem.*, 2002, **41**, 2313.

³⁷ M. Stender, M. M. Olmstead, A. L. Balch, D. Rios and S. Attar, *Dalton Trans.*, 2003, 4282.

simple and stable (NHC)gold(I) complexes to gold(I) centres containing phosphine and imine ligands. A commonality is found in the consistent employment of N-rich heterocycles to effect these novel organometallic and coordination complexes of gold(I). We also set out to contribute further to the rapidly expanding field of (NHC)gold(I) chemistry by the preparation and structural characterisation of the first gold(I) carbene complexes derived from tetrazoles.

4.2 Results and discussion

4.2.1 Tetrazolylidene complexes of gold(I) derived from lithiated tetrazoles.

The lithiation of 1-alkyltetrazoles is known to be a temperature dependent reaction. Brubaker and co-workers³⁸ first reported, in a study directed towards the synthesis of C-tetrazolyl nickel(II) complexes, that 1-methyltetrazol-5-yl lithium appeared thermally stable at -50 °C. Raap demonstrated that the careful addition of a solution of 1-methyltetrazole in thf, to *n*-butyllithium at -60 °C to -65 °C afforded stable precursors to 5-substituted tetrazoles.³⁹ However, at temperatures exceeding -50 °C, an exothermic reaction (with gas evolution) results in the formation of cyanamide by-products, indicating that ring fragmentation occurs. In contrast, Kauer and co-workers⁴⁰ report that by reacting 5-chloro-1-phenyl- and 1-phenyltetrazole with *n*-butyllithium or Mg results in the formation of phenylcyanamide exclusively, and it appears that the N¹ substituent plays an important role in the stability of lithiated tetrazole derivatives. In the successful preparation of medicinally important 1,5-disubstituted tetrazole compounds from 1-benzyltetrazol-5-yl lithium, Satoh and co-workers⁴¹ have shown the worth of this synthon in organic synthesis.

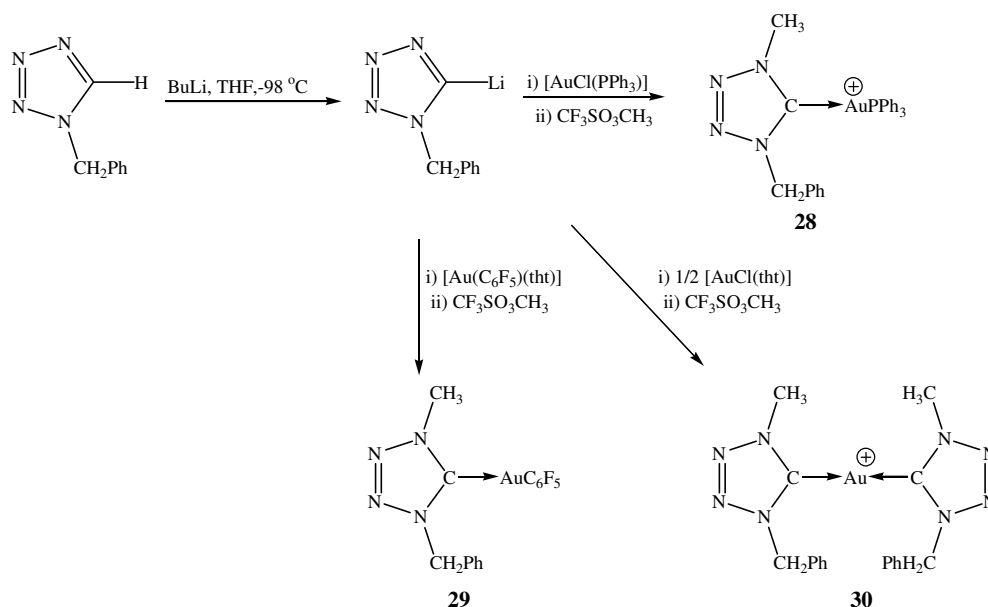
Scheme 4.4 illustrates the methodology used in the preparation of various novel (tetrazolylidene)gold(I) complexes. This involves sequential lithiation of the CH-acidic tetrazole, transmetallation involving a gold(I) substrate, and finally alkylation of the resultant aurate complex. The unexpected alternative and unique reaction products obtained in this investigation will be discussed in section 4.2.2.

³⁸ L.L. Garber and C.H. Brubaker, Jr, *J. Am. Chem. Soc.*, 1968, **90**, 309.

³⁹ R. Raap, *Can. J. Chem.*, 1971, **49**, 2139.

⁴⁰ J. C. Kauer and W. A. Sheppard, *J. Org. Chem.*, 1967, **32**, 3580.

⁴¹ Y. Satoh and N. Marcopulos, *Tetrahedron Lett.*, 1995, **36(11)**, 1759.



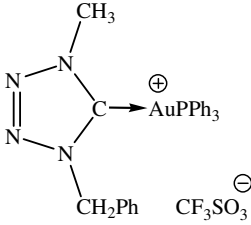
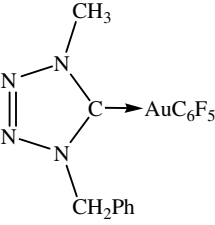
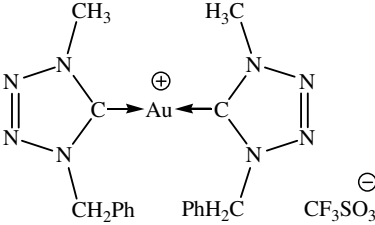
Scheme 4.4 The synthetic route towards mono- and bis(tetrazolylidene)gold(I) complexes; the counterion, CF_3SO_3^- , is omitted in cationic complexes.

A. Preparation of (1-benzyl-4-methyltetrazol-5-ylidene)(triphenylphosphine) gold(I) triflate, **28, (1-benzyl-4-methyltetrazol-5-ylidene)(pentafluorophenyl) gold(I), **29**, bis(1-benzyl-4-methyltetrazol-5-ylidene)gold(I) triflate, **30**.**

The cationic mono(carbene)gold(I) complex **28** was prepared by lithiation of 1-benzyltetrazole in thf with *n*-butyllithium at low temperature (-98°C), followed by the addition of $[\text{Au}(\text{C}_6\text{F}_5)(\text{tht})]$ and direct alkylation with $\text{CF}_3\text{SO}_3\text{CH}_3$ at -68°C . Although complex **28** could initially be isolated in microcrystalline form, it appeared unstable in solution and underwent a gradual homoleptic rearrangement. The rearrangement afforded the corresponding bis(carbene)gold(I) and bis(triphenylphosphine)gold(I) triflate complexes, and their formation, followed by ^1H NMR measurements is discussed in Section 4.2.4. Numerous attempts to recrystallise **28** only yielded the homoleptic by-products, and no X-ray single crystal structure analysis was carried out. Furthermore, in the solid state complex **28** is highly hygroscopic which ruled accurate elemental analysis out. The cationic complex is soluble in dichloromethane, acetone and thf, and insoluble in apolar solvents. The neutral mono(carbene)gold(I) complex **29** was prepared by treatment of a thf solution, containing lithiated 1-benzyltetrazole, with $[\text{Au}(\text{C}_6\text{F}_5)(\text{tht})]$ at -98°C . The aurate salt was not isolated but directly alkylated with $\text{CF}_3\text{SO}_3\text{CH}_3$ at low temperature. The neutral complex was extracted from residual product with a diethyl ether/*n*-pentane (1:1) mixture. The colourless microcrystalline material of complex **29** is thermodynamically stable in air at room temperature. Alternative reaction products were obtained using a different solvent system and will be discussed, together with examples of unique lithium coordination complexes, in section 4.2.2. The cationic bis(carbene)gold(I)

complex **30** was prepared in very much a similar fashion as described for **28** and **29**. The addition of half a molar amount of [AuCl(tht)] to a solution of 1-benzyltetrazol-5-yl lithium in thf at -98 °C afforded the corresponding aurate complex, which was directly alkylated with CF₃SO₃CH₃ at slightly elevated temperature (-68 °C) to yield complex **30** in high yield. An analytically pure sample of **30** could be obtained by the recrystallisation from a dichloromethane solution layered with *n*-pentane at -20 °C. The colourless needle-like crystals are thermodynamically stable in air at room temperature, and appeared very stable in solution. The formation of trace amounts of an isomeric product to **30** was confirmed by a ¹⁵N NMR investigation which will be discussed in section 4.2.2. The analytical data for complexes **28-30** are summarised in Table 4.1.

Table 4.1 Analytical data for complexes **28-30**

Complex			
	28	29	30
M.p(°C)	61-63	136-139	118-120 (decomp.)
Colour	colourless	colourless	colourless
Yield(%)	71	77	69
<i>M_r</i>	782.10	538.05	694.10
Analysis(%) [*]	not pure	not pure	C ₁₉ H ₂₀ AuF ₃ N ₈ O ₃ S
C			32.55 (32.86)
H			2.76 (2.90)
N			16.29 (16.14)

* Required calculated values given in parenthesis.

B. Spectroscopic characterisation of complexes **28-30**.

Nuclear magnetic resonance spectroscopy

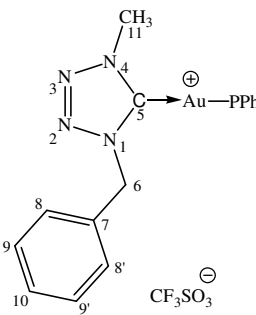
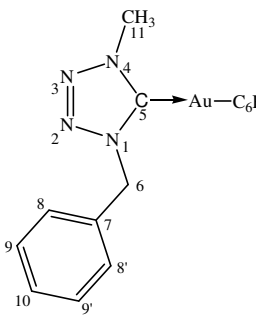
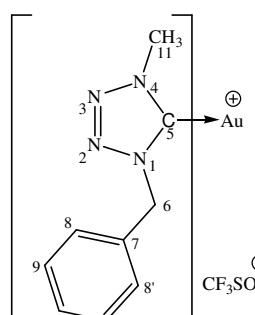
The ¹H, ¹³C{¹H}, ³¹P{¹H}, ¹⁹F and ¹⁵N NMR spectroscopic data for complexes **28-30** are summarised in Table 4.2.

In the ¹H NMR spectra of **28** and **30** the singlet signals at δ 4.26 and 4.36, respectively assigned to the three and six NMe protons in the cationic complexes, confirm the formation of carbene complexes. The corresponding resonance in **29** appears slightly

upfield at δ 3.85, in close agreement with that of (1,3-dimethylimidazol-5-ylidene)(pentafluorophenyl)gold(I) (δ 3.82).²⁶ The ^{13}C NMR spectra reveal characteristic NMe resonances for **28** (δ 38.7), **29** (δ 38.4) and **30** (δ 39.9).²⁶ The carbene carbon in **28** resonates as a sharp singlet at δ 180.6, and the phenyl carbons appear as uncharacteristic broad singlets, devoid of distinguishing C-P coupling patterns. This phenomenon is due to phosphine group exchange, during the homoleptic rearrangement of **28** in solution. In agreement, the ^{31}P NMR spectrum of this complex, reveals a broad singlet (δ 44.0) assigned to the nuclei in **28** and a sharp singlet (δ 31.1) for the homoleptic gold(I) product, bis(triphenylphosphine)gold(I) triflate. Further evidence, with regards to the formation of these by-products, is given in section 4.2.2. Well-defined singlet signals at δ 186.6 and δ 182.6, are assigned to the carbene carbons in **29** and **30**, respectively. These resonances are again in close agreement with reported values for the related complexes, (1,3-dimethylimidazol-5-ylidene)(pentafluorophenyl)gold(I) (δ 189.5) and bis(1,3-dimethylimidazol-5-ylidene)gold(I) chloride (δ 185.7).²⁶ The complex coupling patterns for the C_6F_5 ligand in **29** is well resolved, and the presence of the ligand is also confirmed by three sets of multiplet signals in the ^{19}F NMR spectrum.

The ^{15}N chemical shifts of the nitrogen atoms of **28** and **30** could be determined in a ^1H detected ^1H , ^{15}N gHMQC experiment. The shielded nitrogens, sp^3 hybridised N^1 and N^4 , appear at highest field for both complex **28** and **30**. Large downfield shifts are observed for N^1 in **28** ($\Delta\delta$ 21.7) and **30** ($\Delta\delta$ 20.0) with relation to the free ligand, 1-benzyltetrazole. In this regard, the most distinguishing difference is the pronounced upfield shift found for the N^4 resonance in both **28** ($\Delta\delta$ 81.8) and **30** ($\Delta\delta$ 83.2). This confirms that N^4 changes from an sp^2 to more of an sp^3 nucleus, and that electron density in the carbene complexes is mostly delocalised to the gold centre and adjacent onto N^4 nitrogen atoms.

Table 4.2 ^1H , $^{13}\text{C}\{^1\text{H}\}$, $^{31}\text{P}\{^1\text{H}\}$, ^{19}F and ^{15}N NMR spectroscopic data for **28-30**

Complex	 <p style="text-align: center;">28</p>	 <p style="text-align: center;">29</p>	 <p style="text-align: center;">30</p>
Solvent Temperature (°C) ^1H NMR (300 MHz) $^{13}\text{C}\{^1\text{H}\}$ NMR (75 MHz) ^{15}N NMR (61 MHz) ^{19}F NMR (376 MHz) $^{31}\text{P}\{^1\text{H}\}$ NMR (121 MHz)	CD ₂ Cl ₂ 25 H ⁶ 5.82 (s, 2H) H ⁸⁻¹⁰ 7.16-7.42 (m, 5H) H ¹¹ 4.36 (s, 3H) PPh 7.51-7.67 (m, 15H) C ⁵ 180.6 (s) C ⁶ 55.4 (s) C ⁷ 128.9 (s) C ⁸ , C ^{8'} 129.7 (s) C ⁹ , C ^{9'} 129.2 (s) C ¹⁰ 129.3 (s) C ¹¹ 38.70 (s) PPh-C ^{ipso} 129.4 (bs) PPh-C ^{ortho} 134.7 (bs) PPh-C ^{meta} 130.3 (bs) PPh-C ^{para} 129.3 (bs) C ₆ F ₅ -C ^{ipso} C ₆ F ₅ -C ^{ortho} C ₆ F ₅ -C ^{meta} C ₆ F ₅ -C ^{para} CF ₃ SO ₃ N ¹ -119.9 (s) N ² -11.2 (s) N ³ -11.5 (s) N ⁴ -132.5 (s) F ^{ortho} F ^{meta} F ^{para} P 44.0 (bs)	[CD ₃] ₂ CO 25 5.91 (s, 2H) 7.28-7.52 (m, 5H) 3.85 (s, 3H) 186.6 (s) 55.6 (s) 131.2 (s) 131.2 (s) 131.1 (s) 129.9 (s) 38.4 (s) 134.2 (tm, $J_{\text{C-F}} = 61.2$ Hz) 150.6 (dm, $J_{\text{C-F}} = 227.6$ Hz) 138.1 (dm, $J_{\text{C-F}} = 250.5$ Hz) 139.7 (dm, $J_{\text{C-F}} = 230.8$ Hz) 123.0 (q, $J_{\text{C-F}} = 320.9$ Hz)	[CD ₃] ₂ CO 25 5.96 (s, 2H) 7.41-7.56 (m, 5H) 4.36 (s, 3H) 182.6 (s) 56.7 (s) 130.8 (s) 131.4 (s) 131.0 (s) 131.3 (s) 39.9 (s) 123.6 (q, $J_{\text{C-F}} = 322.8$ Hz) -123.0 (s) -14.4 (s) -12.7 (s) -134.2 (s) -115.6 (m) -163.5 (m) -160.3 (m)

Mass spectrometry

The mass spectrum of neutral complex **29** exhibits a prominent molecular ion peak (m/z 538) as well as a diagnostic fragmentation peak at m/z 538, due to the loss of dinitrogen. No molecular ion peaks are detected for complexes **28** and **30**, however the cationic fragments are present at m/z 633 and m/z 545, respectively. In addition, the bis(tetrazole)-containing complex, **30**, reveals a step-wise loss of dinitrogen molecules (m/z 517 and m/z 489).

Table 4.3 Mass spectrometric data for **28-30**

Fragment	m/z (%)		
	28	29	30
{[M]} ⁺	-	538 (12)	-
{[M]-CF ₃ SO ₃ } ⁺	633 (2)		545 (7)
{[M]-CF ₃ SO ₃ -N ₂ } ⁺	-	510 (7)	517 (13)
{[M]-CF ₃ SO ₃ -2N ₂ } ⁺			489 (9)
{[M]-PPh ₃ } ⁺	371 (2)		
{AuPPh ₃ } ⁺	459 (15)		
{AuC ₆ F ₅ } ⁺		364 (2)	
{C ₁₂ F ₁₀ } ⁺		334 (15)	

C. X-ray structure determination of complex **30**.

The crystal and molecular structure of compound **30** (Figure 4.1) was determined by single crystal X-ray diffraction. Selected bond lengths and bond angles are summarised in Table 4.4, numbered according to the figure. Compound **30** crystallises in the orthorhombic space group, Pna2(1). The molecular structure of **30** embodies a two-coordinated, cationic bis(carbene) complex with the angle about the Au(I) centre approximately linear [C(21)-Au(1)-C(11) 177.3(3) Å]. The two planar coordinated tetrazole rings are only slightly twisted [torsion angles N(11)-C(11)-C(21)-N(21) and N(14)-C(11)-C(21)-N(21), respectively -6.6 ° and 174.4 °] in relation to each other, in agreement with the perfectly co-planar complex, bis(1,3-dimethylbenzimidazol-2-ylidene)gold(I) pentafluorophosphate²⁷ but in contrast to the larger interplanar angles of the dimeric bis(1-benzylimidazol-2-ylidene)gold(I) chloride [52.7 ° and 49.8 °]⁴² and bis(1,3-diethylbenzimidazol-2-ylidene)gold(I) pentafluorophosphate [52.96 °].²⁷ The Au(1)-C(11) and Au(1)-C(21) separations [2.035(7) Å and 2.001(7) Å respectively] are similar and correspond to Au(I)-NHC bonds in related compounds, bis(1-benzylimidazol-2-ylidene)gold(I) chloride [2.01(1) Å, 2.02(1) Å],⁴² (1,3-dimethylimidazol-5-ylidene)(1-

⁴² F. Bonati, A. Burini and B. R. Pietroni, *J. Organomet. Chem.*, 1989, **375**, 147.

methylimidazol-5-ylidene gold(I) triflate [1.99(1) Å, 2.00(2) Å],⁴³ bis(1,3-dimethylbenzimidazol-2-ylidene)gold(I) pentafluorophosphate [2.05(1) Å], bis(1,3-diethylbenzimidazol-2-ylidene)gold(I) pentafluorophosphate [2.02(1) Å] and bis(1-methylpyridin-2-ylidene)gold(I) chloride [2.03(2) Å, 2.02(2) Å].²⁷ It is worth noting that the N-N bond lengths of the tetrazole ring in **30** are consistent with lengths in the free ligand, 1-benzyltetrazole (see Chapter 3). The only notable difference occurs in the N(14)-C(11) and N(24)-C(21) bond lengths [1.36(1) Å and 1.34(1) Å, respectively], which are consistent with single bond lengths, in contrast to the related double bond length in the free ligand [1.315(8) Å]. The organisation in the crystal lattice, along the c-axis is shown in Figure 4.2, and best illustrates the π - π stacking of the phenyl and 5-membered rings of adjacent molecules (3.504 Å and 3.639 Å). The lack of intermolecular Au...Au interactions can partly be ascribed to the steric bulk of the triflate anion and the N1-benzyl substituent, which prevent a close approach of the metal centres. Bonati and co-workers⁴², reported that bis(1-benzylimidazol-2-ylidene)gold(I) chloride, aggregates as two independent molecules with Au...Au interactions [3.2630(5) Å]. In this instance, the benzyl moieties are in a *trans* configuration with regard to the Au(carbene)₂ core. This allows two chlorine ions to join the two cations through four hydrogen bond bridges. The organisation of the cations, however, is in agreement with the monomeric structure of (1,3-dimethylimidazol-5-ylidene)(1-methylimidazol-5-ylidene)gold(I) triflate, which has no aurophilic interactions.⁴³

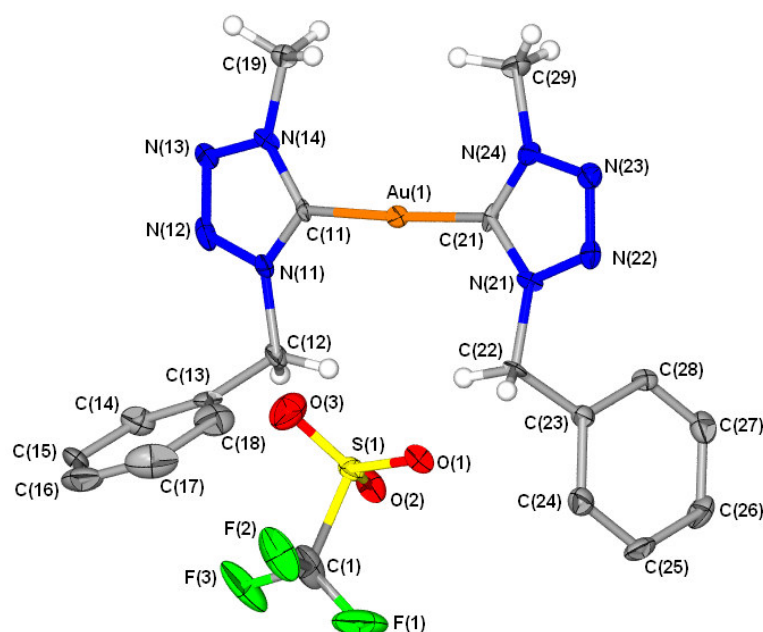


Figure 4.1 Molecular structure of **30** showing the numbering scheme; phenyl hydrogen atoms omitted for clarity.

⁴³ G. J. Kruger, P. J. Olivier, L. Lindeque and H. G. Raubenheimer, *Acta Cryst.*, 1995, **C51**, 1814.

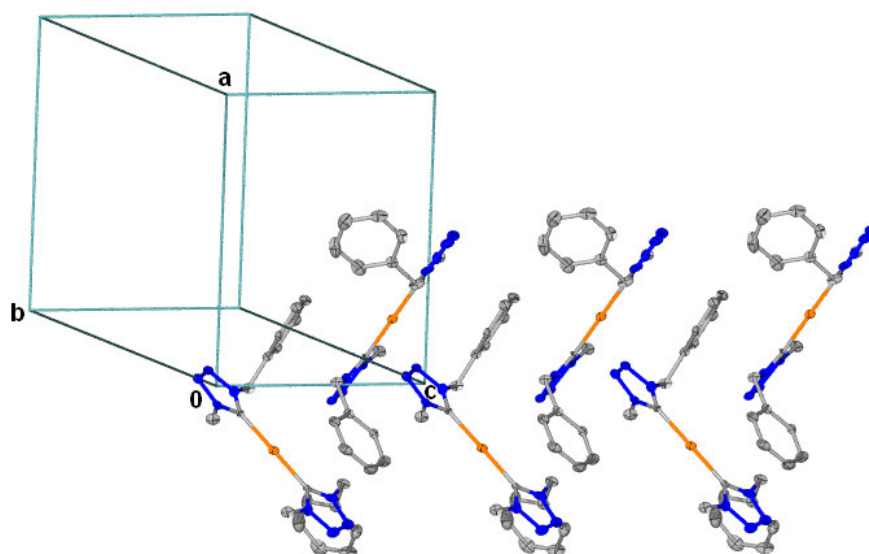


Figure 4.2 Unit cell and packing pattern along the *c*-axis in the crystal lattice of **30**, showing π - π interactions between the phenyl and tetrazole rings.

Table 4.4 Selected bond lengths (Å) and angles (°) for complex **30** with e.s.d.s in parenthesis

Bond lengths		Bond angles	
Au(1)-C(11)	2.035(7)	C(21)-Au(1)-C(11)	177.3(3)
Au(1)-C(21)	2.001(7)	N(11)-C(11)-N(14)	103.2(7)
C(11)-N(11)	1.31(1)	N(11)-C(11)-Au(1)	132.2(6)
C(11)-N(14)	1.36(1)	N(14)-C(11)-Au(1)	124.6(6)
N(11)-N(12)	1.35(1)	C(11)-N(11)-N(12)	112.1(7)
N(12)-N(13)	1.29(1)	C(11)-N(11)-C(12)	129.1(8)
N(13)-N(14)	1.36(1)	N(13)-N(12)-N(11)	107.4(7)
C(21)-N(21)	1.35(1)	N(12)-N(13)-N(14)	107.2(7)
C(21)-N(24)	1.34(1)	C(11)-N(14)-N(13)	110.2(7)
N(21)-N(22)	1.38(1)	C(11)-N(14)-C(19)	129.3(7)
N(22)-N(23)	1.28(1)	N(21)-C(21)-Au(1)	129.9(6)
N(23)-N(24)	1.37(1)	N(24)-C(21)-Au(1)	128.7(6)
		C(21)-N(21)-N(22)	111.2(7)
		C(21)-N(21)-C(22)	130.8(8)
		N(23)-N(22)-N(21)	107.9(7)
		N(22)-N(23)-N(24)	106.0(7)
		C(21)-N(24)-N(23)	113.5(6)

4.2.2 Unexpected reactions observed in the attempted preparation of carbene complexes derived from lithiated tetrazoles.

A still expanding involvement in transition metal carbene chemistry in our research group during the past two decades, has unearthed numerous atypical features for simple carbene complexes, especially with gold(I) as the central metal. The preparation and characterisation of an array of metal carbene complexes derived from lithiated heterocycles, mainly azoles, accompanied by unusual features exhibited, have been reported.²¹ In the following discussion, a further complement of unexpected results

obtained during the preparation of tetrazolyl and tetrazolylidene complexes of gold(I) derived from lithiated tetrazoles, is introduced.

4.2.2.1 Homoleptic rearrangement of mono(carbene)gold(I) complex, **28**.

The spontaneous rearrangement of carbene complexes of gold(I) containing mixed ligands have been described on a few occasions in the literature (Equation 4.10). Shaw and co-workers⁴⁴ found that for neutral gold(I) complexes of the type $[\text{Au}(\text{CN})\text{PR}_3]$, a ligand scrambling reaction occurs to afford ionic mixtures of by-products, namely $\text{Au}(\text{CN})_2^-$ and $\text{Au}(\text{PR}_3)_2^+$. Similar reactions occur for anionic gold(I) complexes of the type $[\text{Au}(\text{CN})\text{SR}]^-$ to yield the dicyanate and dithiolate gold(I) complexes.⁴⁵



Equation 4.10

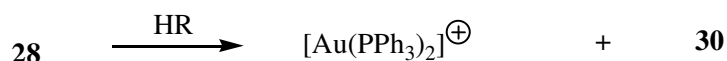
Within our research group, the preparation of bis(diamino)carbene complexes from $[\text{AuCl}(\text{PPh}_3)]$ or $[\text{Au}(\text{C}_6\text{F}_5)(\text{tbt})]$ and lithiated imidazole substrates, followed by alkylation or protonation has been investigated extensively, as a product of homoleptic rearrangement (HR).²⁶ In the instance when isothiazole is used as N-heterocyclic substrate in the neutral complex (pentafluorophenyl)(isothiazol-5-ylidene)gold(I), this rearrangement occurs slowly and can be followed by ¹H NMR.⁴⁶ It has been established that trace amounts of the rearranged product formed within days and that the reaction reached equilibrium after 18 days. This reaction occurred more rapidly for the precursor complex, (pentafluorophenyl)(isothiazol-5-yl)gold(I), which prompted an *in situ* carbene preparation by immediate alkylation to avoid complicating reactions. In contrast, (triphenylphosphine)(isothiazol-5-yl)gold(I) appears very stable in solution and could be isolated in pure form. However, subsequent alkylation of this product again afforded a mixture of ionic homoleptically-rearranged by-products.⁴⁶

In Chapter 2 the varying success obtained by using strongly bonded (azolyl)phosphine ligands, as ancillary ligands for mono(carbene)gold(I) complexes is described. Now the ligand rearrangement that occurs in the cationic (tetrazol-5-ylidene)complex **28**, which renders this complex unstable in solution (Equation 4.11, with counterions ignored) and affords **30** as one of the by-products will be discussed.

⁴⁴ A. L. Hormann, C. F. Shaw III, D. W. Benett and W. M. Reiff, *Inorg. Chem.*, 1986, **25**, 3953.

⁴⁵ G. Lewis and C. F. Shaw III, *Inorg. Chem.*, 1986, **25**, 58.

⁴⁶ H. G. Raubenheimer, M. Desmet and G. J. Kruger, *J. Chem. Soc., Dalton Trans.*, 1995, 2067.



Equation 4.11

Using the same methodology as described above, i.e. circumvention of the isolation of the (tetrazol-5-yl)aurate complex by immediate alkylation of the reaction product at low temperature (-78°C), a white microcrystalline solid was obtained, after the precipitation of the cationic product, **28**, with diethyl ether. However, ³¹P NMR analysis of the crystalline material revealed a broadened singlet signal at δ 44.05, typical of an exchanging phosphorus atom (Figure 4.3). Furthermore, crystallisation from the NMR tube, by slow evaporation of the solvent, afforded colourless crystals of [Au(PPh₃)₂][CF₃SO₃]. The phosphorus resonance at δ 31.80, assigned to this bis(phosphine) complex is in close agreement with the signal for [Au(PPh₃)₂]Cl at δ 29.71⁴⁷.

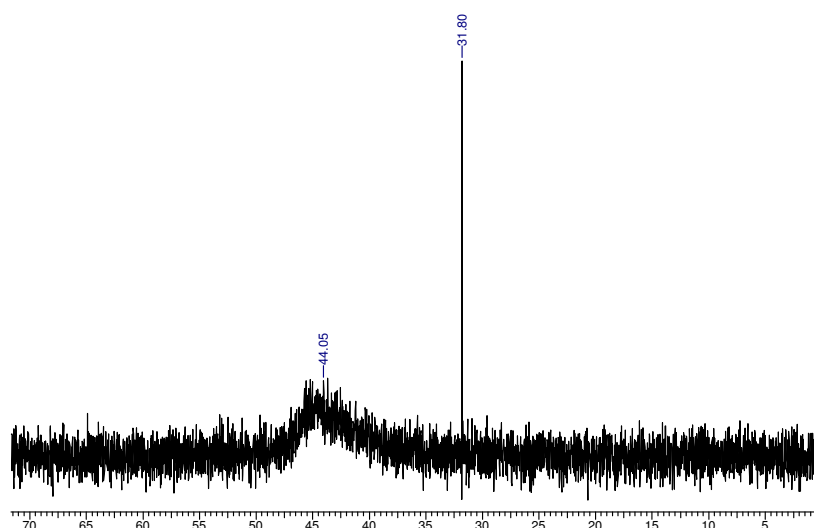


Figure 4.3 ³¹P NMR spectra of **28** showing a broadened singlet peak at δ 44.05, assigned to an exchanging phosphorus atom, and a sharp singlet peak at δ 31.80 assigned to the homoleptically rearranged product, [Au(PPh₃)₂]⁺.

The ¹⁵N chemical shifts of the nitrogen atoms in complex **28** were measured in a ¹H-detected ¹H, ¹⁵N gHMQC experiment in which a specified proton resonance could be used to locate coupling N atoms that are removed by two to three bonds. This spectrum thus represents not only signals pertaining to complex **28**, but also the homoleptic, rearranged product, **30**. Figure 4.4 shows two sets of four closely related nitrogen resonances, separated as shielded (alkyl substituted nitrogens) and deshielded (imine) nuclei. In each case the nitrogen atoms can be related to the proton (resonance) two or three bonds removed. Two further resonances are also noted, and they have been ascribed to the

⁴⁷ G. H. Woehrle, L. O. Brown and J. E. Hutchison, *J. Am. Chem. Soc.*, 2005, **127**, 2172.

possible formation of cyanamide compounds as products of ring fragmentation. In this instance the benzylic proton resonance is correlated to only the two remaining nitrogen atoms, after the loss of dinitrogen in the cyanamide product.

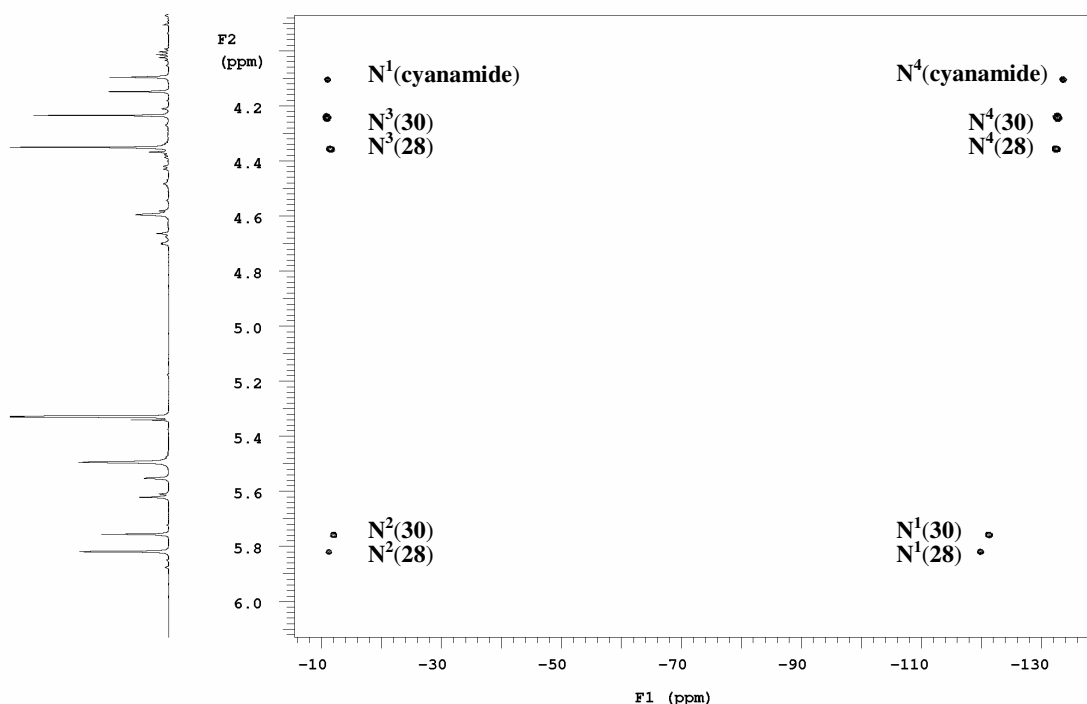


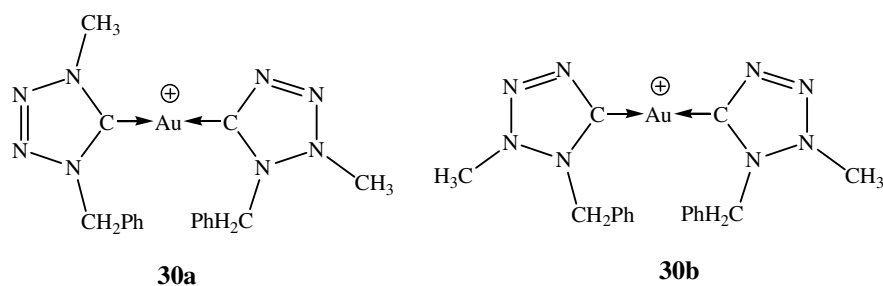
Figure 4.4 $^1\text{H},^{15}\text{N}$ gHMQC experiment of **28**, collected over a 24 h period in CD_2Cl_2 at ambient temperature; for **28** [δ -119.9 (N^1), δ -11.2 (N^2), δ -11.5 (N^3), δ -132.5 (N^4)] and **30** [δ -121.3 (N^1), δ -12.0 (N^2), δ -10.9 (N^3), δ -132.8 (N^4)].

4.2.2.2 Carbene complex formation by alkylation on a remote nitrogen atom, a ^{15}N NMR interpretation.

Members of our research group have shown that by using the lithiation-transmetallation-protonation route atypical Öfele-type carbene complexes can be prepared from precursors in which the nucleophilic heteroatom is located γ to the co-coordinated carbon atom and not in the conventional α -position.⁴⁸ The reaction of phenylpyrazol-5-yllithium, and $[\text{Fe}(\text{Cp})(\text{CO})_2\text{Cl}]$, followed by protonation, yields the amino(organo)carbene complex, (1-phenylpyrazol-5-ylidene)iron(I). This result represents a carbene complex formation mediated by a remote protonation on a nitrogen atom more than one bond removed from the metal-coordinated carbon atom. This procedure was extended to include complexes in which the nucleophilic heteroatom in the precursor substrate is located outside the coordinated ring and separated from the coordinated carbon by more than two bonds, in the preparation of organo(thio)carbene complexes, using various N-heterocyclic derivatised thienyl ligands.⁴⁸

⁴⁸ H. G. Raubenheimer, M. Desmet, P. Olivier and G. J. Kruger, *J. Chem. Soc, Dalton Trans.*, 1996, 4431.

In the preparation and structural characterisation of **30**, it was established that alkylation of the bis(1-benzyltetrazol-5-yl)gold(I) precursor complex on the N atom in the α position relative to the coordinated carbon is favoured above alkylation of the nitrogen atoms in the β positions. This elucidates the findings by Wehlan and co-workers³⁰, who reported that the protonation of sodium tetrakis(tetrazol-5-yl)aurate(III), affords a monocarbene complex by alkylation on one of the four tetrazole rings. This finding however could not be confirmed by either structural or ¹⁵N NMR analysis. ¹H NMR analysis of the reaction mixture of **30** revealed that trace amounts of secondary products, which share common diagnostic resonances, i.e. benzylic and NMe protons, with complex **30**, were present. Such by-products could arise from the alkylation of the nitrogen atom in the β position relative to the coordinated carbon, in very much a similar manner as was observed for carbene complexes derived from 1-phenylpyrazole, as a result of a conjugation across the heterocyclic system. We thus propose that apart from the major product **30**, secondary products **30a** and **30b** could form during this reaction, and that the related weaker auxiliary signals (Figure 4.5) can be assigned to **30a** and **30b** (Scheme 4.5). This is supported by the observation of three sets of four ¹⁵N resonances in the ¹H detected ¹H, ¹⁵N gHMQC experiment which was conducted using the reaction product. The respective carbene carbon resonances that should differ from those observed for complex **30**, were not clearly distinguishable in the ¹³C NMR and could not be assigned with certainty.



Scheme 4.5 The proposed alternative reaction products in the synthesis of complex **30**; the counterion, CF_3SO_3^- , is omitted in the cationic complexes.

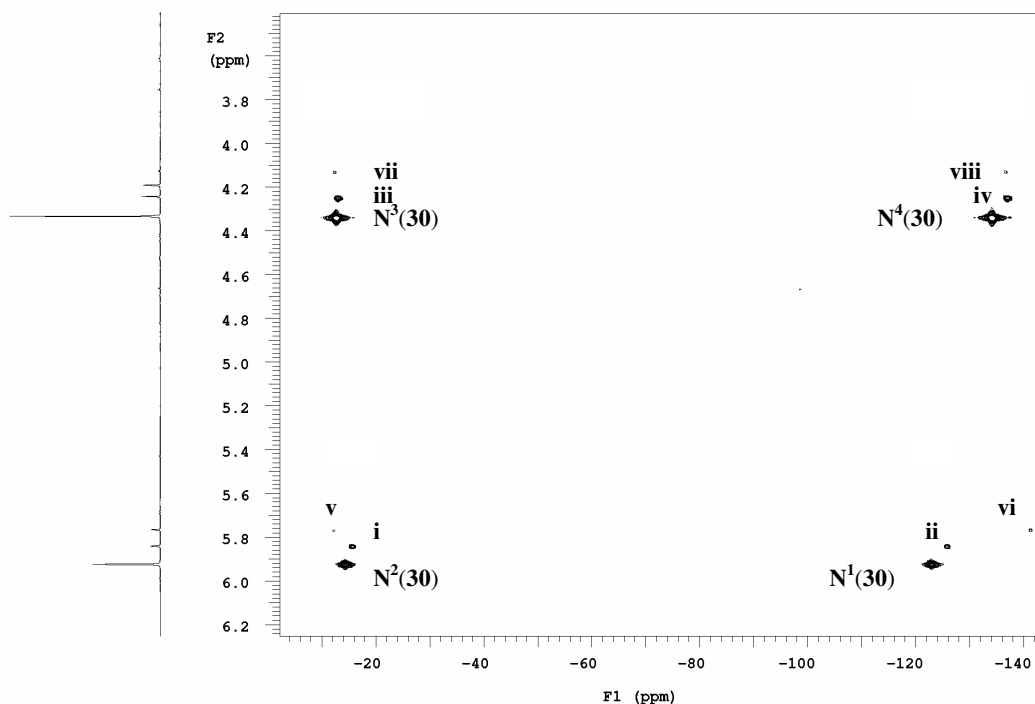
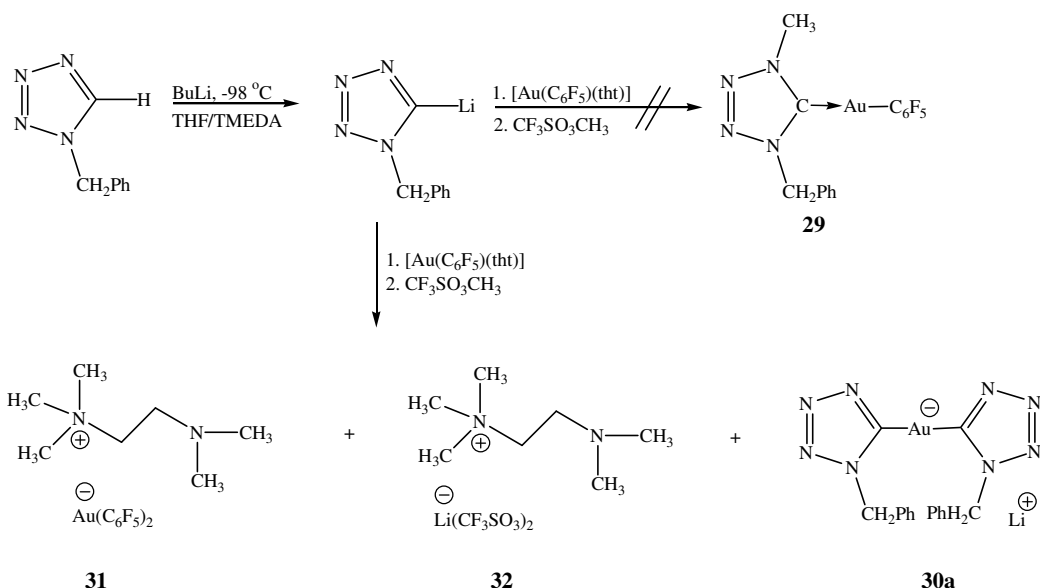


Figure 4.5 ^1H , ^{15}N gHMQC experiment of **30**, collected over a 24 h period in CD_2Cl_2 at ambient temperature; for **30** [δ -123.0 (N^1), δ -14.4 (N^2), δ -12.7 (N^3), δ -134.2 (N^4)] and weak signals for **30a** or **30b** [δ -15.7 (i), δ -125.9 (ii), δ -13.1 (iii), δ -137.0 (iv), δ -12.2 (v), δ -141.3 (vi), δ -12.4 (vii), δ -136.7 (viii)].

4.2.2.3 Homoleptic rearrangement of a gold(I) aurate complex, in the presence of an ammonium salt.

Satoh and Marcopulos in their investigation of 5-substituted tetrazoles, found that by the addition of a 10 % tetramethylethylenediamine (TMEDA) solution in thf to the lithiated substrates, the reactive intermediates are stabilised and very few by-products are formed in the subsequent electrophilic addition reactions.⁴¹ The effect of an electron donor solvent or additive is to reduce the electron deficiency of the reagents, and enhances both their nucleophilicity and their basicity and promotes metallation of the acidic azole substrates. The treatment of 1-benzyltetrazole with *n*-BuLi at -98 °C, in TMEDA-thf solutions instead of pure thf, resulted in the formation of a clear orange solution with regioselective lithiation evident from the absence of products arising from deprotonation of benzylic or aromatic protons. Using the same methodology employed for the preparation of mono(carbene)gold(I) complex, **29**, but with the addition of a 10 % TMEDA solution in thf, an alternative product spectrum to the one previously described (Scheme 4.6) was obtained.



Scheme 4.6 Alternative reaction products obtained in the presence of an ammonium salt. The counterions, CF_3SO_3^- and Li^+ are not shown.

Crystallisation of the solid material from a dichloromethane solution layered with *n*-pentane, afforded stable colourless crystals of **31** and fragile colourless crystals of **32**. The latter crystals appeared very brittle, and rapidly lose morphology when stored in hydrocarbon oil. The formation of **30a** and indeed whether this anionic complex is stable in solution, could not be confirmed. However distinctive signals in the ^1H and ^{13}C NMR, that are comparable to resonances reported for the analogous carbene complex **30** and the isolable compound **A** (*vide infra*), suggests that **30a** could be a product of homoleptic rearrangement. Furthermore, although the nucleophilicity of the azole nitrogen atoms in the precursor aurate complex to **29**, may be comparable to those in the aliphatic tertiary amine in TMEDA, the latter is present in an overwhelming excess and alkylation would have been favoured on the TMEDA molecule. The separation of the mixture of ionic complexes was extremely difficult and analytically pure samples could not be obtained for analysis.

As mentioned previously, a second unique lithium coordination complex, [Li(triflate)(diethylether)] **33** closely related to **32**, was isolated from the initial reaction mixtures of complex **29** (see section 4.2.1), and is discussed here. Although, the work-up procedure entails the removal of these lithium salts, their partial solvation by thf allows for trace amounts to be co-extracted with the reaction products. Subsequent crystallisation from dichloromethane solutions layered with diethyl ether afforded an interesting self-assembly of lithium salt and solvent. The colourless crystals displayed a similar plate-like morphology to complex **32**, and became opaque after only a few minutes when stored in

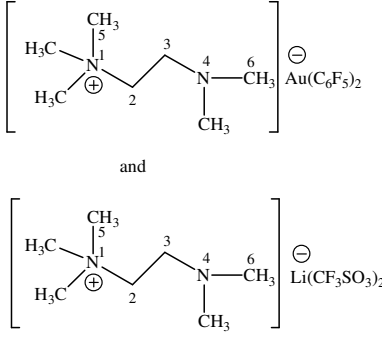
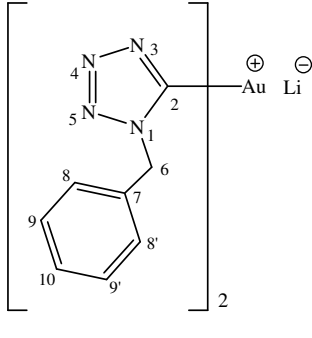
hydrocarbon oil at room temperature, presumably due to the loss of diethyl ether molecules from the crystal lattice.

A. Spectroscopic characterisation of complexes **30a**, **31** and **32**.

Nuclear magnetic resonance spectroscopy

The ^1H , $^{13}\text{C}\{^1\text{H}\}$ and ^{19}F NMR spectroscopic data for complexes **30a**, **31** and **32** are summarised in Table 4.5. Note that, both alkylated TMEDA cations (TMEDAMe), present in **31** and **32**, appear non-interactive to the anions in the respective crystal lattices.

Table 4.5 ^1H , $^{13}\text{C}\{^1\text{H}\}$ and ^{19}F NMR spectroscopic data for **30a**, **31** and **32**

Complex	 <p style="text-align: center;">31 and 32</p>	 <p style="text-align: center;">30a</p>
Solvent Temperature (°C) ^1H NMR (400 MHz) $^{13}\text{C}\{^1\text{H}\}$ NMR (101 MHz) ^{19}F NMR (376 MHz)	CD ₂ Cl ₂ 25 3.44 (t, 2H, $J = 5.75$ Hz.) 2.70 (m, 2H) 3.22 (s, 9H) 2.23 (s, 6H) PPh C ² 63.1 (s) C ³ 54.4 (s) C ⁵ 54.3 (s) C ⁶ 45.0 (s) C ⁷ C ⁸ , C ^{8'} C ⁹ , C ^{9'} C ¹⁰ C ₆ F ₅ -C ^{ipso} 128.7 (t, $J_{\text{CF}} = 52.9$ Hz) C ₆ F ₅ -C ^{ortho} 149.2 (ddm, $J_{\text{CF}} = 223.0$ Hz, $J_{\text{CF}} = 24.1$ Hz) C ₆ F ₅ -C ^{meta} 137.3 (dm, $J_{\text{CF}} = 270.1$ Hz) C ₆ F ₅ -C ^{para} 138.0 (dm, $J_{\text{CF}} = 248.3$ Hz) CF ₃ SO ₃ 121.1 (q, $J_{\text{CF}} = 320$ Hz) F ^{ortho} -121.5 (m) F ^{meta} -169.1 (m) F ^{para} -167.7 (t, $J = 19.9$ Hz) CF ₃ SO ₃ -84.3 (s)	CD ₂ Cl ₂ 25 5.68 (s, 4H) 7.19-7.31 (m, 10H) 184.9 (s) 63.1 (s) 137.3 (s) 128.8 (s) 128.9 (s) 128.2 (s)

The ^1H NMR spectrum of the product mixture, exhibits a singlet resonance at δ 5.68, which integrating for two protons and assignable to the benzylic protons; in agreement a

multiplet in the aromatic region is assigned to five phenyl protons (δ 7.26), of the (tetrazolyl)aurate complex **30a**. Upfield, strong singlet signals at δ 2.23 and δ 3.22 for NMe_2 (H^6) and $^+\text{NMe}_3$ (H^5) respectively, a multiplet δ 2.70 (H^3) and a triplet signal δ 3.44 (H^2), pertaining to the ethylene bridge protons, confirms the alkylation of TMEDA that features as counterions in both complex **31** and **32**.

The ^{13}C NMR spectroscopic data further confirm the presence of the tetrazole-containing gold(I) complex with strong singlet resonances at δ 63.1 and δ 184.9, for the benzylic and metal-coordinated carbon atoms. The chemical shift of the latter nucleus is in close agreement with the gold-coordinated carbon atom in the analogous, bis(1-methylimidazol-2-yl)aurate(I) complex (δ 185.8)²⁶ and appears slightly downfield from the carbene-carbon atom resonance in **30** (δ 182.6). A quartet signal at δ 121.1 ($J_{\text{CF}} = 320$ Hz) is assigned to the triflate counterion in compound **32**. Strong C-F coupling multiplets are exhibited for the four inequivalent phenyl carbon atoms, complemented by three sets of multiplet signals for the aromatic F-F coupling in ^{19}F NMR. The resonances assigned to the pentafluorophenyl groups (δ -121.5, -167.7 and -169.1) integrate for five fluorine atoms, in agreement to the sharp singlet resonance at δ -84.3 assigned to the six fluorine atoms in the two triflate molecules (coordinated to the lithium atoms in the solid state) of complex **32**.

B. X-ray structure determination of complexes 31-33.

The crystal and molecular structures of compounds **31**, **32** and **33** were determined by single crystal X-ray diffraction. The molecular structure of **31** is depicted in Figure 4.6 and selected bond lengths and bond angles are summarised in Table 4.6, numbered according to the figure. Complex **31** crystallises in the monoclinic space group $\text{P2}_1/\text{c}$ as colourless needle-like crystals. It is composed of non-interacting bis(pentafluorophenyl)gold(I) anions and 2-dimethylamino(ethylene)trimethylammonium (TMEDAMe^+) cations. The geometry about the central metal atom is approximately linear, [$\text{C}(11)\text{-Au}(1)\text{-C}(21)$ $179.31(16)^\circ$] with typical Au-C bonds [$\text{Au}(1)\text{-C}(11)$ $2.044(5)$ Å and $\text{Au}(1)\text{-C}(21)$ $2.046(5)$ Å]. Both these structural parameters are in agreement with bond lengths and angles in related compounds, reported in the literature and in this dissertation, e.g. **20** [$177.8(2)$ Å, $2.047(7)$ Å and $2.057(7)$ Å] [compare also (imine)(pentafluorophenyl)gold(I) complexes **16-19**].

The quaternary ammonium cation appears to dictate the ordering within the crystal lattice and the aurate molecules are prevented from intermolecular interaction, by the interdispersed bulky cations (Figure 4.7). The planes of the pentafluorophenyl substituents approaches co-planarity [torsion angles at 32.0°], which differ from the angles between the aryl planes of the homoleptic, rearranged products in [bis(*o*-phenylene)bis(dimethylarsine)gold(I) bis(pentafluorophenyl)gold(I) [$\sim 0^\circ$] ⁴⁹ and bis(pentafluorophenyl)gold(I) tetra-N-butyl-ammonium [81.1(4)] but are almost identical to **20** [32.7°].⁵⁰

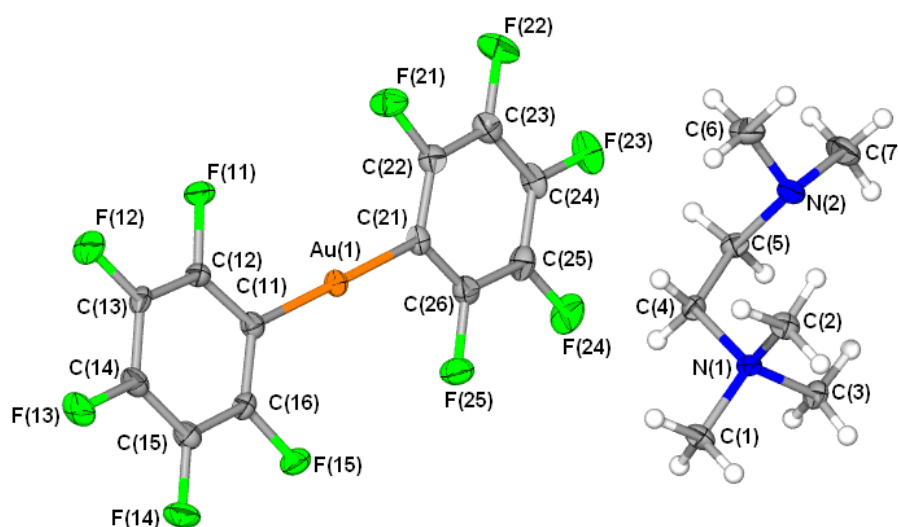


Figure 4.6 Molecular structure of **31** showing the numbering scheme.

Table 4.6 Selected bond lengths (Å) and angles (°) for complex **31** with e.s.d.s in parenthesis

Bond lengths		Bond angles	
Au(1)-C(11)	2.044(5)	C(11)-Au(1)-C(21)	179.3(2)
Au(1)-C(21)	2.046(5)	C(16)-C(11)-C(12)	113.1(4)
N(1)-C(3)	1.498(5)	C(16)-C(11)-Au(1)	124.0(3)
N(1)-C(1)	1.510(5)	C(12)-C(11)-Au(1)	122.9(3)
N(1)-C(2)	1.510(5)	C(3)-N(1)-C(4)	111.4(3)
N(1)-C(4)	1.518(5)	C(1)-N(1)-C(4)	108.2(3)
N(2)-C(7)	1.456(6)	C(7)-N(2)-C(5)	110.6(3)
N(2)-C(5)	1.468(5)	C(5)-N(2)-C(6)	110.8(3)
N(2)-C(6)	1.474(5)	C(5)-C(4)-N(1)	116.0(3)
C(4)-C(5)	1.517(6)	N(2)-C(5)-C(4)	115.4(3)

⁴⁹ R. Usón, A. Laguna, J. Vicente, J. Garcia, P. G. Jones and G. M. Sheldrick, *J. Chem. Soc., Dalton Trans.*, 1981, 655.

⁵⁰ P. G. Jones, *Z. Kristallogr.*, 1993, **208**, 347.

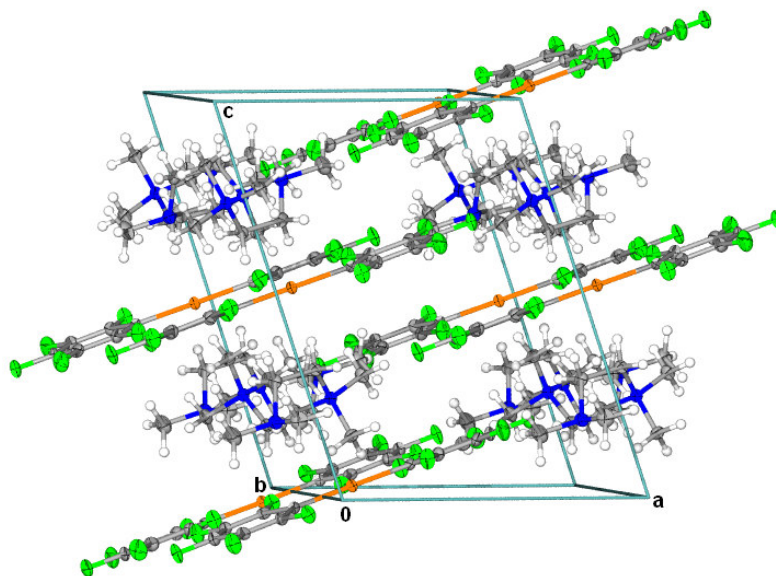


Figure 4.7 Unit cell and packing pattern viewed along the b-axis in the crystal lattice of **31**.

The molecular structure of **32**, is shown in Figure 4.8 and selected bond lengths and bond angles are summarised in Table 4.7, numbered according to the figure. Compound **32** crystallises in the monoclinic space group $P2_1/c$ as colourless needle-like crystals. The molecular structure consists of one Li^+ cation, two triflate anions and one non-interacting (TMEDAMe^+) cation in the asymmetric unit. The Li^+ cations are coordinated to four different triflate anions through oxygen atoms. The triflate anions are further coordinated in a bidentate fashion to a secondary Li^+ cation, to form a chain-like structure (Figure 4.9). Hence, two bidentate triflate anions, link two Li^+ cations to create the links of an eight-membered, dinuclear heterometallacycle. The remnants of the two triflate anions ($-\text{CF}_3$ groups) are arranged in an up and down fashion across the coordination centre, to impose an almost chair-like conformation on the cyclic substructure. The pseudo-tetrahedral geometry about the Li^+ cations propagates, through a centre of inversion, a true chain-like polymeric arrangement. These one-dimensional polymeric chains are flanked by TMEDAMe^+ cations, which are evenly dispersed in the crystal lattice (Figure 4.10). Surprisingly, the coordination of pure Li^+ -cations to triflate anions are not that common. A related structures reported by Henderson *et al.*,⁵¹ [$\text{Li}_2(\text{triflate})_2(\text{diglyme})$], contain both four and five coordinate Li^+ cations and triflate and triflate-diglyme anions that similarly form polymeric chains. The only other closely related structure are [$\text{Li}(\text{triflate})(\text{diglyme})$] and [$\text{Li}(\text{triflate})(\text{polyethylene-oxide})_3$], which show similar bidentate coordination to triflate anions but are additionally stabilised by oxygen coordinated ether.⁵²

⁵¹ W. A. Henderson, V. G. Young Jr, N. R. Brooks and W. H. Smyrl, *Acta Cryst.*, 2002, **C58**, m501.

⁵² C. P. Rhodes and R. Frech, *Macromolecules*, 2001, **34**, 2660.

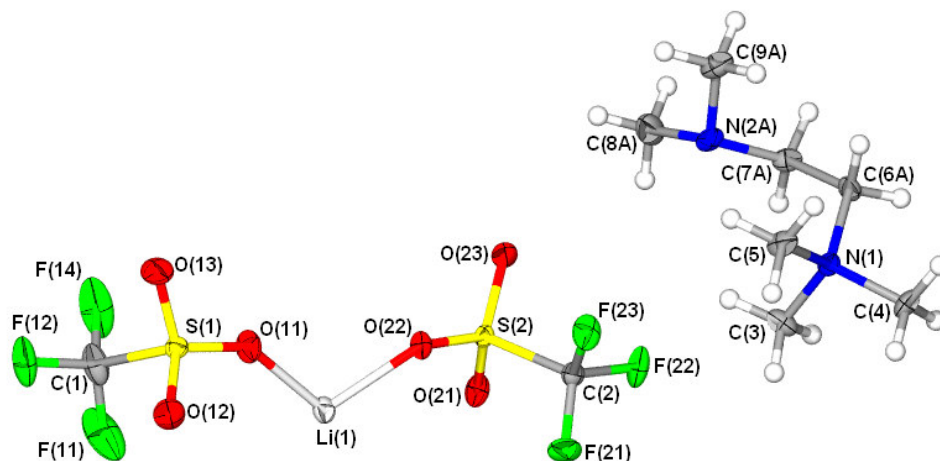


Figure 4.8 Molecular structure of **32** showing the asymmetric unit numbering scheme.

The Li-O bonds and angles are similar and comparable to those found in the four coordinate moieties of [Li(triflate)(diglyme)] and [Li₂(triflate)₂(diglyme)].⁵¹ However, the O-Li-O angles differ significantly from the ideal tetrahedral 109.5° angle [102.0(2)-119.4(3)°] and from the regular tetrahedral geometry observed for [Li₂(triflate)₂(diglyme)] with the largest deviation from this ideal geometry found in the angles, O(12)-Li(1)-O(11), O(21)-Li(1)-O(11) and O(22)-Li(1)-O(11), at 119.4(3), 102.0(2) and 105.2(2), respectively, has a lengthening of the Li(1)-O(11) bond [1.952(5) Å] to effect compared to other Li-O bond lengths [Li(1)-O(12) 1.919(5) Å, Li(1)-O(21) 1.932(5) Å and Li(1)-O(22) 1.939(5) Å].

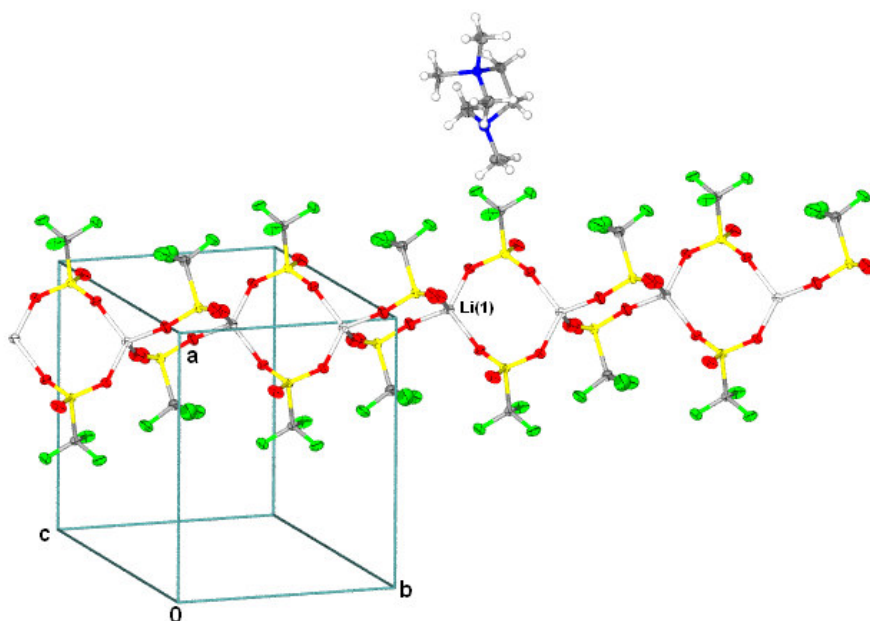


Figure 4.9 Unit cell and packing pattern along the c-axis in the crystal lattice of **32**, showing the chain-like linkage of the chelated lithium ions.

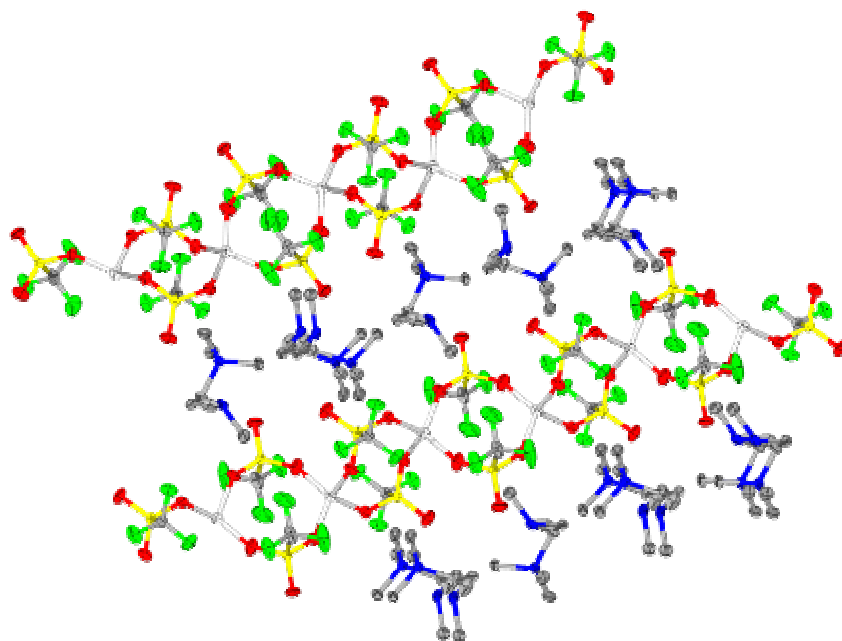


Figure 4.10 Unit cell and packing pattern of crystalline **32**, which shows the location of the cations dispersed between the rows of anions.

Table 4.7 Selected bond lengths (Å) and angles (°) for complex **32** with e.s.d.s in parenthesis

Bond lengths		Bond angles	
Li(1)-O(12)	1.919(5)	O(13)-S(1)-O(12)	14.1(1)
Li(1)-O(21)	1.932(5)	O(13)-S(1)-O(11)	113.7(1)
Li(1)-O(22)	1.939(5)	O(12)-S(1)-C(1)	103.6(2)
Li(1)-O(11)	1.952(5)	O(11)-S(1)-C(1)	104.4(1)
S(1)-O(13)	1.429(2)	C(3)-N(1)-C(4)	108.1(2)
S(1)-O(12)	1.432(2)	C(3)-N(1)-C(5)	109.6(2)
S(1)-O(11)	1.440(2)	C(4)-N(1)-C(5)	108.8(2)
S(2)-O(23)	1.428(2)	O(12)-Li(1)-O(21)	110.6(2)
S(2)-O(21)	1.444(2)	O(12)-Li(1)-O(22)	108.0(2)
S(2)-O(22)	1.445(2)	O(21)-Li(1)-O(22)	111.5(2)
		O(12)-Li(1)-O(11)	119.4(3)
		O(21)-Li(1)-O(11)	102.0(2)
		O(22)-Li(1)-O(11)	105.2(2)

The molecular structure of **33**, is shown in Figure 4.11 and selected bond lengths and bond angles are summarised in Table 4.8, numbered according to the figure. Compound **33** crystallises in the monoclinic space group $C2/c$ as colourless needle-like crystals. The molecular structure consists of a Li^+ cation, triflate anion and equimolar amount of an interacting diethyl ether molecule. The Li^+ cations are coordinated to three different triflate anions through oxygen atoms, and the oxygen atom of a diethyl ether molecule occupies the fourth coordination site. Each triflate anion is tridentately coordinated to three different Li^+ cations, to again furnish a one dimensional polymeric chain, consisting in this instance of rectangular eight-membered metallacycles. Adjoining approximate rectangular links share an axis, which alternates to form the longest and shortest side of a

near rectangle (Fig 4.12a). This affords a staircase architecture to the polymeric structure, i.e. the cycles as steps and the remnants of the triflate and diethyl ether molecules the balustrade of the staircase.

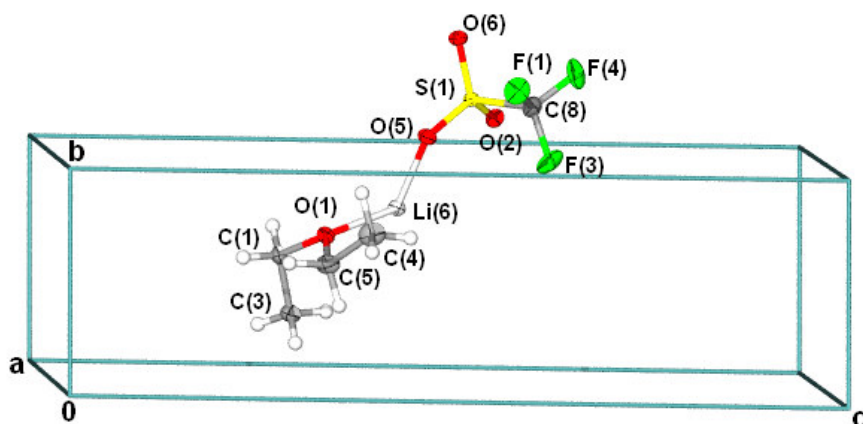


Figure 4.11 Molecular structure of **33** showing the asymmetric unit numbering scheme.

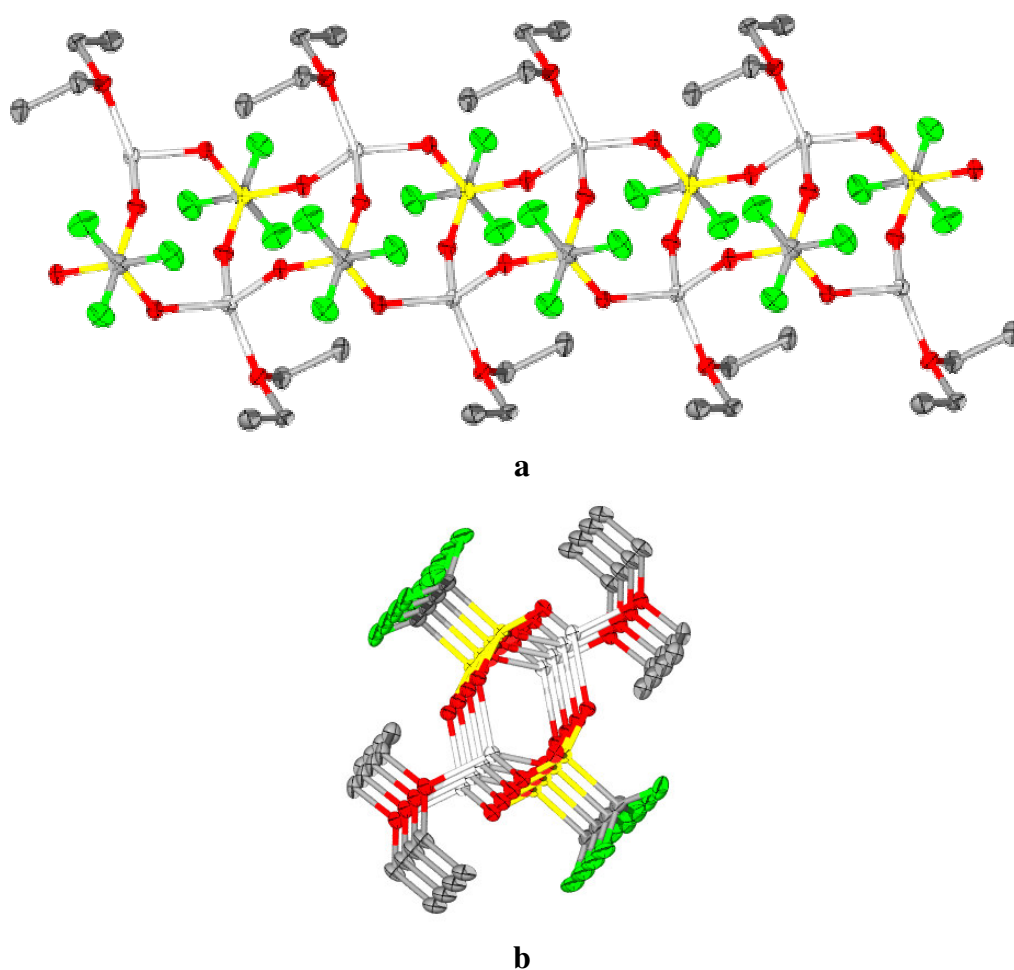


Figure 4.12 Molecular structure of **33** showing **a)** the staircase type polymeric structure, and **b)** the view along the channel created by the eight membered rings, propagated by translation in b-axis.

This example of a Li⁺ cation coordination is closely related to [diglyme(triflate)₂Li₂], which also features tridentate triflate coordination of the Li⁺ cations there replaced by five coordinate Li⁺ cations featuring a tridentate coordination of a diglyme molecule.⁵¹ The crystal structure of **33** contains one inversion centre located on the centroid of the eight membered ring, which joins two two-coordinate Li(ether)(triflate) fragments together. Infinite polymeric chains, connected by an inversion centre, create channels composed of eight membered rings along the b-axis (Fig 4.12b). The Li-O bonds are similar and comparable to those found in the **32**, and the four coordinate moieties of [Li(triflate)(diglyme)] and [Li₂(triflate)₂(diglyme)].⁵¹ However, in contrast to **33**, but in agreement with [Li₂(triflate)₂(diglyme)], the O-Li-O angles approach an ideal tetrahedral geometry with angles not deviating more than 5°, [105.56(1)-114.6(1)°] from 109.5°.⁵¹

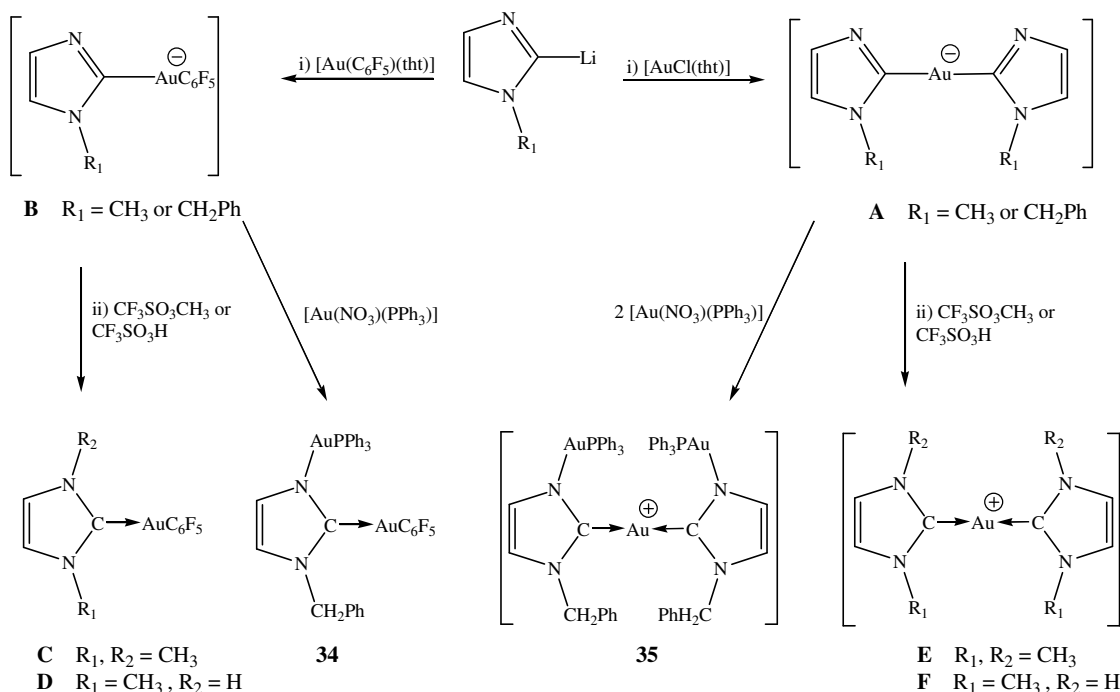
Table 4.8 Selected bond lengths (Å) and angles (°) for complex **33** with e.s.d.s in parenthesis

Bond lengths		Bond angles	
S(1)-O(2)	1.439(1)	O(2)-S(1)-O(5)	114.75(6)
S(1)-O(5)	1.441(1)	O(2)-S(1)-O(6)	115.02(6)
S(1)-O(6)	1.44(1)	O(5)-S(1)-O(6)	114.65(6)
O(2)-Li(6)	1.938(3)	S(1)-O(2)-Li(6)	136.0(1)
O(5)-Li(6)	1.936(3)	S(1)-O(5)-Li(6)	128.0(1)
O(6)-Li(6)	1.923(3)	S(1)-O(6)-Li(6)	144.5(1)
O(1)-Li(6)	1.947(3)	C(5)-O(1)-Li(6)	120.3(1)
		C(1)-O(1)-Li(6)	118.52(1)
		O(6)-Li(6)-O(5)	106.7(1)
		O(6)-Li(6)-O(2)	107.6(1)
		O(5)-Li(6)-O(2)	110.7(1)
		O(6)-Li(6)-O(1)	111.9(1)
		O(5)-Li(6)-O(1)	114.3(1)
		O(2)-Li(6)-O(1)	105.6(1)

4.2.2.4 Reactions of AuPPh₃⁺ cations and nucleophilic aurate complexes: Reactions towards bi and trinuclear (diamino)carbene complexes of gold(I).

The synthesis and characterisation of neutral and cationic (diamino)carbene complexes of gold(I) derived from lithiated imidazole substrates, has received much attention within our research group.^{21,26} Reaction of 1-methylimidazol-2-yl lithium with [AuCl(tht)], affords the bis(1-methylimidazol-2-yl)aurate complex, **A**. Reaction of the same lithiated azole with [Au(C₆F₅)(tht)] yields the mono(imidazol-2-yl)(pentafluorophenyl)aurate, **B**, (Scheme 4.7). Where the anionic bis(imidazolyl)gold(I) complex is isolable as a lithium salt, the mono(imidazolyl) complex spontaneously rearranges to form homoleptic gold(I) complexes. However, by *in situ* alkylation or protonation of **B**, with CF₃SO₃CH₃ or CF₃SO₃H, the mono(diaminocarbene)gold(I) complexes, **C** and **D** are formed.²⁶ Similarly,

by protonation or alkylation of **A**, the related bis(carbene)gold(I) complexes, **E** and **F** are obtained. The question that arose from this, is whether the electrophilic additions of isolobal equivalents to H^+ and CH_3^+ such as $AuPPh_3^+$, could indeed effect carbene complex formation from lithium aurate precursor complexes?

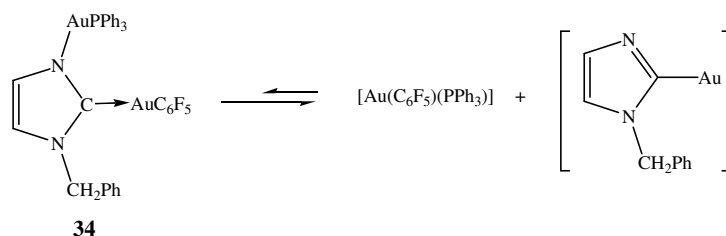


Scheme 4.7 The synthetic route towards bi and trinuclear (diamino)carbene complexes of gold(I); the counterions $CF_3SO_3^-$ and Li^+ are omitted.

An investigation into the preparation of di and tri-nuclear gold(I) complexes, **34** and **35**, further explored a central theme of introducing a multitude of metal centers onto gold(I)-coordinated nitrogen-rich heterocycles. Furthermore, the reactivity of imine coordination sites, in both aurate complexes were probed, to ultimately afford compounds featuring metal centers with different ligand coordination. Our final aim was to use the methodology developed up to this stage, to increase the metal to ligand ratio but simultaneously to retain the solubility of the compounds. Different synthetic routes were investigated towards such compounds with tetrazoles as substrates. The first entailed the derivatisation of (1-tetrazolyl)(triphenylphosphine)gold(I), **24**. Lithiation of this complex in the C^5 position was envisaged, followed by transmetalation and ligand substitution yielding a trinuclear-gold tetrazole compound. The alkylation of this compound could furnish a tetrazolyl carbene complex containing three gold(I)-centres. The unstable nature of the resultant product obtained upon lithiation of **24**, however, prompted the development of an alternative method that circumvents the formation of the lithiated tetrazolyl gold complex, by introducing the secondary metal center at a later stage in the reaction as a metallating reagent.

A. Preparation of [3-(triphenylphosphine)gold(I)-1-benzylimidazol-5-ylidene][pentafluorophenyl]gold(I), **34, bis[3-(triphenylphosphine)gold(I)-1-benzylimidazol-5-ylidene]gold(I) nitrate, **35**.**

The addition of an equimolar amount of $[\text{Au}(\text{NO}_3)(\text{PPh}_3)]$, at low temperature ($-78\text{ }^\circ\text{C}$) to (1-benzylimidazol-2-yl)(pentafluorophenyl)aurate, afforded a mixture of predominantly binuclear complex **34** and a rearranged by-product, $[\text{Au}(\text{C}_6\text{F}_5)(\text{PPh}_3)]$. Although these two compounds were of fairly similar polarity, extraction with *n*-hexane of the dried reaction mixture obtained, afforded $[\text{Au}(\text{C}_6\text{F}_5)(\text{PPh}_3)]$ exclusively. However, dissolution of **34** in diethyl ether or dichloromethane, led to slow and continuous formation of the by-product. It is likely that although complex **34** forms as the major product of the reaction, this complex is unstable in solution rearrange to form $[\text{Au}(\text{C}_6\text{F}_5)(\text{PPh}_3)]$. It was not established whether the rearrangement stops at an equilibrium position (Equation 4.12).



Equation 4.12

Spectral characterisation by ^1H , $^{13}\text{C}\{^1\text{H}\}$ and $^{31}\text{P}\{^1\text{H}\}$ NMR and ESI-MS analysis of the product residue confirmed the presence of both species. Stable $[\text{Au}(\text{C}_6\text{F}_5)(\text{PPh}_3)]$ crystallises readily but its molecular structure is known.⁵³

The addition of two molar equivalents of $[\text{Au}(\text{NO}_3)(\text{PPh}_3)]$ to bis(1-benzylimidazol-2-yl)aurate, at low temperature ($-78\text{ }^\circ\text{C}$), produced a colourless microcrystalline product that contains of largely $[\text{Au}(\text{NO}_3)(\text{PPh}_3)]$ and small amounts of the bis(carbene) complex **35**. This result is in agreement with a previous attempt to prepare **35**, which furnishes large quantities of $[\text{AuCl}(\text{PPh}_3)]$, presumably an ion exchange product of the electrophilic AuPPh_3^+ species and LiCl (a by-product of transmetallation). The addition of a molar equivalent of AgBF_4 as a chlorine scavenger to rid the solution of chlorine atoms, and prevent the formation of the gold phosphine halide, circumvented this side reaction. However, although a $^{31}\text{P}\{^1\text{H}\}$ NMR revealed the presence of two phosphine containing products the bulk of the species in solution consisted of $[\text{Au}(\text{NO}_3)(\text{PPh}_3)]$. Spectral characterisation by ^1H , $^{13}\text{C}\{^1\text{H}\}$ NMR and ESI-MS established the presence of both

⁵³ R. W. Baker, P. J. Pauling, W. Ramsay and R. Forster, *J. Chem. Soc., Dalton Trans.*, 1972, 2264.

products, with single crystal X-ray diffraction confirming the presence of $[\text{Au}(\text{NO}_3)(\text{PPh}_3)]$.

B. Spectroscopic characterisation of complexes **34** and **35**.

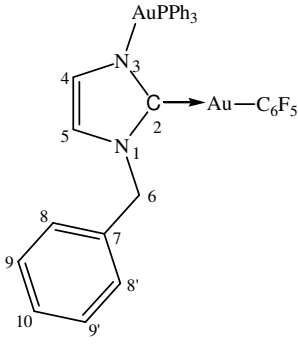
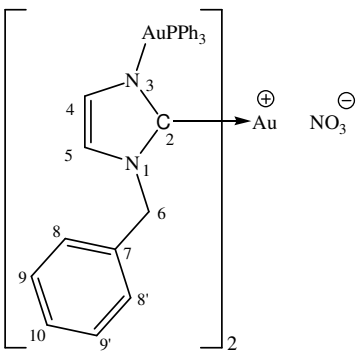
Nuclear magnetic resonance spectroscopy

The ^1H , $^{13}\text{C}\{^1\text{H}\}$, $^{31}\text{P}\{^1\text{H}\}$ NMR spectroscopic data for complexes **34** and **35** are summarised in Table 4.9.

In the ^1H NMR spectra of **34** and **35** the singlet signals at δ 5.38 and δ 5.30, are respectively assigned to the benzylic protons in the complexes. The small allylic couplings ($J = 1.60$ and 1.63 Hz) between the H^4 and H^5 imidazole protons in **34** at δ 6.96 and δ 7.17 appear as unresolved broad singlet signals in **35** at δ 7.19 and δ 7.29. Distinctive phosphorus-carbon coupling to all four phenyl carbons is present in the $^{13}\text{C}\{^1\text{H}\}$ NMR spectra of both **34** and **35**, although in the latter case the overlapping signals due to $[\text{Au}(\text{NO}_3)(\text{PPh}_3)]$, make the assignment more difficult. The four sets of C-F coupled multiplet signals for **34** appear weak and unresolved. However, a strong singlet signal in this spectrum at δ 169.2, approximately 10 ppm upfield from where coordinated carbon resonances are expected to appear (see **28-30**), implies a somewhat atypical carbene character for the C^2 nucleus and that the negative charge of the complex is delocalised onto the AuPPh_3 unit. The spectrum for **35** displays a similar characteristic, with two signals at δ 164.4 and δ 167.8 (s), however due to the low concentrations of **35** present in the sample, these signals appear weak and could not be assigned with absolute certainty.

As a result of the ambiguity of the assignment of the carbene resonance, and the absence of any assenting evidence with regards to the molecular structure, the nature of the metal-coordination cannot be confirmed entirely. Thus whether true carbene complex formation exists or to what extent delocalisation is effected onto the AuPPh_3 in the carbene complex, could only be ascertained from the crystallographic data of **34**. Unfortunately, no crystals could be grown for X-ray diffraction analysis.

Table 4.9 ^1H , $^{13}\text{C}\{^1\text{H}\}$, $^{31}\text{P}\{^1\text{H}\}$ NMR spectroscopic data for **34** and **35**

Complex	 <p style="text-align: center;">34</p>	 <p style="text-align: center;">35</p>
Solvent Temperature (°C) ^1H NMR (300 MHz) $^{13}\text{C}\{^1\text{H}\}$ NMR (75 MHz) $^{31}\text{P}\{^1\text{H}\}$ NMR (121 MHz)	$[\text{CD}_3]_2\text{CO}$ 25 H^4 6.96 (d, 1H, $J = 1.60$ Hz) H^5 7.17 (d, 1H, $J = 1.63$ Hz) H^6 5.38 (s, 2H) H^{8-10} 7.23-7.43 (m, 5H) PPh 7.47-7.66 (m, 15H) C^2 169.2 (s) C^4 128.7 (s) C^5 119.6 (s) C^6 53.2 (s) C^7 138.4 (s) $\text{C}^{8-8'}$ 129.2 (s) $\text{C}^{9-9'}$ 128.1 (s) C^{10} 128.3 (s) PPh- C^{ipso} 130.4 (d, $J = 55.1$ Hz) PPh- C^{ortho} 134.9 (d, $J = 13.8$ Hz) PPh- C^{meta} 129.8 (d, $J = 11.3$ Hz) PPh- C^{para} 132.3 (d, $J = 2.5$ Hz) C_6F_5 - C^{ipso} 121.0 (m) C_6F_5 - C^{ortho} 149.8 (m) C_6F_5 - C^{meta} 138.2 (m) C_6F_5 - C^{para} 139.1 (m) P 42.6 (bs)	CD_2Cl_2 25 7.19 (bs) 7.29 (bs) 5.30 (s, 2H) 7.32-7.42 (m, 5H) 7.52-7.73 (m, 15H) 164.4 (s) / 167.8 (s) 129.8 (s) 121.4 (s) 52.8 (s) 140.3 (s) 128.6 (s) 127.8 (s) 129.1 (s) 130.0 (d, $J = 62.0$ Hz) 134.7 (d, $J = 13.7$ Hz) 130.1 (d, $J = 11.6$ Hz) 133.4 (d, $J = 2.8$ Hz) 45.5 (s)

In agreement with the proposed formation of $[\text{Au}(\text{C}_6\text{F}_5)(\text{PPh}_3)]$, the ^{31}P NMR spectrum of the hexane extract which contained **34** displays a broad singlet at δ 43.5. This value is in close agreement to the sharp singlet at δ 42.6 assigned to the phosphorus resonance in **34**. The corresponding resonance in **35** at δ 45.5 however can clearly be distinguished from the strong signal at δ 28.9 assigned to the phosphorus nucleus in $[\text{Au}(\text{NO}_3)(\text{PPh}_3)]$.

Mass spectrometry

The ESI-MS spectrometric data for complexes **34** and **35** show apart from strong molecular ion peaks for **34** at m/z 981 (M^+) and a cationic fragment for **35** at m/z 1430 ($\text{M}^+ - \text{NO}_3^-$) also diagnostic fragmentation peaks thereof (Table 4.10). The mass spectrum

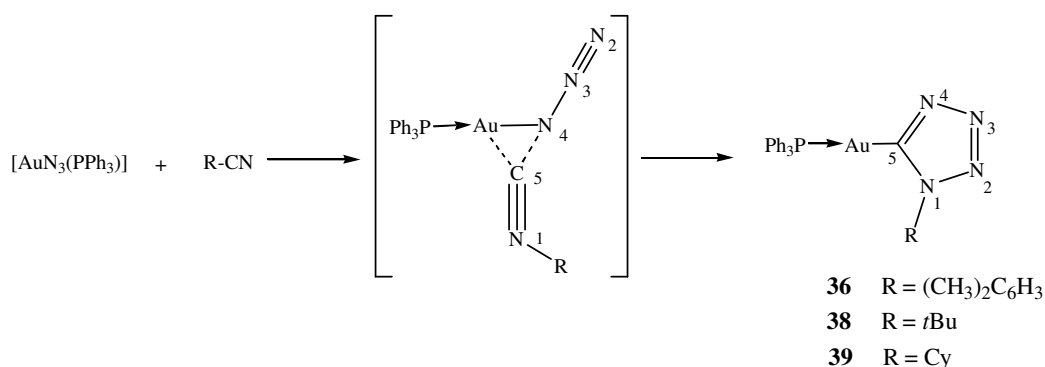
of **34** exhibits a base peak at m/z 619, which is assigned to the fragment formed from the molecular ion upon loss of AuC_6F_5 . For **35**, the gradual fragmentation of the cationic fragment is noted by the peaks at m/z 970 and m/z 531, which respectively represent fragments formed after the loss of one and two AuPPh_3^+ units.

Table 4.10 Mass spectrometric data for **34** and **35**

Fragment	m/z (%)	
	34	35
$\{[\text{M}]^+\}^+$	980 (92)	-
$\{[\text{M}]-\text{NO}_3^-\}^+$	-	1430 (88)
$\{[\text{M}]-\text{AuC}_6\text{F}_5\}^+$	619 (100)	-
$\{[\text{M}]-\text{AuPPh}_3\}^+$	-	970 (68)
$\{[\text{M}]-2\text{AuPPh}_3\}^+$	-	513 (33)
$\{\text{AuPPh}_3\}^+$	459 (89)	-
$\{(\text{AuPPh}_3)_2\}^+$	721 (95)	721 (100)

4.2.3 C-tetrazolyl and NHC-carbene complexes of gold(I) derived from isocyanide precursors.

The reaction of metal azides with isocyanides, first reported by Beck and co-workers,²⁹ represents a straightforward and elegant route to a series of novel carbon-bonded metal tetrazolates. This group report that under very mild conditions, the addition of large excesses (25 fold) of isocyanides (methylisocyanide, cyclohexylisocyanide and phenylisocyanide) to a dichloromethane solution of azido(triphenylphosphine)gold(I), $[\text{Au}(\text{N}_3)(\text{PPh}_3)]$, affords after precipitation by the addition of diethyl ether the neutral isocyanide(tetrazol-5-yl)gold(I) complexes (Scheme 4.8). It is further reported that, these complexes upon exposure to air immediately decompose to form highly insoluble yellow luminescent products.



Scheme 4.8 The synthetic route towards C-tetrazolyl gold(I) complexes.

It was only recently shown that these reactions are strongly dependant on the metal azide, and isocyanide used and even upon the solvent employed. In the preparation of rhodium(III), palladium(III) and gold(III) C-tetrazolyl complexes, Wehlan and co-workers

³⁰ report that reactivity of the isocyanides increases with their assumed nucleophilicity, i.e. 1-*tert*-butylisocyanide > 1-cyclohexylisocyanide ~ 2,6-dimethylphenyl-isocyanide, thus ascribing the highest reactivity to *tert*-butyl isocyanides. Apart from the tetrakis(tetrazolate) metal complexes that form, certain reactions proceed with the evolution of dinitrogen, and the formation of cyanamide ([M]-N{R}-C≡N and carbodiimide ([M]-N=C=NR) complexes.

A. Preparation of [1-(2,6-dimethylphenyl)tetrazol-5-yl](triphenylphosphine)gold(I), **36, [1-(2,6-dimethylphenyl)-4-methyltetrazol-5-ylidene](triphenylphosphine)gold(I) triflate, **37**, [1-(*tert*-butyl)tetrazol-5-yl](triphenylphosphine)gold(I), **38**, [1-(cyclohexyl)tetrazol-5-yl](triphenylphosphine)gold(I), **39**.**

In a further investigation of the 1,3-dipolar cycloaddition reactions of metal azides to isocyanides, we now report alternative products that are obtained when [Au(N₃)(PPh₃)] is reacted with a smaller excess of related isocyanides. The reaction of 2,6-dimethylphenylisocyanide (10 fold excess) with [Au(N₃)(PPh₃)] at ambient temperature while protected from light, affords after 17 h [1-(2,6-dimethylphenyl)tetrazol-5-yl](triphenylphosphine)gold(I), **36**, in good yield. The colourless crystalline solid is stable in air at room temperature and is readily soluble in dichloromethane, acetone and thf, and insoluble in diethyl ether and pentane. Colourless prisms of complex **36** can be obtained overnight at -20 °C, from a dichloromethane solution layered with diethyl ether.

Alkylation of the aurate complex, **36**, at low temperature (-70 °C) affords the mono(carbene)gold(I) complex, **37**, in almost quantitative yield. Although alkylation of C-bonded (tetrazolate)gold(I) complexes are favoured on the more nucleophilic N⁴ atom (*vide supra*), ¹⁵N NMR analysis of the crude reaction product from which complex **30**, was isolated, suggests the presence of isomeric products, which we suspect are possibly N² alkylated carbene complexes.

Furthermore, the related complex, **28** displayed a rapid homoleptic rearrangement to afford complexes containing like ligands. In a striking contrast to both the observations mentioned above, complex **37** appears as the exclusive product of alkylation. This result is illustrated in the comparative ¹H NMR spectra of the 1-benzyltetrazole and 1-(2,6-dimethylphenyl)tetrazole derived gold(I) complexes (Figure 4.13).

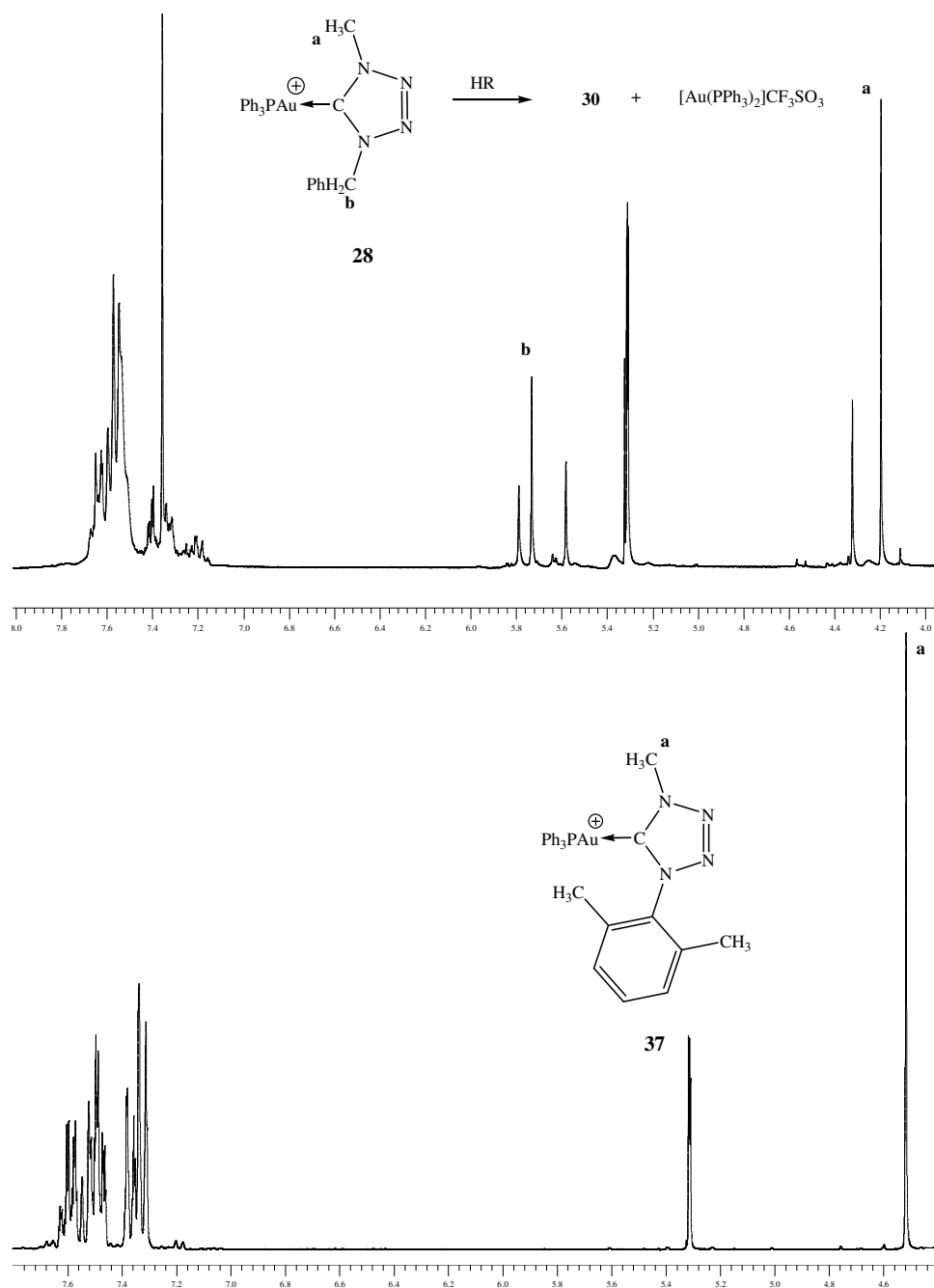


Figure 4.13 Comparative ^1H NMR-spectra of **30** and **37** showing the absence of secondary products in the preparation of **37**.

Kim *et al.*,^{32,33} reported that the reaction of bis(azido)palladium(II) complexes, $[\text{Pd}(\text{N}_3)_2\text{L}_2]$ ($\text{L} = \text{PMe}_3$, PEt_3 and PMe_2Ph) with two mole equivalents of 2,6-dimethylphenylisocyanide, affords *trans* (diphosphine)palladium(II) complexes, containing tetrazolate and carbodiimide ligands. These complexes can, upon mild heating, be converted to the bis(carbodiimide) $\text{Pd}(\text{II})$ complexes. In contrast, the same reactions with *tert*-butyl- and cyclohexylisocyanide did not produce the mono or bis(carbodiimide) complexes and only produced the bis(tetrazolate) complexes. It was thus suggested that the steric bulk of the 2,6-dimethylphenyl substituent on the tetrazole ring effected dinitrogen elimination, and carbodiimide formation.^{32,33} In the instance of complex **37**, the

steric bulk and/or an additional electronic effect of the N¹ substituent, may play a role in directing alkylation on the N⁴ atom. The propensity of mono-NHC of (phosphines)gold(I) complexes to convert to the homoleptic bis(carbene)gold(I) complexes is evident from the limited number of structurally characterised mono(carbene) complexes described in literature. One such example has been described by Böhler and co-workers⁵⁴ in the synthesis of {1,3-bis(5*H*-dibenzo[*a,d*]cycloheptenyl)imidazol-2-ylidene}(triphenyl phosphine)gold(I) chloride. Regardless of the steric congestion within the mixed NHC(phosphine)gold(I) complex, it can be isolated as a stable, crystalline solid. Baker and co-workers¹⁹ very recently reported on the preparation and structural characterisation of [1,3-di(*tert*-butyl)imidazol-2-ylidene](triphenylphosphine)gold(I) hexafluorophosphate, from the [1,3-di(*tert*-butyl)imidazol-2-ylidene]gold(I) chloride, by the ligand substitution of a chloride with a triphenylphosphine ligand. Pyykkö and co-workers⁵⁵ have concluded that the structural, NMR and solution equilibrium data describing homoleptic rearrangement of neutral gold(I) complexes of the type LAuX (L = donor ligand, X = anionic ligand), suggest that reactants and products energetically do not differ much. However, it remains tempting to ascribe the stability (relative to the two literature examples given) of **37**, in part to the sterically bulky N¹ substituent.

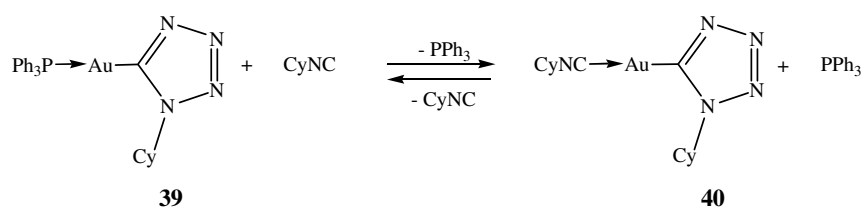
Using the same methodology as for the preparation of complex **37**, the related aurate complex, [1-(*tert*-butyl)tetrazol-5-yl](triphenylphosphine)gold(I), **38**, could be obtained from the metal azide and *tert*-butylisocyanide (10 fold excess). However, where complex **36** was isolated by the precipitation from a dichloromethane solution after the addition of diethyl ether, **38** formed overnight as an insoluble precipitate from the reaction mixture. The isolated colourless microcrystalline solid appeared very stable in air at room temperature. Subsequent alkylation of this compound to afford the corresponding mono(carbene)gold(I) complex, was unsuccessful due to its insolubility in most common organic solvents. Numerous attempts to obtain suitable crystals for X-ray structure analysis were fruitless, however this complex could be characterized by NMR (slight solubility in d₆-DMSO), and FAB-MS spectrometry (in an *m*-nitrobenzylalcohol matrix).

The reaction of 20 mole quantities of cyclohexylisocyanide against one of [Au(N₃)(PPh₃)] afforded, after the usual work-up (*vide supra*), (1-cyclohexyltetrazol-5-yl)(triphenyl phosphine)gold(I) complex, **39**. However in solution and in the presence of residual

⁵⁴ C. Böhler, D. Stein, N. Donati and H. Grützmacher, *New J. Chem.*, 2002, **26**, 1291.

⁵⁵ P. Pyykkö, W. Schneider, A. Bauer, A. Bayler and H. Schmidbaur, *Chem. Commun.*, 1997, 1111.

amounts of free isocyanide (evident from the characteristic odour of the reaction product), a substitution product, (cyclohexylisocyanide)(1-cyclohexyltetrazol-5-yl)gold(I), **40**, had formed which appeared to be in equilibrium with the phosphine complex **39** (Scheme 4.9).



Scheme 4.9 The synthetic route towards the simultaneous formation of complexes **39** and **40**.

In agreement to the findings of Beck and co-workers²⁹ complex **40**, upon exposure to air formed a bright yellow luminescent product almost immediately. This result gives evidence that amounts of complex **40**, indeed exist in the isolated product. Further evidence such as infrared spectrometry, as well as the spontaneous formation of two acyclic carbene complexes derived from **40** (see section 4.2.4), confirms this conclusion. The analytical data for complexes **36-38** are summarised in Table 4.11.

Table 4.11 Analytical data for complexes **36-38**

Complex			
	36	37	38
M.p(°C)	97-98	165-167	146(decomp.)
Colour	colourless	colourless	colourless
Yield(%)	69	91	74
M_r	632.14	796.12	584.14
Analysis(%) [*]	$C_{27}H_{24}AuN_4P$	$C_{29}H_{27}AuF_3N_4O_3PS$	$C_{23}H_{24}AuN_4P$
C	51.77 (51.28)	43.50 (43.73)	47.00 (47.27)
H	3.62 (3.82)	3.33 (3.42)	4.55 (4.14)
N	9.01 (8.86)	7.61 (7.03)	9.29 (9.59)

* Required calculated values given in parenthesis.

B. Spectroscopic characterisation of complexes 36-40.

Nuclear magnetic resonance spectroscopy

The ^1H , $^{13}\text{C}\{^1\text{H}\}$, $^{31}\text{P}\{^1\text{H}\}$ NMR and ^{15}N NMR spectroscopic data for complexes **36-40** are summarised in Table 4.12.

In the ^1H NMR spectra of **36** and **37** the slightly broad singlet signals at δ 1.94 and δ 2.05, are respectively assigned to the six benzylic protons. The only other proton resonance at high field, is a sharp singlet resonance at δ 4.51, assigned to the three NMe protons in **37**, confirming that carbene complex formation had indeed taken place. It is noteworthy that this value differs from the related resonance in the neutral(monocarbene)gold(I) complex, **29**, (δ 3.85), but correlates with the NMe proton resonances reported previously for cationic (carbene)gold(I) complexes, **28** (δ 4.24) and **30** (δ 4.36).

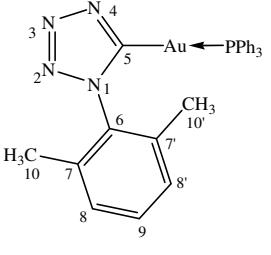
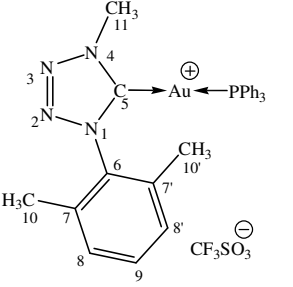
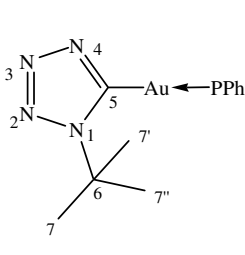
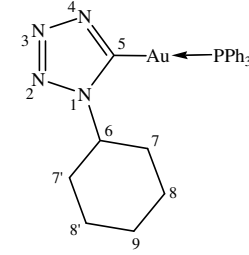
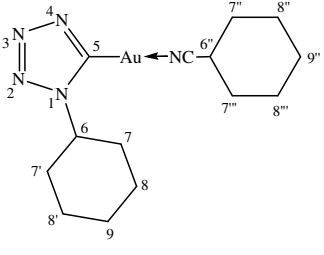
The $^{13}\text{C}\{^1\text{H}\}$ NMR spectrum reveals a characteristic NMe resonance for complex **37** at δ 39.0, in addition to the single carbon resonance (δ 18.0) observed for the chemically equivalent methyl phenyl carbons. The latter observation suggests a free rotation of the 2,6-dimethylphenyl substituent about the $\text{N}^1\text{-C}^6$ axis, a crucial impediment towards N^2 alkylation. For both complex **36** and **37**, the carbon signals of the phosphine ligands were well resolved, showing distinctive phosphorus coupling to all four chemically inequivalent carbon atoms. This result is in contrast to the broad singlet resonances, suggestive of a dynamic system, reported previously for complex **28**. The diagnostic carbene resonance of **37** appears as a strong doublet resonance at δ 186.9 (d, $^2J_{\text{C-P}} = 121.6$ Hz), similar to the same chemical shift in **36** (δ 186.6). This is also in agreement with the carbene carbon-phosphorus coupling *via* a gold(I) centre, observed for (3,4-dimethylthiazol-2-ylidene)(triphenylphosphine)gold(I) triflate (209.8, $^2J_{\text{C-P}} = 126$ Hz).⁵⁶ The $^{31}\text{P}\{^1\text{H}\}$ NMR exhibits a small upfield shift ($\Delta\delta$ 1.6) for the phosphorus nuclei bonded to an “electron-rich” gold centre in complex **37** (δ 39.7) compared to linkage to a more “electron-deficient” metal centre in complex **37** (δ 41.3). This is in agreement with the pattern observed for (isothiazol-5-yl)(triphenylphosphine)gold(I) (δ 45.6) and the corresponding carbene complex, [2-methylisothiazol-5-ylidene][triphenylphosphine] gold(I) triflate (δ 41.5).⁴⁶ Due to the low solubility of complex **38** in d_6 -DMSO, the signals in the ^1H , $^{13}\text{C}\{^1\text{H}\}$ and $^{31}\text{P}\{^1\text{H}\}$ NMR spectra appear weak and broadened. The *tert*-butyl proton

⁵⁶ H. G. Raubenheimer, F. Scott, G. J. Kruger, J. G. Toerien, R. Otte, W. van Zyl, I. Taljaard, P. Olivier and L. Linford, *J. Chem. Soc., Dalton Trans.*, 1994, 2091.

resonance appears as a broad singlet at δ 1.75, which integrates correctly for nine protons with respect to the 15 phenyl protons in the multiplet at δ 7.64. The $^{13}\text{C}\{^1\text{H}\}$ NMR spectrum reveals weak signals for the *tert*-butyl carbons (δ 28.7 and δ 31.1), and the phenyl carbons with their carbon-phosphorus coupling patterns. The metal-bonded carbon atom could not be assigned with certainty and is tentatively assigned to a broad singlet at δ 172.9. The $^{31}\text{P}\{^1\text{H}\}$ NMR spectrum shows a single resonance at δ 26.7.

Due to the fact that the attempted synthesis of **39** also afforded the formation of related complex **40**, an unambiguous assignment of signals in the ^1H and $^{13}\text{C}\{^1\text{H}\}$ NMR spectra of the product mixture to **39** was not possible. However, in their preparation of **40**, Beck and co-workers,²⁹ reported the proton resonances, which could now be ignored in the spectrum of the mixture of **40** and **39**. Furthermore, using a two-dimensional gHSQC experiment, $^{13}\text{C}\{^1\text{H}\}$ NMR resonances could be assigned to carbon nuclei in **39**. The ^1H NMR spectrum of **39** and **40** reveals two sets of proton resonances, which integrate in an approximately 1:2 ratio, for the *ipso*-H signal of the Cy-groups. The well-resolved multiplet at δ 4.65 is assigned to the tetrazole H^6 protons occurring in both **39** and **40**. The corresponding resonance in the Cy-group, $\text{H}^{6''}$ attached to the coordinated isocyanide appears as a broad singlet at δ 3.71. The H^7 , $\text{H}^{7'}$, H^8 and $\text{H}^{8'}$ resonances of the tetrazole-bonded Cy-group can be differentiated from the corresponding resonances in the isocyanide bonded Cy-group ($\text{H}^{7''}$, $\text{H}^{7'''}$, $\text{H}^{8''}$ and $\text{H}^{8'''}$). However, the three sets of H^4 protons overlap and could not be assigned independently. In the $^{13}\text{C}\{^1\text{H}\}$ NMR spectrum a singlet at δ 59.4 is assigned to the *ipso*- C^6 which occurs in both **39** and **40**. The carbon resonances of the two inequivalent Cy-rings can be assigned with correlation to the ^1H NMR resonances. Four sets of doublet signals are assigned to the phenyl carbons exhibiting characteristic carbon-phosphorus coupling patterns. The coordinated isocyanide carbon atom in **40** is not resolved and a weak signal at δ 181.7, is tentatively assigned to the metal-bonded tetrazole carbon atoms. The $^{31}\text{P}\{^1\text{H}\}$ NMR spectrum shows a single broadened singlet at 38.3, assigned to the coordinated phosphine in **39**.

Table 4.12 ^1H , $^{13}\text{C}\{^1\text{H}\}$, $^{31}\text{P}\{^1\text{H}\}$ NMR spectroscopic data for **36-40**

Complex	 <p style="text-align: center;">36</p>	 <p style="text-align: center;">37</p>	 <p style="text-align: center;">38</p>	 <p style="text-align: center;">39</p>	 <p style="text-align: center;">40</p>
Solvent Temperature (°C) ^1H NMR (300 MHz) $^1\text{H}^6/\text{H}^{6''}$ $\text{H}^7, \text{H}^{7'}/\text{H}^{7''}, \text{H}^{7''''}$ $\text{H}^8, \text{H}^{8'}$ $\text{H}^9, \text{H}^{9''}$ H^{10} H^{11} $^{13}\text{C}\{^1\text{H}\}$ NMR (75 MHz) PPh C^5 $\text{C}^6/\text{C}^{6''}$ $\text{C}^7, \text{C}^{7'}/\text{C}^{7''}, \text{C}^{7''''}$ $\text{C}^8, \text{C}^{8'}/\text{C}^{8''}, \text{C}^{8''''}$ $\text{C}^9/\text{C}^{9''}$ $\text{C}^{10}, \text{C}^{10'}$ C^{11} $\text{PPh-C}^{\text{ipso}}$ $\text{PPh-C}^{\text{ortho}}$ $\text{PPh-C}^{\text{meta}}$ $\text{PPh-C}^{\text{para}}$ CF_3SO_3 $^{31}\text{P}\{^1\text{H}\}$ NMR (121 MHz)	CD ₂ Cl ₂ 25 7.23 (d, 2H, $^3J = 1.24$ Hz) 7.21 (dd, 1H, $^3J = 1.34$ Hz, $^3J = 1.36$ Hz) 1.94 (bs, 6H) 7.34-7.56 (m, 15H) 186.6 (bs) 137.0 (s) 136.7 (s) 128.7 (s) 129.9 (s) 17.9 (s) 129.8 (d, $^1J_{\text{C-P}} = 56.6$ Hz) 134.7 (d, $^2J_{\text{C-P}} = 13.9$ Hz) 129.8 (d, $^3J_{\text{C-P}} = 11.4$ Hz) 132.3 (d, $^4J_{\text{C-P}} = 2.2$ Hz) 41.3 (s)	CD ₂ Cl ₂ 25 7.33 (m, 2H) 7.31 (m, 1H) 2.05 (bs, 6H) 4.51 (s, 3H) 7.46-7.63 (m, 15H) 186.9 (d, $^2J_{\text{C-P}} = 121.6$ Hz) 134.1 (s) 136.3 (s) 129.7 (s) 132.4 (s) 18.0 (s) 39.0 (s) 127.8 (d, $^1J_{\text{C-P}} = 60.8$ Hz) 134.7 (d, $^2J_{\text{C-P}} = 13.8$ Hz) 130.2 (d, $^3J_{\text{C-P}} = 11.9$ Hz) 133.1 (d, $^4J_{\text{C-P}} = 2.6$ Hz) 121.6 (q, $^1J_{\text{C-F}} = 322.5$ Hz) 39.7 (s)	CD ₂ Cl ₂ 25 1.75 (bs, 9H) 7.51-7.75 (m, 15H) 172.9 (bs) 28.7 (s) 31.1 (s) 129.3 (d, $^1J_{\text{C-P}} = 63.4$ Hz) 134.1 (d, $^2J_{\text{C-P}} = 13.7$ Hz) 129.8 (d, $^3J_{\text{C-P}} = 11.9$ Hz) 132.3 (d, $^4J_{\text{C-P}} = 2.8$ Hz) 26.7 (s)	CD ₂ Cl ₂ 25 4.65 (m, 1H)/ 2.08 (m, 4H) 1.38 (m, 2H) 1.24 (m, 2H) 7.47-7.62 (m, 15H) 181.7 (s) 59.4 (s) 34.6 (s) 25.9 (s) 25.0 (s) 129.9 (d, $^1J_{\text{C-P}} = 58.1$ Hz) 134.7 (d, $^2J_{\text{C-P}} = 13.9$ Hz) 129.8 (d, $^3J_{\text{C-P}} = 11.6$ Hz) 132.4 (d, $^4J_{\text{C-P}} = 2.5$ Hz) 38.3 (bs)	CD ₂ Cl ₂ 25 4.65 (m, 1H)/ 3.71 (bs, 1H) 2.08 (m, 4H)/ 1.70 (m, 4H) 1.38 (m, 2H)/ 1.89 (m, 2H) 1.24 (m, 2H)/ 1.24 (m, 2H) 181.7 (s) 59.4 (s)/- 34.6 (s)/ 32.5 (s) 25.9 (s)/ 25.5 (s) 25.0 (s)/ 23.0 (s)

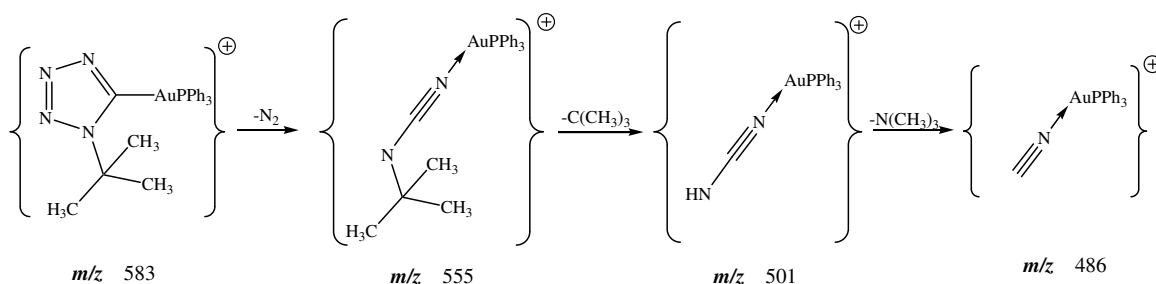
Mass spectrometry

The electron impact mass spectrometric data for complexes **36** and **37** provide apart from fragmentation peaks for the AuPPh₃ moiety, m/z 459 (M⁺) and m/z 262 for PPh₃⁺, no additional peaks that can be assigned to the complexes or fragments thereof. However, the ESI-MS spectra of **37** and **39** (Table 4.13), gives further evidence for the formation of cationic complexes.

Table 4.13 Mass spectrometric data for **37** and **39**

Fragment	m/z (%)		
	37	38	39
{[M]} ⁺	-	-	611 (10)
{[M]-CF ₃ SO ₃ } ⁺	647 (49)	583 (13)	-
{[M]-CF ₃ SO ₃ -N ₂ } ⁺	619 (91)	555 (3)	-
{[M]-N ₂ } ⁺	-	-	-
{[M]-CF ₃ SO ₃ -PPh ₃ } ⁺	385 (2)	-	-
{[M]-CF ₃ SO ₃ -C ₄ H ₉ } ⁺	-	501 (3)	-
{AuPPh ₃ CN} ⁺	-	486 (3)	-
{AuPPh ₃ } ⁺	459 (7)	-	459 (3)
{(AuPPh ₃) ₂ } ⁺	721 (100)	-	-

The strong signal at m/z 647 is assigned to the cationic fragment of complex **37**, and fragmentation peaks thereof at m/z 619 (-N₂), and m/z 385 (-PPh₃) are also present. A similar fragmentation pattern is evident from the FAB-MS data for **38**, depicted in Scheme 4.10. The molecular ion peak of the related neutral complex **39** is observed in the FAB-MS, but with no further characteristic tetrazole fragmentation patterns.



Scheme 4.10 Fragmentation pattern for complex **38**.

Infrared spectroscopy

The IR spectra of **39** and **40** are devoid of the antisymmetric N₃ stretching vibrations normally visible in the range 2050 cm⁻¹, but shows very prominent bands between 2861 and 3050 cm⁻¹ ascribed to ν (CH) frequencies. A characteristic ν (CN) band is very prominent at 2251 cm⁻¹, clearly distinguishable from the corresponding ν (CN) vibrations in cyclohexylisocyanide (2139 cm⁻¹).

C. X-ray structure determination of complexes **36** and **37**.

The crystal and molecular structures of compounds **36** and **37** were determined by single crystal X-ray diffraction. The molecular structure of **36** is shown in Figure 4.14 and selected bond lengths and bond angles are summarised in Table 4.14, numbered according to the figure. Compound **36** crystallises in the monoclinic space group $P2_1/c$. The gold centre is coordinated to a phosphorus atom of a PPh_3 moiety and to an azole carbon on the tetrazole ring. The coordination about the metal is distorted from linearity, $[C(1)-Au(1)-C(1) \ 172.60(3)^\circ]$, in contrast to the essentially linear (isothiazol-5-yl)(triphenylphosphine)gold(I) $[177.1(2)^\circ]$,⁴⁶ and [1,3-di(*tert*-butyl)imidazol-2-ylidene](triphenylphosphine)gold(I) hexafluorophosphate $[177.0(1)^\circ]$,¹⁹ but comparable to {1,3-bis(5*H*-dibenzo[*a,d*]cycloheptenyl)imidazol-2-ylidene}(triphenylphosphine)gold(I) chloride $[173.8(2)^\circ]$.⁵⁴

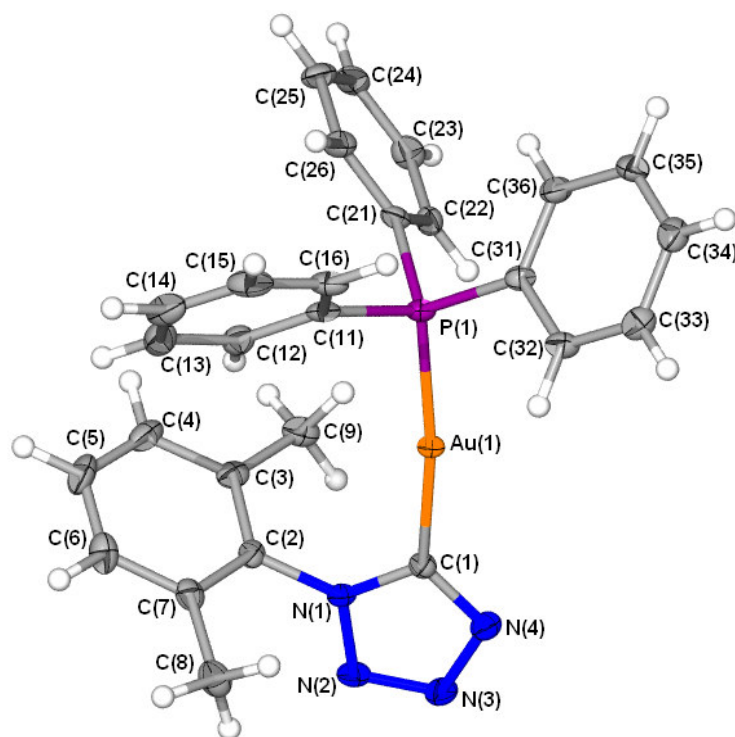


Figure 4.14 Molecular structure of **36** showing the numbering scheme; the included dichloromethane is omitted for clarity.

The Au(1)-C(1) and Au(1)-P(1) bond separations $[2.031(3) \text{ \AA}$ and $2.2777(7) \text{ \AA}$ respectively] are normal and correspond closely to the C-bonded azolyl(phosphine)gold(I) compounds, (isothiazol-5-yl)(triphenylphosphine)gold(I) $[2.032(7) \text{ \AA}$ and $2.290(2) \text{ \AA}]$,⁴⁶ and the aryl(phosphine)gold(I) compound, (2,6-methoxyphen-1-yl)(triphenylphosphine)gold(I), $[2.050(4) \text{ \AA}$ and $2.284(1) \text{ \AA}]$.⁵⁷ Unfortunately, due to the

⁵⁷ P. E. Riley and R. E. Davis, *J. Organomet. Chem.*, 1980, **192**, 283.

unsatisfactory refinement of the parent carbene complex, **37**, a critical assessment cannot be made with regard to common structural parameters found in these complexes. However, compared to the two reported mixed phosphine, NHC gold(I) structures, the Au-P bonds appear not to change significantly upon carbene complex formation, i.e. {1,3-bis(5*H*-dibenzo[*a,d*]cycloheptenyl)imidazol-2-ylidene}(triphenylphosphine)gold(I) chloride [2.299(2) Å]⁵⁴ and [1,3-di(*tert*-butyl)imidazol-2-ylidene](triphenylphosphine)gold(I) hexafluorophosphate [2.275(1) Å].¹⁹ Consistent with expectation, the Au-C in pure single bond in **37** [2.031(3) Å] differs from the “single bond character” found for the carbene complexes, {1,3-bis(5*H*-dibenzo[*a,d*]cycloheptenyl)imidazol-2-ylidene}(triphenylphosphine)gold(I) chloride [2.111(7) Å],⁵⁴ but surprisingly is identical to the Au-C_{carbene} bond in [1,3-di(*tert*-butyl)imidazol-2-ylidene](triphenylphosphine)gold(I) hexafluorophosphate [2.034(1) Å].¹⁹

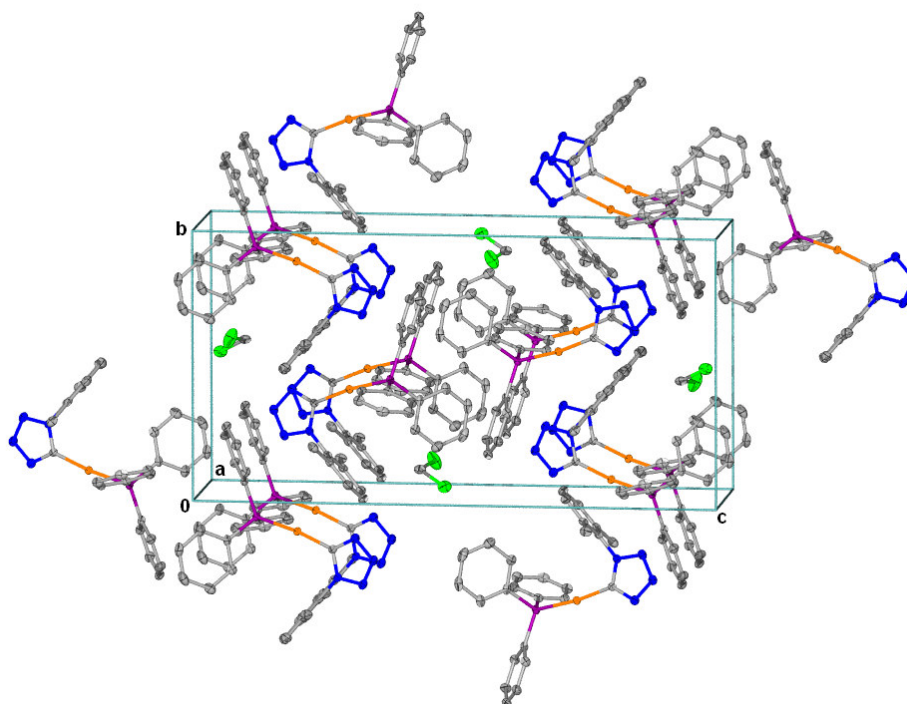


Figure 4.15 Unit cell and packing pattern along the *a*-axis in the crystal lattice of **36**, showing included dichloromethane molecules.

Molecules of **36** pack in regular rows along the *a*-axis as monomeric units (Figure 4.15), and are interspersed with an included amount of dichloromethane. The latter molecule is disordered in two positions with equal occupancy. No intermolecular auriphilic interactions are present, presumably due to the overcrowding around the metal centre of the triphenylphosphine and 2,6-dimethylphenyl moieties.

Table 4.14 Selected bond lengths (Å) and angles (°) for complex **36** with e.s.d.s in parenthesis

Bond lengths		Bond angles	
Au(1)-C(1)	2.031(3)	C(1)-Au(1)-P(1)	172.60(7)
Au(1)-P(1)	2.2777(7)	C(31)-P(1)-C(11)	106.2(1)
P(1)-C(31)	1.811(3)	C(31)-P(1)-C(21)	108.0(1)
P(1)-C(11)	1.814(3)	C(11)-P(1)-C(21)	104.0(1)
P(1)-C(21)	1.817(3)	C(11)-P(1)-Au(1)	110.02(9)
N(1)-C(1)	1.353(3)	C(21)-P(1)-Au(1)	111.60(9)
N(1)-N(2)	1.361(3)	C(31)-P(1)-Au(1)	116.16(9)
N(1)-C(2)	1.445(3)	N(4)-C(1)-N(1)	106.1(2)
N(2)-N(3)	1.295(3)	C(1)-N(1)-N(2)	110.3(2)
N(3)-N(4)	1.371(3)	N(4)-C(1)-Au(1)	132.6(2)
N(4)-C(1)	1.333(3)	N(1)-C(1)-Au(1)	121.2(2)
		N(3)-N(2)-N(1)	105.4(2)
		C(7)-C(2)-N(1)	118.0(2)
		C(1)-N(1)-C(2)	127.6(2)

Single needle-like crystals of **37** suitable for X-ray structural analysis were obtained from a dichloromethane solution. Repeated efforts to obtain a more acceptable data set, including recrystallisation from different solvent systems, were unsuccessful. The best obtained dataset is reported here. All the 5-membered and 6-membered rings have been restrained to ideal pentagons or hexagons. Refinement could be achieved up to $R_1 = 0.1156$ and $wR_2 = 0.29$. Discussion of metric parameters will be reserved to selective bonds and angles, and morphological features with regard to molecular connectivities will be highlighted (Table 4.15). The molecular structure of **37** is depicted in Figure 4.16, and shows two independent, two-coordinate molecules in the asymmetric unit. Compound **37** crystallises in the monoclinic space group $P2_1/c$ as colourless needle-like crystals. The molecules consist of a near linear coordination of an AuPPh₃ moiety to a carbon-bonded tetrazolylidene ligand [C(1)-Au(1)-P(2) and C(91)-Au(2)-P(3), 174.59(1) Å and 178.12(1) Å, respectively]. The Au-C [Au(1)-C(1) 2.034(1) Å and Au(2)-C(91) 2.100(1) Å] and Au-P [Au(1)-P(2) 2.279(1) Å and Au(2)-P(3) 2.258(1) Å] bonds, are typical and in good agreement with those in {1,3-bis(5*H*-dibenzo[*a,d*]cycloheptenyl)imidazol-2-ylidene}(triphenylphosphine)gold(I) chloride [Au-C 2.111(7) Å, Au-P 2.299(2) Å]⁵⁴ and [1,3-di(*tert*-butyl)imidazol-2-ylidene](triphenylphosphine)gold(I) hexafluorophosphate [Au-C 2.044(4) Å, Au-P 2.275(1) Å],¹⁹ the only entries for NHC(phosphine)gold(I) complexes reported in the Cambridge Crystallographic database. The steric bulk of the 2,6-dimethylphenyl N¹ substituent is clearly visible, an exclusive alkylation on the N⁴ atom is confirmed, similar to complex **30**. The two independent molecules are non-interacting and no Au...Au interactions are present.

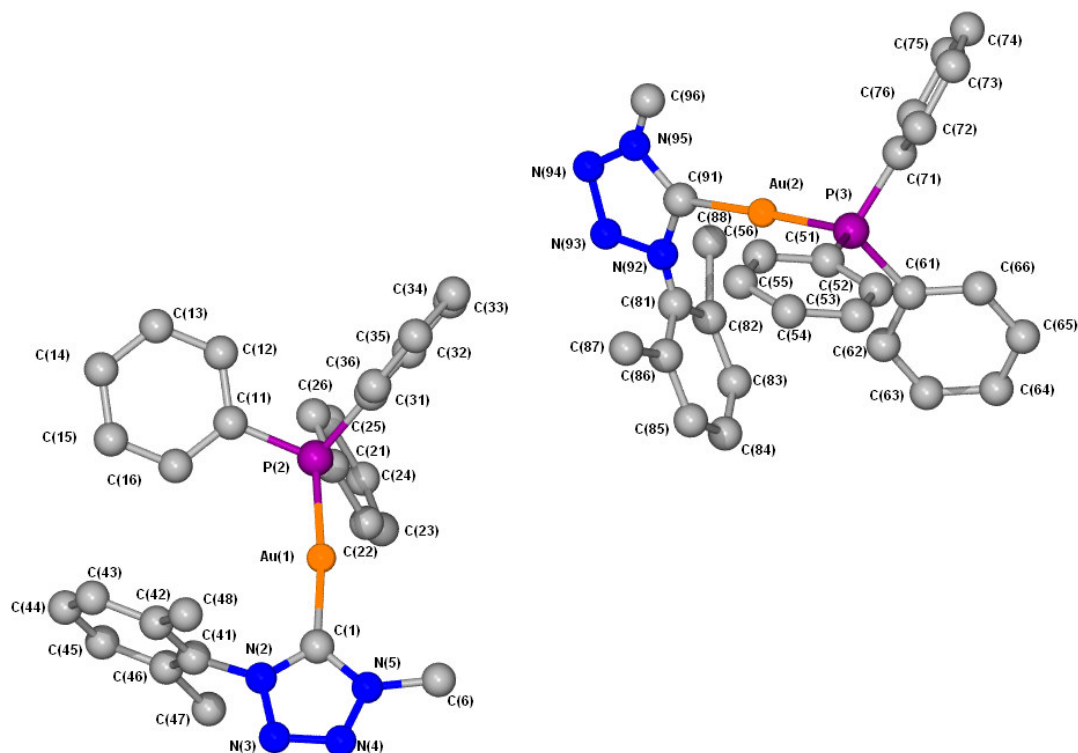


Figure 4.16 The molecular structure of **37**. The hydrogen atoms and two triflate counter anions omitted for clarity.

Table 4.15 Selected bond lengths (Å) and angles (°) for complex **37** with e.s.d.s in parenthesis

Bond lengths		Bond angles	
Au(1)-C(1)	2.034(1)	C(1)-Au(1)-P(2)	174.59(1)
Au(2)-C(91)	2.100(1)	C(91)-Au(2)-P(3)	178.12(1)
Au(1)-P(2)	2.279(1)		
Au(2)-P(3)	2.258(1)		

4.2.4 Acyclic nitrogen-rich carbene complexes of gold(I) derived from isocyanide precursors.

Usón and co-workers³⁵ first reported on the ready substitution of the tht group in [Au(C₆F₅)(tht)] by neutral ligands such as isocyanide. The obtained isocyanide(pentafluorophenyl)gold(I) complexes provide very stable precursors, in comparison to the analogous pentachlorophenyl and pentabromophenyl complexes, for further derivatisations. Bonati and Minghetti,⁵⁸ proposed that nucleophilic additions of amines and alcohols to afford gold(I) carbene complexes proceed by nucleophilic attack on the isocyanide carbon atom. The outcome of these reactions are dependant largely on the basicity of the nucleophile, reactivity of the coordinated isocyanide and to a lesser extent on the electronic nature of the ligand in the *trans* position. The reaction of isocyanide(pentafluorophenyl)gold(I) complexes with a variety of amines, ammonia and alcohols, proceeds in general faster than those of related pentahalophenyl derivatives.³⁵

⁵⁸ F. Bonati and G. Minghetti, *J. Organomet. Chem.*, 1973, **59**, 403.

However, the course of the reactions is mainly governed by the reactivity of the nucleophile, which decreases in the sequence: primary aliphatic amines > ammonia > secondary aliphatic amines > aromatic amines > alcohols.

In the following discussion a few key aspects of this well-established field of study are described as found in the preparation of a novel isocyanide(pentafluorophenyl)gold(I) complex and its derivatisation to a carbene complex by the addition of a pseudo-aromatic 1,2,4-triazol-3-ylamine. We have used these methods to obtain complexes that contain nitrogen rich heterocycles, which in the case of aminotriazole, provide not only a water-soluble product but allows for further potential coordination to gold(III) by the di-amino moiety. Furthermore, the reactivity of imine coordination sites could be probed, which could ultimately afford a compound featuring multiple metal centers with different ligand coordination.

The spontaneous formation and co-crystallisation of an alkoxy(amino) and di(amino)carbenegold(I) complex from the same parent isocyanide(tetrazolyl)gold(I) substrate, demonstrates the propensity of gold(I) species to aggregate by aurophilic interactions while even using two co-crystallising compounds.

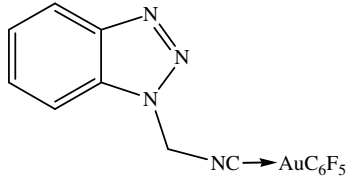
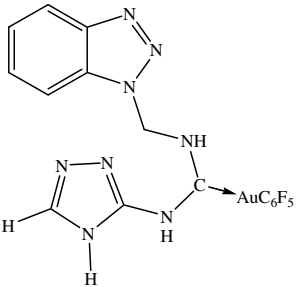
A. Preparation of (benzotriazol-1-ylmethylisocyanide)(pentafluorophenyl)gold (I), 41, {[N-(1,2,4-triazol-3-yl)amine][N'-benzotriazol-1-ylmethylamine]ylidene}(pentafluorophenyl)gold(I), 42.

Reaction of benzotriazol-1-ylmethylisocyanide with $[\text{Au}(\text{C}_6\text{F}_5)(\text{tht})]$ produced a microcrystalline solid, **41**, that displayed interesting solvo-luminescent properties. The colourless ether extract appeared luminescent upon removal of solvent *in vacuo*, and subsequently became insoluble in diethyl ether. Dissolution of the yellow solid in dichloromethane produced a colourless solid upon removal of the solvent. The colourless solid is then readily soluble in diethyl ether. The crystal packing of electron-rich, coordinated isocyanides reportedly plays a role in their luminescent properties.⁵⁹ In this regard, solvent included in the crystal associates with the constituent molecules and effects the close-packing in the crystal lattice. The neutral complex, **41**, crystallises as yellow microcrystalline needles (from diethyl ether), and repeated efforts to obtain crystals suitable for X-ray structure analysis was unsuccessful. Reaction of the coordinated isocyanide with a fourfold excess of 1,2,4-triazol-3-ylamine, resulted in the formation of the corresponding carbene complex **42**. The course of the reaction was monitored (26 h)

⁵⁹ I. Ino, J. Chu Zhong, M. Munakata, T. Kuroda-Sowa, M. Maekawa, Y. Suenaga and Y. Kitamori, *Inorg. Chem.*, 2000, **39**, 4273.

by IR spectroscopy until the $\nu(\text{C}\equiv\text{N})$ vibration of the coordinated isocyanide was no longer present. The isolated product was obtained, after extraction of the reaction residue with thf, filtration through a short silica column, and concentration of the eluent *in vacuo*. The moisture- and air-stable microcrystalline solid is moderately soluble in thf and in water, and insoluble in other common organic solvents. Complex **42** displays none of the luminescent properties observed for **41**. The analytical data for complexes **41** and **42** are summarised in Table 4.16

Table 4.16 Analytical data for complexes **41** and **42**

Complex	 <p style="text-align: center;">41</p>	 <p style="text-align: center;">42</p>
M.p.(°C)	140(decomp.)	158(decomp.)
Colour	Yellow	colourless
Yield(%)	88	80
M_r	522.02	606.06
Analysis(%)*	$\text{C}_{14}\text{H}_6\text{AuF}_5\text{N}_4$	$\text{C}_{16}\text{H}_{10}\text{AuF}_5\text{N}_8$
C	32.05	31.54
	(32.20)	(31.70)
H	1.23	1.71
	(1.16)	(1.66)
N	11.05	18.22
	(10.73)	(18.48)

* Required calculated values given in parenthesis.

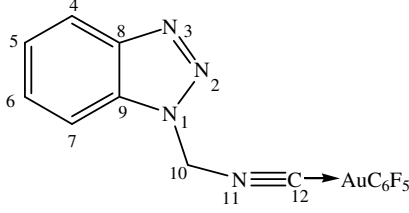
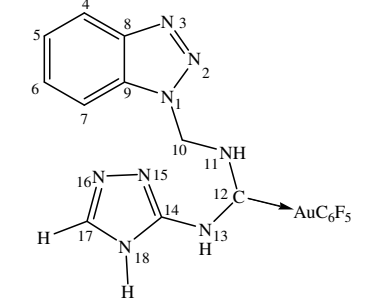
B. Spectroscopic characterisation of complexes **41** and **42**.

Nuclear magnetic resonance spectroscopy

The ^1H , $^{13}\text{C}\{^1\text{H}\}$, ^{19}F NMR spectroscopic data for complexes **41** and **42** are summarised in Table 4.17. In the ^1H NMR spectrum of **41** the benzotriazole group is represented by four distinguishable doublet signals in the aromatic region. The CH_2 protons appear upfield at δ 3.29 as a singlet resonance. The $^{13}\text{C}\{^1\text{H}\}$ NMR spectrum only reveals five clear signals for the benzotriazole moiety, however with enhanced resolution of the slightly broadened singlet at δ 127.2, this signal is resolved as two overlapping singlets, for the C^5 and C^6

nuclei. Furthermore, in conjunction with ^{19}F NMR spectra, the presence of AuC_6F_5 moieties, in the noted distinctive four C-F and three F-F multiplet signals is confirmed.

Table 4.17 ^1H , $^{13}\text{C}\{^1\text{H}\}$, ^{19}F NMR spectroscopic data for **41** and **42**

Complex	 <p style="text-align: center;">41</p>	 <p style="text-align: center;">42</p>
Solvent Temperature ($^{\circ}\text{C}$) ^1H NMR (41, 300 MHz) (42, 600 MHz) $^{13}\text{C}\{^1\text{H}\}$ NMR (41, 75 MHz) (42, 150 MHz) ^{19}F NMR (41 376 MHz) (42 564 MHz)	$[\text{CD}_3]_2\text{CO}$ 25 H^4, H^7 8.13 (d, 1H, $J = 8.4$ Hz), 8.16 (d, 1H, $J = 8.8$ Hz) H^5, H^6 7.76 (d, 1H, $J = 7.2$ Hz), 7.58 (d, 1H, $J = 7.5$ Hz) H^{10} 3.29 (s, 2H) H^{11} H^{13} H^{17} H^{18} C^4, C^7 122.3 (s), 112.0 (s) C^5, C^6 127.2 (s), 127.2 (s) C^8 134.7 (s) C^9 131.2 (s) C^{10} 59.9 (s) C^{12} 148.3 (s) C^{14} C^{17} $\text{C}_6\text{F}_5\text{-C}^{\text{ipso}}$ 121.4 (tm, $J_{\text{CF}} = 65.3$ Hz) $\text{C}_6\text{F}_5\text{-C}^{\text{ortho}}$ 151.4 (ddm, $J_{\text{CF}} = 225.0$ Hz, $J_{\text{CF}} = 24.3$ Hz) $\text{C}_6\text{F}_5\text{-C}^{\text{meta}}$ 139.1 (dm, $J_{\text{CF}} = 251.3$ Hz) $\text{C}_6\text{F}_5\text{-C}^{\text{para}}$ 141.3 (dm, $J_{\text{CF}} = 246.8$ Hz)	$d^8\text{-thf}$ 25 H^4, H^7 8.05 (d, 1H, $J = 8.4$ Hz), 8.45 (d, 1H, $J = 8.4$ Hz) H^5, H^6 7.40 (d, 1H, $J = 8.0$ Hz), 7.56 (d, 1H, $J = 8.0$ Hz) H^{10} 3.43 (dd, 1H, $^2J = 6.14$ Hz, $^3J = 5.37$ Hz) 3.53 (dd, 1H, $^2J = 6.40$ Hz, $^3J = 5.37$ Hz) H^{11} 11.68 (t, 1H, $J = 5.89$ Hz) H^{13} 11.74 (bs, 1H) H^{17} 8.31 (s, 1H) - C^4, C^7 120.5 (s), 111.8 (s) C^5, C^6 128.5 (s), 124.8 (s) C^8 133.3 (s) C^9 128.2 (s) C^{10} 61.1 (s) C^{12} 163.2 (s) C^{14} 147.4 (s) C^{17} 143.6 (s) $\text{C}_6\text{F}_5\text{-C}^{\text{ipso}}$ 119.3 (m) $\text{C}_6\text{F}_5\text{-C}^{\text{ortho}}$ 147.5 (m) $\text{C}_6\text{F}_5\text{-C}^{\text{meta}}$ 142.4 (m) $\text{C}_6\text{F}_5\text{-C}^{\text{para}}$ 146.2 (dm)
F^{ortho} (41 376 MHz) F^{meta} (42 564 MHz) F^{para}	F^{ortho} -116.0 (m) F^{meta} -162.4 (t, $J_{\text{FF}} = 19.9$ Hz) F^{para} -165.0 (m)	F^{ortho} -116.3 (m) F^{meta} -161.7 (t, $J_{\text{FF}} = 19.8$ Hz) F^{para} -164.4 (m)

A weak signal at δ 148.3 is tentatively assigned to the carbon-coordinated isocyanide, C^{12} . Importantly, the H^{10} singlet in **42** now resonates as two sets of doublets of doublets, which signifies the geminal coupling between the two chemically non-equivalent H^{10} protons and the NH proton. A diagnostic triplet signal at δ 11.68 ($J = 5.89$ Hz) for the amine proton confirms derivatisation of the coordinated isocyanide group. The H^{13} proton signal of equal intensity occurs at δ 11.74 as a broad singlet. Diagnostic signals in the $^{13}\text{C}\{^1\text{H}\}$

NMR spectrum of the mono(carbene) complex, **42**, include a downfield shifted ($\Delta\delta$ 14.9) coordinated isocyanide carbon at δ 163.2, which is in close agreement to the value reported in the related (diamino)carbene gold(I) complex, $(\text{ArNH})_2\text{CAuCl}$ [δ 160.7].⁶⁰ The complex C-F coupling patterns are not resolved, however, three distinctive multiplet signals in the ^{19}F NMR are assigned to the three types of fluorine atoms of the pentafluorophenyl ligand.

Mass spectrometry

The molecular (M^+) ion peaks for both compound **41** (m/z 523) and **42** (m/z 607) are represented in ESI-MS spectra (Table 4.18). Important fragmentation peaks for **41** and **42** include a loss of a C_6F_5 group, with the remaining ions at m/z 357 and m/z 439. Interestingly, for the carbene complex, strong peaks for the sodium adducts are present observed at m/z 629 ($\{[\text{M}]\text{Na}\}^+$) and 1235 ($\{2[\text{M}]\text{Na}\}^+$).

Table 4.18 Mass spectrometric data for **41** and **42**

Fragment	m/z (%)	
	41	42
$\{[\text{M}]\}^+$	523 (20)	607 (30)
$\{[\text{M}]\text{Na}\}^+$	-	629 (80)
$\{2[\text{M}]\text{Na}\}^+$	-	1235 (25)
$\{[\text{M}]-\text{C}_6\text{F}_5\}^+$	357 (23)	439 (20)

Infrared spectroscopy

The infrared spectrum of **42** shows the disappearance of the strong $\nu(\text{C}\equiv\text{N})$ band at 2231 cm^{-1} observed for the parent compound **41**, and the concomitant appearance of multiple new bands at 2925, 3051, 3194, 3320 and 3399 cm^{-1} attributable to the two aliphatic and the three tautomeric triazole $\nu(\text{NH})$ bands.

Fluorescence spectroscopy

Microcrystalline material of complex **41** isolated from a diethyl ether solution exhibits intense yellow luminescence at room temperature. The emission and excitation spectra of **41** are given in Figure 4.17. The excitation profile shows a maximum at 320 nm. The strong, broad emission for **41** occurs at a maximum of 382 nm.

⁶⁰ G. Banditelli, F. Bonati, S. Calogero, G. Valle, F. E. Wagner and R. Wordel, *Organometallics*, 1986, **5**, 1346.

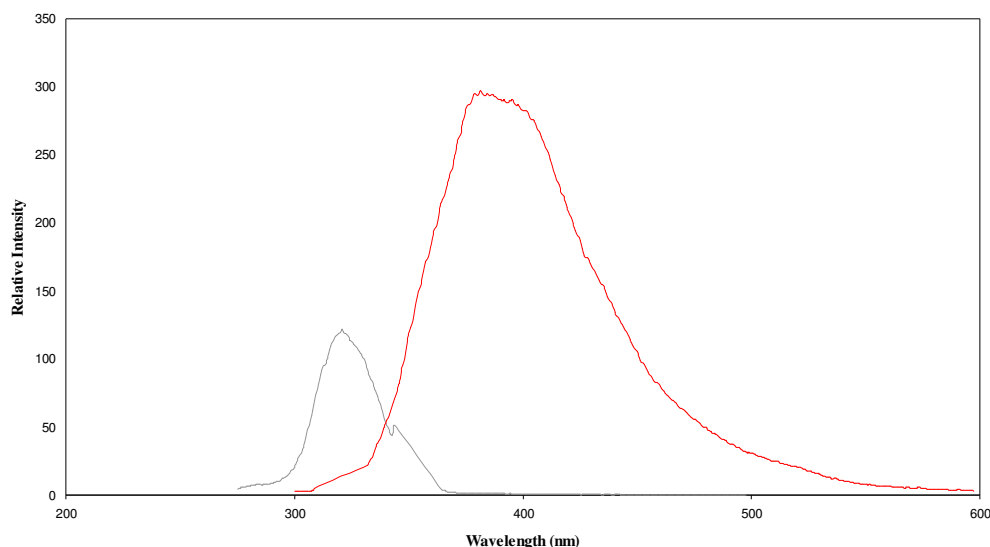
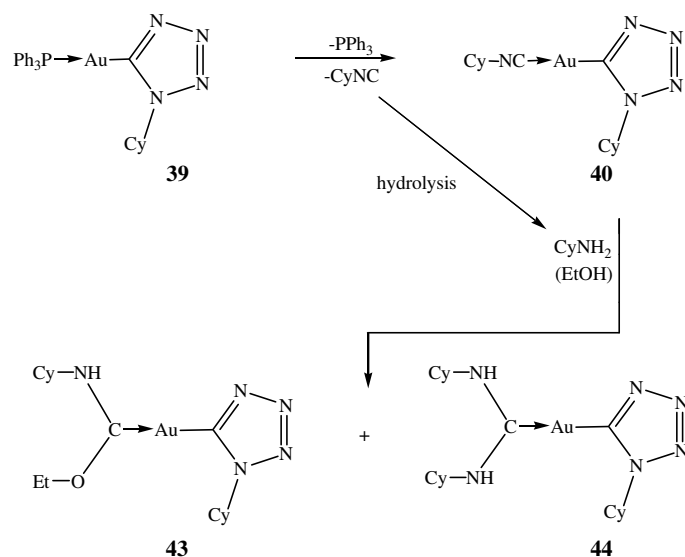


Figure 4.17 The excitation (grey) and emission spectra (red) for **41** measured in a dichloromethane solution (excitation at 320 nm).

C. Spontaneous formation and co-crystallisation of di(amino)carbene and amino(ethoxy)carbene complexes of gold(I).

In Section 4.4.2 the preparation of the C-bonded tetrazole gold(I) complex, **39**, as well as the simultaneous formation of a substitution product, (1-cyclohexylisocyanide)(1-cyclohexyltetrazol-5-yl)gold(I), **40** is discussed. In an attempt to crystallise **39**, from ethanol and pentane a mixed crystalline product of the Fischer-type carbene complex, **43**, and a Bonati-Minghetti-type product, **44**, was isolated. The necessary conversions to afford such gold(I) carbene complexes are indicated in Scheme 4.11. Ethanol and cyclohexylamine addition to the gold (I) isocyanide are invoked. The amine is probably a hydrolysis product of **39** or free isocyanide. Schmidbaur and coworkers⁶¹ reported a similar instance, where the formation of a (isocyanide)(diaminocarbene)gold(I) chloride resulted from the addition of an alkylamine, present due to the hydrolysis of the free isocyanide, to bis (isocyanide)gold chloride. Compounds **43** and **44** were isolated as a co-crystallised product (referred to as **43·44**, henceforth) from the crystallisation mixture.

⁶¹ H. Ehlich, A. Schier and H. Schmidbaur, *Organometallics*, 2002, **21**, 2400.



Scheme 4.11 Spontaneous self-assembly towards the formation of amino(ethoxy)carbene, **43** and di(amino)carbene, **44**, complexes of gold(I).

The transformation of gold(I)-isocyanide complexes to carbene complexes by nucleophilic addition reactions with alcohols and amines, is well documented. Aliphatic and aromatic amines react readily in low concentrations and under mild conditions, whereas alcohols normally require prolonged reaction times at higher temperatures. This variance in nucleophilicity, is elegantly illustrated in this reaction (at $-20\text{ }^{\circ}\text{C}$ over 8 months) which only required a limited amount of amine in comparison to the overwhelming excess of alcohol present to effect a similar nucleophilic addition, however, with the knowledge that the co-crystallisation of **43** and **44**, does not necessitate the formation of the complexes in equal concentrations.

Nuclear magnetic resonance spectroscopy

Unfortunately only a few crystals of **43·44** could be obtained and characterisation by ^1H and $^{13}\text{C}\{^1\text{H}\}$ NMR analysis was not possible.

Mass spectrometry

The FAB-MS spectra of **43·44** is shown in Figure 4.18. The molecular ion peaks for complex **43** (m/z 504) and **44** (m/z 557) are present, as well as characteristic fragmentation peaks thereof. Peaks at m/z 507 and m/z 560 are both exactly three mass units larger than the respective molecular ion peaks of **43** and **44**, and indicate further protonation in the mass spectrometer.

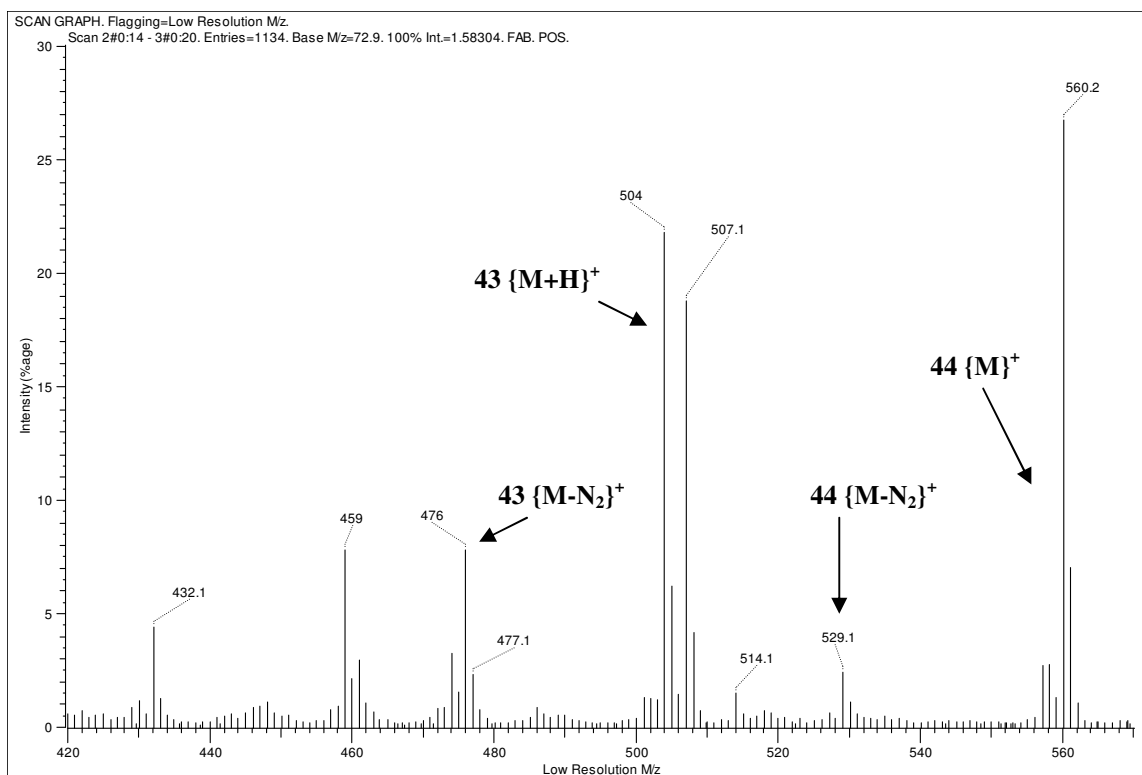


Figure 4.18 FAB-MS spectrum for **43·44** with significant fragmentation peaks denoted.

D. X-ray structure determination of complex **43** and **44**.

Colourless crystals that contain both carbene complexes, [alkoxy(amino)carbene][tetrazol-5-yl]gold(I), **43**, and (diaminocarbene)(tetrazol-5-yl)gold(I), **44** were isolated. The crystal and molecular structures of **43·44** were determined by single crystal X-ray diffraction. The molecular structures are shown in Figure 4.19 and selected bond lengths and bond angles are summarised in Table 4.19, numbered according to the figure. The compounds **43·44** crystallise in the triclinic space group $P\bar{1}$.

Two independent molecules occur in the asymmetric unit (Figure 4.19). Bis(cyclohexylamine)- and ethoxy(cyclohexylamine) substituents are coordinated to each (1-cyclohexyltetrazol-5-yl)gold(I) unit.

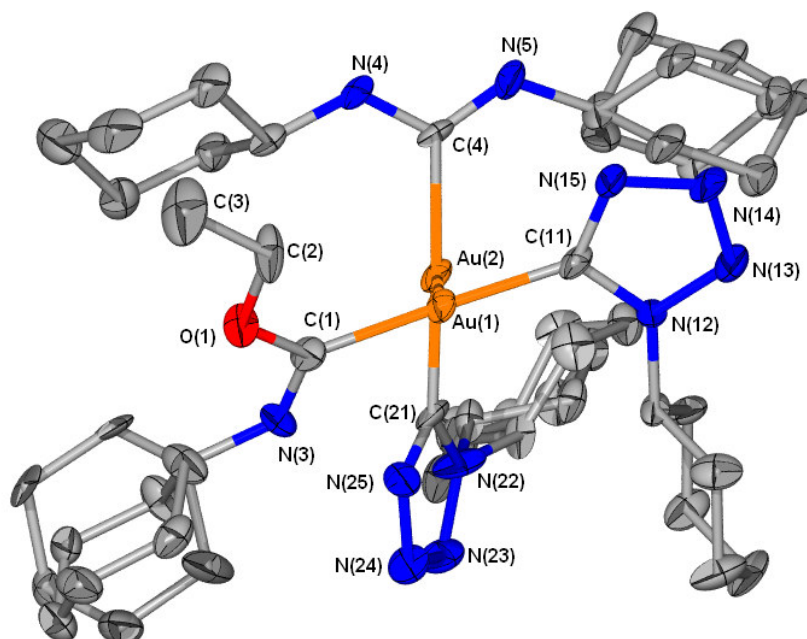


Figure 4.19 Molecular structure of **43·44** showing the numbering scheme.

Coordination around the metal centers is essentially linear [C(4)-Au(2)-C(21) 178.1(4)^o and C(1)-Au(1)-C(11) 176.7(4)^o]. It is noteworthy that all four trigonally planar metal bonded carbon atoms, have equal bond distances [C(1)-Au(1) 2.02(1) Å, C(11)-Au(1) 2.01(1) Å, C(4)-Au(2) 2.07(1) Å and C(21)-Au(2) 2.02(1) Å]. These bond lengths are in good agreement with related compounds, [{*cis,cis*-(*p*-MeC₆H₄NH)(EtO)C₂Au(I)] [ClO₄] [2.03(3) Å and 1.93(3) Å],⁶⁰ [(ArNH)(EtO)CAuCl] [2.04(4) Å and 1.98(3) Å],⁶⁰ [{(MeNH)(Me₂N)C₂Au(I)] [PF₄] [2.050(3) Å]⁶² and [{(MeNH)₂C₂Au(I)] [Cl·H₂O] [2.039(4) Å].³⁶ Schmidbaur and co-workers⁶¹ reported a closely related, [(CyNC){(CyNH)₂C}Au(I)] [Cl], with an identical ligand to complex **44**, but which contains an 1-cyclohexylisocyanide ligand compared to the 1-cyclohexyltetrazol-5-yl ligand in **44**. In these complexes the similar metal-carbene bonds differ somewhat in length [Au-C(carbene) 2.03(1) Å and Au(2)-C(4) 2.07(1) Å], however the Au-C (isocyanide) [2.03(1) Å] and C(21)-Au(2) [2.03(1) Å] bonds are identical. The two molecular structures which co-crystallises illustrates that the relative *trans* influence of ethoxy- and di(amino)-carbene substituents are very similar. Baker and co-workers²⁴ illustrated that in a series of (pseudo)halo[1,3-di(*tert*-butyl)imidazol-2-ylidene]gold(I) complexes, the Au-C(carbene) bond length increases parallel with the σ -donor ability of the ancillary ligand. In both complexes **43** and **44**, the acyclic carbene ligands are rotated at an angle to the plane of the heterocyclic rings. Within the crystalline lattice, the two

⁶² R.L. White-Morris, M. M. Olmstead, F. Jiang, D. S. Tinti and A. L. Balch, *J. Am. Chem. Soc.*, 2002, **124**, 2327.

carbene complex types aggregate by relatively weak Au(I)...Au(I) interactions [3.2880 (9) Å] (Figure 4.20). The two molecules approach each other at an almost perpendicular angle [torsion angles C(11)-Au(1)-Au(2)-C(21), C(1)-Au(1)-Au(2)-C(21), at 109.6(4)° and -69.1(4)°, respectively]. Three of the four cyclohexyl rings [N(3), N(5) and N(22)] are disordered in two positions, the modelled disorder is shown in Figure 4.21.

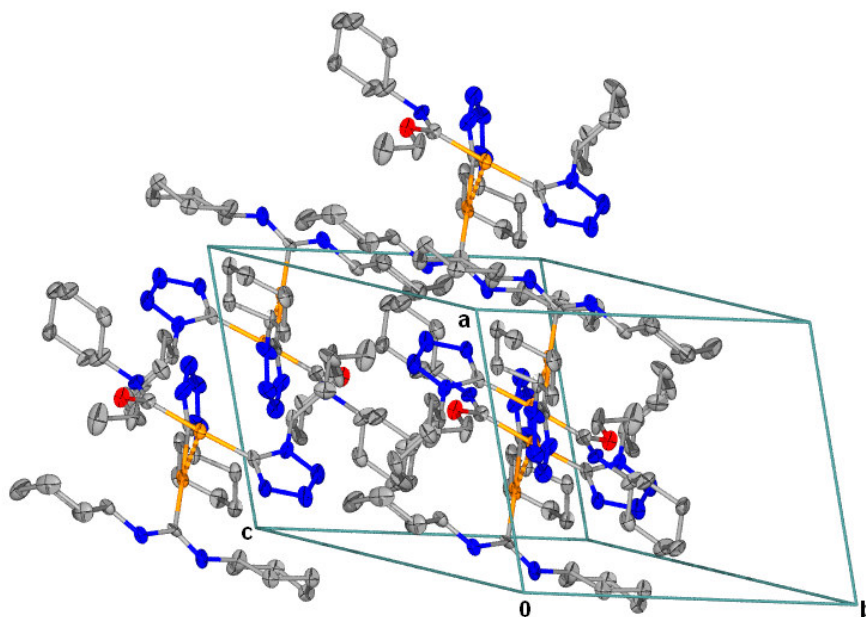


Figure 4.20 Unit cell and packing pattern in the crystal lattice of **43·44** viewed along the c-axis.

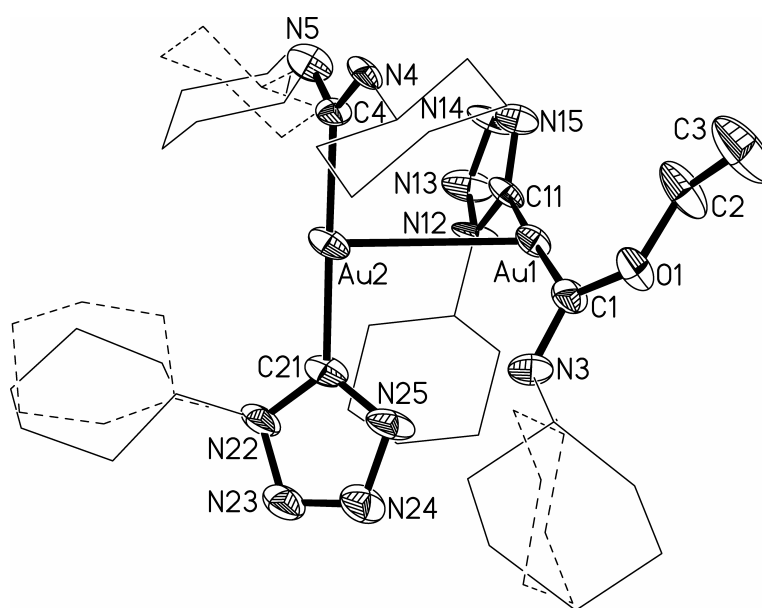


Figure 4.21 Molecular structure of **43·44** with the modelled disorder in the cyclohexyl rings.

Table 4.19 Selected bond lengths (Å) and angles (°) for **43·44** with e.s.d.s in parenthesis

Bond lengths		Bond angles	
Au(1)-C(11)	2.01(1)	C(11)-Au(1)-C(1)	176.8(4)
Au(1)-C(1)	2.02(1)	C(11)-Au(1)-Au(2)	89.0(3)
Au(2)-C(21)	2.02(1)	C(1)-Au(1)-Au(2)	93.9(3)
Au(2)-C(4)	2.07(1)	C(21)-Au(2)-C(4)	178.1(4)
Au(1)-Au(2)	3.2880(9)	C(21)-Au(2)-Au(1)	91.4(3)
C(11)-N(15)	1.33(1)	C(4)-Au(2)-Au(1)	88.2(3)
C(11)-N(12)	1.37(1)	N(3)-C(1)-O(1)	112(1)
N(12)-N(13)	1.35(1)	O(1)-C(1)-Au(1)	126.7(8)
N(12)-C(12)	1.47(1)	N(15)-C(11)-N(12)	105.2(9)
N(13)-N(14)	1.27(1)	N(15)-C(11)-Au(1)	129.1(8)
N(14)-N(15)	1.40(1)	N(5)-C(4)-N(4)	118(1)
C(21)-N(25)	1.33(1)	N(4)-C(4)-Au(2)	119.0(8)
C(21)-N(22)	1.37(1)	N(25)-C(21)-N(22)	105.3(9)
N(22)-N(23)	1.36(1)	N(25)-C(21)-Au(2)	126.4(8)
N(23)-N(24)	1.29(1)	C(1)-O(1)-C(2)	115.5(8)
N(24)-N(25)	1.36(1)		
O(1)-C(1)	1.33(1)		
O(1)-C(2)	1.46(1)		
C(4)-N(5)	1.32(1)		
C(4)-N(4)	1.34(1)		

4.3 Conclusion

Gold(I) complexes that contain tetrazole units are rare, and their C-bonded or carbene complexes have not been structurally characterised before. In the present study we have shown that novel stable tetrazolyl and tetrazolylidene complexes of gold(I) can be prepared by two classic methodologies.

First, by following a lithiation-transmetallation-alkylation sequenced procedure, neutral and cationic mono(carbene)gold(I) complexes can be obtained. (1-Benzyltetrazol-5-ylidene)(triphenylphosphine)gold(I) triflate, in accord with the related imidazolylaurate and imidazolylidene complexes, displayed a rapid homoleptic rearrangement of ligands when in solution. In a related reaction, the presence of an ammonium salt during the preparation of (pentafluorophenyl)(1-benzyltetrazol-5-ylidene)gold(I), a similar reaction was confirmed by isolating and structurally characterising the [bis(pentafluorophenyl)gold(I)][TMEDAMe]. From the same reaction mixture, two closely related coordination polymers, [Li(CF₃SO₃)₂][TMEDAMe] and [Li(CF₃SO₃)(diethyl ether)]⁻ wherein the coordinated Li⁺-ions play an important ligand coupling role within extended structures – were also isolated. Single crystal X-ray diffraction studies revealed that the macroscopic similarity (i.e in morphology) of the crystals in these two complexes, can also be related to their microscopic crystalline organisation. The first X-ray structure analysis performed on a C-bonded tetrazole derived carbene gold(I) complex, bis(1-benzyltetrazol-5-

ylidene)gold(I) triflate, **30**, revealed the inequivalency of the three imine nitrogen atoms present: alkylation to afford carbene complex formation occurs selectively on the nucleophilic N⁴ heteroatom.

Second, the elegant route to carbon-bonded tetrazolyl metal complexes first reported by Beck, Fehlhammer and co-workers²⁹ was revisited. This method has surprisingly received limited attention, and only recently have Au(III), Pd, Rh and Pd complexes been prepared. In the present study we have shown that the simultaneous 1,3-cycloaddition and ligand substitution reactions to afford various neutral isocyanide(tetrazol-5-yl)gold(I) complexes, are strongly dependant on the reactivity and concentration of isocyanide employed. A series of phosphine-containing (tetrazolyl)gold(I) complexes, different from the Fehlhammer complexes, were prepared and structurally characterised. Furthermore, these isolable compounds are precursors to new NHC compounds of gold(I), as illustrated by the successful isolation of the mono(carbene) complex, [1-(2,6-dimethylphenyl)-4-methyltetrazol-5-ylidene](triphenylphosphine)gold (I), **37**. Structural analysis of this compound revealed that even without a formal negative charge (in comparison to **30**) on the metal centre, electrophilic addition is favoured on the N⁴ position.

In our contribution to the Bonati-Minghetti approach towards carbene complex formation, the preparation of a luminescent isocyanide(pentafluorophenyl)gold(I) complex, **41**, followed by functionalisation to a non-luminescent acyclic di(amino)carbene complex, **42** demonstrate that these carbene complex types can also be effected by a primary amine functionality, in the presence of a tautomeric-type secondary amine, contained in a nitrogen-rich heterocycle.

Finally, in a serendipitous discovery of an amino(ethoxy)carbene complex of gold, **43**, and a di(amino)carbene complex, **44**, co-crystallises together and incurred complex conversions.

4.4 Experimental

4.4.1 General procedures and instruments

Reactions were carried out under argon using standard Schlenk and vacuum-line techniques. Tetrahydrofuran (thf), *n*-hexane, *n*-pentane and diethyl ether were distilled under N₂ from sodium benzophenone ketyl, dichloromethane from CaH₂, ethanol and methanol from magnesium. 2,6-dimethylphenyl-, *tert*-butyl-, 1-cyclohexyl-, benzotriazole-

1-ylmethyl-isocyanide, 1,2,4-triazol-3-ylamine and CF₃SO₃Me were purchased from Aldrich. Butyllithium (1.6 M solution *n*-hexane) and TMEDA were purchased from Merck. Literature methods were used to prepare 1-benzyltetrazole,⁴¹ [AuCl(tht)],⁶³ [Au(C₆F₅)(tht)],⁶⁴ [AuCl(PPh₃)],⁶⁵ [Au(NO₃)(PPh₃)]⁶⁶ and [Au(N₃)(PPh₃)].⁶⁷

Melting points were determined on a Stuart SMP3 apparatus and are uncorrected. Mass spectra were recorded on an AMD 604 (EI, 70 eV), VG Quattro (ESI, 70 eV methanol, acetonitrile) or VG 70 SEQ (FAB, 70 eV) instrument. In the instance of EI and FAB MS the isotopic distribution patterns were checked against the theoretical distribution. All NMR spectra were recorded on a Varian 300 FT or INOVA 600 MHz spectrometer (¹H NMR at 300/400/600 MHz, ¹³C{¹H} NMR at 75/100/150 MHz, ³¹P{¹H} NMR at 121/162/243 MHz, ¹⁵N NMR at 60.8 MHz, ¹⁹F NMR at 284/376/564 MHz). Chemical shifts (δ) are reported relative to solvent resonance or external reference of 85 % H₃PO₄ (³¹P), NH₃NO₂ (¹⁵N) and CFC₃(¹⁹F). Infrared spectra recorded on a Thermo Nicolet Avatar 330FT-IR with Smart OMNI ATR (attenuated total reflectance) sampler. Elemental analysis were carried out at the School of Chemistry, University of the Witwatersrand. Fluorescent spectroscopy were recorded on a Perkin Elmer LS50B luminescence spectrometer (emission range scanned 300-600 nm). Certain characterisation data (elemental analysis, melting point and also yields) are given in the main text. For elemental analysis, products were evacuated under high vacuum for 10 h.

4.4.2 Preparations and procedures

4.4.2.1 Preparation of (1-benzyl-4-methyltetrazol-5-ylidene)(triphenylphosphine) gold(I) triflate, 28.

A solution of 1-benzyltetrazole (0.24 g, 1.5 mmol) in thf (15 ml) was treated with *n*-butyllithium in hexane (1.0 ml, 1.5 mmol) at -98 °C. After 30 min of stirring [AuCl(PPh₃)] (0.74 g, 1.5 mmol) in thf (10 ml) was added to the orange coloured solution. The reaction mixture was stirred for a further 1.5 h between -98°C to -78°C during which time the solution became colourless. The product was treated with CF₃SO₃CH₃ (0.18 ml, 1.6 mmol) at -78°C, reacted for 1h, and slowly allowed to reach room temperature. The

⁶³ R. Usòn and A. Laguna, in *Organometallic Synthesis*, eds. R. B. Lang and J. J. Eisch, Elsevier, Amsterdam, 1986, vol. 3, p. 325.

⁶⁴ R. Usòn and A. Laguna, in *Organometallic Synthesis*, eds. R. B. Lang and J. J. Eisch, Elsevier, Amsterdam, 1986, vol. 3, p. 326.

⁶⁵ M. I. Bruce, B. K. Nicholson and O. Bin Shawkataly, *Inorg. Synth*, 1989, 324.

⁶⁶ L. Malatesta, L. Naldini, G. Simonetta and F. Cariati, *Coord. Chem. Rev.*, 1966, **1**, 25.

⁶⁷ G. Beuter and J. Strähle, *J. Organomet. Chem.*, 1989, **372**, 67.

solvent was removed *in vacuo* to yield a colourless oily residue. The residue was extracted sequentially with a diethyl ether/*n*-pentane mixture (1:1, 30 ml), and dichloromethane (30 ml) and the extracts were filtered individually through MgSO₄. The dichloromethane extract was concentrated *in vacuo* to afford a colourless microcrystalline solid, **28** (0.83 g, 71 %).

4.4.2.2 Preparation of (1-benzyl-4-methyltetrazol-5-ylidene)(pentafluorophenyl)gold(I), **29**.

A solution of 1-benzyltetrazole (0.14 g, 0.87 mmol) in thf (20 ml) was treated with *n*-butyllithium in hexane (0.56 ml, 0.87 mmol) at -98 °C. After 30 min of stirring [Au(C₆F₅)(tht)] (0.39 g, 0.87 mmol) in thf (10 ml) was added to the orange coloured solution. The reaction mixture was stirred for a further 2 h between -98°C to -78°C during which time the solution became colourless. The product was treated with CF₃SO₃CH₃ (0.10 ml, 0.87 mmol) at -78°C, reacted for 1h, and slowly allowed to reach room temperature. The solvent was removed *in vacuo* to yield a colourless oily residue. The residue was extracted sequentially with a diethyl ether/*n*-pentane mixture (1:1, 30 ml), and dichloromethane (30 ml) and the extracts were filtered individually through MgSO₄. The ether/pentane extract was concentrated *in vacuo* to afford a colourless microcrystalline solid, **29** (0.36 g, 77 %).

4.4.2.3 Preparation of bis(1-benzyl-4-methyltetrazol-5-ylidene)gold (I) triflate, **30**.

A solution of 1-benzyltetrazole (0.31 g, 1.9 mmol) in thf (20 ml) was treated with *n*-butyllithium in hexane (1.3 ml, 1.9 mmol) at -98 °C. After 30 minutes of stirring [AuCl(tht)] (0.31 g, 0.98 mmol) in thf (10 ml) was added to the orange coloured solution. The reaction mixture was stirred for a further 2 h between -98°C to -78°C during which time the solution became colourless. The product was treated with CF₃SO₃CH₃ (0.22 ml, 1.9 mmol) at -78°C, reacted for 1h, and slowly allowed to reach room temperature. The solvent was removed *in vacuo* to yield a colourless oily residue. The residue was extracted sequentially with diethyl ether/*n*-pentane mixture (1:1, 30 ml), and dichloromethane (30 ml) and the extracts were filtered individually through MgSO₄. The dichloromethane extract was concentrated *in vacuo* to afford a colourless solid, which was recrystallised from a dichloromethane solution layered with diethyl ether at -20 °C to yield colourless needles, **30** (0.47 g, 69 %).

4.4.2.4 *The attempted synthesis of complex 29, in the presence of TMEDA.*

A solution of 1-benzyltetrazole (0.16 g, 1.0 mmol) in thf (9.0 ml) and TMEDA (0.9 ml) was treated with *n*-butyllithium (0.66 ml, 1.0 mmol) in hexane at -98 °C. After 5 minutes of stirring [Au(C₆F₅)(tht)] (0.45 g, 1.0 mmol) in thf (10 ml) was added to the orange coloured solution. The reaction mixture was stirred for a further 2 h between -98°C to -78 °C during which time the solution became colourless. The product was treated with CF₃SO₃CH₃ (0.11 ml, 1.0 mmol) at -78 °C, reacted for 1h, and slowly allowed to reach room temperature. The solvent was removed *in vacuo* to yield a colourless oily residue. The residue was extracted sequentially with a diethyl ether/*n*-pentane mixture (1:1, 50 ml), and dichloromethane (50 ml) and the extracts were filtered individually through MgSO₄. The dichloromethane extract was concentrated *in vacuo* to afford a colourless microcrystalline solid (0.49 g), a mixture of complexes **31** and **32**. Recrystallisation of the mixture from a dichloromethane solution layered with diethyl ether at -20 °C, afforded colourless needles of both **31** and **32**.

4.4.2.5 *The attempted synthesis of [3-(triphenylphosphine)gold(I)-1-benzylimidazol-5-ylidene][pentafluorophenyl]gold(I) nitrate, 34.*

A solution of 1-benzylimidazole (0.08 g, 0.5 mmol) in thf (20 ml) was treated with *n*-butyllithium in hexane (0.3 ml, 0.5 mmol) at -98 °C . After 30 minutes of stirring [Au(C₆F₅)(tht)] (0.23 g, 0.50 mmol) in thf (10 ml) was added to the yellow coloured solution. The reaction mixture was stirred for a further 2 h at -78 °C during which time the solution became colourless. The product was treated with a solution of [Au(NO₃)(PPh₃)] (0.24 g, 0.50 mmol) in thf (10 ml) at -78 °C and slowly allowed to reach room temperature over 2 hours. The solvent was removed *in vacuo* to yield a colourless oily residue. The residue was extracted sequentially with diethyl ether (30 ml) and, dichloromethane (30 ml) and the extracts were filtered individually through MgSO₄. The ether extract afforded a mixture of gold-containing products (0.21 g), which consisted predominantly of [Au(C₆F₅)(PPh₃)] and trace amounts of **34**.

4.4.2.6 *The preparation of bis[3-(triphenylphosphine)gold(I)-1-benzylimidazol-5-ylidene]gold(I) nitrate, 35.*

A solution of 1-benzylimidazole (0.16 g, 1.0 mmol) in diethyl ether (20 ml) was treated with *n*-butyllithium in hexane (0.63 ml, 1.0 mmol) at -78 °C. After 30 min of stirring a suspension of [AuCl(tht)] (0.16 g, 0.49 mmol) in diethyl ether (20 ml) was added to the yellow coloured solution. The reaction mixture was stirred for a further 2 h at -78 °C

during which time the solution became colourless. The solution was treated with a suspension of AgBF_4 (0.10 mg, 0.50 mmol) in diethyl ether (10 ml) stirred and allowed to slowly reach room temperature over a 2 h period. The product mixture was filtered through MgSO_4 to obtain a clear solution, which was treated with a solution of $[\text{Au}(\text{NO}_3)(\text{PPh}_3)]$ (0.52 g, 1.0 mmol) in ether at $-78\text{ }^\circ\text{C}$. The product mixture was allowed to reach room temperature over a 2 h period. The solvent was removed *in vacuo* to yield a colourless oily residue. The residue was extracted sequentially with diethyl ether (30 ml) and, dichloromethane (30 ml) and the extract were filtered individually through MgSO_4 . The ether extract was concentrated *in vacuo* to yield a white solid, a mixture of unreacted $[\text{Au}(\text{NO}_3)(\text{PPh}_3)]$ and **35** (0.19 g).

4.4.2.7 The preparation of [1-(2,6-dimethylphenyl)tetrazol-5-yl](triphenylphosphine) gold(I), 36.

A solution of $[\text{Au}(\text{N}_3)(\text{PPh}_3)]$ (0.23 g, 0.46 mmol) in dichloromethane (25 ml) was reacted with 2,6-dimethylphenylisocyanide (0.91 g, 6.9 mmol) in dichloromethane (10 ml). The reaction was protected from sunlight and left unstirred for 17 h, upon which the solution was concentrated to approximately 15 ml. The addition of diethyl ether to the solution produced a colourless precipitate, which upon recrystallisation from a dichloromethane solution layered with diethyl ether afforded colourless prisms of **36** (0.20 g, 69 %).

4.4.2.8 The preparation of [1-(2,6-dimethylphenyl)-4-methyltetrazol-5-ylidene] (triphenylphosphine)gold(I) triflate, 37.

A solution of **37** (0.14 g, 0.22 mmol) in dichloromethane (10 ml) was cooled to $-70\text{ }^\circ\text{C}$, treated with $\text{CF}_3\text{SO}_3\text{Me}$ (0.03 ml, 0.2 mmol) and stirred for 30 min whereafter, the mixture was allowed to reach room temperature. The solvent was removed *in vacuo* to yield a dark brown residue. The residue was extracted sequentially with diethyl ether (30 ml) and dichloromethane (30 ml) and the extracts were filtered individually through MgSO_4 . The ether extract was concentrated *in vacuo* to yield a colourless solid. Recrystallisation from a dichloromethane solution layered with diethyl ether afforded colourless needles of **37** (0.13 g, 91 %).

4.4.2.9 The preparation of [1-(tert-butyl)tetrazol-5-yl](triphenylphosphine) gold (I), 38.

A solution $[\text{Au}(\text{N}_3)(\text{PPh}_3)]$ (0.30 g, 0.60 mmol) in dichloromethane (25 ml) was reacted with *tert*-butylisocyanide (0.50 g, 6.0 mmol) in dichloromethane (10 ml). The reaction was protected from sunlight and stirred for 15 h at room temperature, upon which the

solution was concentrated to approximately 15 ml. The addition of diethyl ether to the solution produced a colourless microcrystalline product, **38** (0.26 g, 74 %).

4.4.2.10 The preparation of [1-(cyclohexyl)tetrazol-5-yl](triphenylphosphine)gold(I), **39 and [1-cyclohexylisocyanide][1-(cyclohexyl)tetrazol-5-yl]gold (I), **40**.**

A solution [Au(N₃)(PPh₃)] (0.50 g, 1.00 mmol) in dichloromethane (40 ml) was reacted with 1-cyclohexylisocyanide (2.18 g, 20.0 mmol) in dichloromethane (10 ml). The reaction was protected from sunlight and left unstirred for 17 h, upon which the solution was concentrated to approximately 15 ml. The addition of diethyl ether to the solution formed a colourless microcrystalline product, a mixture of complexes **39** and **40** (0.37 g).

4.4.2.11 Preparation of (benzotriazol-1-ylmethylisocyanide)(pentafluorophenyl)gold(I), **41.**

The addition of a solution of benzotriazole-1-ylmethylisocyanide (0.10 g, 0.66 mmol) in dichloromethane (15 ml) to a solution [Au(C₆F₅)(tbt)] (0.30 g, 0.66 mmol) in diethyl ether (20 ml) produces a cloudy solution. The mixture was stirred for 4 h at room temperature upon which the solution was reduced to dryness *in vacuo*. The residue was redissolved in diethyl ether, filtered through anhydrous MgSO₄ and the filtrate concentrated *in vacuo* to yield a luminescent yellow microcrystalline solid, **41** (0.30 g, 88 %).

4.4.2.12 Preparation of {[N-(1,2,4-triazol-3-yl)amine][(N'-benzotriazol-1-ylmethylamine)ylidene]}(pentafluorophenyl)gold(I), **42.**

A solution of 1, 2, 4-triazol-3-ylamine (0.70 g, 0.83 mmol) in thf (20 ml) was added with stirring to a solution of **41** (0.10 g, 0.20 mmol). The reaction was protected from sunlight and stirred for 48 h at room temperature, upon which the solution was rapidly filtered through a short silica column. The filtrate was concentrated *in vacuo* to yield a colourless microcrystalline solid, **42** (0.10 g, 80 %).

4.4.2.13 The formation of complexes, [1-cyclohexyltetrazol-5-yl][cyclohexylamine(ethoxy)ylidene]gold(I), **43, and [1-cyclohexyltetrazol-5-yl][bis(cyclohexylamine)ylidene]gold(I), **44**.**

Complex **39**, in addition to residual amounts of 1-cyclohexylisocyanide, in freshly distilled ethanol layered with *n*-pentane, was stored in a narrow schlenk tube at -20 °C for 8 months. Apart from a bright yellow luminescent microcrystalline solid which formed towards the base of the gas-inlet tap and cap, colourless needle-like crystals, a co-crystallate of **43** and **44**, formed from the solution.

4.4.2.14 X-Ray crystal structure determinations.

Crystal data collection and refinement details for complexes **30**, **31**, **32**, **33**, **36** and **43·44** are summarised in Tables 4.20-4.22. Data sets were collected on a Bruker SMART Apex CCD diffractometer⁶⁸ with graphite monochromated MoK α radiation ($\lambda = 0.71073 \text{ \AA}$). Data reduction was carried out with standard methods from software package Bruker SAINT.⁶⁹ Empirical corrections were performed using SCALEPACK⁷⁰ and data were treated with SADABS.^{71,72}

All the structures were solved in collaboration with Dr S. Nogai, using direct methods or interpretation of a Patterson synthesis which yielded the position of the metal atoms, and conventional difference Fourier methods. All non-hydrogen atoms were refined anisotropically by full-matrix least squares calculations on F^2 using SHELX-97⁷³ within the X-seed environment.⁷⁴ The hydrogen atoms were fixed in calculated positions. Figures were generated with X-seed⁷⁴ and POV Ray for Windows, with the displacement ellipsoids at 50% probability level. Further information is available from Prof. H.G. Raubenheimer at the Department of Chemistry and Polymer Science, Stellenbosch University.

⁶⁸ SMART Data Collection Software, Version 5.629, Bruker AXS Inc., Madison, WI, 2003.

⁶⁹ SAINT, Data Reduction Software, Version 6.45, Bruker AXS Inc., Madison, WI, 2003.

⁷⁰ L. J. Ferrugia, *J. Appl. Crystallogr.*, 1999, **32**, 837.

⁷¹ R. H. Blessing, *Acta Crystallogr.*, 1995, **A51**, 33.

⁷² SADABS, Version 2.05, Bruker AXS Inc., Madison, WI, 2002.

⁷³ G. M. Shelrick, SHELX-97. Program for Crystal Structure Analysis, University of Göttingen, Germany, 1997.

⁷⁴ L. J. Barbour, *J. Supramol. Chem.* 2001, **1**, 189.

Table 4.20 Crystallographic data for **30** and **31**

	30	31
Empirical formula	C ₁₉ H ₂₀ AuF ₃ N ₈ O ₃ S	C ₁₉ H ₁₉ AuF ₁₀ N ₂
<i>M_r</i>	694.46	662.33
Temp. (K)	100(2) K	143(2) K
Wavelength (Å)	0.71073 Å	0.71073 Å
Crystal system	Orthorhombic	Monoclinic
Space group	Pna2 ₁	P2 ₁ /c
a (Å)	11.812(2)	10.005(17)
b (Å)	22.452(3)	16.421(17)
c (Å)	8.892(1)	13.600(14)
α (°)	90	90
β (°)	90	107.68(6)
γ (°)	90	90
Volume (Å ³)	2358.1(5)	2129(5)
Z	4	4
<i>d</i> _{calcd} (g/cm ³)	1.956	2.067
Absorption coefficient (μ, mm ⁻¹)	6.390	7.006
Absorption correction	Semi-empirical from equivalents	Semi-empirical from equivalents
F(000)	1344	1264
Crystal size (mm ³)	0.20 x 0.20 x 0.10	0.20 x 0.10 x 0.10
θ-range for data collection (°)	1.81 to 26.72	2.14 to 26.73
Index range	-10 ≤ h ≤ 14, -25 ≤ k ≤ 28, -11 ≤ l ≤ 11	-9 ≤ h ≤ 12 -18 ≤ k ≤ 20 -17 ≤ l ≤ 16
No. of reflections collected	12896	12536
No. independent reflections	4842 [R(int) = 0.0356]	4494 [R(int) = 0.0319]
Max. and min. transmission	0.5280 and 0.3181	0.4976 and 0.3891
Refinement method	Full-matrix least-squares on F ²	Full-matrix least-squares on F ²
Data/restraints/parameters	4842 / 1 / 318	4494 / 0 / 294
Goof on F ²	1.108	1.016
Final R-indices [I > 2σ >(I)]	R ₁ = 0.0407 wR ₂ = 0.0854	R ₁ = 0.0279 wR ₂ = 0.0592
R indices (all data)	R ₁ = 0.0517 wR ₂ = 0.0890	R ₁ = 0.0358 wR ₂ = 0.0623
Largest diff. peak and hole (e.Å ⁻³)	2.900 and -1.222	1.088 and -0.608
Weighing scheme	a = 0.0355 / b = 3.4720	a = 0.0313

Table 4.21 Crystallographic data for **32** and **33**

	32	33
Empirical formula	C ₉ H ₁₉ F ₆ LiN ₂ O ₆ S ₂	C ₅ H ₁₀ F ₃ LiO ₄ S
M_r	436.32	230.13
Temp. (K)	100(2) K	100(2) K
Wavelength (Å)	0.71073 Å	0.71073
Crystal system	Monoclinic	Monoclinic
Space group	P2 ₁ /c	C2/c
a (Å)	10.6609(14)	21.885(3)
b (Å)	8.4235(11)	5.2170(6)
c (Å)	20.265(3)	19.210(3)
α (°)	90	90
β (°)	99.807(2)	114.060(4)
γ (°)	90	90
Volume (Å ³)	1793.2(4)	2002.7(5)
Z	4	8
d_{calcd} (g/cm ³)	1.616	1.527
Absorption coefficient (μ , mm ⁻¹)	0.385	0.353
Absorption correction	Semi-empirical from equivalents	Semi-empirical from equivalents
F(000)	896	944
Crystal size (mm ³)	0.20 x 0.10 x 0.10	0.40 x 0.30 x 0.30
θ -range for data collection (°)	1.94 to 25.68	2.04 to 25.68
Index range	-12 ≤ h ≤ 13 -10 ≤ k ≤ 10 -21 ≤ l ≤ 24	-24 ≤ h ≤ 26 -6 ≤ k ≤ 6 -22 ≤ l ≤ 23
No. of reflections collected	9405	5183
No. independent reflections	3368 [R(int) = 0.0255]	1897 [R(int) = 0.0181]
Max. and min. transmission	None	None
Refinement method	Full-matrix least-squares on F ²	Full-matrix least-squares on F ²
Data/restraints/parameters	3368 / 8 / 279	1897 / 0 / 129
Goof on F ²	1.083	1.042
Final R-indices [I > 2 σ > (I)]	R ₁ = 0.0453 wR ₂ = 0.1074	R ₁ = 0.0284 wR ₂ = 0.0778
R indices (all data)	R ₁ = 0.0558 wR ₂ = 0.1122	R ₁ = 0.0316 wR ₂ = 0.0797
Largest diff. peak and hole (e.Å ⁻³)	0.509 and -0.289	0.493 and -0.269
Weighing scheme	a = 0.0413 / b = 2.9207	a = 0.0492 / b = 0.9755

Table 4.22 Crystallographic data for **36** and **43·44**

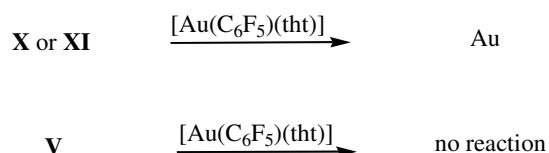
	36.CH₂Cl₂	43·44
Empirical formula	C ₂₈ H ₂₆ AuCl ₂ N ₄ P	C ₃₆ H ₆₃ Au ₂ N ₁₁ O
M_r	717.36	1059.91
Temp. (K)	100(2)	173(2)
Wavelength (Å)	0.71073	0.71073
Crystal system	monoclinic	Triclinic
Space group	P2 ₁ /c	P $\bar{1}$
a (Å)	8.6440(8)	10.569(3)
b (Å)	12.7376(12)	12.484(3)
c (Å)	24.885(2)	16.827(5)
α (°)	90	95.641(4)
β (°)	94.429(2)	98.979(4)
γ (°)	90	110.714(4)
Volume (Å ³)	2731.8(4)	2022.8(9)
Z	4	2
d_{calcd} (g/cm ³)	1.744	1.740
Absorption coefficient (μ , mm ⁻¹)	5.664	7.287
Absorption correction	Semi-empirical from equivalents	Semi-empirical from equivalents
F(000)	1400	1044
Crystal size (mm ³)	0.30 x 0.20 x 0.10	0.20 x 0.10 x 0.10
θ -range for data collection (°)	2.29 to 26.76	1.77 to 25.35
Index range	-10 \leq h \leq 10 -16 \leq k \leq 16 -29 \leq l \leq 31	-12 \leq h \leq 12 -15 \leq k \leq 15 -20 \leq l \leq 20
No. of reflections collected	5797	19845
No. independent reflections	5333 [R(int) = 0.0239]	7361 [R(int) = 0.0635]
Max. and min. transmission	0.4182 and 0.6012	0.5294 and 0.3235
Refinement method	Full-matrix least-squares on F ²	Full-matrix least-squares on F ²
Data/restraints/parameters	5797/0/355	7361 / 258 / 599
Goof on F ²	1.054	1.077
Final R-indices [$I > 2\sigma > (I)$]	R ₁ = 0.0205 wR ₂ = 0.0470	R ₁ = 0.0589 wR ₂ = 0.1180
R indices (all data)	R ₁ = 0.0233 wR ₂ = 0.0481	R ₁ = 0.0874 wR ₂ = 0.1283
Largest diff. peak and hole (e.Å ⁻³)	1.172 and -0.388	2.108 and -2.521
Weighing scheme	a = 0.0226/ b = 1.9230	a = 0.0582 / b = 0.2758

ADDENDUM 1

A1.1 Reactions of ligands IV, V, VIII, X and XI with gold(I) substrates.

A1.1.1 Attempted synthesis of (pentafluorophenyl)gold(I) imine complexes.

The reaction of ligands **IV**, **X** and **XI** with $[\text{Au}(\text{C}_6\text{F}_5)(\text{tht})]$ were investigated. The ligand substitution reactions were carried out in acetone, which affected dissolution of the otherwise insoluble ligand. An assessment of two coordination motifs (tetrazole and imidazole imine) in one molecule was envisioned, in the attempted bidentate coordination of **X** and **XI** to neutral gold(I) units (Scheme A1.1). These complexes bearing a hydrophilic tetrazolyl substituent were designed to improve solubility in water, owing to the acidity of tetrazole ($\text{pK}_a = 4.89$ in H_2O) and the stable anions formed at physiological pH range.



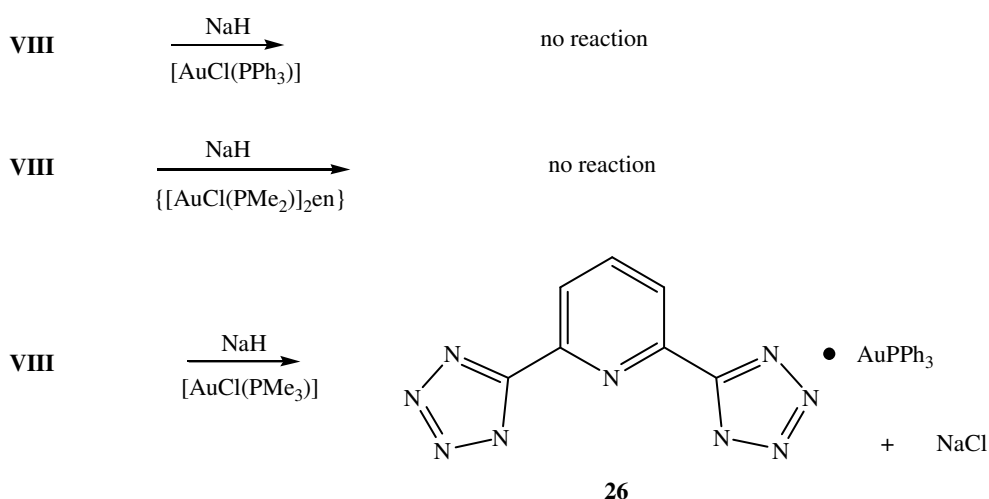
Scheme A1.1 Synthetic route towards (pentafluorophenyl)gold(I) imine complexes.

However, the reactions of ligand **X** or **XI** and $[\text{Au}(\text{C}_6\text{F}_5)(\text{tht})]$ were characterised by marked metal decomposition during the initial stages of the reaction. This result was surprising owing to the previously described strong imine coordination abilities of imidazole substrates (see **12-14**, **15-18**). This result is in agreement with previously described unsuccessful coordination of $[\text{Au}(\text{C}_6\text{F}_5)(\text{tht})]$ to 1*H*-tetrazole (Section 3.2.2), and it appears that the imine donor potential, of 1- or 5-substituted tetrazoles to neutral gold(I) centres, is delicately balanced. It has previously been shown that tetrazole derivatives containing strong electron withdrawing substituents in the N¹ position, such as phenyl or pyridyl rings, have impeded imine coordination to gold(I) (section 3.2.2). Furthermore, there are few examples in literature where the coordination of an AuC_6F_5 group to secondary amines are described and specifically no neutral gold(I) complexes are described that are derived from ligands containing acidic NH protons.¹ The possible tautomerism of 5-substituted tetrazoles, and how it effects the imine coordination potential to gold(I) centres should also not be underestimated.

¹ S. D. Bunge, O. Just and W. S. Rees, Jr., *Angew. Chem., Int. Ed., Engl.*, 2000, **39**, 3082.

A1.1.2 Attempted synthesis of (phosphine)gold(I) amide complexes.

To complement the preparation of mononuclear gold(I) complexes derived from tetrazolate anionic ligands, the synthesis of binuclear gold amido compounds contained in a pyridyl pincer were attempted using different chloro(phosphine)gold(I) starting materials (Scheme A1.3). Suspensions of ligand **VIII** and $[\text{AuCl}(\text{PMe}_3)]$, $[\text{AuCl}(\text{PPh}_3)]$ or $[\mu\text{-}1,2\text{-bis}(\text{dimethylphosphine})\text{ethane}]\text{bis}[\text{chlorogold}(\text{I})]$ $\{[\text{AuCl}(\text{PMe}_2)]_2\text{en}\}$ were treated with sodium hydride, and the reactions were characterised by an immediate formation of a white precipitate (NaCl). Due to the high insolubility of **VIII** these reactions did not proceed to completion and hindered further purification. In the instance where $[\text{AuCl}(\text{PPh}_3)]$ was used, DMF was employed as solvent, the formation of the white precipitation was followed immediately by metal decomposition, evident by a violet colour due to the presence of finely divided metallic gold. No reaction product could be identified where $\{[\text{AuCl}(\text{PMe}_2)]_2\text{en}\}$ was used, and both ligand and gold(I) starting material were recovered in almost quantitative yield after prolonged reaction times.



Scheme A1.2 Synthetic route towards (phosphine)gold(I) amide complexes.

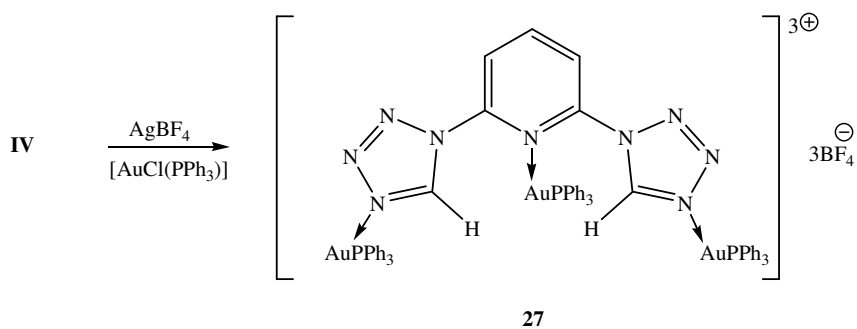
The most successful reaction occurred in the instance where $[\text{AuCl}(\text{PMe}_3)]$ was used as starting compound. Monitoring this reaction by TLC (silica, methanol/dichloromethane/*n*-hexane; 1:5:5) revealed that a strong fluorescent gold containing product, with a relative intermediate polarity to the starting reagents, had formed. Duati and coworkers² had reported similar luminescent properties of Ru(II) tridentate complexes of **VIII**. Infrared spectroscopic measurement of the white solid isolated suggested that the ligand coordinates to the metal centre as a tetrazolate anion rather than as a neutral ligand, due to the absence of the N-H stretching vibrational bands observed in the free ligand. The

² M. Duati, S. Tasca, F. C. Lynch, H. Bohlen and J. G. Vos, *Inorg. Chem.*, 2003, **42**, 8377.

complex mass spectrometric data could not successfully be assigned to either a molecular ion or characteristic fragmentation products for either a mono or disubstituted product. ^1H and ^{13}C NMR data of **26** show apart from a strong doublet resonance at δ 1.57 ($^2J = 9.20$ Hz) and δ 15.8 ($^1J = 38.1$ Hz) for the trimethylphosphine group, a downfield (δ 8.03, dd, $^3J = 8.01$ Hz) and upfield shift (δ 8.21, d, $^3J = 7.72$ Hz) for the protons in the 4 and 3-position of the pyridine ring, respectively. A complex ^{31}P NMR spectrum (broad multiplet at δ -6.8 and a further sharp singlet resonance at δ 37.7) signifies that apart from the coordination to the tetrazolate anion, a further neutral coordination of the cationic metal species to the pyridyl nitrogen may have occurred. Suitable crystals for X-ray diffraction studies could not be grown, and no conclusive evidence exists to confirm the molecular structure of **26**.

A1.1.3 Attempted synthesis of cationic(phosphine)gold(I) imine complexes.

A modified approach as described by Navarro *et al.*³ and Blackie *et al.*⁴ for the preparation of cationic (phosphine)gold(I) imine complexes from pyridyl derivatives, was also used. The addition of a THF solution of $[\text{AuCl}(\text{PPh}_3)]$ and **IV** to AgBF_4 in THF, formed an immediate white precipitate (Scheme A1.3). The reaction that was protected from light was stirred for a further 12 h, whereupon the white solid was removed by filtration.



Scheme A1.3 Synthetic route towards pyridyl-tetrazole imine coordinations.

The concentration of the mother liquor afforded a yellow solid, which included apart from $[\text{AuCl}(\text{PPh}_3)]$ one other gold containing product. ^{31}P NMR confirms that these two products are present in a 4:1 ratio (δ 31.1 and 46.0), in agreement with the multiple proton multiplet resonances arising from triphenylphosphine groups at δ 7.67-7.83. A correlation of this multiplet with the diagnostic peaks of the pyridyl ligand (δ 8.85, 8.62 and 11.18) indicates that the other phosphine containing product is related to ligand **IV**. A notable

³ M. Navarro, F. Vásquez, R. A. Sánchez-Delgado, H. Pérez, V. Sinou and J. Schrével, *J. Med. Chem.*, 2004, **47**, 5204.

⁴ M. A. L. Blackie, P. Beagley, K. Chibale, C. Clarkson, J.R. Moss and P.J. Smith, *J. Organomet. Chem.*, 2003, **688**, 144.

downfield shift of H⁴ (δ 8.85, dd, $^3J = 7.6$ Hz, $^3J = 7.7$ Hz), H³ (δ 8.62, d, $^3J = 8.0$ Hz) and large downfield shift for the two acidic CH protons ($\Delta\delta$ 1.59, at 11.18) further substantiates this observation. ¹³C NMR signals showing distinctive phosphorous coupling patterns to all four chemically inequivalent carbon atoms are duplicated, and the pyridyl carbons are all consistently shifted downfield ($\Delta\delta$ 3.5). However no definite long range carbon-phosphorous coupling of the CH or C² carbon, which would have to be across one ring nitrogen, and would confirm gold(I) imine coordination, could be observed. Furthermore, low solubility of the ligand and complex hampered an ¹⁵N NMR study to elucidate the nature and presence of gold(I) coordination. The positive-ion FAB-MS of the residual mixture mainly showed {Ph₃PAu}⁺ (m/z 459) and {(Ph₃P)₂Au}⁺ (m/z 721) fragmentation peaks. Strong signals at m/z 592 and m/z 1051 could not be assigned with certainty to any coordination product. Attempted crystallisation of the product mixture using different solvent systems was unsuccessful and only confirmed the presence of unreacted [AuCl(PPh₃)].

A1.2 Experimental

A1.2.1 Preparations and procedures

A1.2.1.1 Attempted synthesis of (pentafluorophenyl)gold(I) imine complexes from ligands IV, X and XI.

A similar preparative route was followed as for **13** using **IV** (0.09 g, 0.5 mmol), **X** (0.13 g, 0.50 mmol) and **XI** (0.09 g, 0.5 mmol) with [Au(C₆F₅)(tht)] (0.46 g, 1.0 mmol) in acetone (20 ml), respectively. A prolonged reaction time at room temperature was accompanied by metal decomposition. At this point in the reaction, the reaction mixtures were filtered through celite and MgSO₄. The colourless filtrate was concentrated *in vacuo*, and extracted with diethyl ether to recover unreacted [Au(C₆F₅)(tht)]. Analysis of the insoluble residue confirmed that no reactions had taken place.

A1.2.1.2 The reaction of the sodium tetrazolate salt of VIII with chloro(trimethylphosphine)gold(I).

A suspension of sodium hydride (0.05 g, 2 mmol) and pyridine ligand **VIII** (0.11 g, 0.50 mmol) in THF (10 ml) was heated to 50 °C and stirred for 15 hr. The reaction mixture was cooled to room temperature, treated with [AuCl(PMe₃)] (0.31 g, 1.0 mmol) in THF (10 ml) and stirred for a 15 h at room temperature. The resultant off-white suspension was filtered through celite and MgSO₄, and the clear solution evaporated to dryness. The white solid was recrystallised from methanol layered with diethyl ether, to afford colourless

microcrystalline material, (0.22 g) at -20 °C. A similar preparative route was followed where [AuCl(PPh₃)] and {[AuPMe₂Cl]₂en} was employed as gold starting material. No reaction was observed in these instances.

A1.2.1.3 The reaction of the VIII with chloro(triphenylphosphine)gold(I) in the presence of a silver salt.

A solution of AgBF₄ (0.19 mg, 1.0 mmol) in THF was added to a mixture of ligand **VIII** (0.22 g, 0.50 mmol) and [AuCl(PPh₃)] (0.49 g, 1.0 mmol) in THF (10 ml). An immediate precipitate formed. The reaction mixture was protected from light and stirred for 12 hr. The resultant off-white suspension was filtered through celite and MgSO₄, and the clear solution evaporated to dryness. The yellow solid was extracted sequentially with ethanol, and concentrated *in vacuo*, and then recrystallised from dichloromethane layered with *n*-pentane, to afford yellow microcrystalline material, (0.20 g) at -20 °C.